# INVESTIGATION OF THE EFFECTS OF KETOGENIC DIET THERAPY IN A MOUSE MODEL OF GM2 GANGLIOSIDOSIS

**A Thesis Submitted to the**
**Graduate School of Engineering and Sciences of**
**Izmir Institute of Technology**
**in Partial Fulfillment of the Requirements for the Degree of**

**DOCTOR OF PHILOSOPHY**

**in Molecular Biology and Genetics**

**by**
**Orhan Kerim İNCİ**

**March 2024**
**İZMİR**

We approve the thesis of **Orhan Kerim İNCİ.**

**Examining Committee Members:**

**Prof. Dr. Volkan SEYRANTEPE**
Department of Molecular Biology and Genetics, Izmir Institute of Technology

**Prof. Dr. Bünyamin AKGÜL**
Department of Molecular Biology and Genetics, Izmir Institute of Technology

**Prof. Dr. Şerife Esra ERDAL BAĞRIYANIK**
Department of Basic Medical Sciences, Dokuz Eylül University

**Assoc. Prof. Dr. Şükrü GÜLEÇ**
Department of Food Engineering, Izmir Institute of Technology

**Assist. Prof. Dr. Yavuz OKTAY**
Department of Basic Medical Sciences, Dokuz Eylül University

**21 March 2024**

**Prof.Dr. Volkan SEYRANTEPE**
Supervisor, Department of Molecular Biology and Genetics
Izmir Institute of Technology

**Prof.Dr. Özden Yalçın ÖZUYSAL**
Head of Department of Molecular Biology and Genetics

**Prof. Dr. Mehtap EANES**
Dean of Graduate School of Engineering and Sciences

# ACKNOWLEDGEMENTS

Initially, I would like to express my sincere gratitude and thankfulness to my supervisor, Prof. Dr. Volkan SEYRANTEPE for his guidance, encouragement, support, and extensive knowledge throughout my thesis.

I would like to express special thanks to Prof. Dr. Bünyamin Akgül, Assoc. Dr. Şükrü Güleç for being my thesis committee members as well as their suggestions and attention.

I would like to thank also The Scientific and Technological Research Council of Turkey (TÜBİTAK) (218S824) and the Council of Higher Education (YOK) 100/2000 Doctoral Scholarship program for their financial support in completing my thesis research.

I have special thanks to my lab friends, Selman Yanbul, llker Gümüş, and Tufan Utku Caliskan, for their encouragement and support during my thesis. I also have special thanks and gratitude to my lab pair, Nurselin Ates, for their infinite assistance and encouragement. I would like to thank other lab members, Hatice Hande Basirli, Melike Can Ozgür, Beyza Kaya, Ebru Ada, and undergraduate students (Esin Simge Güler, Halil Kaan Türk, Mustafa Can Turali, Hayri Tolga Yıldız). Moreover, I am immensely grateful to alum members of Seyrantepe Lab (Tekin Can Sobacı, Berkan Kanmaz, Tugce Sengül Turan, Barıs Colpan) for their help during thesis research. Secil Akyıldız Demir also deserved special thanks for sharing excellent lab experiences with me.

Finally, I am deeply grateful to my parents, Gürsel Inci, Nesrin Inci, and Gokce Inci, for their endless trust and support. Their support allowed me to continue my thesis research without getting tired. Last but not least, I would like to give very special thanks to my fiancee, Tugba Firik, because she made me who I am now.

# ABSTRACT

## INVESTIGATION OF THE EFFECTS OF KETOGENIC DIET THERAPY IN A MOUSE MODEL OF GM2 GANGLIOSIDOSIS

GM2 gangliosidosis is an autosomal recessive lysosomal storage disorder in which GM2 ganglioside is accumulated, especially in the brain. GM2 gangliosidosis is divided into three different variants: Tay Sachs (B-variant or type I), Sandhoff (O-variant or type 2), and GM2AP deficiency (AB-variant). Accumulation of the GM2 ganglioside in brain causes disease pathology as neurodegeneration and neuroinflammation. Our lab first displayed the novel GM2 gangliosidosis type-I mouse model (*Hexa-/-Neu3-/-*). Compared to control, this model could survive a maximum of five-months due to severe pathologies, neurodegeneration, and neuroinflammation. The ketogenic diet is high-fat and low-carbohydrate/protein diet that triggers burning fat instead of carbohydrates. The ketogenic diet is used comprehensively in neurodegenerative disorders such as Sandhoff, Alzheimer's, and Parkinson's to regulate inflammation, neurodegeneration, and autophagy. In addition, elevation of *CCL2* expression in *Hexa-/-Neu3-/-* mice resulted in increased amounts of active microglia and astrocytes. Therefore, the CCL2/CCR2 signaling inhibitor of propagermanium was used in addition to ketogenic diet. Thus, reducing neuroinflammation is aimed to be more effective as a combined therapy. In my Ph.D. thesis, expression and protein levels of autophagy and inflammation-associated genes were analyzed in the mouse brain to exhibit whether beneficial effects on autophagic flux and neuroinflammation are found after the ketogenic diet and propagermanium treatment. The pathology of the GM2 gangliosidosis mouse type-I brain was illustrated by thin-layer chromatography and immunofluorescence staining to display whether the ketogenic diet affects the ganglioside metabolism. Briefly, ketogenic diet therapy and its anti-inflammatory and neuroprotective effects were explored in the GM2 gangliosidosis mouse model.

# ÖZET

## GM2 GANGLİOSİDOZ FARE MODELİNDE KETOJENİK DİYET TEDAVİSİNİN ETKİLERİNİN ARAŞTIRILMASI

GM2 gangliosidoz, GM2 gangliositinin özellikle beyinde biriktiği bir tür otozomal resesif lizozomal depo bozukluğudur. GM2 gangliosidoz, Tay Sachs (B varyantı veya tip I), Sandhoff (O varyantı veya tip 2) ve GM2AP eksikliği (AB varyantı) olmak üzere üç farklı varyanta bölünür. GM2 gangliositinin beyinde birikmesi, nörodejenerasyon ve nöroenflamasyon gibi hastalık patolojilerine neden olur. Özgün GM2 gangliosidosis tip I fare modeli (*Hexa-/-Neu3-/-)* ilk olarak laboratuvarımız tarafından sergilendi. Bu model, kontrole göre nörodejenerasyon ve nöroenflamasyon gibi ciddi patolojiler nedeniyle maksimum beş ay yaşayabilmiştir. Ketojenik diyet, karbonhidrat yerine yağ yakımını tetikleyen yüksek yağ ve düşük karbonhidrat/protein diyetidir. Ketojenik diyet, iltihabı, nörodejenerasyonu ve otofajiyi düzenlemek için Sandhoff, Alzheimer, Parkinson hastalıkları gibi nörodejeneratif rahatsızlıklarda kapsamlı bir şekilde kullanılmaktadır. Ayrıca, *Hexa-/-Neu3-/-* farelerinde artan *CCL2* ekspresyonu, farelerde aktif mikroglia ve astrosit miktarlarında artışa sebebiyet vermiştir. Bu yüzden, ketojenik diyete ek olarak CCL2/CCR2 yolağını bozan bir inhibitör olan propagermanyum kullanılmıştır. Böylelikle, kombine terapi olarak nöroenflamasyondaki azalmanın daha etkili olması amaçlanmıştır. Doktora tezimde, ketojenik diyet ve propagermanium tedavilerinden sonra otofajik yolak ve nöroenflamasyon üzerinde faydalı etkilerin bulunup bulunmadığını göstermek için otofaji ve inflamasyonla ilişkili genlerin ekspresyon ve protein seviyeleri fare beyninde analiz edilmiştir. Ketojenik diyetin gangliosit metabolizması üzerinde herhangi bir etkisi olup olmadığını göstermek içinse, GM2 gangliosidoz tip I fare beyninin patolojisi, ince tabaka kromatografisi ve immünohistokimyasal boyamalarla gösterilmiştir. Kısaca, ketojenik diyet tedavisinin anti-enflamatuvar ve nöroprotektif etkileri, GM2 gangliosidoz fare modelinde araştırılmıştır.

# TABLE OF CONTENTS

# LIST OF FIGURES

**Figure** **Page**

# LIST OF TABLES

# CHAPTER 1

# INTRODUCTION

## 1.1 Ganglioside Metabolism

Gangliosides are the one type of glycosphingolipids that contains sialic-acid residues (terminal sugar). They are expressed cell-specific and widely abundant in neuronal plasma membranes (Sandhoff and Sandhoff 2018). De novo synthesis of the gangliosides begins first at the cytoplasmic leaflet of the endoplasmic reticulum by synthesizing 3-keto sphinganine/3-keto dihydrosphingosine (KdS) (Mandon et al. 1992). KdS is converted to the ceramide, which is the last product at ER, step by step. Ceramide is transported either by vesicular transport or transporter proteins, which is the ceramide transport protein (CERT) to the Golgi apparatus to generate glycosphingolipids via the stepwise addition of monosaccharides to the ceramides (Kolter and Sandhoff 1999). Ceramide is converted to glycosylceramide (GlcCer), followed by GlcCer is glycosylated to the lactosylceramide (LacCer) by B4Galt5 and B4Galt6 in the Golgi lumen (Nishie et al. 2010)(Tokuda et al. 2013). The first ganglioside of GM3 is produced by sialic-acid addition to the galactose moiety of the LacCer via ST3Gal5 (GM3-Synthase) (Ishii et al. 1999). Higher ganglioside production occurs by stepwise addition of sialic acids at the Golgi lumen or trans-Golgi network. As a classification, gangliosides are categorized using Svennerholm's terminology. The 0 a-, b-, and c-series, respectively, include gangliosides with 0, 1, 2, and 3 sialic acid residues attached to the innermost galactose (Svennerholm 1994). Four major gangliosides (GD1a, GM1, GD1b, and GT1b), which are the most common ones, constitute >90% of brain gangliosides in mammal brains (Tettamanti et al. 1973). Gangliosides play an essential role in stabilizing neuronal membranes with sphingomyelin as well as cell adhesion and development processes (Jennemann et al. 2005)(Fukushi, Hakomori, and Shepard 1984)(Kolter, Magin, and Sandhoff 2000). Since gangliosides play a critical role in maintaining CNS homeostasis, both a deficiency of gangliosides and an overabundance lead to severe neurological and lysosomal storage disorders such as Sandhoff and Tay-Sachs disorders (Platt et al. 2018).

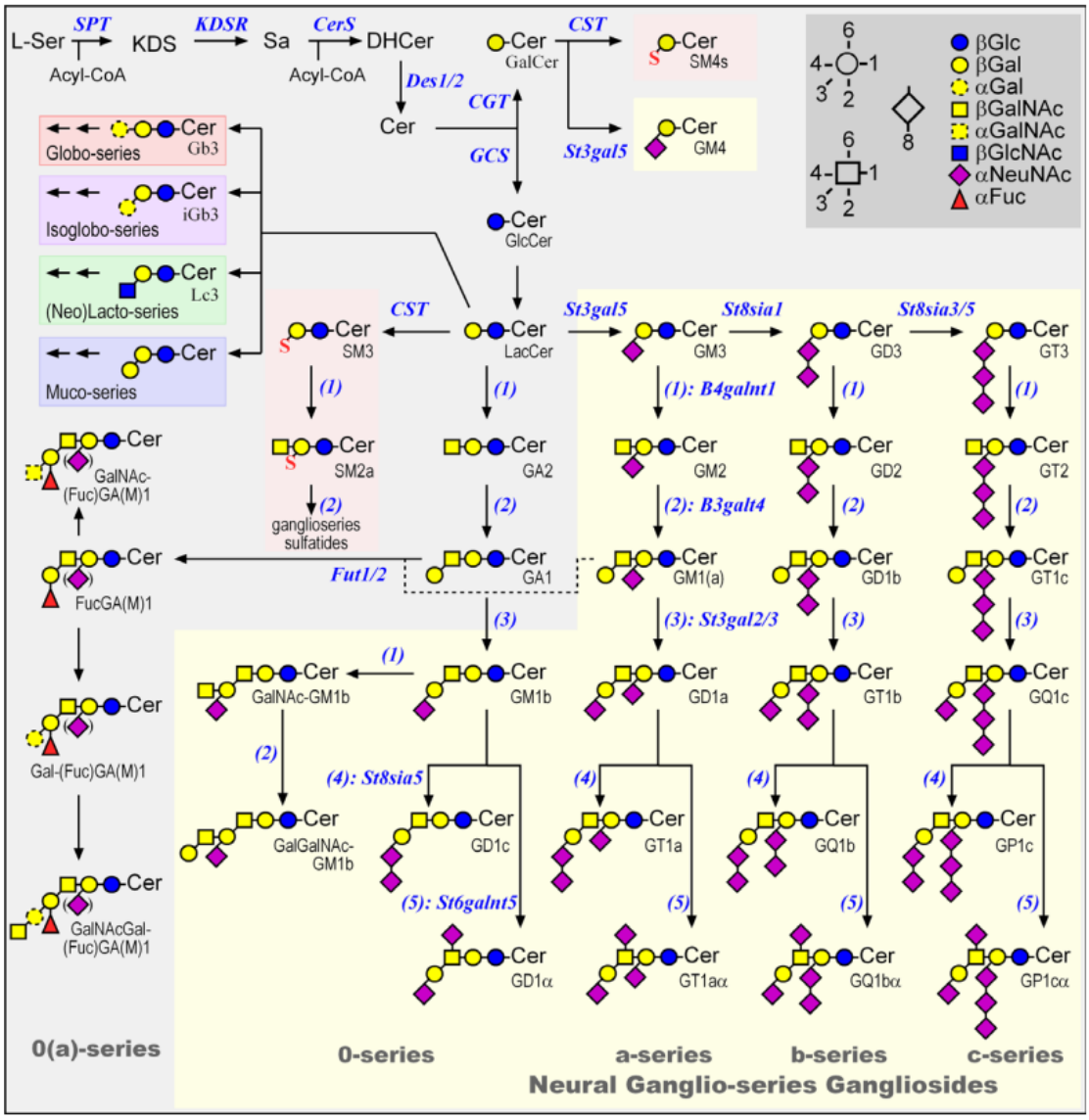


Figure 1.1 Visualization of the ganglioside biosynthetic pathway. Names of gangliosides are classified according to Svennerholm's nomenclature (Source: Sandhoff and Sandhoff 2018).

## 1.2 Lysosomal Storage Disorders

Lysosomal storage disorders are a group of rare metabolic diseases caused by the defective function of lysosomal enzymes. Dysfunction of the lysosomal enzymes and proteins leads to the accumulation of undegraded metabolites such as sphingolipids gangliosides (Abed Rabbo et al. 2021). Progressively accumulating the undegraded metabolites induces devastating neurodegeneration and neuroinflammation at early onset. Moreover, the severity of the diseases is associated with the percentage of enzyme activity, and lower enzyme activity displays a more severe disease phenotype. Lysosomal

storage disorders are divided into five groups according to accumulated substrates in the body: mucopolysaccharidoses, mucolipidoses, glycoproteinoses, glycogen storage disease, and sphingolipidoses. Mucopolysaccharidoses (MPS) are one of the groups of lysosomal storage disorders due to failure of glycosaminoglycan degradation, such as dermatan sulfate keratan sulfate. Organomegaly, severe neurological deterioration, and cartilage abnormalities were observed in MPS types (Ballabio and Gieselmann 2009). Mucolipidoses (ML) are also other groups of lysosomal storage disorders that occur due to N-acetylglucosamine 1- phosphotransferase mutation, which plays roles in the multiple lysosomal enzymes (Aronson 2008). Mucolipidoses generally cause an accumulation of the sialyl oligosaccharides and glycolipids in the lysosomes. Since accumulating the undegraded metabolites, ML patients display severe neurological signs and organomegaly like MPS. Glycoproteinoses show a deficiency of the glycan-degrading enzymes which regulate glycoproteins. Disorders in glycoproteinoses are named according to undegraded sugar, such as fucosidosis and aspartylglucosaminuria. As for lysosomal accumulation of glycoproteinoses, only oligosaccharide accumulation is shown, except for extra glycoprotein accumulation in the patient with fucosidosis. Accumulated metabolites not only cause impairment of the lysosomal activity but also affect cellular actions such as endocytosis, exocytosis, and autophagy (Schultz et al. 2011). The glycogen storage disorders are a group of rare genetic diseases caused by abnormality of the glycogen metabolism. Clinical symptoms predominantly take place in the muscle and liver. For example, Pompe disease is a type of glycogen storage disorder caused by a deficiency of α-glycosidase in which glycogen accumulation was observed in all cell types, especially muscle and liver (Engel et al. 1973). The last group of lysosomal storage disorders are sphingolipidoses caused by failure of the sphingolipid degradation pathway (Puri et al. 1999). Sphingolipidosis is composed of multiple disorders such as GM1 gangliosidosis, GM2 gangliosidosis (Tay-Sachs, Sandhoff disease), Niemann Pick disease, etc., according to the type of accumulated sphingolipids, and enzyme deficiency. Sphingolipidoses, which contain gangliosidosis, display various clinical manifestations in the body, such as neurological and cardiovascular abnormalities (Gilbert-Barness 2004). The primary response of the accumulated substrates in sphingolipidosis exhibits higher lysosome productions in the cell because accumulation prevents the functionality of the lysosome. Besides, the new lysosomes are also abnormal, and the lysosomal system eventually halts in this way, which triggers an inflammatory response, ending cellular death (Hoops, Kolter, and Sandhoff 2009). Most of the genes encoding the

sphingolipidosis-related enzymes are targeted to cell lines and animal models to understand disease pathology and compare patients (Kunihiko Suzuki, Vanier, and Suzuki 1998).

### 1.2.1 Tay-Sachs Disease

Tay-Sachs disease or GM2 gangliosidosis type I is a rare neurodegenerative metabolic disorder caused by the accumulation of the GM2 ganglioside in neuronal cells due to deficiency of the lysosomal β-hexosaminidase A (HexA) enzyme. The enzyme is composed of dimerization of the enzyme subunits, which are α and β subunits, and α-subunit mutations prevent the activity of both the HexA (α-β) and HexS (α-α) enzymes. According to The Human Gene Mutation Database, 181 different mutations were reported for Tay-Sachs disease containing splicing, indels, missense, and nonsense mutations (Stenson et al. 2017). The highest prevalence of Tay-Sachs disease is observed among Ashkenazi Jews. As a function, Hexa enzyme catabolizes GM2 ganglioside to GM3 ganglioside conversion through the cleavage of N-acetylgalactosamine residue in normal conditions (Cachon-Gonzalez, Zaccariotto, and Cox 2018). Impairment of the enzyme causes GM2 ganglioside and related glycolipid accumulations, triggering progressive neuronal deterioration such as motor deficits, macrocephaly, and hyperacusis in the first year (Masingue et al. 2020). Moreover, a cherry-red spot of the macula in the eye is also one of the pathological signs of Tay-Sachs disease. Tay-Sachs disease is divided into four subtypes: early-onset (infantile), juvenile, late (adult), and chronic form according to residual enzyme activity. In early-onset, progressive accumulation of the GM2 ganglioside, especially in the neuronal cells, leads to a secondary cascade of cell death and eventually death between 2-4 years of age (Fernandes Filho and Shapiro 2004). In contrast to the early-onset form, disease progression displays milder symptoms in the juvenile and adult forms (Leinekugel et al. 1992). In juvenile-onset, impaired motor activity, seizures, and intellectual disability were observed (Maegawa et al. 2006). The most common form is the adult onset, where quadriceps weakness and iliopsoas are observed (Leinekugel et al. 1992). In chronic form, the patient suffers from various clinical phenotypes: spinocerebellar impairment, dystonia, and spinal muscular atrophies (Masingue et al. 2020). Tay-Sachs disease still lacks an identified primary treatment. There are lots of treatment strategies have been tried up to now to cure Tay-Sachs disease,

such as stem cell therapy (Stepien et al. 2018)(Jacobs et al. 2005), substrate reduction/enzyme replacement therapies (Bembi et al. 2006)(Espejo-Mojica et al. 2020) and gene therapies (Martino et al. 2005)(Akli et al. 1996) (Leal et al. 2022). Multiple animal models have been used until now to develop therapeutic strategies to ameliorate Tay-Sachs disease.

### 1.2.2 Tay-Sachs Disease Mouse Model

Tay-Sachs mouse model (*Hexa-/-*) was generated by disruption of the *Hexa* in embryonic stem cells via homologous recombination; however, disruption of the *Hexa* did not exhibit severe clinical pathology in mouse model like Tay-Sachs disease (Yamanaka et al. 1994). Accordingly, the *Hexa-/-* mouse model is not appropriate for studying human early-onset Tay-Sachs disease, but this mouse model also displayed milder symptoms like late-onset Tay-Sachs disease. Moreover, it has been shown that the asialylated form of GM2, GA2, also accumulates in *Hexa-/-* mice in contrast to human patients. The other type of GM2 ganglioside mouse model (*Hexb-/-*) displays disease pathology like Sandhoff disease. The role of sialidases has been explained by showing that they prevent the pathology of Tay-Sachs disease by degrading accumulated GM2 gangliosides to GA2 gangliosides through a bypass mechanism (Yuziuk et al. 1998).

Sialidases or neuraminidases are the specific type of exoglycosidase family that catalyze the cleavage of the non-reducing sialic acids from the glycoconjugates (Monti et al. 2010). Mammals contain four different sialidases, which are Neu1 (lysosomal sialidase), Neu2 (cytoplasmic sialidase), Neu3 (plasma-membrane sialidase), and Neu4 (mitochondria/lysosome/ER sialidase) sialidases (Miyagi and Yamaguchi 2012). Except for Neu2 sialidase, all sialidase types cleave sialic acids from the gangliosides and have a role in glycoconjugate metabolism. To determine which kind of sialidase degrades GM2 gangliosides, *Hexa-/-* mice were bred with *Neu4-/-* mice to create the *Hexa-/-Neu4-/-* mouse, a double knockout model (Seyrantepe et al. 2010). Although *Hexa-/-Neu4-/-* exhibited neurological deficits, Neu4 sialidase is not the only sialidase involved in the metabolic bypass mechanism for GM2 ganglioside degradation. Accordingly, Neu4 sialidase was determined as a modifier gene in GM2 ganglioside catabolism. Next, the plasma membrane sialidase of the Neu3 deficient mouse was mated with the *Hexa-/-* mouse model to determine whether Neu3 sialidase plays the primary role in the metabolic

bypass mechanism of GM2 degradation. *Hexa-/-Neu3-/-* mouse model elicits severe phenotypes like the infantile form of Tay-Sachs disease (Seyrantepe et al. 2018). TLC analysis from brain samples displayed abnormal accumulation of the GM2 and slightly GA2 gangliosides against *Hexa-/-* mice. As a pathological feature, *Hexa-Neu3-/-* mice show lysosomal vacuolization, Purkinje cell deterioration, and neuronal cell death. At the last stage of life, tremors and hind limb spasticity were observed, like in the Tay-Sachs patient. Developmental abnormalities were also observed in *Hexa-/-Neu3-/-* mice because the body size of *Hexa-/-Neu3-/-* mice was lower, between 15% and 20% percent, than the control mice. Severe phenotypes, mainly CNS-related, like ataxia and tremors, have started to be observed (Seyrantepe et al. 2018). Furthermore, visceral organs also contain abnormal GM2 ganglioside accumulation, but the effects of accumulation in visceral organs can be elucidated by further investigations. Accumulation of GM2 ganglioside in the *Hexa-/-Neu3-/-* mouse model causes secondary effects in the CNS, like neuroinflammation. It has been demonstrated that the *Hexa-/-Neu3-/-* mouse model shows progressive chronic neuroinflammation due to microglia/astrocyte activation and macrophage infiltration triggering astrogliosis (Demir et al. 2020).

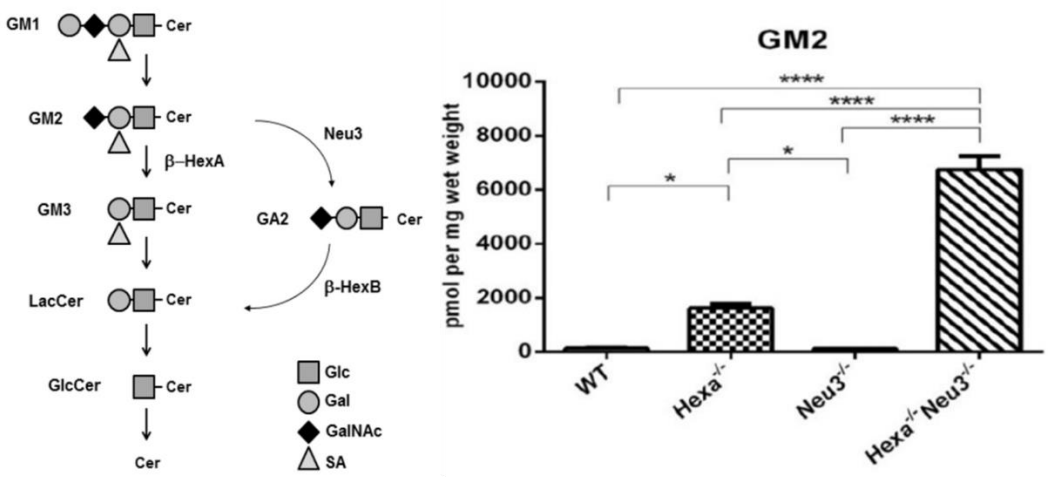


Figure 1.2 The GM2 ganglioside bypass mechanism for degradation in *Hexa-/-Neu3-/-* mice.

## 1.3 Ketogenic Diet

The ketogenic diet is a high fat/low carbohydrate dietary regimen at a ratio of 3-4:1 to trigger ketone body (KB) synthesis in the body. Diet was developed at the beginning of the 20$^{th}$ century to cure epileptic seizures depending upon the antiseizure effect

followed by multiple neurodegenerative disorders were studied in Alzheimer's disease, Pelizaeus-Merzbacher disease, Sandhoff disease, etc. (Pietrzak et al. 2022) (Stumpf et al. 2019) (Denny et al. 2010). Ketone body synthesis or ketogenesis mainly occurs in the liver and the astrocytes. Ketone bodies are classified into three types which are acetoacetate, β-hydroxybutyrate, and acetone (Longo et al. 2019). A ketogenic diet especially mimics fasting and prolonged exercises because they trigger ketone body production by β-oxidation of the fatty acids in the liver to generate a ketosis-like condition. Accordingly, glucose level reduction is inversely proportional to ketone body levels, and ketone bodies become the primary energy source in the brain under low-carbohydrate availabilities. Since the ketone body is the primary energy source due to low glucose, neurological problems of GLUT1 mutation and pyruvate dehydrogenase deficiencies were partially ameliorated with ketogenic diet intervention (Kass et al. 2016). Except for neurologic disorders, a ketogenic diet was utilized to treat a wide range of dysfunctions like obesity, cancer, and weight loss (Brouns 2018). Moreover, ketogenic diet intervention has some disadvantages, such as acidosis, hypercholesterolemia, and mineral deficiencies, but supplements could reverse (Bergqvist et al. 2005). The ketogenic diet is divided into four different types according to macronutrient distribution: classical ketogenic diet, medium-chain triglyceride diet (MCT), modified Atkins diet, and low glycemic index treatments (Barzegar et al. 2021). The classic ketogenic diet was found by Woodyatt in 1921, and the ratio of fat/carbohydrate+protein is 4:1. The majority of the fat composition in the traditional ketogenic diet consists of long-chain fatty acids (Wheless 2008). Due to low carbohydrate and high-fat levels, 80%-90% of energy requirement is supplied by fat. MCT diet is thought to be a more ketone-producing diet but causes gastrointestinal adverse effects. MCT diet is composed of mainly C8 (caprylic) and C9 (pelargonic) fatty acids (Y. M. Liu and Wang 2013). The other diet is the Atkins diet, which is considered less restrictive and more palatable. Although it has been suggested that it may be less effective than the traditional ketogenic diet, it is often well-accepted and is used as a therapeutic diet for epileptic children who find it difficult to follow the traditional KD (Kossoff 2023). Low glycemic index therapy is an alternative nutritional approach introduced in 2005 to ameliorate drug-resistant epilepsy (Pfeifer and Thiele 2005). In this diet, carbohydrate restriction is limited to low glycemic index carbohydrates with a glycemic index below 50 to keep stable blood glucose levels (Pfeifer, Lyczkowski, and Thiele 2008).

### 1.3.1 Ketone Body Metabolism

Ketone bodies, acetoacetate, β-hydroxybutyrate, and acetone, are predominantly converted from free fatty acids in the liver and are used as a primary energy source in CNS and muscle. Low glucose levels display low insulin and high glucagon levels in the blood serum, followed by glucose levels that are kept balanced by glycogenolysis and gluconeogenesis in the liver (Rui 2014). Reduction of the insulin level triggers free acid circulations and their β-oxidation to generate ketone bodies in the liver mitochondria. Since fatty acids cannot cross the blood-brain barrier during ketogenesis, the central nervous system cannot use fatty acids as an energy source. However, while glucose is normally the only energy source for the human brain, after prolonged fasting or a low-carbohydrate diet, the central nervous system requires an alternative energy source (Mitchell et al. 1995). The necessary alternative energy source is provided by the conversion of acetyl-CoA into ketone bodies during ketogenesis (Murakami and Tognini, 2022). The ketone bodies produced cannot be used directly by the liver, so they are transported to extrahepatic tissues, predominantly the brain and retina, where they can be metabolized and produce energy (McPherson and McEneny 2012). As a biochemical mechanism, various regulating enzymes and co-factors transform free fatty acids into acetyl-CoA, which enter the TCA cycle or are metabolized into ketone bodies. Specifically, two acetyl-CoA molecules are combined to generate acetoacetyl-CoA by acetoacetyl-CoA thiolase followed by additional acetyl-CoA is merged to acetoacetyl-CoA to generate intermediate product of beta-hydroxy-methylglutarylCoA (HMG-CoA) by HMG-CoA-synthase 2 (HMGCS2). The intermediate product is partitioned off to the first ketone body of acetoacetate and acetyl-CoA by HMG-CoA lyase. Acetoacetate follows two different pathways: In the first pathway, acetoacetate is converted to β-hydroxybutyrate by the enzyme β-hydroxybutyrate dehydrogenase with NADH oxidation, while in the second pathway, it can be converted to acetone by decarboxylation (Puchalska and Crawford 2017). Ketone bodies are passed into the extrahepatic tissues by monocarboxylate transporters (MCT) via concentration gradient and then are metabolized to produce energy in mitochondria by ketolysis. In CNS, ketone bodies can be passed through the blood-brain barrier (BBB) by MCT1 and MCT-2 into astrocytes and neurons, respectively. In ketolysis, ketone bodies are reconverted to the acetyl-CoA, which the Krebs cycle utilizes to produce GTP and ATP and additional NAD+ reduction.

The ketolysis involves three steps; the first step is the conversion of the β-hydroxybutyrate to the acetoacetate by beta-hydroxybutyrate dehydrogenase 1 (BDH1) enzyme, and then acetoacetate is degraded to the acetoacetyl-CoA by succinyl-CoA:3-ketoacid CoA transferase (SCOT) and followed by conversion of the acetoacetyl-CoA to the acetyl-CoA by 2-methylacetoacetyl-coenzyme A thiolase (MAT) (Fukao et al. 1997). Converted two molecules of acetyl-CoA enter the citric acid or Krebs cycle to produce energy.

### 1.3.2 Ketogenic Diet in LSDs

The ketogenic diet utilized various lysosomal storage disorders to reduce the adverse effects of the disease pathologies. Firstly, a ketogenic diet combined with miglustat was used in infantile GM1 and GM2 gangliosidosis patients, and this combined treatment mediated palliative care by decreasing gastrointestinal side effects of miglustat and prolonged survival in both GM1 and GM2 gangliosidosis patients (Jarnes Utz et al. 2017). The other example of the beneficial effects of the ketogenic diet in LSD is the improvement of the myoclonus and gait stability and mitigation of the seizure frequency in GM1 gangliosidosis patients. (Myers et al., 2018). The ketogenic diet has also been combined with miglustat in Sandhoff's disease, another lysosomal storage disease, to improve cardiac function and seizure control in these patients (Villamizar-Schiller et al. 2015). Moreover, the ketogenic diet displayed neuroprotection and beneficial effects for the seizure frequency in Neimann-Pick type C patients (Höller et al. 2021). In the Sandhoff mouse model, a ketogenic diet was used to enhance the therapeutic effect of miglustat by facilitating its passage across the blood-brain barrier (*Hexb-/-*) (Denny et al. 2010).

## 1.4 Propagermanium (Bis(2-carboxyethylgermanium) Sesquioxide)

Propagermanium (Poly-*trans*-[(2-carboxyethyl) germasesquioxane]) is a germanium-based compound that was synthesized first by Dr. Oikawa in 1967. Toxicity tests in animal models were examined while their safety was confirmed (Anger et al. 1991). Propagermanium (PG) is also classified as a C-C chemokine receptor 2 (MCP-1R) inhibitor, which has a role in monocyte/macrophage migration and macrophage-based

inflammation. PG inhibits CCR2 because its effects need glycosylphosphatidylinositol (GPI)-anchored proteins. PG shows specific activity only for CCR-2 and inhibits the function of this receptor without causing any damage to the receptor and its ligands (Yokochi et al. 2001). PG treats many inflammatory diseases, such as chronic hepatitis type B and cerebral ischemia/reperfusion injury, based on its anti-inflammatory properties. (Rumi et al. 1993) (He et al. 2019)

As a mouse model utilization, PG was used to improve hepatic steatosis and insulin resistance to prevent obesity after a high fat/high sugar diet in the db/db mouse model (Tamura et al. 2008).

## 1.5 Neuroinflammation

Neuroinflammation is the response of the brain cells against cellular infections, accumulation of the undegraded metabolites and cellular death mechanisms, and infiltration of the adaptive and innate immune system components into the brain (Ransohoff et al. 2015). The perception of DAMPs and PAMPs by microglia and astrocytes initiates inflammatory events in the CNS, leading to the mobilization of peripheral leukocytes into the CNS. Furthermore, elevation of the neuroinflammation level causes impairment of the brain metabolism by secretion of the cytokines, chemokines, and activation of the neuroglia cells (Yong et al. 2019). The secretion of mediators is provided by resident CNS neuroglia cells, particularly microglia, and astrocytes, where various consequences, such as immune, biological, and physiological responses, occur. The severity of neuroinflammation varies according to the context, duration, and progression of the primary stimulus or insult. Astrocytes are the subtype of the glial cells that play an essential role in regulating the innate and adaptive immune response to CNS injuries (Cordiglieri and Farina 2010). In addition, astrocytes are one of the main types of cells in the maintenance of blood-brain-barrier integrity. Activation of astrocytes causes secretion of pro-inflammatory cytokines/chemokines such as CCL2, CCL3, CCL5, and CXCL10, and their activation was detected by GFAP expression (Verkhratsky, Nedergaard, and Hertz 2015). Microglia are the primary resident immune cells in the CNS that have a dominant role in maintaining brain metabolism, as these cells show a marked sensitivity to mitigate any disturbances in the brain. Microglia is divided into two forms, which are ramified or inactive and reactive forms. Ramified microglia

release fewer immune molecules such as IL-1β, IL-6, and Tnf-α and do not phagocytize cells like activated or ameboid microglia (Thameem Dheen, Kaur, and Ling 2007). In addition to the negative aspects of neuroinflammation, there are also positive effects. For example, the neuroinflammation markers IL-4 and IL-1 also have an essential promoting role in learning and memory, and IL-4-mediated macrophage repolarization ameliorates axonal growth in traumatic brain injury (Derecki et al. 2010).

### 1.5.1 Neuroinflammation in LSDs

Lysosomal storage disorders (LSDs) are a rare genetic disorder group caused by enzymatic deficiencies that result from the accumulation of toxic undegraded metabolites in the lysosomes. The accumulation of these metabolites triggers cellular immune response, especially in the CNS, leading to disease progression. Accumulated substrates due to enzymatic defects include GM1, GM2, globotriaosylceramide (Gb3), sphingosine, cholesterol, etc. Abnormal accumulation of these molecules in lysosomal storage disorders such as Gaucher disease, GM1/GM2 gangliosidosis, etc., impair various cell types such as microglia, astrocytes, oligodendrocytes, monocytes, and macrophages. Disruption of these cells triggers neuroinflammatory responses and the secretion of pro-inflammatory cytokines/chemokines associated with cellular damage and devastating consequences, particularly in the CNS and PNS (Manoj Kumar Pandey 2023). These cells secrete specific molecules against substrate accumulation, including IL1-β, TNF-α (tumor necrosis factor-alpha), IL-6, and various C-C and C-X-C motif ligands (CCL2, CCL3, CXCL10) (Vitner 2020). The abundance of these molecules is also vital for regulating CNS and PNS homeostasis since they damage the blood-brain barrier (BBB) and blood-nerve barrier (BNB) integrity (J. Yang et al. 2022). The blood-brain barrier is a specialized semipermeable barrier that provides separation of the blood from the cerebrospinal fluid. The barrier protects and nourishes the brain by regulating the entry of nutrients or harmful substances (Blanchette and Daneman 2015). The blood-nerve barrier is another special barrier that divides peripheral nerve tissue from blood. Like the BBB, BNB controls the passage of nutrients and waste products inside the peripheral tissue. Damage to the BNB causes infiltration of the toxic substances and pro-inflammatory mediators, which can lead to nervous tissue dysfunctions (Ubogu 2020).

The diversity of substances accumulated in lysosomal storage disorders can lead to different immune responses by the nervous system during disease progression. In Gaucher disease, glucosylceramide (GC) and glycosphingosine (GS) accumulate in the macrophages and microglia due to acid β-glucosidase enzyme deficiency (GCase) (Manoj K Pandey et al. 2017). Accumulated substances induce especially neurological symptoms: ataxia, epilepsy, and seizure. Apart from neurological symptoms, GC and GS trigger elevation of the pro-inflammatory cytokines/chemokines such as Ifn-γ, IL6, and Tnf-α both in patient and mouse models (Manoj Kumar Pandey and Grabowski 2013; Manoj Kumar Pandey et al. 2012). In addition, the GBA mouse model displays increasing CCL2, CCL3, CCL5, and CXCL10 secretion in the brain (Manoj K Pandey et al. 2017). In GM1 gangliosidosis, the Glb1 gene encoding β-Galactosidase (β-Gal) is mutated and excessive amounts of GM1 accumulate in the CNS, as well as keratan sulfate and oligosaccharides. Accumulated GM1 and other molecules cause extreme neurological symptoms, especially in the central nervous system, and systemic deterioration throughout the body (Brunetti-Pierri and Scaglia 2008). The mouse model of GM1 gangliosidosis (*Glb-/-*) displays similar pathology to the patients due to GM1 accumulation, especially in macrophages and microglial cells, which trigger overproduction of pro-inflammatory mediators such as Tnf-α, IL-1β and IL-6 (Jeyakumar et al. 2003). GM2 gangliosidosis is divided into three different types, which are Tay-Sachs (B-variant), Sandhoff (0-variant), and GM2AP deficiency (AB-variant). Tay-Sachs disease, Sandhoff disease, and GM2-gangliosidosis AB-variant are caused by mutation of the *HEXA*, *HEXB*, and *GM2AP* genes, respectively. Mutation of these genes mainly results in excessive accumulation of the GM2 ganglioside. In addition to GM2 ganglioside, GA2 ganglioside also accumulates in Sandhoff disease patient and mouse models (Toro, Zainab, and Tifft 2021). Tay-Sachs and Sandhoff patients have CNS pathologies such as tremors, ataxia, and paralysis, while Sandhoff patients have not only CNS abnormalities but also visceral abnormalities such as hepatosplenomegaly and respiratory problems, etc. (Myerowitz et al. 2002). Enhanced GM2 and GA2 ganglioside accumulation in the brain and spinal cord induces the secretion of pro-inflammatory cytokines, microgliosis, and astrogliosis in the Sandhoff mouse model (*Hexb-/-).* The activation of astrocytes and microglial cells leads to neuronal cell death due to excessive inflammatory responses (Wada, Tifft, and Proia 2000). Unlike the Sandhoff mouse model (*Hexb-/-*), which has a short life span of ~4 months, showing a severe phenotype due to excessive GM2 and GA2 gangliosides accumulation, no severe phenotype was observed

in the Tay-Sachs mouse model (*Hexa-/-*) due to accumulation of the GM2 ganglioside only in limited regions. The explanation for this is that alternative ganglioside degradation pathways are not present in humans in the absence of the Hexa enzyme found in mice and that this bypass mechanism found by Seyrantepe et al. converts GM2 to GA2 with Neu3 sialidase in mice, thus bypassing the requirement for Hexa enzyme-dependent activity (Seyrantepe et al. 2018). The generation of *Hexa-/-Neu3-/-* mice, which mimic the neuropathological and clinical abnormalities of classic early-onset TSD patients, has been an ideal TSD mouse model that could provide a precious tool for treatment development (Leal et al. 2020). Progressive accumulation of the GM2 ganglioside results in premature death for the *Hexa-/-Neu3-/-* mice (Seyrantepe et al. 2018). Similar to *Hexb-/-* mice, the *Hexa-/-Neu3-/-* mouse model exhibits chronic neuroinflammation by secretion of pro-inflammatory cytokine/chemokines in the brain (Demir et al. 2020). Furthermore, Demir et al. showed that neuroinflammation in *Hexa-/-Neu3-/-* mice precedes neurodegeneration by activating microglia and astrocytes. Understanding the mechanisms of innate and adaptive immune-mediated neuroinflammation in GM2 gangliosidoses may provide new insights into the pathogenesis of such disorders and may identify potential targets for therapeutic intervention.

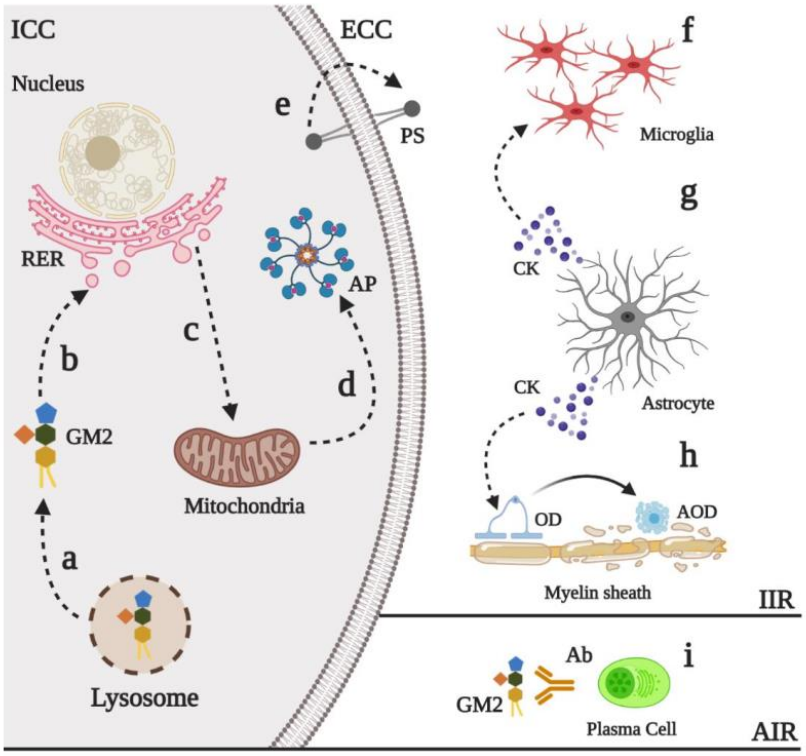


Figure 1.3 Adaptive (AIR) and innate (IIR) immune responses for GM2 accumulation in GM2 gangliosidosis physiopathology. (Source: (Leal et al. 2020))

### 1.5.2 Ketogenic Diet and Neuroinflammation

The ketogenic diet is a combination of the high fat, low carbohydrate/protein diet in which fat becomes the primary energy source instead of carbohydrates. While this diet was initially used only in the treatment of epilepsy, recent studies have shown that the ketogenic diet can also have a positive effect on neurodegenerative diseases. Furthermore, the ketogenic diet has been shown to have a protective and anti-inflammatory effect on neuroinflammation mechanisms (Koh, Dupuis, and Auvin 2020). As a neuroprotective effect, the ketogenic diet has an active role in various cellular pathways: energy supply, regulation of the amino acid metabolism, improvement of mitochondrial activity, reduction of oxidative stress, and neurotrophic factors. Firstly, ketone bodies triggered by the ketogenic diet exert neuroprotective effects by increasing mitochondrial respiration and activating ATP (adenosine triphosphate) production. Considering this, it has been shown that β-hydroxybutyrate, one of the ketone bodies, may provide more energy in the brain than glucose (Masino and Rho 2012). Moreover, consumption of the KD from murine triggers increased expression levels of the insulin-like growth factor 1 (IGF1) and specific glucose transporters expression levels (GLUT1 and GLUT3) (Cheng et al. 2003). Secondly, the transition from glucose to ketone bodies as a primary energy source affects amino acid metabolism by reducing the conversion of glutamate to aspartate and inducing decarboxylation of glutamate to form GABA (Yudkoff et al. 2001; Daikhin and Yudkoff 1998). Third, ketone bodies, βHB and AcAc, have an essential role in attenuating oxidative stress and ROS production by augmenting NADH oxidation and also protecting from mitochondrial membrane permeabilization (Masino and Rho 2012; Pinto et al. 2018). Lastly, KD intervention regulates neurotrophic factors. In a study, βHB has been found to increase BDNF expression against excitotoxicity and oxidative stress as a neuroprotective mechanism in the cerebral cortex (Marosi et al. 2016). Another study shows that KD intervention for seven days results in the elevation of the insulin-like growth factor (IGF1R) and glutamate receptor 1 (GLUT1) gene expressions to provide neuroprotection in rats (Cheng et al. 2003). One of the beneficial effects of KD is its anti-inflammatory effect, and this has been demonstrated by some molecular and biochemical mechanisms as follows. The KD treatment shows an anti-inflammatory effect by inhibiting nuclear factor kappa-B (NfκB) activation and NLRP3 inflammasome activation, irrespective of polyunsaturated fatty acids (Dupuis et al. 2015; Pinto et al.

2018). Another study is that while the MCAO mouse model was intervened with KD, βHB activates the HCA2 in macrophages. The activation of the HCA2 induces prostaglandin D2 (PDG2) secretion, which inhibits NfκB activation and pro-inflammatory cytokine secretion by activating the COX1 and HPGDS enzymes (Rahman et al. 2014). Furthermore, in a KD-fed glaucoma mouse model, HCA1, the target of BHB, along with increased expression of ARRB2, has been shown to inhibit NLRP3 inflammasome function, leading to decreased NLRP3 and IL-1β levels (Harun-Or-Rashid and Inman 2018). Apart from these, high concentrations of the βHB and long-term KD intervention trigger activation of the pro-inflammatory mediators of IL-1β, TNF-α, and IL-6 (Shi et al. 2014; Goldberg et al. 2020).

### 1.5.3 CCL2/CCR2 Axis in Neuroinflammation

The chemokine C-C motif 2 (CCL2) or monocyte chemotactic protein 1 (MCP-1) is a chemoattractant protein that signals through binding its specific receptor of chemokine receptor type 2 (CCR2) (Bose and Cho 2013). CCL2 plays a vital role in mediating the migration and infiltration of monocytes/macrophages and does so through its complex with the CCR2 receptor (Rollins 1996; Lu et al. 1998). Different cell types in the brain, such as astrocytes, microglia, and endothelial cells, produce CCL2 constitutively or in response to a range of agents or metabolic states, including growth factors, cytokines, and oxidative stress (Semple, Kossmann, and Morganti-Kossmann 2010). Similar to CCL2, CCR2 is secreted by astrocytes, microglia, and endothelial cells (Dorf et al. 2000; Boddeke et al. 1999; Banisadr et al. 2005).

The interaction of chemokine CCL2 and its receptor CCR2 (CCL2/CCR2 axis) has been associated with neuroinflammation-related pathology in various neurodegenerative and lysosomal storage disorders (Conductier et al. 2010; Vitner 2020). In Alzheimer's disease, CCL2 levels significantly increase in the patient's CSF, which was associated with the severity of the disease (Galimberti et al. 2006). In addition, overexpression of the CCL2 expression in the APP mouse model triggers microgliosis and amyloid β-plaque formation (Kiyota et al. 2009). In multiple sclerosis (MS), acute and chronic term-derived MS plaques from patients exhibited elevation levels of the CCL2, secreted from microglia and astrocytes (Conductier et al. 2010). The lack of the CCL2 gene in the EAE mouse model displays delayed and reduced disease symptoms (D. R. Huang et al. 2001).

However, the inactivity of CCL2 observed in the EAE mouse model of MS lacking the CCR2 gene is explained by the absence of encephalopathic pathology (D. Huang et al. 2005). Moreover, the elimination of the CCL2/CCR2 axis also mitigates neuroinflammation and subsequent neuronal cell death by STAT3 activation and inhibiting IL-1β secretion in the kainic-acid-induced status epilepticus mouse model (Tian et al. 2017). Gaucher disease, a type of lysosomal storage disorder, exhibits overproduction of the pro-inflammatory mediators, particularly CCL2, and is characterized by macrophage activation and immune activity in the brain (Manoj Kumar Pandey and Grabowski 2013). In addition, the Farber disease mouse model (Asah1P361R/P361R) is damaged by excessive ceramide and ganglioside accumulation in Schwann cells, which in turn damages the CNS and PNS, primarily by inducing CCL2 and various pro-inflammatory chemokines/cytokines (Dworski et al. 2017). Last, the GM2 gangliosidosis mouse model (*Hexa-/-Neu3-/-*) exhibits elevation of the *CCL2* gene expressions in cortex and cerebellum tissue compared to controls. Elevation of the *CCL2* gene expressions might cause activation of the astrocyte and microglia with the assist of the CCR2 receptor that, led to astrogliosis (Demir et al. 2020).

The intracellular signaling of the CCL2/CCR2 axis in the CNS takes place by binding the CCL2 ligand to the G-protein coupled receptor of the CCR2. The interaction of the CCL2 and CCR2 is mainly responsible for the monocyte recruitment first. CCL2/CCR2 axis is also related to the intracellular mechanisms of phosphatidylinositol-3 kinase, mitogen-activated protein kinase, and protein kinase C pathways (Stamatovic et al. 2005; Wain, Kirby, and Ali 2002).

## 1.6 Autophagy

Autophagy is a conserved cellular process that eliminates unnecessary/dysfunctional components and damaged organelles to stabilize intracellular homeostasis. In general, autophagy plays a protective role for the cell, but disruption of autophagy mechanisms or excessive autophagic flux often leads to cell death as it disrupts cell homeostasis. Autophagy also takes place in response to any signal or stress like starvation, infection, or growth factor depletion (Dikic and Elazar 2018).

There are three different types of autophagic mechanisms: macroautophagy, microautophagy, and chaperone-mediated autophagy, which are distinguished by the way in which the degraded substances are transported to the lysosome. Microautophagy is the

process by which small particles to be degraded are taken into the lysosome and degraded through indentations in the membrane (Levine and Kroemer 2019). Chaperone-mediated autophagy is the transport of cytosolic proteins with specific peptide sequences to lysosomes after binding to chaperone proteins and recognition by the carrier Hsp73 protein. This autophagy pathway does not require vesicular trafficking (Y. Liu, Tan, and Tan 2023). The last and the most common autophagic pathway is macroautophagy, in which large particles and organelles are taken in through autophagosomes, transported to the lysosome, and fused with lysosomes (Mehrpour et al. 2010).

The regulation of the autophagic flux is provided by highly conserved *ATG* genes, which are responsible for the autophagic process of nucleation, elongation, and fusion (Levine and Kroemer 2019). Initiation of autophagy occurs by the formation of the phagophore structure from the organelles such as mitochondria, Golgi apparatus, and endoplasmic reticulum (ER). The ULK1 complex regulates this structure, and mTORC1 and AMP-kinase control the ULK1 complex through inhibition and activation, respectively (Holczer et al. 2019). The nucleation step occurs with the class III phosphatidylinositol 3-kinase (PtdIns3K) complex, composed of PI3K, Vps34, Atg14, and the main protein Beclin-1. Beclin-1 regulates autophagic initiation and other cellular death mechanisms (Kang et al. 2011). After that, the expanded phagophore structure conjugates with the Ubl protein complexes, which are ATG12-ATG5 and MAP1LC3-I/LC3-II complexes. LC3-I is the most abundant form of LC3 protein, which is converted to LC3-II upon induction of the autophagy, but LC3-II plays a pivotal role in the formation of autophagosomes and the degradation of autophagic cargo through interaction with the p62/SQSTM1 protein in response to autophagic signaling (Young et al. 2006). In the last step, the autophagosome fuses with the lysosome to form an autolysosome with the assistance of the N-ethylmaleimide–sensitive factor attachment protein receptor (SNARE) complex, which binds to ATG14 for completion of the fusion process. In the end, LC3-II and cargo proteins are finally degraded by lysosomal enzymes (Nakamura and Yoshimori 2017; Mizushima and Yoshimori 2007).

### 1.6.1 Autophagy in LSDs

Lysosomes are intracellular organelles with an acidic intrinsic pH that perform crucial roles in cellular clearance. Lysosomal hydrolytic enzyme deficiencies in

lysosomal storage disorders (LSD) display progressive accumulation of the cellular macromolecules, which causes disease pathologies. In spite of different accumulations of the undegraded macromolecules in the cell, LSDs show pathologic similarities such as neurodegeneration (Settembre et al. 2008).

Lysosomes play a core role in the autophagic pathway by fusing with autophagosomes and digesting cargo products. The discovery of transcription factor EB (TFEB), a master gene that regulates the synthesis and activity of both lysosomes and autophagosomes, as well as an overarching regulatory gene network (CLEAR), provides new evidence for the cooperative and integrated roles of lysosomes and autophagosomes (Settembre et al. 2011; Sardiello and Ballabio 2009). By looking at lysosomal effects in the autophagic pathway, it seems that LSDs are at the core of autophagic studies. Autophagic vacuoles accumulate and expand in the Pompe disease mouse muscle due to autophagic impairment. Furthermore, electron microscopy revealed the accumulation of the lysosomal membrane marker LAMP1 and LC-3 positive cargoes in the muscle tissues of Pompe disease mice (S. Xu et al. 2010). In the MPS mouse model, LC-3, which indicates the presence of autophagosomes, accumulates in the brain without colocalizing with LAMP1. This may be due to disruption of autophagosome-lysosome fusion (Settembre et al. 2008). The autophagic impairment results in accumulation of the secondary autophagic substrates, such as damaged mitochondria and ubiquitinated proteins. Autophagic impairment was also shown in GM2 gangliosidosis mouse models: the Sandhoff mouse model (*Hexb-/-*) and the Tay-Sachs mouse model (*Hexa-/-Neu3-/-*). Sandhoff mouse model displays the accumulation of the LC3-II protein during autophagic flux, indicating an autophagic abnormality in the autophagosome-lysosome fusion step or the inability of the lysosomal degradation. Moreover, the autophagic cargo protein of the p62/SQSTM1 also accumulates in the *Hexb-/-* mouse brain due to dysfunctional autophagosomal-lysosomal turnover (Keilani et al. 2012). The Tay-Sachs mouse model (*Hexa-/-Neu3-/-*) shows that autophagic flux is disrupted by the accumulation of LC3-II and p62/SQSTM1 in addition to GM2 ganglioside through the failure of the termination step of autophagy (Sengul et al. 2023).

## 1.6.2 Ketogenic Diet and Autophagy

The ketogenic diet-induced ketone body production plays a regulatory role in autophagic flux to maintain cell survival and homeostasis. This autophagic triggering is

mediated through multiple signaling mechanisms. The main ketone body of the BHB elevates the NAD+, activating sirtuin 1/2 (SIRT1/2) through the SIRT1-AMPK pathway. AMPK stimulates autophagy by inhibition of mTORC1 and activation of ULK1 via phosphorylation because, under normal conditions, mTORC1 inhibits ULK1 activity, which is responsible for the autophagosome formation (Egan et al. 2011). SIRT2 triggers autophagy by activating FOXO1/3a, different from the SIRT1/AMPK pathway (McCarty, DiNicolantonio, and O'Keefe 2015). Moreover, ketone bodies also induce transcription factor EB (TFEB), Peroxisome proliferator-activated receptor alpha (PPARα), Peroxisome proliferator-activated receptor (PPAR) gamma coactivator 1 alpha (PGC1) expressions to mediate lysosome production. Elevation of these genes by ketone body induction disrupts lysosome-associated membrane protein 2 (LAMP2) and autophagic contents in NMDA-injected and MCAO-induced brain-injured rodent brains (Montiel et al. 2020; 2023). In addition to other mechanisms of autophagic induction via ketone bodies, there is also inhibition of mTORC1, although the α-subunit of eukaryotic initiation factor 2 (eIF2), protein kinase C (PKC) and c-Jun N-terminal Kinase (JNK) pathways are activated due to increased fatty acid levels (K. H. Kim and Lee 2014). BHB also interacts with and inhibits histone deacetylases (HDACs), which are included in histone modifications and triggering FOXO3a activities which induce autophagic flux by regulation of the ATG proteins, Beclin-1, etc. (Shimazu et al. 2013). Furthermore, since BHB inhibits mTOR, it also indirectly inhibits the Akt mechanism, which leads to the triggering of autophagy flux (Yamada et al. 2010). In summary, by regulating autophagy flux, ketone bodies may contribute to autophagy induction, allowing cell survival when energy availability is limited.

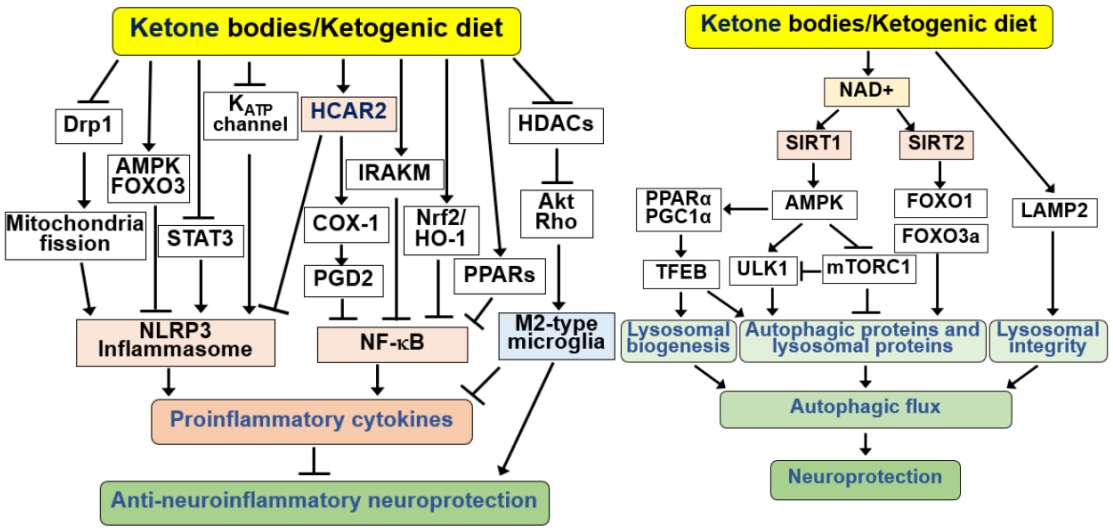

Figure 1.4 Regulation of neuroinflammation and autophagy signaling through ketogenic diet intervention (Source: (Jang et al. 2023)).

## 1.7 The Aim of the Thesis

The neuroinflammatory response and impairment of the autophagic flux have been shown in the *Hexa-/-Neu3-/-* mouse model. The purpose of the thesis is the elucidation of the efficacy of combined ketogenic diet and anti-inflammatory drug (propagermanium) therapy on the neuroinflammation and autophagy in the GM2 gangliosidosis mouse model. The purpose was also whether which strategy (short-term or long-term ketogenic diet therapy) is more effective when combined with the anti-inflammatory drug treatment to ameliorate neuroinflammation and autophagy due to abnormal GM2 accumulation.

# CHAPTER 2

# MATERIALS AND METHODS

## 2.1 Mouse Genotyping

The Turkish Council on Animal Care (TCAC), a recognized animal facility of the Izmir Institute of Technology, provided the breeding and maintenance of the mice. Animals were kept at a steady temperature and exposed to 12-hour cycles of light and darkness. Ad libitum access to food and drink was provided. According to the Turkish Institute of Animal Health's manual for handling and using laboratory animals, all animal experiments were conducted on animals.

The *Hexa-/-* mouse model was crossed with the *Neu3-/-* mouse model to create the GM2 gangliosidosis mouse model (*Hexa-/-Neu3-/-*). In F1, heterozygous (H*exa+/-Neu3+/-*) male and female mice were generated. Afterward, heterozygous female and male mice were bred to create the *Hexa-/-Neu3-/-* mouse model (Table 2.1).

Table 2.1 Generation of *Hexa-/-Neu3-/-* mouse model

| | **Breeding** | **Genotypes** |
|---|---|---|
| **F1 Generation** | *Hexa-/-* ♀ X *Neu3-/-* ♂<br>or<br>*Hexa-/-* ♂ X *Neu3-/-* ♀ | *Hexa+/-Neu3+/-* |
| **F2 Generation** | *Hexa+/-Neu3+/-* ♀<br>X<br>*Hexa+/-Neu3+/-* ♂ | ***Hexa+/+Neu3+/+* (1/16)**<br>***Hexa-/-Neu3+/+* (1/16)**<br>***Hexa-/-Neu3-/-* (1/16)** |

Genotypes of mice were determined after each breeding with genomic DNA isolation from the mice's tail and polymerase chain reactions (PCR). First, a small tail cut was put in the 1.5 mL Eppendorf tube. 250 mL lysis buffer (10% 1M Tris pH 7.6, 20% SDS, 2.5% 0.2M EDTA, and 4% 5M NaCl) and 6 µL Proteinase K (25 ug/ul stock solution) were added to this tube. Eppendorf tubes were put into the shaker incubator at

55℃ overnight. After overnight incubation, samples were centrifuged at 14000 rpm for 10 minutes. The supernatant was taken and transferred to the fresh tube to continue further DNA isolation steps. The same supernatant volume of 100% isopropanol was added to the samples, and the solution was gently mixed. Precipitated DNA was transferred to the new tube, which included 70% ethanol. Samples were then centrifuged at 15000 rpm for 1 min. After centrifugation, the supernatant was discarded, and the samples were air-dried at room temperature for 10 min. In the last step, samples were dissolved with the 100 µl distilled water and then incubated at 55℃ for 1 hour. DNA samples were stored at -20℃ for PCR reactions.

Two PCR reactions for Hexa and Neu3 genes were performed for each mouse to detect whether the mouse was a double knockout. To amplify the Hexa and Neu3 genes by PCR reaction, the designed primers illustrated in Table 2 were used. The PCR reaction for Hexa was prepared with 100 ng genomic DNA and 25 µl of the PCR reaction mix, including 1X PCR buffer (GeneDireX Inc, Taiwan), 50 pmol of each primer, 10 mM dNTPs, 1.5 mM $MgCl_2$, 2.5 units of Taq polymerase (GeneDireX Inc, Taiwan). Conditions of HexA PCR: 1 cycle 30 seconds at 95˚C, 30 cycles 30 seconds at 95˚C, 45 seconds at 60˚C, 45 seconds at 72˚C, and 1 cycle 5 minutes at 72˚C.

The PCR reaction of Neu3 was carried out with 100 ng genomic DNA and 50 µl PCR reaction mix containing the same components except primers like Hexa PCR. Neu3 PCR conditions: 1 cycle of 3 minutes at 94℃, 35 cycles of 50 seconds at 94℃, 45 seconds at 58℃, 2 minutes at 72℃, and 1 cycle of 10 minutes at 72℃.

Table 2.2 Primer sequences for mouse genotyping.

| **Genes** | **Primer Sequences** | **Product Size** |
|---|---|---|
| Hexa-F | 5’-GGCCAGATACAATCATACAG-3’ | *WT*: 420 bp |
| PGK-R | 5’-CACCAAAGAAGGGAGCCGGT-3’ | KO: 210 bp |
| Hexa-R | 5’-CTGTCCACATACTCTCCCCACAT-3’ | |
| Neu3-F | 5’-AAGCAGAGAACATTCTTGAGAGAGCACAGC-3’ | *WT*: 1100 bp |
| Neu3-552R | 5’TCGTGCTTTACGGTATGCCCGCTCCCGATT-3’ | KO: 600 bp |
| Neu3-553R | 5’GTGAGTTCAAGAGCCATGTTGCTGATGGTG-3’ | |

## 2.2 Ketogenic Diet Intervention

*WT*, *Hexa-/-* and *Hexa-/-Neu3-/-* mice were divided into two main groups according to the time range of diet interventions: long-term ketogenic diet (LTKD) and short-term ketogenic diet (STKD). These two main groups were subdivided into four groups, illustrated in Table 2.3 and Table 2.4. (Standard Diet (SD), Ketogenic Diet (KD), Propagermanium (Propa or PG), and combined Ketogenic diet and Propagermanium (KD+PG). Mice were divided into distinct groups to evaluate diet consumption and body weight effectively. STKD group of mice was fed a standard diet (C1000, (Altromin, Germany) until the ketogenic diet intervention. The control diet is composed of 13% fat, 20% protein, and 67% carbohydrate. The control diet was restricted due to the weight loss requirement of approximately 15%-18% for 10 days before the ketogenic diet intervention. All the mice were starved in the last 16 hours before starting a ketogenic diet. The short-term ketogenic diet group was intervened by ketogenic diet ad-libitum for 10 days. The ketogenic diet is composed of 84% fat, 11% protein, and 5% carbohydrate.

LTKD group of mice was fed a standard diet only 10 days after weaning to adapt to the ketogenic diet. When calorie reduction was ended after 10 days, the ketogenic diet intervention was maintained ad-libitum until the sacrification of the mice.

Table 2.3 STKD treatment strategies for each genotype.

| **Treatment Strategies** | ***WT*** | ***Hexa-/-*** | ***Hexa-/-Neu3-/-*** |
|---|---|---|---|
| Standard Diet | + | + | + |
| Ketogenic Diet | + | + | + |
| Propagermanium | - | + | + |
| Ketogenic Diet + Propagermanium | - | + | + |

Table 2.4 LTKD treatment strategies for each genotype.

| **Treatment Strategies** | ***WT*** | ***Hexa-/-*** | ***Hexa-/-Neu3-/-*** |
|---|---|---|---|
| Standard Diet | + | + | + |
| Ketogenic Diet | + | + | + |
| Propagermanium | - | + | + |
| Ketogenic Diet + Propagermanium | - | + | + |

## 2.3 Drug Administration

When the mice were 119-day-old, propagermanium (PG) was mixed with drinking water (8 mg/kg/day) and administered for 21 days until sacrification. Furthermore, the combination of the ketogenic diet and propagermanium started ten days before sacrification for the STKD group, while this procedure lasted 21 days for the LTKD group until sacrification.

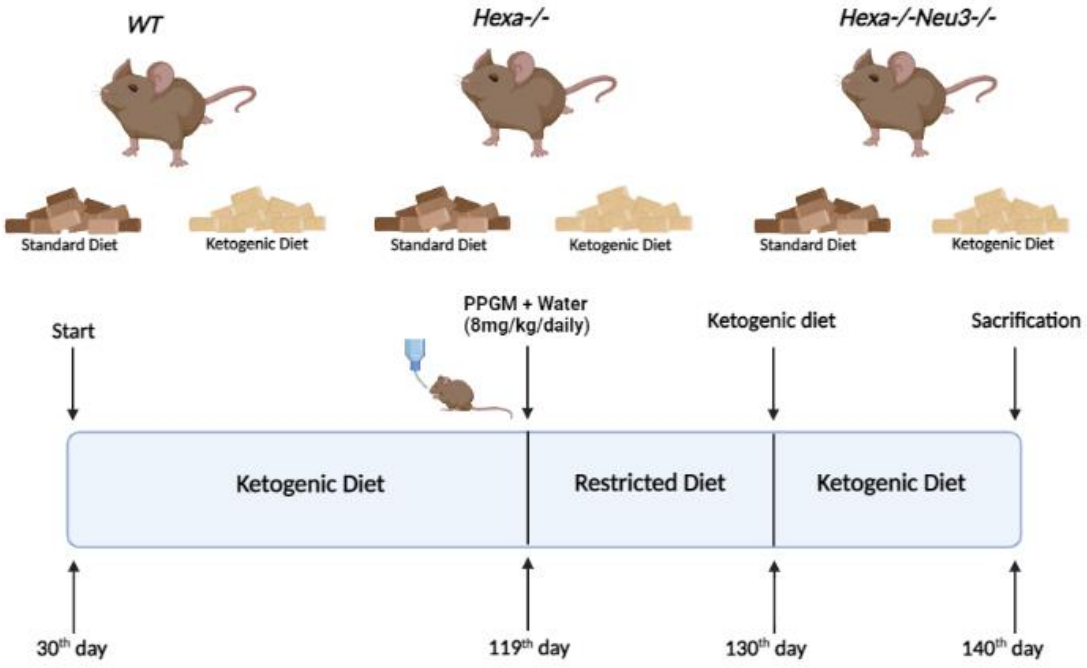


Figure 2.1 Illustration of the short-term ketogenic diet and propagermanium treatment strategies for *WT*, *Hexa-/-* and *Hexa-/-Neu3-/-* mouse model.

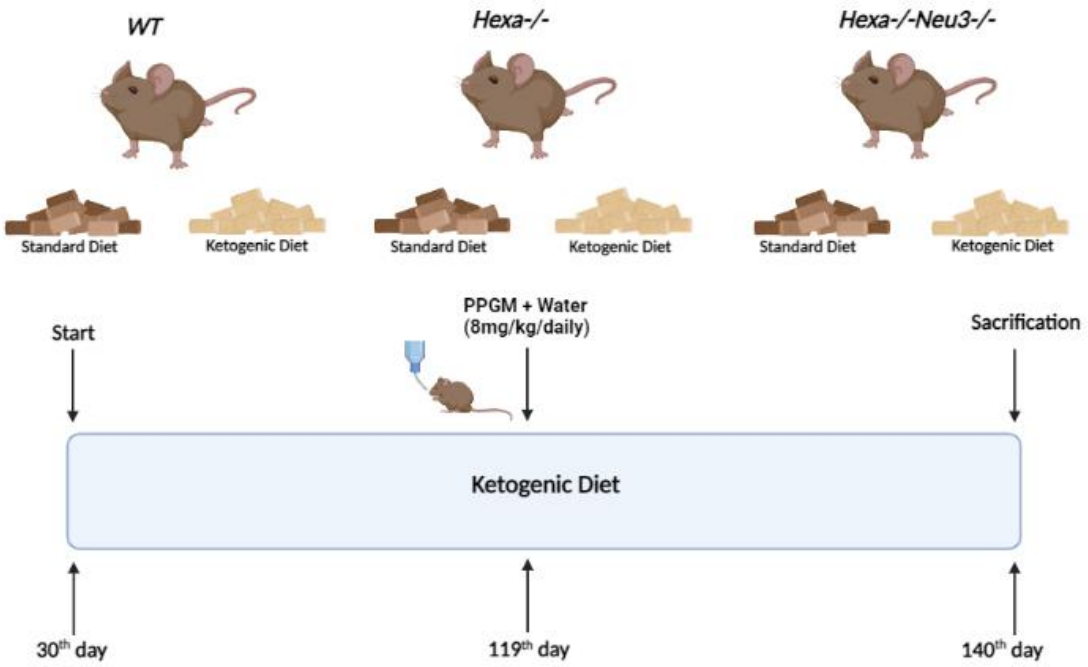


Figure 2.2 Illustration of the long-term ketogenic diet and propagermanium treatment strategies for *WT*, *Hexa-/-* and *Hexa-/-Neu3-/-* mouse model.

## 2.4 Body Weight Measurement

Body weights of each genotype *WT*, *Hexa-/-* and *Hexa-/-Neu3-/-* mice were measured every three days, which started after one month of age for each mouse until sacrification. Ketogenic diet consumption was also recorded simultaneously as body weight measurement.

## 2.5 Ketone Body Measurement

Ketone body level was measured as mmol/L before and after each treatment to determine whether the ketogenic diet and propagermanium affect ketone body metabolism. A small tail piece was cut to measure the ketone body, and blood was put on the ketone test strips (Abbott Diabetes Care, Inc., cat no. #7074565). The ketone strip was placed in the Precision Xtra meter device (Abbott Diabetes Care, Inc., cat no. #9881465).

## 2.6 Brain Tissue Handling

Brain tissues were collected from 140-day-old *WT*, *Hexa-/-* and *Hexa-/-Neu3-/-* after each treatment strategy. Either collected fixed or dissected brain tissues were stored at -80℃ until usage.

### 2.6.1 Brain Tissue Dissection

Aged-matched short-term and long-term ketogenic diet/propagermanium treated or untreated 140-day-old *WT*, *Hexa-/-* and *Hexa-/-Neu3-/-* mice were sacrificed via cervical dislocation. After that, brain tissues were dissected by a dissector blade as two halves of cortex and cerebellum, which were focused on the experiments of the thesis. All brain tissue was frozen with dry ice and stored at -80℃.

### 2.6.2 Brain Fixation

The brain was fixed by transcardiac perfusion for immunofluorescence and histological staining. First, mice were anesthetized with ketamine and xylazine (200/10 mg/kg) by intraperitoneal injection. Each mouse was first perfused with a 0.9% NaCl solution and then fixed with 4% paraformaldehyde (PFA). Three animals were fixed from each genotype for each treatment strategy. Anesthetized animals were immobilized by tape on the stage while they were laid down. Mouse skin was griped, and an incision revealed a xiphoid. The xiphoid was griped, with two side lateral incisions under the ribcage to expose visceral organs. The needle was inserted from the heart's left ventricle and parallel to the heart. Before the perfusion was started, an incision was made from the right atrium. 15 mL of 0.9% NaCl solution was passed, and the liver turned pale. The solution was switched from 0.9% NaCl to 4% PFA in 1xPBS for fixation. Mice became very stiff due to perfusion with approximately 20 mL of 4% PFA. The mice were decapitated, and their brains were dissected by micro spatula. Dissected brains were put into the 4% PFA overnight at 4℃. After overnight incubation in 4% PFA, a sucrose gradient was performed to discard excessive water inside the brain. First, brains were put into the 10% sucrose in 1xPBS (pH=7.4) for 2 hours at 4℃, and then brains were transferred to the 20% sucrose solution for 2 hours. Finally, brains were incubated

overnight in the 30% sucrose solution at 4°C. On the last day, brains were embedded inside the embedding molds containing OCT (Optimal Cutting Temperature). Embedding molds were placed into the dry ice to mediate the slow freezing of the embedded mouse brain inside the OCT. Fixed brains were stored at -80°C until cryosectioning.

### 2.6.3 Cryosectioning

Fixed brain tissues were first placed into the cryostat (CM1850-UV, Leica, Wetzlar, Germany) to reach optimal cutting temperature (-22/-23 °C). The mouse brain was cut 10 µm of coronal sections, collected on the poly-lysine coated HistoBond (Marienfeld, Germany) slides. The slides were stored at -80°C until immunofluorescence and histological staining.

## 2.7 Thin Layer Chromatography (TLC)

### 2.7.1 Ganglioside Isolation

Thin layer chromatography illustrated the acidic and neutral gangliosides from each treatment group of 140-day-old *WT*, *Hexa-/-* and *Hexa-/-Neu3-/-* mice cortex and cerebellum. Brain samples (Short-Term group: 10 samples cortex, 10 samples cerebellum; Long-Term group: 10 samples cortex, 10 samples cerebellum) stored at -80°C were measured as 50 mg for ganglioside isolation. Brain samples were put into the borosilicate tube, and 2 mL $dH_2O$ was added. The samples were homogenized by Ultra Turax homogenizer (IKA T10, Sigma, Darmstadt, Germany) at 6000 rpm for 45 seconds. Borosilicate tubes were put into the ice-cold water, and a sonicator (Bandelin, Berlin, Germany) performed sonication for four cycles of 1.5 minutes to mediate cell lysis. After that, borosilicate tubes were put into the heated water with a Reacti-Therm Heating module (Thermo, Massachusetts, USA) at 37°C. Heated water and $N_2$ flow accelerated the evaporation of the water. Extraction of the ganglioside process began after this step. Dried pellets were dissolved in 3 mL 100% acetone by vortex and incubated for 2 minutes at RT. After incubation, samples were centrifuged at 2000 rpm for 5 minutes, and supernatants were removed. This process is repeated two times. Next, pellets were extracted twice by adding 1.5 mL chloroform/methanol/$dH_2O$ (10/10/1) solution. After

each addition, samples were centrifuged at 2000 rpm for 5 minutes, and then supernatants were collected by Pasteur pipettes in the fresh neutral tubes. Methanol/chloroform/water (60/30/8) solution was added twice to the samples and centrifuged at 200 rpm for 5 minutes. Supernatants were put over the same neutral tubes. A total mixture of acidic and neutral gangliosides was obtained after these steps. DEAE Sephadex A-25 ion exchange columns were prepared to get neutral gangliosides from the collected ganglioside mixture.

The ion exchange columns were prepared by incubating 2 gr Sephadex A-25 resin with 20 ml of chloroform/methanol/0.8M sodium acetate (30:60:8) solution for 5 minutes. The mixture was centrifuged at 2000 rpm for 2 minutes, and the supernatant was removed. After repetition of this step, the resin was incubated overnight with the same solution. The next day, the solution was removed, and the resin was washed with 20 ml of chloroform/methanol/water (60/30/8) three times. After this step, the resin was ready to use for the ion exchange procedure. The column was prepared with glass Pasteur pipettes, glass woolen, and resin. First, the glass woolen was placed into the Pasteur pipettes, and resin was added 2 cm over the glass woolen to prepare the separation column. Each column was washed with 1 mL of chloroform/methanol/water (10:10:1) solution and 1 mL of chloroform/methanol/water (30:60:8) solution, respectively. New neutral tubes were loaded under the columns, and then collected ganglioside mixtures were added into the column. Next, neutral gangliosides were obtained when 4 mL of 100% methanol was added to each column. Later, new neutral tubes were placed under the column, and 4 mL of 500 mM potassium acetate in methanol was added into each column to elute acidic glycosphingolipids. Acidic glycosphingolipids were eluted to acidic gangliosides using the SupelClean$^{TM}$ LC-18 SPE column (Sigma-Aldrich, USA). SPE columns were placed on the ChromaBond Vacuum manifold, and the vacuum was arranged to 3-4 Hg. Firstly, columns were washed with 2 mL methanol and then 2 mL of 500 mM potassium acetate in methanol. After the washing steps, the acidic glycosphingolipid mixtures were added to the columns. Next, 10 mL of water was added to each column and flowed through. New neutral tubes were placed into the vacuum manifold, and then 4 mL of methanol and 4 mL of chloroform/methanol (1/1) were added to each column, respectively. After the addition of these solutions, the acidic gangliosides flowed through the columns were the acidic gangliosides. Neutral and acidic gangliosides collected at the end of neutral tubes were placed in a Reacti-Therm Heating module (Thermo, Massachusetts, USA), which heats the water to 37 °C. These tubes evaporated with $N_2$ and heated water.

### 2.7.2 Chromatographic Analysis

Neutral and acidic gangliosides were loaded onto the 20x20 cm silica gel plates (Merck, USA) to visualize ganglioside patterns. In the first step, TLC running solution was prepared into the tank, which included half a volume of methanol/chloroform/0.2% $CaCl_2$ (35:60:8). Tank was incubated with running solution for at least 2 hours 15 minutes. Before loading neutral or acidic gangliosides onto the silica plate, the silica plate was heated at 100℃ for 30 minutes. Dried samples for neutral or acidic gangliosides were loaded onto the silica plates by the Linomat 5 device (Camag, Muttenz, Switzerland). Dried neutral or acidic ganglioside samples were dissolved with 100 ul of chloroform/methanol/water (10:10:1) solution. Then, 20 ul neutral and 45 ul acidic ganglioside samples were taken with a 100 ul Hamilton syringe and loaded automatically onto the 20x20 silica plates, respectively. After loading the samples, plates were run 10 cm into the TLC tank.

### 2.7.3 Visualization of the Silica Plates

Visualization of the silica plates was performed by orcinol staining. 0.6 gr of orcinol (Sigma-Aldrich, USA) was dissolved with 15 mL 25% sulfuric acid solution into the 50 mL glass TLC sprayer (Sigma-Aldrich, USA). The spray solution is incubated at room temperature to cool because a hot solution could cause a black spot after spraying. After incubation, orcinol solution was sprayed to the silica plates, and then plates were placed onto the TLC heater (CAMAG, Switzerland) at 120-125 ℃ until ganglioside bands were observed. In the end, plates were scanned by HP Scanner, and ganglioside band intensities were measured by NIH ImageJ software (Fiji).

## 2.8 qRT-PCR Analysis

Ganglioside metabolism, neuroinflammation and autophagy-related genes were performed relative mRNA expression of 140-day-old mice brain cortex and cerebellum. RNA primer sequences are shown in Table 2.5. Ganglioside metabolism was analyzed by *B4Galnt1*, *B3Galnt4*, *GM3S*, *GD3S* and *HexB* gene expressions. For neuroinflammation,

*CCL2*, *CCL3*, *CCL5*, *CXCL10*, and *GFAP* expressions were analyzed while for autophagy, *Beclin-1*, *Atg7*, *Atg9*, *p62/SQSTM1* and *Lamp-2* gene expressions were analyzed. Gapdh was used as a housekeeping gene to normalize gene expressions.

### 2.8.1 RNA Isolation

The mouse brain cortex and cerebellum were weighed at 50 mg and put into the 2 mL Eppendorf tubes. 500 µL Genezol (Geneaid, Taiwan) and one magnetic bead were added to each Eppendorf tube. Magnetic beads included samples were homogenized by homogenizer (Retsch MM100) for 30 seconds at $1^{-25}$ frequency. This step could be performed twice if the tissue is not totally homogenized. After homogenization, samples were incubated at RT for 5 minutes and transferred to fresh 1.5 mL Eppendorf tubes. 100 µL chloroform for 500 µl Genezol was added to each sample. The samples were gently inverted after chloroform addition for 15 seconds. Next, the samples were centrifuged at 15.000g for 15 minutes at 4°C to separate the RNA phase from the DNA and proteins. Supernatants were transferred to the new 1.5 mL Eppendorf tubes to precipitate the RNA by 1 volume addition of 100% isopropanol. After that, samples were incubated for 10 minutes at RT before performing centrifugation of samples at 15.000g for 10 minutes at 4°C. Supernatants were removed, and 1 mL of 70% ethanol was added to each sample for washing. Centrifugation was performed the last time for each sample at 7.500g for 5 min at 4°C. Samples were incubated at RT for 5 min to dry after removal of supernatants. After 5 minutes, 30-50 µL RNA-free water was added to dissolve the RNA pellet, which was incubated in a water bath at 55°C for 15 minutes.

### 2.8.2 cDNA Synthesis

cDNA isolation was performed after RNA isolation from the cortex and cerebellum. According to the manufacturer's instructions, RNAs from the cortex and cerebellum were converted to 50 ng/µL of cDNA by a cDNA conversion kit (BioRad, USA). RNA concentrations of each sample were measured by nanodrop before preparation of the reaction mixture, which includes 1x RT buffer, 4 mM dNTP mix, OligodT Primers, and 50 Units Reverse Transcriptase enzyme except calculated volume of water and RNA mixture depending upon RNA concentrations. PCR conditions for 20

μL mixture: 1 cycle of 15 minutes at 42°C, 1 cycle of 5 minutes at 85°C, and 1 cycle of 15 minutes at 65°C. To demonstrate whether cDNA was converted from an RNA mixture, Gapdh PCR was performed. Gapdh PCR comprised 1x reaction buffer, 0.8 mM Gapdh primers, 10 mM dNTPs, and 1.75 units Taq polymerase (GeneDirex, Taiwan) for 50 ng of cDNA. The reaction occurred by these conditions: 1 cycle of 2 minutes at 95˚C, 30 cycles of 20 seconds at 95˚C, 15 seconds at 65˚C, 22 seconds at 72˚C, and 1 cycle of 3 minutes at 72˚C. PCR bands were illustrated by agarose gel electrophoresis (1% agarose gel) at 100 V for 30 minutes.

### 2.8.3 qRT-PCR Reaction

Relative mRNA expression of neuroinflammation and autophagy-related primer, which were shown in Table x., were carried out by Roche LightCycler 480 SYBR Green I Master Mix using Roche LightCycler® 96 System. The real-time PCR reaction comprised 0.4 μM forward and reverse primers, SYBR Green I Master Mix, and 50 ng cDNA. These conditions performed the reaction: 1 cycle of 10 minutes at 95℃, 45 cycles of 20 seconds at 95℃, 15 seconds at 60℃, and 22 seconds at 72℃. Samples were loaded three times, and three results were averaged to be accurate. In addition, each gene expression result was normalized to the Gapdh expression. Statistical analysis was completed by using one-way ANOVA on GraphPad Prism.

Table 2.5 Primer sequences for the relative gene expression analysis of neuroinflammation and autophagy-related markers

| | **Gene** | **Primer Sequences** | **Size** |
|---|---|---|---|
| **Ganglioside Metabolism Markers** | *B4Galnt1* | **F:**5’ **-**GGGCGGTTGACCTCACTAAA**-** 3’<br>**R:**5’ -GGAGAACCGGACTGTGTCTG- 3’ | **431 bp** |
| | *B3Galnt4* | **F:**5’ -GGCAGTGCCCCTTCTGTATT- 3’<br>**R:**5’ -GTGCAGTCCTCTCCCCATTC- 3’ | **407 bp** |
| | *GM3S* | **F:**5’ -GCTGCCCGAACATGACTTTC- 3’<br>**R:**5’ -TGAAGTGCTTTGGCTGGAGT- 3’ | **389 bp** |
| | *GD3S* | **F:**5’ -AGGAGATTGTGCAAGGGGTG- 3’<br>**R:**5’ -TGGCGAATTATGCTGGGGTT- 3’ | **418 bp** |
| | *HexB* | **F:** 5’ -AGTGCGAGTCCTTCCCTAGT- 3’ | **412 bp** |

| | | | |
|---|---|---|---|
| | | **R:**5’ -ATCCGGACATCGTTTGGTGT- 3’ | |
| **Neuroinflammation Markers** | *CCL2* | **F**:5’-ATGCAGTTAATGCCCCACTC-3’<br>**R**:5’-TTCCTTATTGGGGTCAGCAC-3’ | **167 bp** |
| | *CCL3* | **F**:5’-TCTGTACCATGACACTCTGC-3’<br>**R**:5’-AATTGGCGTGGAACTTTCCG-3’ | **103 bp** |
| | *CCL5* | **F**:5’-AGTGCTCCAATCTTGCAGTC-3’<br>**R**:5’-AGCTCATCTCCAAATAGTTG-3’ | **108 bp** |
| | *CXCL10* | **F**:5’-ACCATGAACCCAAGTGCTGCCGT-3’<br>**R**:5’-AGGAGCCCTTTTAGACCTTTTTTG-3’ | **297 bp** |
| | *GFAP* | **F**:5’-AGTAACATGCAAGAGACAGAG-3’<br>**R**:5’-TAGTCGTTAGCTTCGTGCTTG-3’ | **113 bp** |
| **Autophagy Markers** | *Beclin-1* | **F**:5’-GAGGAGCAGTGGACAAAAGC-3’<br>**R**:5’-CAAACATCCCCTAAGGAGCA-3’ | **112 bp** |
| | *Atg7* | **F**:5’-CCTGTGAGCTTGGATCAAAGGC-3’<br>**R**:5’-GAGCAAGGAGACCAGAACAGTG-3’ | **147 bp** |
| | *Atg9* | **F**: 5’-GTTAGCTGTGGAACACGTCCTC-3’<br>**R**: 5’-GCAAGAATCACTCGGAGCAGCT-3’ | **126 bp** |
| | *p62/SQSTM1* | **F**:5’- TGTGGAACATGGAGGGAAGAG -3’<br>**R**:5’- TGTGCCTGTGCTGGAACTTTC -3’ | **67 bp** |
| | *Lamp-2* | **F**:5’- TAACATCAACCCTGCCACAA-3’<br>**R**:5’- AAGCTGAGCCATTAGCCAAA-3’ | **176 bp** |
| | *Gapdh* | **F**:5’-CCCCTTCATTGACCTCAACTAC-3’<br>**R**:5’- ATGCATTGCTGACAATCTTGAG-3’ | **347 bp** |

## 2.9 Western Blotting

The cortex and cerebellum tissues from each treatment group of 140-day-old *WT*, *Hexa-/-* and *Hexa-/-Neu3-/-* mice. Isolated proteins were illustrated with NfκB and IkB antibodies for neuroinflammation and p62/SQSTM1 and LC3 antibodies for autophagic flux.

### 2.9.1 Protein Isolation

The cortex and cerebellum tissues were homogenized with a mini homogenizer after the addition of 500 µL of tissue lysis buffer, which was composed of 1% Triton X-100, 10% Glycerol, 50mM Tris-Base, 50mM HEPES, 150mM NaCl, 1% PMSF, and 1% protease inhibitor. Protein samples were put on ice for 1 hour when homogenization was completed. Next, each sample was centrifuged at 15.000g for 15 minutes at 4°C. The supernatant (isolated total protein) was transferred to the fresh Eppendorf tubes and stored at -20°C.

### 2.9.2 Bradford Assay

Isolated proteins were diluted at a 1/10 ratio (2 µL protein + 18 µL $dH_2O$) to carry out the Bradford assay at 595 nm. A BSA standard curve was drawn with the different concentrations (100,80,40,20,10 µg/mL) of BSA solutions to prepare equal protein stocks for each sample. Diluted samples and each BSA solution were loaded twice into the 96-well plates. After that, 200 µL of Bradford solutions were added to each well, and 96-well plates were incubated in the dark for 5 minutes. After incubation in the dark, protein absorbance values were measured at 595 nm by iMark™ Microplate Absorbance Reader (BioRad, USA). A standard curve was plotted by different concentrations of BSA solution absorbances. Equation from the standard curve was used to prepare the same quantity of the protein stock volume (20 µg) from each sample. Later, prepared protein samples were mixed with the 4:1 ratio of loading dye solution (40% Glycerol, 240mM Tris-HCl pH: 6.8, 8% SDS, 0.04% Bromophenol Blue, and 5% β-mercaptoethanol). Protein mixtures were boiled at 95°C for 10 minutes and then stored at 4°C.

### 2.9.3 SDS-PAGE

SDS-PAGE was performed by preparation of two different gels, which were resolving and stacking gels. Gel concentrations and components are illustrated in Table 2.6. First, resolving or lower gel was prepared and poured between western blot glass plates held stable with the clamp. After polymerization of the resolving gel, stacking gel or upper gel was prepared and poured. Once the stacking gel was poured onto the

resolving gel, the comb was placed into the stacking gel solution. The prepared gel was put into the running tank filled with running buffer (0.25M Tris-Base, 1.92M Glycine, 1%SDS) while the stacking gel was solidified. The comb was carefully removed from the stacking gel, and protein samples were loaded each well. Proteins into each well were separated at 80V for 2 hours through SDS-PAGE, which were then transferred to the nitrocellulose membrane (BioRad, USA) by transfer sandwich. The transfer sandwich was placed into the transfer tank filled with transfer buffer (48 mM Tris-Base, 39 mM Glycine, 20% Methanol, pH: 9.2). Protein transfer to the membrane was performed at 250 mA for 1 hour and 15 minutes. After the transfer step, the blot was blocked by 5% milk in 1xPBS-T (0.005% Tween-20) at RT for 1 hour. The blot was rinsed three times with 1xPBS-T for 5 minutes, and primary antibodies, which were diluted in red solution (5% BSA, 0.02% Na Azide, Phenol Red, in PBS-T pH: 7.5), incubated with blot overnight at 4°C. For neuroinflammation analysis, anti-Nf-κB (1:1000, Cell Signaling, 8242) and anti-IκB-α (1:1000, Cell Signaling, 9242) primary antibodies were used while for autophagy, anti-p62/SQSTM1 (1:1000, Cell Signaling, 16177) and anti-LC-3 (1:1000, Cell Signaling, 2775S), primary antibodies were used. The blot was rinsed three times after overnight incubation, and it was incubated with HRP-conjugated secondary antibody (Jackson ImmunoResearch Lab, UK) at RT for 1 hour. The blot was rinsed again three times with 1xPBS-T before visualization of the protein bands using LuminataTM Forte Western HRP Substrate (Millipore) via western blot imaging system (Fusion SL, Vilber). Protein band concentrations for each antibody were measured using ImageJ (Fiji), and protein levels were normalized to β-actin level. One-way ANOVA illustrated their statistical analyses on GraphPad Prism.

Table 2.6 Requirements of components for preparation of the resolving (10%) and stacking (5%) gel

| **10% Resolving Gel** | **5% Stacking Gel** |
|---|---|
| 4 mL $dH_2O$ | 2.7 mL $dH_2O$ |
| 3.3 mL 30% Acrylamide | 0.67 mL 30% Acrylamide |
| 2.5 mL Lower Buffer<br>(1.5M Tris-HCl pH:8.8) | 0.5 mL Upper Buffer<br>(1M Tris-HCl pH:6.8) |
| 0.1 mL 10% SDS | 0.04 mL 10% SDS |
| 0.1 mL 10% APS | 0.04 mL 10% APS |
| 0.01 mL TEMED | 0.004 mL TEMED |

## 2.10 Immunofluorescence Staining

The poly-lysine coated slides from each treatment group were selected for immunofluorescence stainings which are anti-NeuN (Cell Signaling, USA), anti-CNPase (Cell Signaling, USA), anti-GFAP (Cell Signaling, USA), anti-MOMA-2 (Abcam, UK) for neuroinflammation and anti-p62/SQSTM1 and anti-LC3 colocalized with anti-LAMP1 for autophagy. Firstly, chosen fixed slides were incubated on ice for 15 minutes and then put into the humidified chamber to incubate at 55℃ for 15 minutes. For NeuN, GFAP, and MOMA-2 stainings, slides were put into the 1xPBS twice for 5 minutes. Next, slides were incubated in the ice-cold 100% acetone for 15 minutes to permeabilize the cellular membrane. In CNPase staining, slides were incubated in the ice-cold 100% methanol for 15 minutes for permeabilization. Slides were rewashed with 1xPBS twice for 5 minutes to remove acetone from the sections. After that, each section on the slides was enclosed with a blocker PAP pen (Sigma-Aldrich, USA) and blocking solution (0.3M Glycine, 4% BSA in mg, and 10% normal goat serum and 0.3% Triton X-100 dissolved in 1xPBS) were put on each section which was incubated in a humidified chamber at RT for 1 hour. Primary antibodies were diluted as: anti-CNPase (1:200), anti-NeuN (1:50), anti-GFAP (1:200), anti-MOMA-2 (1:50) for neuroinflammation; anti-SQSTM-1/p62 (1:200), anti-LC3 (1:200) and anti-LAMP1 (1:500) for autophagy. Slides were incubated with primary antibodies in the humidified chamber and placed overnight into the refrigerator at 4℃. After incubation with primary antibodies, slides were washed by 1xPBS three times for 5 minutes, followed by Alexa Fluor 568 secondary antibody (red; Abcam, UK) incubation in the dark for at RT for 1 hour except for autophagic flux. Anti-CNPase, anti-p62, and anti-LC3 were incubated with Alexa Fluor 488 (green; Abcam, UK). Slides were rewashed by 1xPBS three times to remove excess antibody artifacts. Later, slides were mounted using Fluoroshield mounting medium DAPI (blue; Abcam, UK) to stain nuclei. The immunofluorescence staining was visualized by fluorescent Microscopy (BX53, Olympus, Tokyo, Japan) with different wavelength filters. Statistical analysis of the intensities from each staining was analyzed by ImageJ (Fiji) and followed by one-way ANOVA on GraphPad Prism.

## 2.11 Histological Stainings

The coronal sections of the fixed brains were stained by two different histopathological staining: Hematoxylin&Eosin staining and Periodic Acid-Schiff staining.

### 2.11.1 Hematoxylin&Eosin Staining

The slides from each treatment group of mice were put over ice for 15 minutes and then incubated in a humidified chamber at 55℃ for 15 minutes. Slides were washed with $dH_2O$ for 2 minutes and dried with Kimwipes. Each slide was stained by hematoxylin (Merck, Germany) at RT for 3 minutes, and they were washed by running tap water for 5 minutes, followed by $dH_2O$ for 2 minutes. Slides were incubated in 1% HCl in 70% ethanol and then were washed by running tap water for 5 minutes, followed by washing with $dH_2O$ for 2 minutes. Counterstain of eosin (Merck, Germany) was used for 30 seconds to stain the cytoplasm of each section, followed by dehydration of the slides were performed as 70% ethanol, 95% ethanol, and 100% ethanol, respectively. Slides were mounted by Cytoseal XYL (ThermoFisher, UK) while 100% ethanol was evaporated on the slides. Slides were stored at 4℃ until brain sections were visualized by light microscopy (BX53, Olympus, Japan).

### 2.11.2 Periodic Acid-Schiff Reagent Staining

The cryosectioned fixed brains on poly-lysine-coated slides were selected and placed on the ice for 15 minutes. After that, the slides were put in a humidified chamber and incubated at 55℃ for 15 minutes. Then, slides were incubated in Carnoy's solution containing ethanol, chloroform, and acetic acid (6:3:1) at RT for 15 minutes. Slides were rinsed by $dH_2O$ two times for 5 minutes, and then 30 µl of 0.5% Periodic acid solution (Merck, Germany) was dripped on each brain section following incubation at RT for 5 minutes. Slides were washed by running tap water and $dH_2O$ for 3 minutes. After the washing steps, Schiff's reagent was added to each brain section and incubated at RT for 15 minutes. After removing the Schiff reagent, the slides were washed with running tap water and $dH_2O$ for 3 minutes. Next, slides were counterstained with hematoxylin for 2

minutes and then washed by running tap water for 6 minutes. Tissue dehydration was performed by dipping each slide in 70% ethanol, 95% ethanol, and 100% ethanol, respectively.

## 2.12 Behavioral Analysis

Observation of the anxiety-related behavior and locomotor activity of the 140-day-old *WT*, *Hexa-/-* and *Hexa-/-Neu3-/-* mice after STKD and LTKD treatments were performed by open field test and rotarod analysis, respectively.

### 2.12.1 Open Field Analysis

The open-field analysis measured the mice's anxiety-related behavior and locomotor activity. In this test, *WT*, *Hexa-/-,* and *Hexa-/-Neu3-/-* mouse models from each treatment strategy were selected and placed into the 40x40 cm box and transparent walls before the sacrification of each mouse. Movement was recorded by a digital camera, which was above the box. Mice were put in the same corner of the box, and then the record was continued for 5 minutes. Record analysis also was processed in the PanLab SMART Video Tracking System v0.3 (Harvard Apparatus, USA). Statistical analysis was completed by one-way ANOVA using GraphPad Prism.

### 2.12.2 Rotarod Analysis

The rotarod analysis was applied to test the mice's motor coordination and balance capabilities. Mice were accustomed to the rotarod unit at a speed of 4 rpm. *WT*, *Hexa-/-,* and *Hexa-/-Neu3-/-* mice from each treatment strategy were selected, and rotarod analysis was performed before the sacrification of each mouse. After training, mice were tested on the accelerated rod unit from 4 to 40 rpm for 5 minutes. The test was performed three times to obtain accurate results. Mice were rested before repetition of the test for 15 minutes. Latency to fall was recorded for each mouse to constitute statistical analysis by one-way ANOVA in GraphPad Prism.

# CHAPTER 3

# RESULTS

## 3.1 Mouse Genotyping

Determining mouse genotype by controlling for the wild-type and mutant alleles from the Hexa and Neu3 genes was performed by separating the DNA isolated from each mouse by agarose gel electrophoresis. Each allele was labeled on the gel as +/+, +/-, and -/- for *Hexa* (Figure 3.1 A) and *Neu3* (Figure 3.1 B) genes.

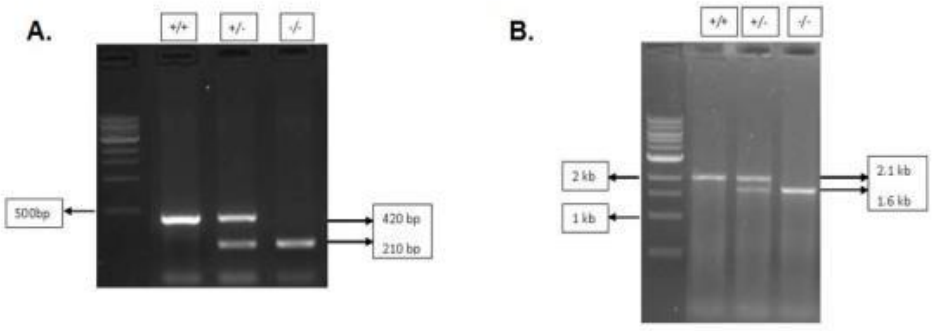


Figure 3.1 Agarose gel electrophoresis image for *Hexa* and *Neu3* PCR for mouse genotyping. While *Hexa* wild-type allele is 500 bp, the mutated allele is 210 bp fragments (A). In the *Neu3*, the wild-type allele is 2 kb while the mutant allele is 1.6 kb fragments. (B).

## 3.2 Measurements

The body weight, ketogenic diet consumption, and ketone body concentrations were measured in *WT*, *Hexa-/-*, and *Hexa-/-Neu3-/-* mice treated with short- and long-term ketogenic diet, propagermanium and their combined.

### 3.2.1 Body Weight

Biweekly body weight measurements were taken for treated or untreated *WT*, *Hexa-/-* and *Hexa-/-Neu3-/-* male-only mice with two strategies ranging from 2 weeks to 18 weeks after weaning.

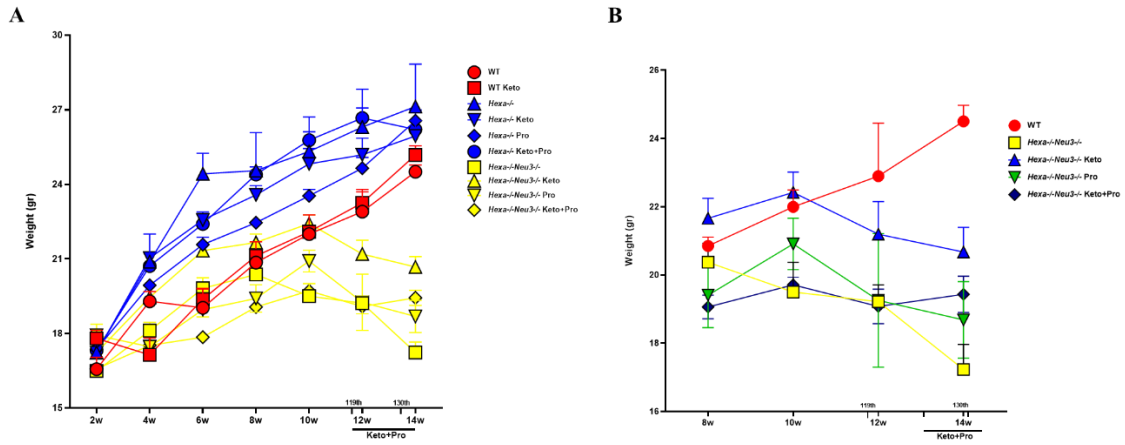


Figure 3.2 Body weight measurements of the short-term ketogenic diet (10 days), propagermanium (21 days), and combined therapy groups of *WT*, *Hexa-/-* and *Hexa-/-Neu3-/-* mice from 6 weeks to 18 weeks. Data show mean ± SEM of measurements. Significant levels of data were determined using the two-way ANOVA. (n=9, *p<0.05, **p<0.01, ***p<0.001 and ****p<0.0001)

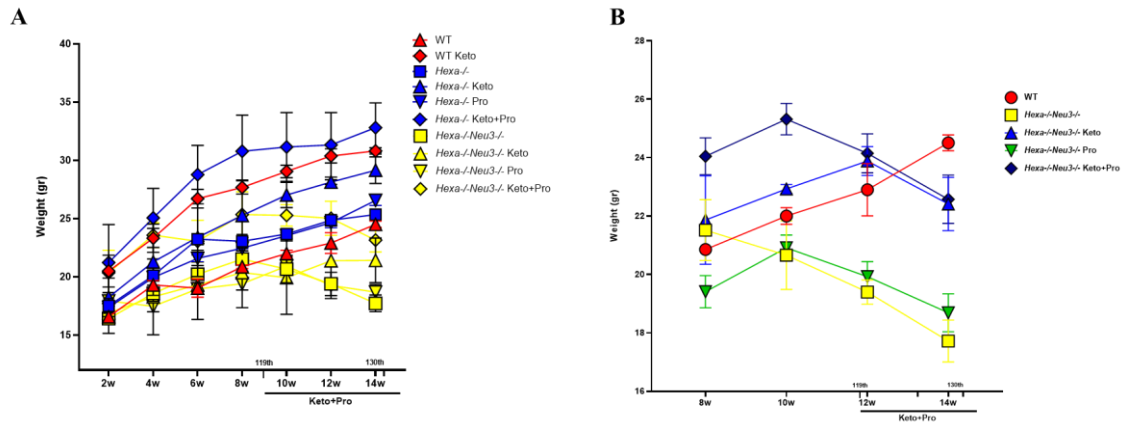


Figure 3.3 Body weight measurements of the long-term ketogenic diet (119 days), propagermanium (21 days), and combined therapy groups of *WT*, *Hexa-/-* and *Hexa-/-Neu3-/-* mice from 6 weeks to 18 weeks. Data show mean ± SEM of measurements. Significant levels of data were determined using the two-way ANOVA. (n=9, *p<0.05, **p<0.01, ***p<0.001 and ****p<0.0001)

According to the results, short-term ketogenic diet, propagermanium, and combined therapies did not change the body weight in *WT* and *Hexa-/-* mice compared to untreated one; however, ketogenic diet and combined ketogenic diet and propagermanium therapies prevented the excessive loss of body weight in *Hexa-/-Neu3-/-* mice compared to untreated ones (Figure 3.2 A-B). After long-term ketogenic diet treatment, *WT* and Hexa-/- mice gained weight compared to untreated mice, whereas *Hexa-/-Neu3-/-* mice prevented excessive weight loss, with a similar outcome to short-term ketogenic diet treatment (Figure 3.3 A-B).

## 3.2.2 Ketone Body Concentration

Ketone body concentration and the amount of ketogenic diet consumed by each mouse were measured to show whether the amount of ketone bodies increases with ketogenic diet consumption in a genotype- and consumption-dependent manner.

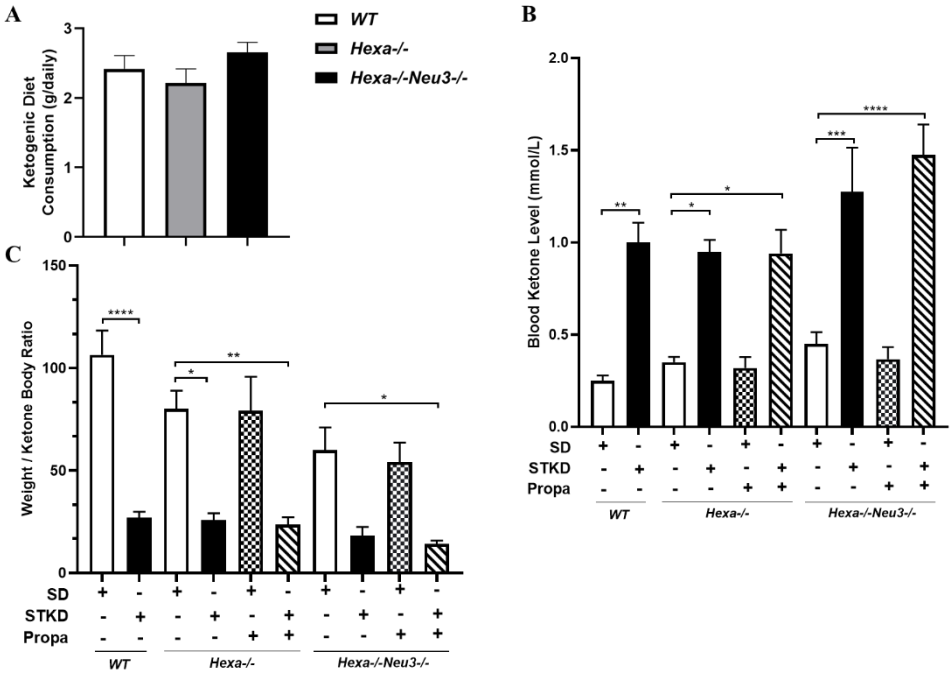


Figure 3.4 Illustration of the daily ketogenic diet consumption for short-term ketogenic diet group for age-matched *WT*, *Hexa-/-* and *Hexa-/-Neu3-/-* (A). Measurements of blood ketone levels (mmol/L) for untreated and treated *WT*, *Hexa-/-* and *Hexa-/-Neu3-/-* mice (B). Illustration of the ratio of mice body weight per ketone body concentration from each genotype and treatment conditions (C). Data show mean ± SEM of measurements. Significant levels

of data were determined using the one-way ANOVA. (n=9, *p<0.05, **p<0.01, ***p<0.001 and ****p<0.0001)

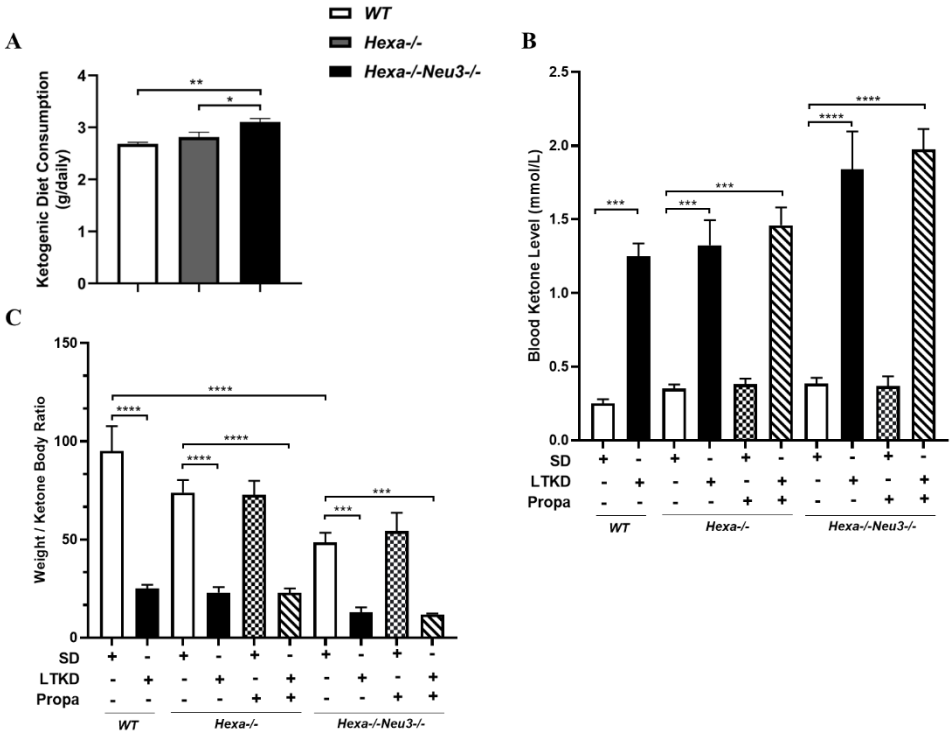


Figure 3.5 Illustration of the daily ketogenic diet consumption for long-term ketogenic diet group for age-matched *WT*, *Hexa-/-* and *Hexa-/-Neu3-/-* (A). Measurements of blood ketone levels (mmol/L) for untreated and treated *WT*, *Hexa-/-* and *Hexa-/-Neu3-/-* mice (B). Illustration of the ratio of mice body weight per ketone body concentration from each genotype and treatment conditions (C). Data show mean ± SEM of measurements. Significant levels of data were determined using the one-way ANOVA. (n=9, *p<0.05, **p<0.01, ***p<0.001 and ****p<0.0001)

Ketogenic diet consumption slightly increased in the *Hexa-/-Neu3-/-* mice compared to *WT* and *Hexa-/-* mice in the short-term ketogenic diet treatment; however, the result was not statistically significant (Figure 3.4 A). After 10 days of ketogenic diet intervention, ketone body concentrations were elevated in each genotype compared to aged-match untreated mice. The propagermanium treatment did not change the ketone body concentration in the *Hexa-/-* and *Hexa-/-Neu3-/-* mice compared to untreated ones (Figure 3.4 B). The weight/ketone body concentration ratio exhibited a meaningful pattern with the ketone body concentration results in the short-term treatment strategy. (Figure 3.4 C).

The ketogenic diet consumption significantly increased for *Hexa-/-Neu3-/-* mice compared to aged-match *WT* and *Hexa-/-* mice in the long-term ketogenic diet strategy (Figure 3.5 A). Long-term ketogenic diet therapy displayed a similar pattern with the

short-term strategy for ketone body concentration and the weight/ketone body concentration ratio (Figure 3.5 B, C).

## 3.3 TLC Analysis for Neutral and Acidic Gangliosides

TLC analysis was performed to analyze acidic and neutral gangliosides in the cortex and cerebellum tissues of 140-day-old *WT*, *Hexa-/-* and *Hexa-/-Neu3-/-* mouse models utilizing two treatment strategies (short-term and long-term treatments). The intensities of the GM2 ganglioside bands were normalized by GD1a ganglioside intensities.

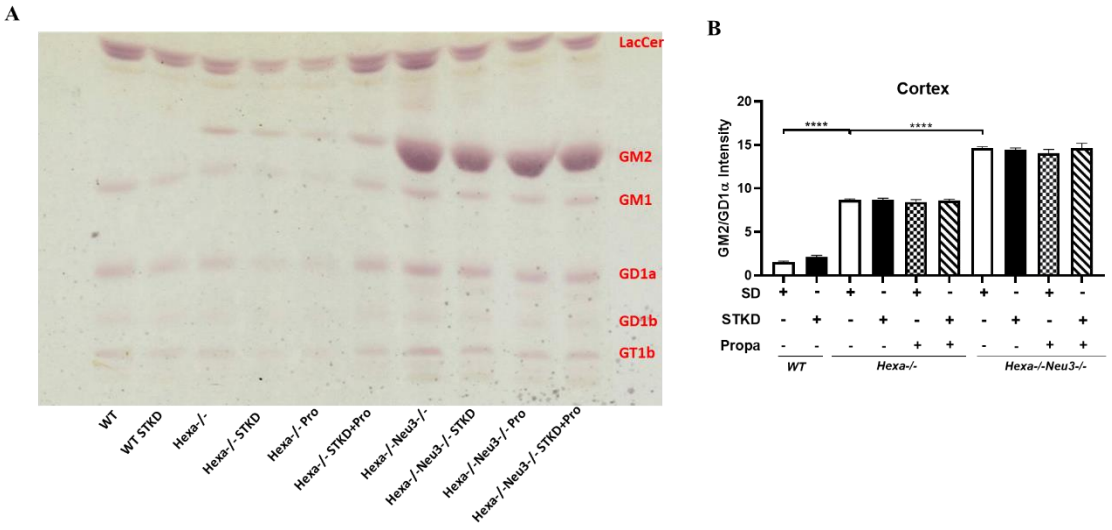


Figure 3.6 Thin layer chromatography showing orcinol stained acidic ganglioside profile extracted from cortex for short-term ketogenic diet strategy of 140-day-old *WT*, *Hexa-/-* and *Hexa-/-Neu3-/-* mice (A). The histogram shows the intensity ratio of GM2/GD1a (B). Intensities were measured via ImageJ program. Data show mean ± SEM of measurements. Significant levels of data were determined using the one-way ANOVA. (n=3, *p<0.05, **p<0.01, ***p<0.001 and ****p<0.0001)

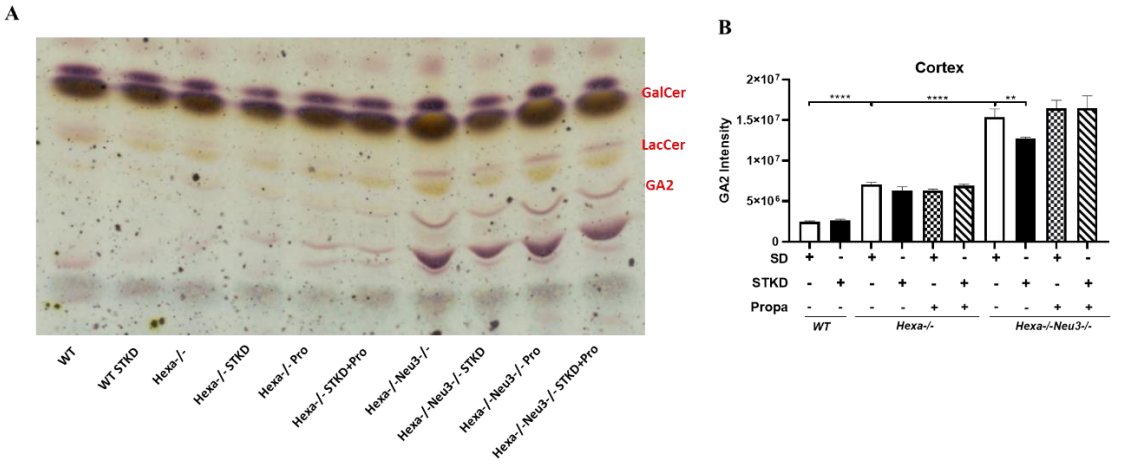


Figure 3.7 Thin layer chromatography showing orcinol stained neutral ganglioside profile extracted from cortex for short-term ketogenic diet strategy of 140-day-old *WT*, *Hexa-/-* and *Hexa-/-Neu3-/-* mice (A). The histogram shows the intensity ratio of GM2/GD1a (B). Intensities were measured via ImageJ program. Data show mean ± SEM of measurements. Significant levels of data were determined using the one-way ANOVA. (n=3, *p<0.05, **p<0.01, ***p<0.001 and ****p<0.0001)

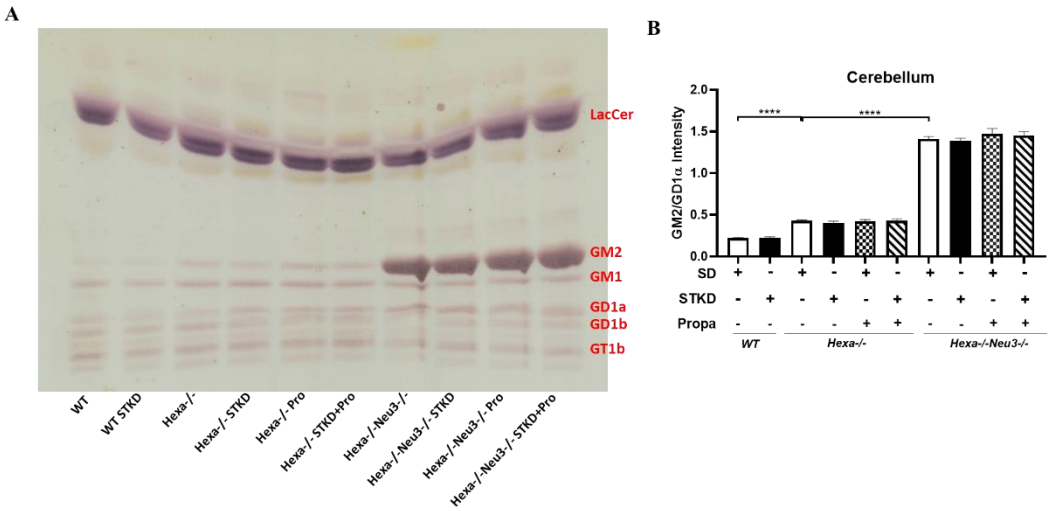


Figure 3.8 Thin layer chromatography showing orcinol stained acidic ganglioside profile extracted from cortex for short-term ketogenic diet strategy of 140-day-old *WT*, *Hexa-/-* and *Hexa-/-Neu3-/-* mice (A). The histogram shows the intensity ratio of GM2/GD1a (B). Intensities were measured via ImageJ program. Data show mean ± SEM of measurements. Significant levels of data were determined using the one-way ANOVA. (n=3, *p<0.05, **p<0.01, ***p<0.001 and ****p<0.0001)

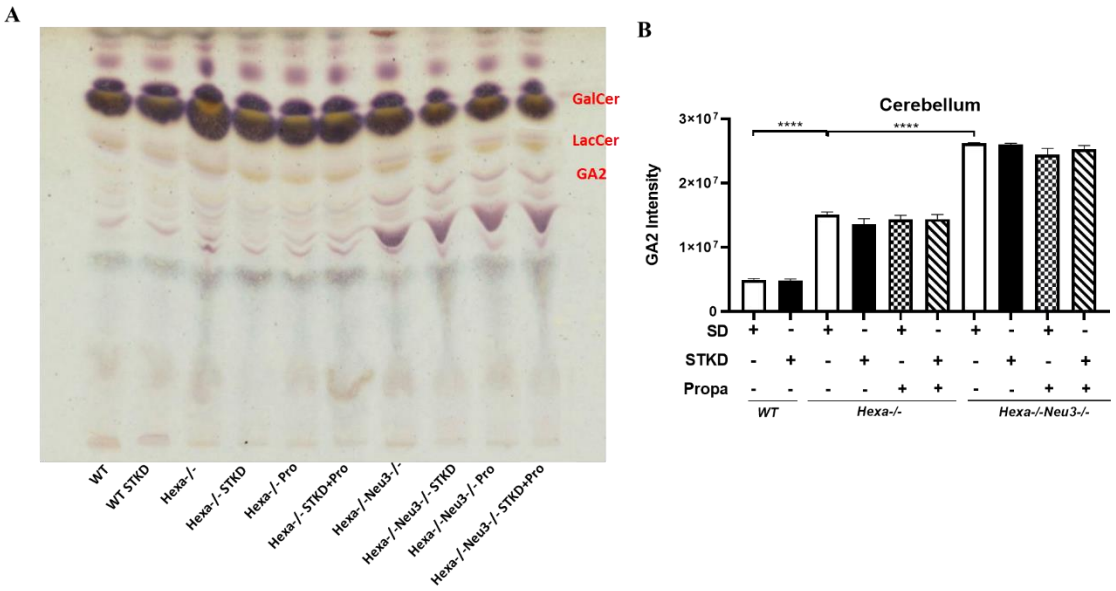


Figure 3.9 Thin layer chromatography showing orcinol stained acidic ganglioside profile extracted from cortex for short-term ketogenic diet strategy of 140-day-old *WT*, *Hexa-/-* and *Hexa-/-Neu3-/-* mice (A). The histogram shows the intensity ratio of GM2/GD1a (B). Intensities were measured via ImageJ program. Data show mean ± SEM of measurements. Significant levels of data were determined using the one-way ANOVA. (n=3, *p<0.05, **p<0.01, ***p<0.001 and ****p<0.0001)

The abnormal GM2 ganglioside accumulation was demonstrated in 140-day-old *Hexa-/-Neu3-/-* mouse model compared to age-matched *WT* and *Hexa-/-* mice as previously published (Seyrantepe et al. 2018). Furthermore, more GM2 ganglioside accumulation was observed in *Hexa-/-* mice than in *WT*. The short-term ketogenic diet and propagermanium treatment did not mitigate abnormal GM2 accumulation in 140-day-old *Hexa-/-Neu3-/-* mice compared to age-matched *WT* and *Hexa-/-* for cortex and cerebellum (Figure 3.6 and Figure 3.8) however, interestingly, the level of GA2, one of the neutral gangliosides, was significantly reduced after short-term ketogenic diet treatment in the *Hexa-/-Neu3-/-* mouse cortex (Figure 3.7) but not in the cerebellum (Figure 3.9).

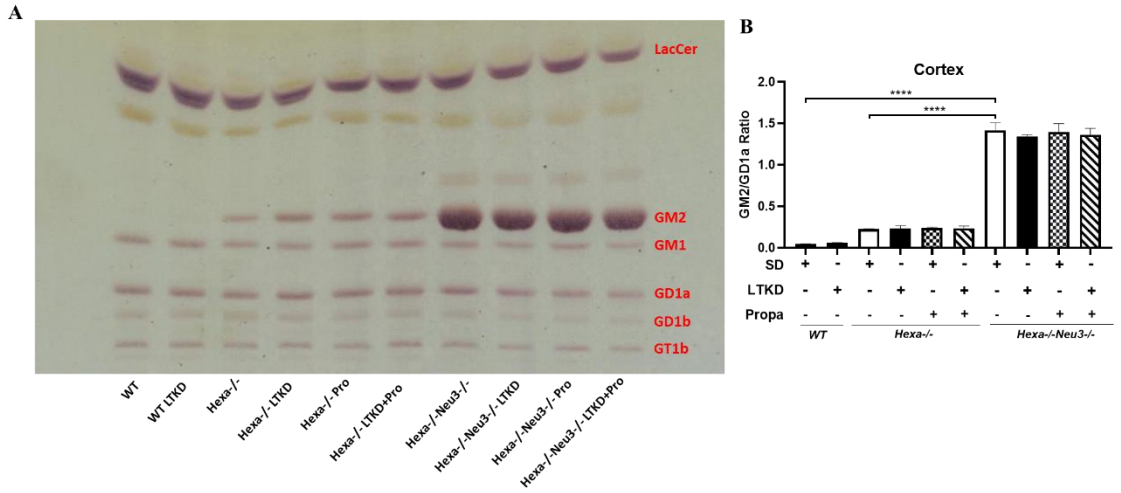


Figure 3.10 Thin layer chromatography showing orcinol stained acidic ganglioside profile extracted from cortex for long-term ketogenic diet strategy of 140-day-old *WT*, *Hexa-/-* and *Hexa-/-Neu3-/-* mice (A). The histogram shows the intensity ratio of GM2/GD1a (B). Intensities were measured via ImageJ program. Data show mean ± SEM of measurements. Significant levels of data were determined using the one-way ANOVA. (n=3, *p<0.05, **p<0.01, ***p<0.001 and ****p<0.0001)

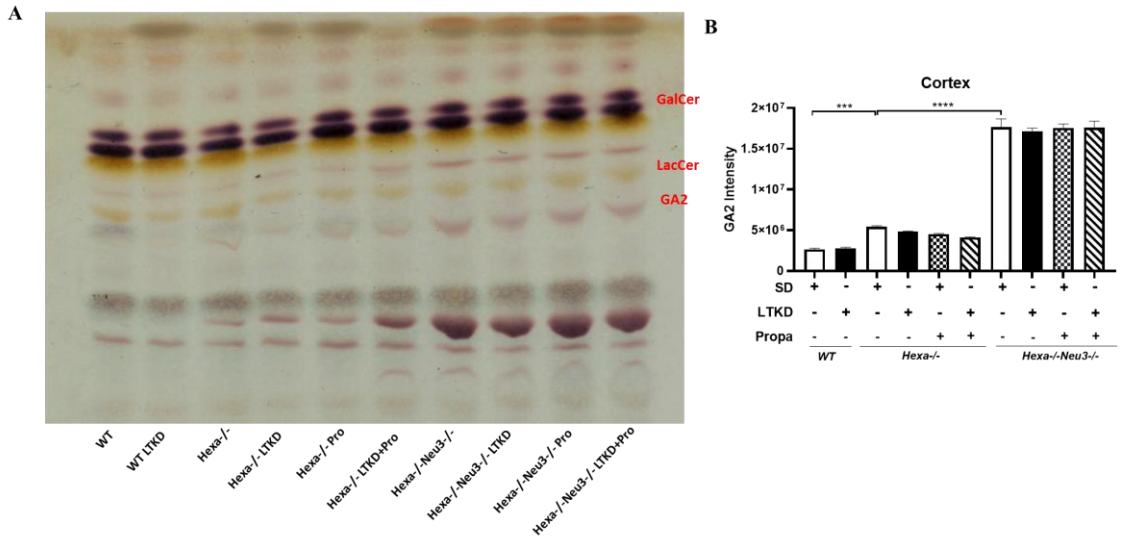


Figure 3.11 Thin layer chromatography showing orcinol stained acidic ganglioside profile extracted from cortex for long-term ketogenic diet strategy of 140-day-old *WT*, *Hexa-/-* and *Hexa-/-Neu3-/-* mice (A). The histogram shows the intensity ratio of GM2/GD1a (B). Intensities were measured via ImageJ program. Data show mean ± SEM of measurements. Significant levels of data were determined using the one-way ANOVA. (n=3, *p<0.05, **p<0.01, ***p<0.001 and ****p<0.0001)

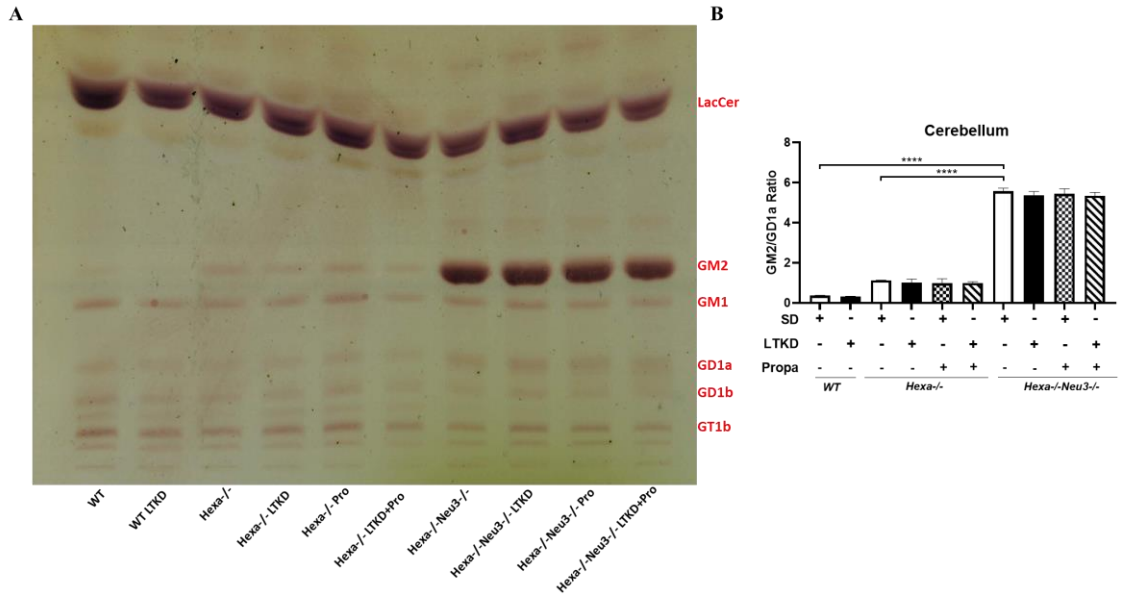


Figure 3.12 Thin layer chromatography showing orcinol stained acidic ganglioside profile extracted from cortex for long-term ketogenic diet strategy of 140-day-old *WT*, *Hexa-/-* and *Hexa-/-Neu3-/-* mice (A). The histogram shows the intensity ratio of GM2/GD1a (B). Intensities were measured via ImageJ program. Data show mean ± SEM of measurements. Significant levels of data were determined using the one-way ANOVA. (n=3, *p<0.05, **p<0.01, ***p<0.001 and ****p<0.0001)

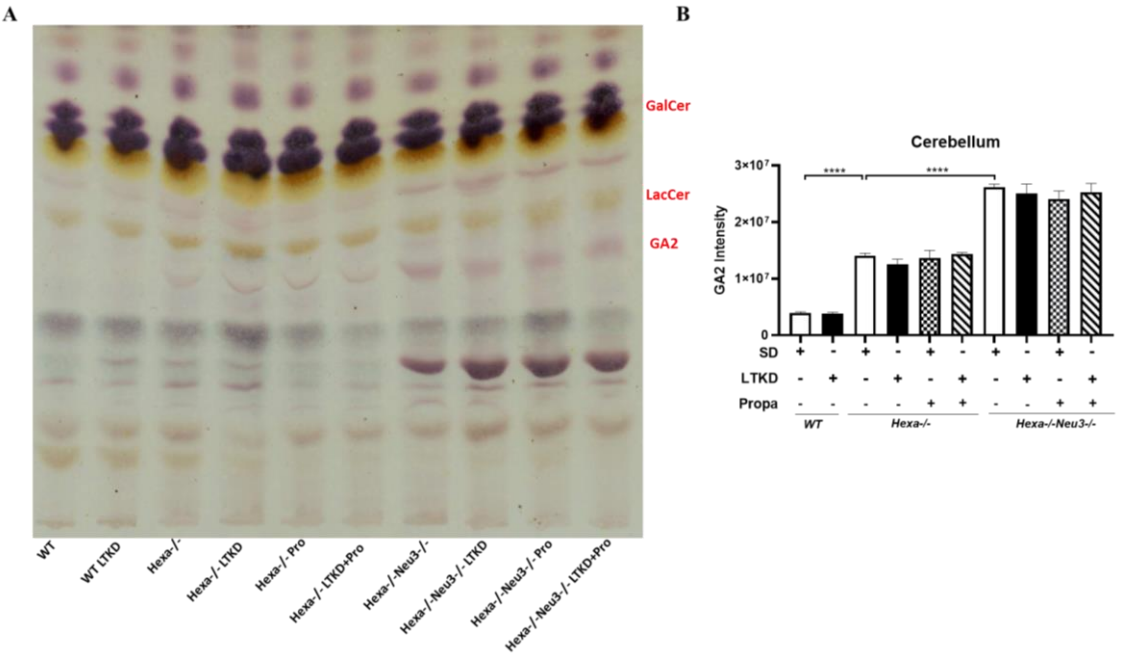


Figure 3.13 Thin layer chromatography showing orcinol stained acidic ganglioside profile extracted from cortex for long-term ketogenic diet strategy of 140-day-old *WT*, *Hexa-/-* and *Hexa-/-Neu3-/-* mice (A). The histogram shows the intensity ratio of GM2/GD1a (B). Intensities were measured via ImageJ program. Data show mean ± SEM of measurements. Significant levels of data were determined using the one-way ANOVA. (n=3, *p<0.05, **p<0.01, ***p<0.001 and ****p<0.0001)

The long-term ketogenic diet did not affect both acidic and neutral ganglioside levels. In the cortex and cerebellum, the long-term ketogenic diet strategy did not alter the abnormal accumulated GM2 ganglioside level that was normalized by GD1a in the 140-day-old *Hexa-/-Neu3-/-* mouse model (Figure 3.10 and Figure 3.11). Moreover, neutral ganglioside of GA2 also did not change in *Hexa-/-Neu3-/-* mice after the long-term ketogenic diet strategy compared to untreated ones in the cortex and cerebellum (Figure 3.12 and Figure 3.13).

## 3.4 Neuroinflammation Analyses

Neuroinflammation-related genes and proteins were analyzed by q-PCR, immunofluorescence staining, and western blotting in the cortex and cerebellum after a short-term and long-term ketogenic diet, and propagermanium treatments for 140-day-old *WT*, *Hexa-/-* and *Hexa-/-Neu3-/-* mouse models.

### 3.4.1 q-RT PCR Analysis

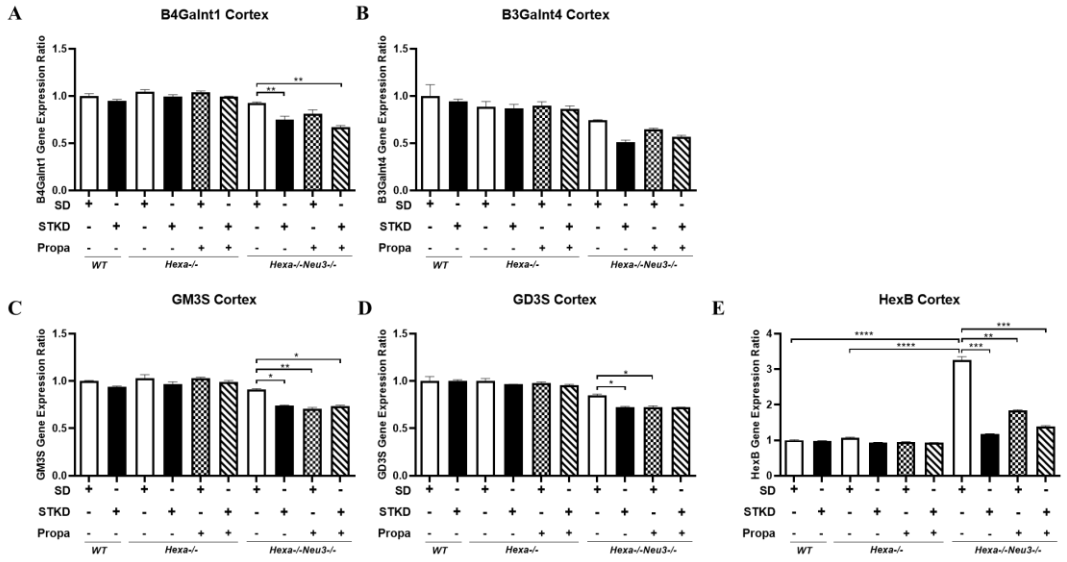


Figure 3.14 Relative expression levels of *B4Galnt1* (A), *B3Galnt4* (B), *GM3S* (C), *GD3S* (D), and *HexB* (E) genes in the short-term ketogenic diet strategy for 140-day-old *WT*, *Hexa-/-* and *Hexa-/-Neu3-/-* mice cortex. Data show mean ± SEM of measurements. Significant levels of data were determined using the one-way ANOVA. (n=3, *p<0.05, **p<0.01, ***p<0.001 and ****p<0.0001)

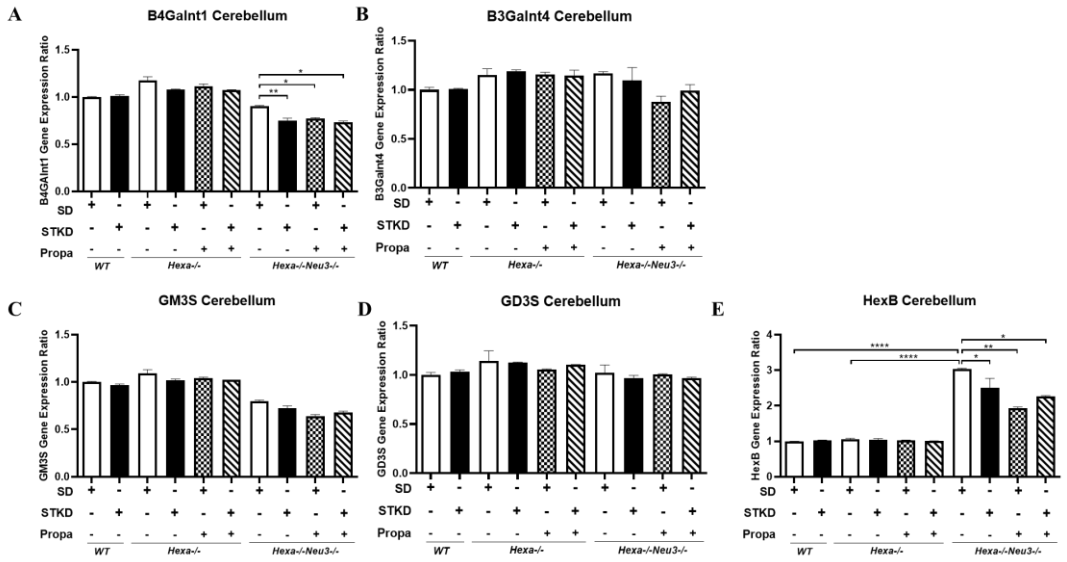


Figure 3.15 Relative expression levels of *B4Galnt1* (A), *B3Galnt4* (B), *GM3S* (C), *GD3S* (D), and *HexB* (E) genes in the short-term ketogenic diet strategy for 140-day-old *WT*, *Hexa-/-* and *Hexa-/-Neu3-/-* mice cerebellum. Data show mean ± SEM of measurements. Significant levels of data were determined using the one-way ANOVA. (n=3, *p<0.05, **p<0.01, ***p<0.001 and ****p<0.0001)

Ganglioside metabolizing enzyme gene expressions were measured to check whether short-term or long-term ketogenic diet and propagermanium treatments transcriptionally alter ganglioside patterns. In the cortex, *B4Galnt1* gene expression significantly decreased in *Hexa-/-Neu3-/-* mice after a short-term ketogenic diet and combined treatments compared to untreated ones (Figure 3.14 A). In addition, *GM3S* and *HexB* gene expressions significantly reduced in *Hexa-/-Neu3-/-* cortex like *B4Galnt1* after ketogenic diet and combined treatments (Figure 3.14 C, E). The *GM3S*, *GD3S,* and *HexB* gene expressions significantly reduced after propagermanium treatment compared to aged-matched untreated *Hexa-/-Neu3-/-* mice. The *B3Galnt4* gene expression level did not change after each treatment in *Hexa-/-Neu3-/-* mice (Figure 3.14 B). In the cerebellum, only *B4Galnt1* and *HexB* gene expressions were affected by the short-term treatment strategy in which each treatment significantly mitigated gene expressions in *Hexa-/-Neu3-/-* mice compared to untreated ones (Figure 3.15 A, E). The other gene expression levels did not change significantly in the *Hexa-/-Neu3-/-* mice cerebellum (Figure 3.15 B, C, D).

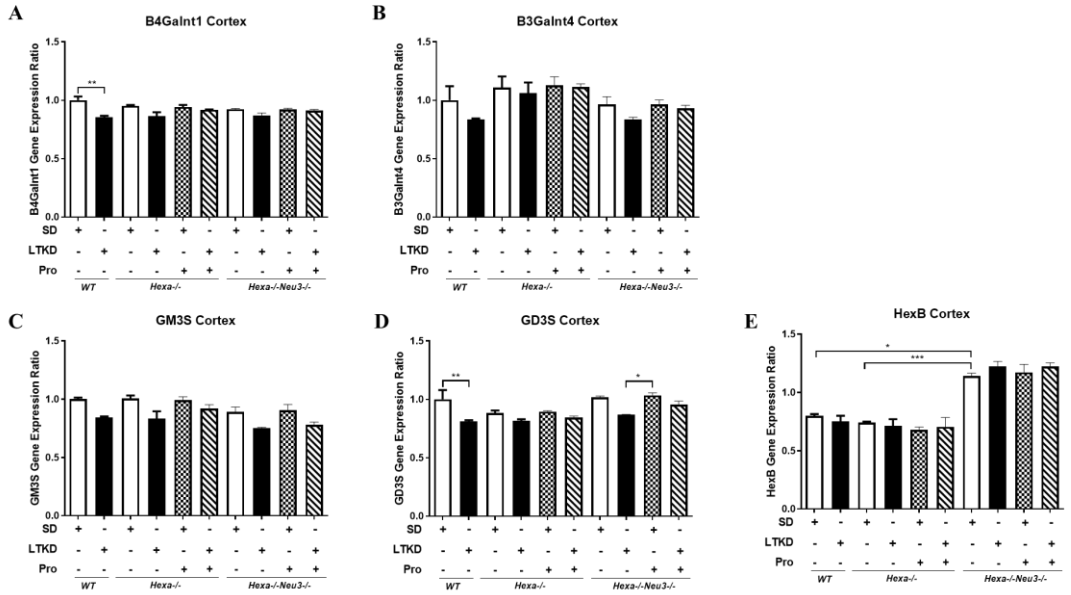


Figure 3.16 Relative expression levels of *B4Galnt1* (A), *B3Galnt4* (B), *GM3S* (C), *GD3S* (D), and *HexB* (E) genes in the long-term ketogenic diet strategy for 140-day-old *WT*, *Hexa-/-* and *Hexa-/-Neu3-/-* mice cortex. Data show mean ± SEM of measurements. Significant levels of data were determined using the one-way ANOVA. (n=3, *p<0.05, **p<0.01, ***p<0.001 and ****p<0.0001)

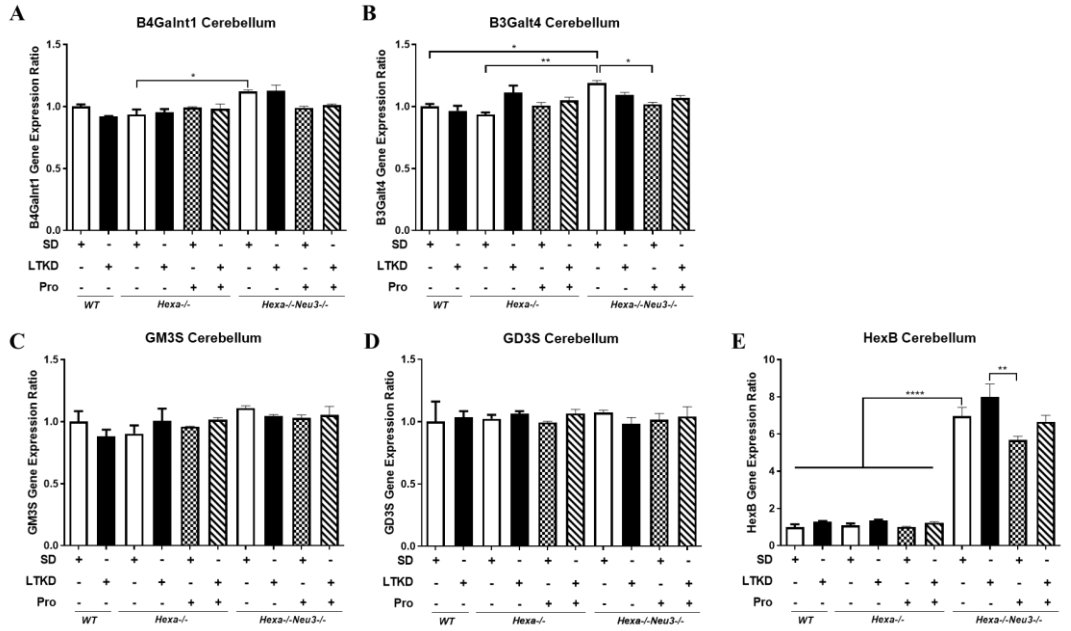


Figure 3.17 Relative expression levels of *B4Galnt1* (A), *B3Galnt4* (B), *GM3S* (C), *GD3S* (D), and *HexB* (E) genes in the long-term ketogenic diet strategy for 140-day-old *WT*, *Hexa-/-* and *Hexa-/-Neu3-/-* mice cerebellum. Data show mean ± SEM of measurements. Significant levels of data were determined using the one-way ANOVA. (n=3, *p<0.05, **p<0.01, ***p<0.001 and ****p<0.0001)

The effect of a long-term ketogenic diet and propagermanium treatment strategy on ganglioside metabolism was investigated, and a significant difference was observed

only for *GD3S* gene expression in *Hexa-/-Neu3-/-* cortex between mice treated with ketogenic diet alone and mice treated with propagermanium alone (Figure 3.16 D). The *B4Galnt1*, *B3Galnt4*, *GM3S, and HexB* gene expressions did not change after treatments in the *Hexa-/-Neu3-/-* mice cortex (Figure 3.16 A, B, C, E). Long-term ketogenic diet treatment interestingly reduced *B4Galnt1* and *GD3S* gene expressions in the *WT* mice cortex compared to untreated ones Figure 3.16 A, D). *B4Galnt1*, *B3Galnt4* and *HexB* gene expressions in the cerebellum were affected by a long-term treatment strategy in which *B3Galnt4* gene expression was reduced with only propagermanium treatment compared to untreated ones (Figure 3.17 A, B, E). Interestingly, long term ketogenic diet increased *HexB* gene expression level compared to untreated *Hexa-/-Neu3-/-* mice cerebellum, and only propagermanium treatment significantly reduced HexB gene expression level compared to long-term ketogenic diet treated *Hexa-/-Neu3-/-* mice. The *GM3S* and *GD3S* gene expression levels were not altered after the long-term treatment strategy (Figure 3.17 C, D).

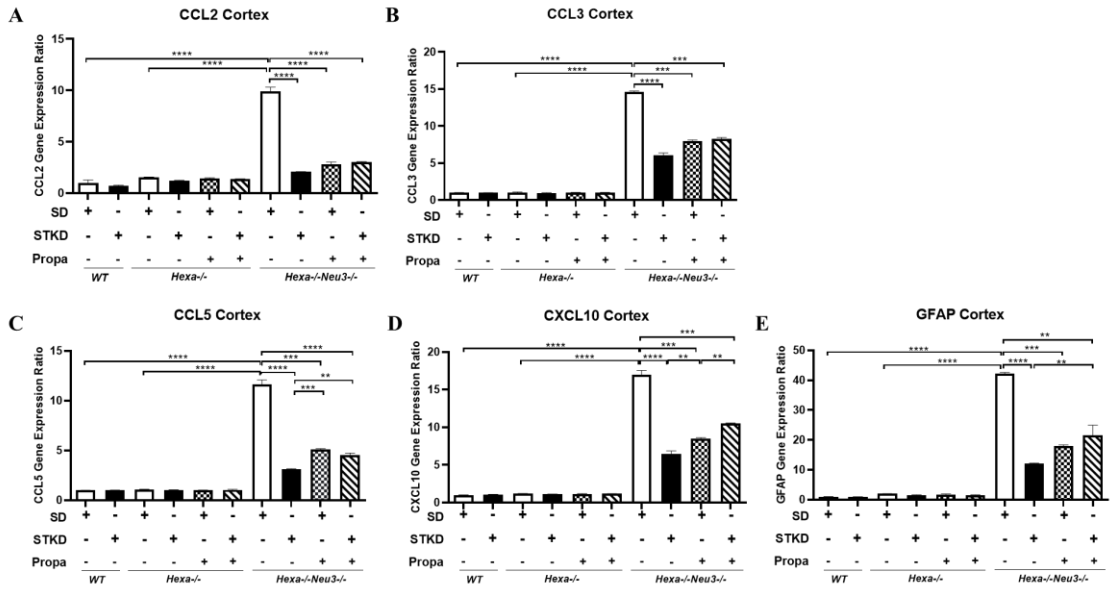


Figure 3.18 Relative expression levels of *CCL2* (A), *CCL3* (B), *CCL5* (C), *CXCL10* (D), and *GFAP* (E) genes in the short-term ketogenic diet strategy for 140-day-old *WT*, *Hexa-/-* and *Hexa-/-Neu3-/-* mice cortex. Data show mean ± SEM of measurements. Significant levels of data were determined using the one-way ANOVA. (n=3, *p<0.05, **p<0.01, ***p<0.001 and ****p<0.0001)

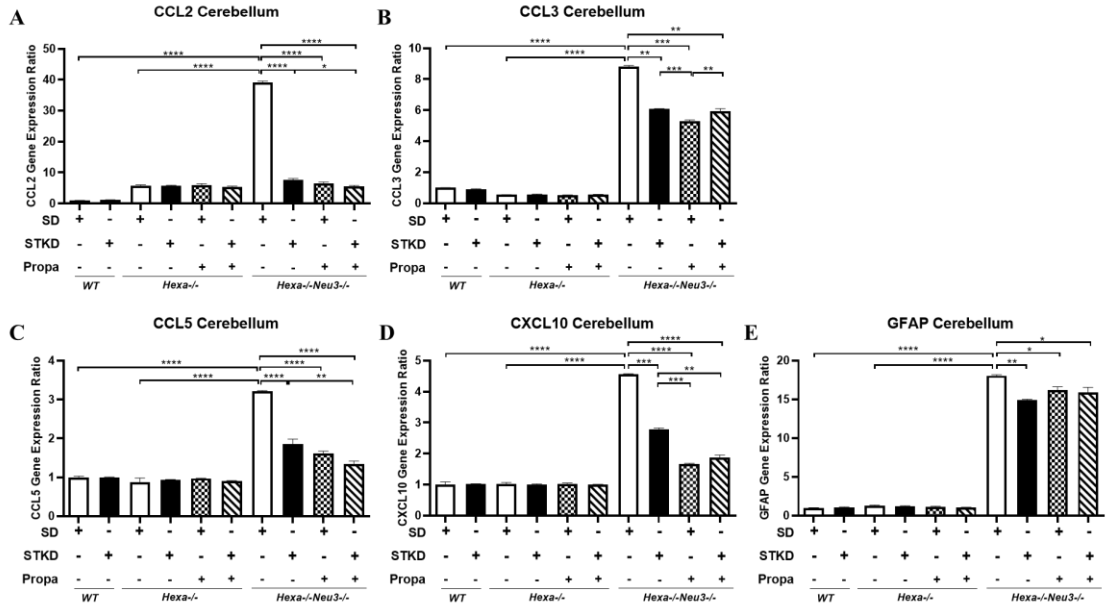


Figure 3.19 Relative expression levels of *CCL2* (A), *CCL3* (B), *CCL5* (C), *CXCL10* (D), and *GFAP* (E) genes in the short-term ketogenic diet strategy for 140-day-old *WT*, *Hexa-/-* and *Hexa-/-Neu3-/-* mice cerebellum. Data show mean ± SEM of measurements. Significant levels of data were determined using the one-way ANOVA. (n=3, *p<0.05, **p<0.01, ***p<0.001 and ****p<0.0001)

Neuroinflammation-related-markers gene expression levels were measured after short-term and long-term ketogenic diet treatment strategies. The pro-inflammatory cytokines/chemokines gene expression levels significantly increased in 140-day-old *Hexa-/-Neu3-/-* mice compared to aged-matched *WT* and *Hexa-/-* mice as previously published. The short-term ketogenic diet, propagermanium, and combined ketogenic diet and propagermanium treatments significantly reduced pro-inflammatory cytokines/chemokines (CCL2, CCL3, CCL5, CXCL10, and GFAP) gene expression levels in 140-day-old *Hexa-/-Neu3-/-* mice cortex and cerebellum (Figure 3.18 and 3.19). Moreover, the ketogenic diet and propagermanium treatment did not alter the gene expression levels of the neuroinflammation-related pro-inflammatory cytokines/chemokines in *WT* and *Hexa-/-* mice cortex and cerebellum (Figure 3.18 and 3.19).

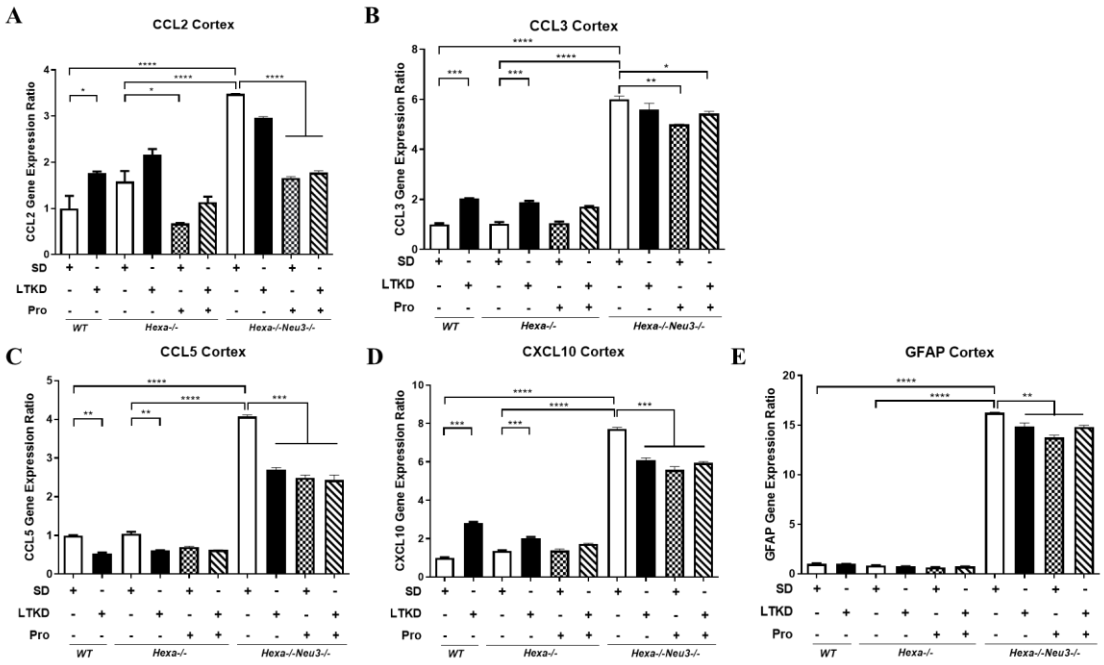


Figure 3.20 Relative expression levels of *CCL2* (A), *CCL3* (B), *CCL5* (C), *CXCL10* (D), and *GFAP* (E) genes in the long-term ketogenic diet strategy for 140-day-old *WT*, *Hexa-/-* and *Hexa-/-Neu3-/-* mice cortex. Data show mean ± SEM of measurements. Significant levels of data were determined using the one-way ANOVA. (n=3, *p<0.05, **p<0.01, ***p<0.001 and ****p<0.0001)

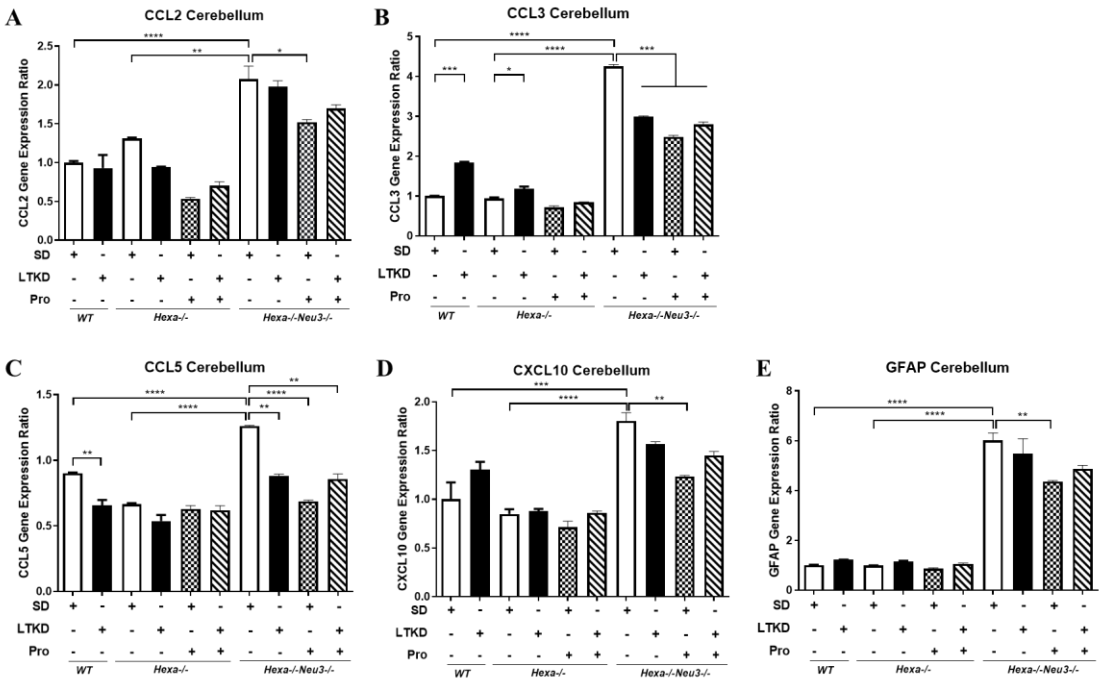


Figure 3.21 Relative expression levels of *CCL2* (A), *CCL3* (B), *CCL5* (C), *CXCL10* (D), and *GFAP* (E) genes in the long-term ketogenic diet strategy for 140-day-old *WT*, *Hexa-/-* and *Hexa-/-Neu3-/-* mice cerebellum. Data show mean ± SEM of measurements. Significant levels of data were determined using the one-way ANOVA. (n=3, *p<0.05, **p<0.01, ***p<0.001 and ****p<0.0001)

Long-term ketogenic diet treatment did not reduce *CCL2* (Figure 3.20 A) and *CCL3* (Figure 3.20 B) gene expression levels in *Hexa-/-Neu3-/-* mice cortex, whereas propagermanium alone and combined ketogenic diet and propagermanium treatments reduced the expression levels of these genes. In addition, long-term ketogenic diet-induced *CCL2* and *CCL3* gene expression in *WT* and *Hexa-/-* mice cortex compared to untreated ones. Interestingly, each treatment condition significantly reduced the CCL5, CXCL10, and *GFAP* gene expression levels in the *Hexa-/-Neu3-/-* mice cortex (Figure 3.20 C, D, E). In contrast to the *CCL2* and *CCL3*, the CCL5 gene expression level was significantly attenuated after *a* long-term ketogenic diet in *WT* and *Hexa-/-* mice (Figure 3.20 C). The *CXCL10* gene expression levels increased like the *CCL2* and *CCL3* gene expression levels in the *WT* and *Hexa-/-* mice cortex (Figure 3.20 D). In the cerebellum, CCL2, *CXCL10*, and GFAP gene expression levels did not reduce significantly after a long-term ketogenic diet alone in the 140-day-old *Hexa-/-Neu3-/-* mice compared to untreated mice. The *CCL2* gene expression levels were only reduced in the cerebellum *of Hexa-/-Neu3-/-* mice after propagermanium treatment alone (Figure 3.21 A). The *CCL3* and *CCL5* gene expression levels significantly decreased after each treatment condition (Figure 3.21 B, C). Like the *CCL2* gene expression levels, *CXCL10* and *GFAP* gene expression levels significantly reduced after propagermanium treatment alone (Figure 3.21 D, E). The *CCL3* gene expression level also increased in both *WT* and *Hexa-/-* mice cerebellum compared to untreated ones (Figure 3.21 B); however, the CCL5 gene expression level decreased in the *WT* after long-term ketogenic diet treatment alone (Figure 3.21 C).

### 3.4.2 Western Blotting

It was shown by western blot method how Nfκb and IκB-α, which are among the major proteins regulating neuroinflammation, would be affected in the cortex and cerebellum regions of the brains of 140-days-old *WT*, *Hexa-/-* and *Hexa-/-Neu3-/-* mice after short-term and long-term ketogenic diet and propagermanium treatments. On the other hand, protein levels were normalized by using β-actin.

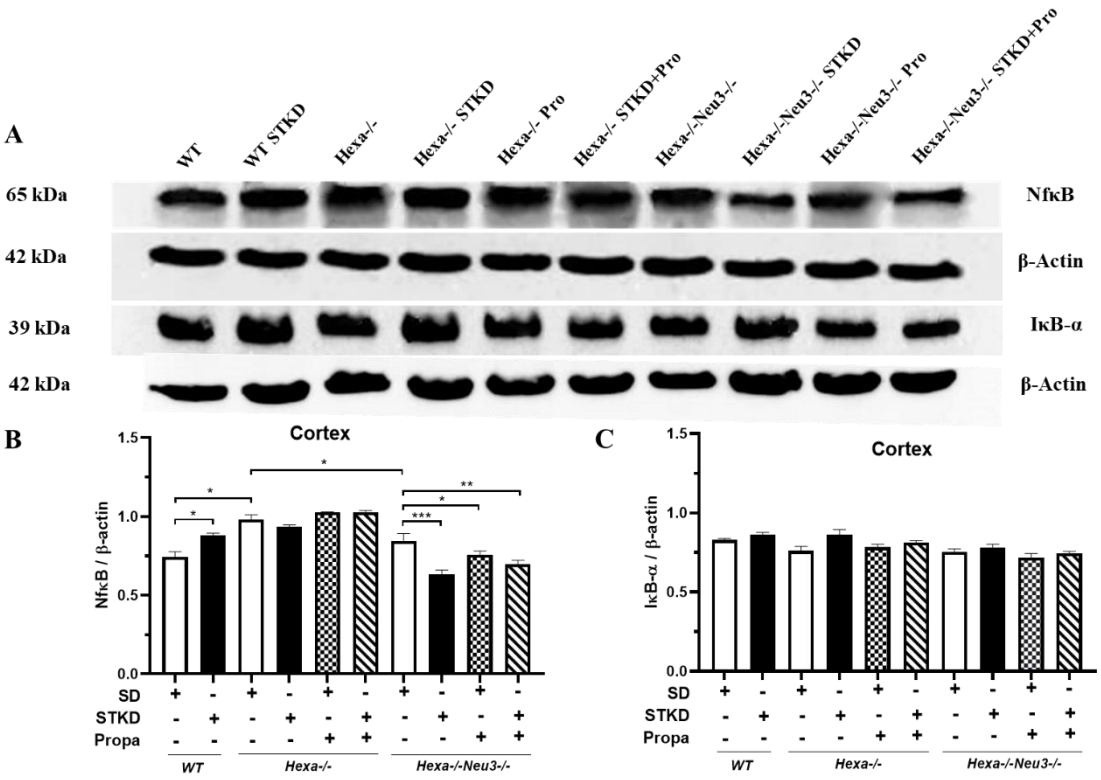


Figure 3.22 Western blotting analysis for NfκB and IκB-α in cortex region of 140-day-old *WT*, *Hexa-/-* and *Hexa-/-Neu3-/-* mice for the short-term ketogenic diet strategy (A). The histogram shows the ratio of NfκB/β-actin (B) and IκB-α/ β-actin (C). Intensities were measured via ImageJ program. Data show mean ± SEM of measurements. Significant levels of data were determined using the one-way ANOVA. (n=3, *p<0.05, **p<0.01, ***p<0.001 and ****p<0.0001)

The NfκB protein level significantly decreased in the *Hexa-/-Neu3-/-* cortex compared to untreated ones after each treatment conditions (Figure 3.22 A, B). Interestingly, the NfκB protein level significantly increased in the *WT* cortex after short-term ketogenic diet treatment. Looking at the protein level of IκB-α, this protein level did not change after each treatment condition in 140-day-old *Hexa-/-Neu3-/-* mice cortex compared to untreated ones. In addition, IκB-α level also did not alter in *WT* and *Hexa-/-* mice cortex (Figure 3.22 A, C).

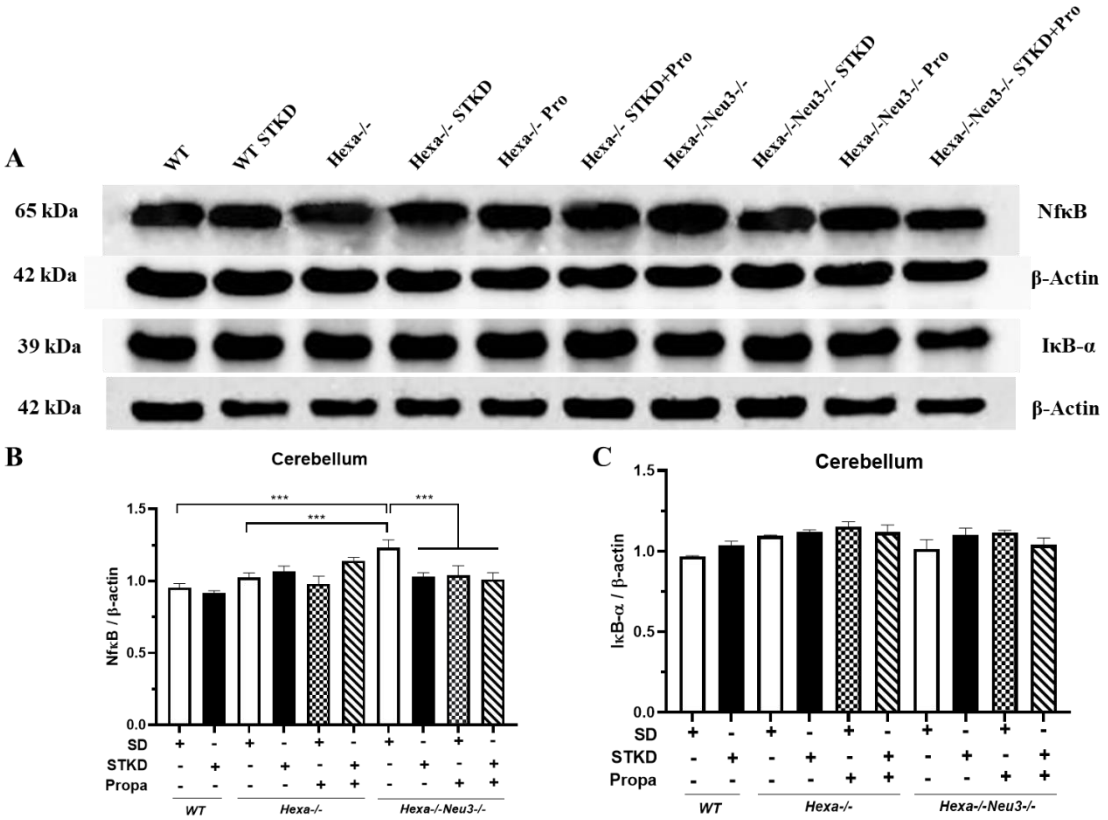


Figure 3.23 Western blotting analysis for NfκB and IκB-α in cerebellum region of 140-day-old *WT*, *Hexa-/-* and *Hexa-/-Neu3-/-* mice for the short-term ketogenic diet strategy (A). The histogram shows the ratio of NfκB/β-actin (B) and IκB-α/β-actin (C). Intensities were measured via ImageJ program. Data show mean ± SEM of measurements. Significant levels of data were determined using the one-way ANOVA. (n=3, *p<0.05, **p<0.01, ***p<0.001 and ****p<0.0001)

The short-term ketogenic diet, propagermanium and combined ketogenic diet and propagermanium treatments significantly reduced the NfκB protein level in the 140-day-old *Hexa-/-Neu3-/-* mice cerebellum compared to untreated ones (Figure 3.23 A, B). The *WT* and *Hexa-/-* displayed a lower NfκB protein level than untreated aged-matched *Hexa-/-Neu3-/-* mice cerebellum. The IκB-α protein level did not change between each genotype before each treatment condition. In addition, the short-term ketogenic diet and propagermanium treatment did not change the IκB-α protein level in the cerebellum (Figure 3.23 B, C).

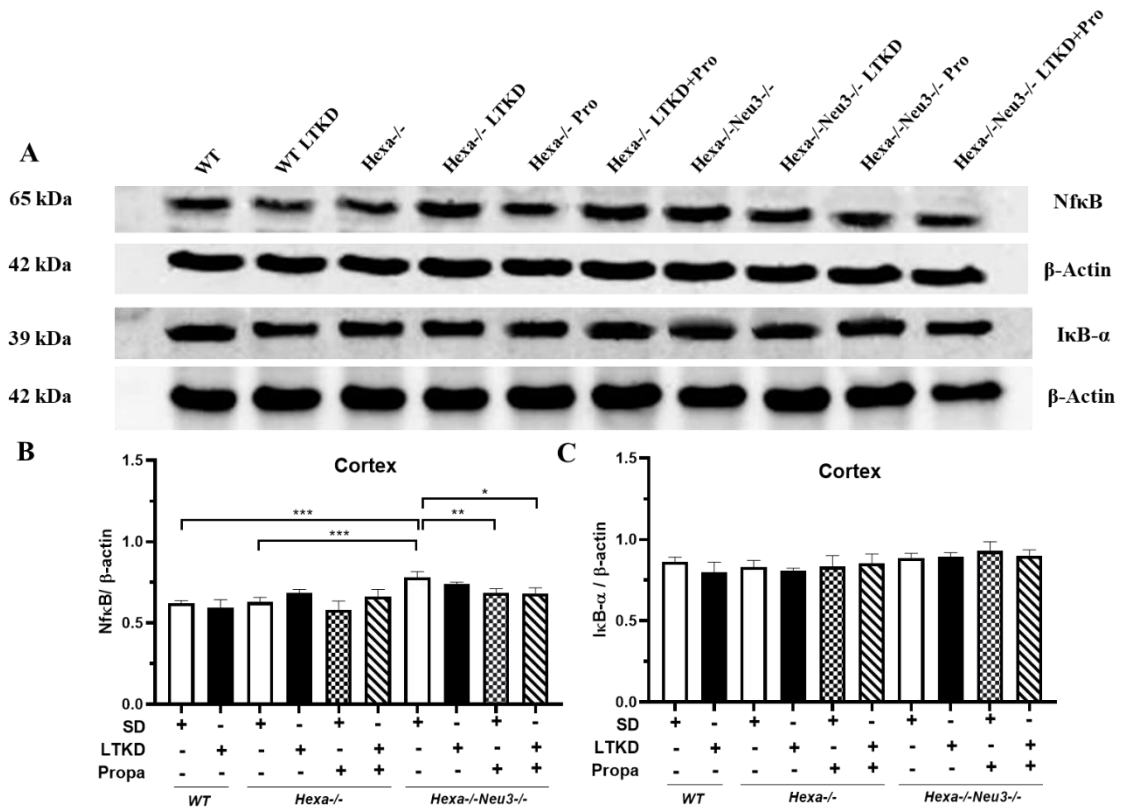


Figure 3.24 Western blotting analysis for NfκB and IκB-α in cortex region of 140-day-old *WT*, *Hexa-/-* and *Hexa-/-Neu3-/-* mice for the long-term ketogenic diet strategy (A). The histogram shows the ratio of NfκB/β-actin (B) and IκB-α/β-actin (C). Intensities were measured via ImageJ program. Data show mean ± SEM of measurements. Significant levels of data were determined using the one-way ANOVA. (n=3, *p<0.05, **p<0.01, ***p<0.001 and ****p<0.0001)

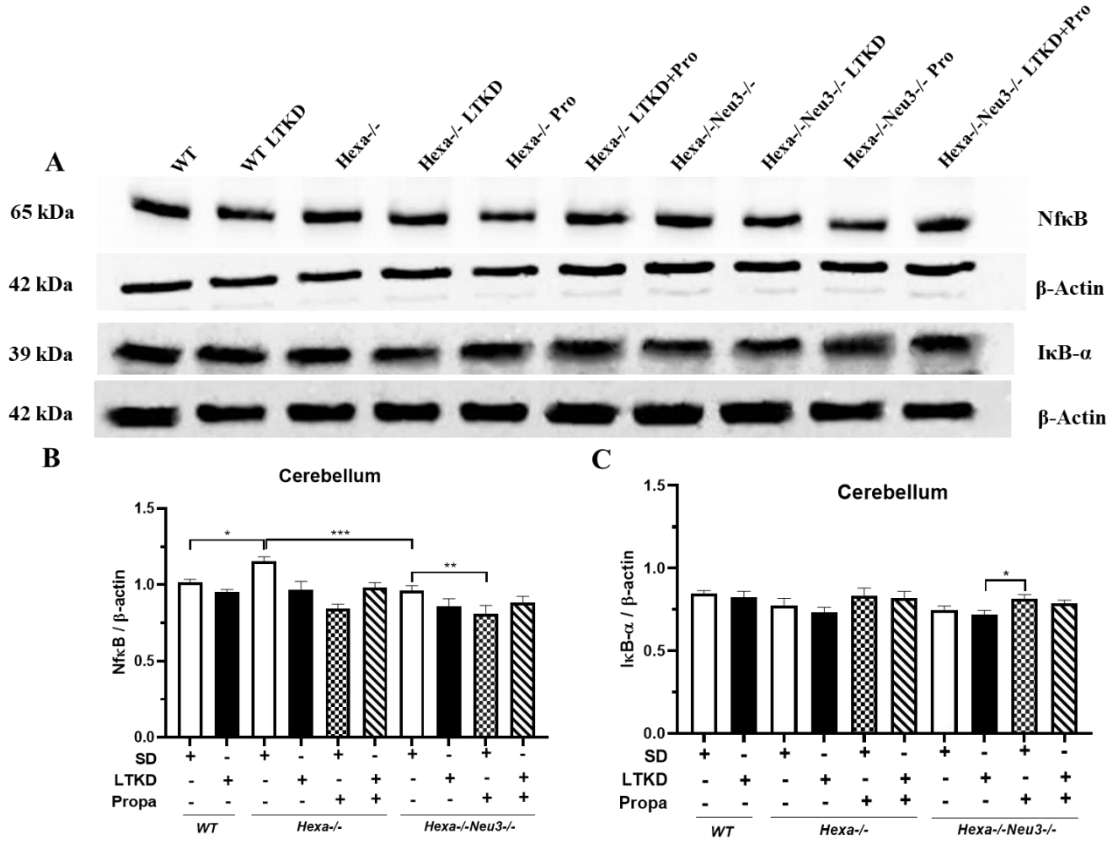


Figure 3.25 Western blotting analysis for NfκB and IκB-α in cerebellum region of 140-day-old *WT*, *Hexa-/-* and *Hexa-/-Neu3-/-* mice for the long-term ketogenic diet strategy (A). The histogram shows the ratio of NfκB/β-actin (B) and IκB-α/β-actin (C). Intensities were measured via ImageJ program. Data show mean ± SEM of measurements. Significant levels of data were determined using the one-way ANOVA. (n=3, *p<0.05, **p<0.01, ***p<0.001 and ****p<0.0001)

The propagermanium and combined long-term ketogenic diet and propagermanium treatments significantly reduced the NfκB protein level in the 140-day-old *Hexa-/-Neu3-/-* mice cortex compared to untreated ones (Figure 3.24 A, B). The NfκB protein level displayed significant elevation in the *Hexa-/-Neu3-/-* mice cortex compared to *WT*. The long-term ketogenic diet alone did not reduce the NfκB level significantly in *Hexa-/-Neu3-/-* mice compared to untreated ones. The IκB-α protein level did not increase after each treatment condition in 140-day-old *Hexa-/-Neu3-/-* mice cortex (Figure 3.24 A, C). The significant difference for IκB-α protein level was not found between each genotype and each treatment (Figure 3.24 A, C). In the cerebellum, the NfκB protein level increased in 140-day-old *Hexa-/-* mice compared to age-matched *WT* and *Hexa-/-Neu3-/-* mice. The propagermanium alone treatment significantly reduced the NfκB protein level in the *Hexa-/-Neu3-/-* mice cerebellum compared to untreated ones (Figure 3.25 A,

B). The IκB-α level significantly increased only in the 140-day-old *Hexa-/-Neu3-/-* mice after propagermanium treatment compared to *Hexa-/-Neu3-/-* mice which were treated by long-term ketogenic diet in the cerebellum (Figure 3.25 A, C).

### 3.4.3 Immunofluorescence Staining

The immunofluorescence staining was performed to determine localization and intensity of the NeuN, GFAP, MOMA-2, and CNPase by fixated brain samples of untreated and treated mice.

#### 3.4.3.1 NeuN Staining

NeuN staining was performed for cortex and cerebellum tissues of 140-day-old *WT*, *Hexa-/-* and *Hexa-/-Neu3-/-* mice, untreated, and two treatment strategies (short-term and long-term) to determine neuronal intensity.

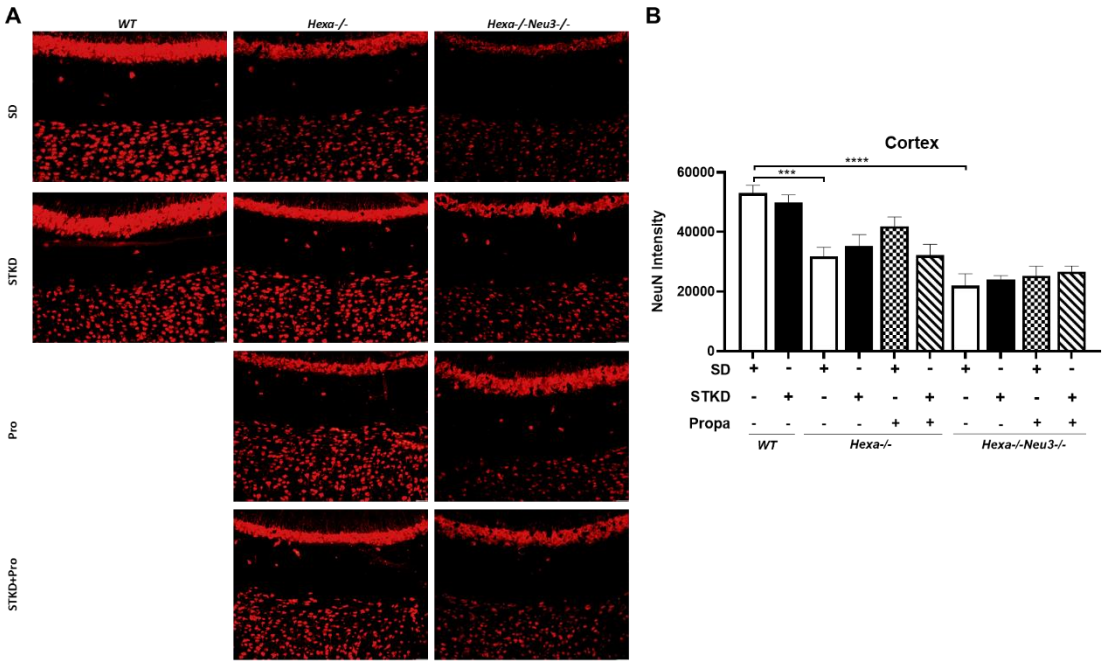


Figure 3.26 Immunostaining of the NeuN in the cortex of 140-day-old *WT*, *Hexa-/-* and *Hexa-/-Neu3-/-* mice brain coronal sections for short-term ketogenic diet strategy (B). Images were taken at 20X magnification and under the same light exposure. The histogram shows the intensity of the NeuN for the treated and untreated of each genotype. Intensities were measured via ImageJ program. Data show mean ± SEM of measurements. Significant levels of data were determined using the one-way ANOVA. (n=3, *p<0.05, **p<0.01, ***p<0.001 and ****p<0.0001)

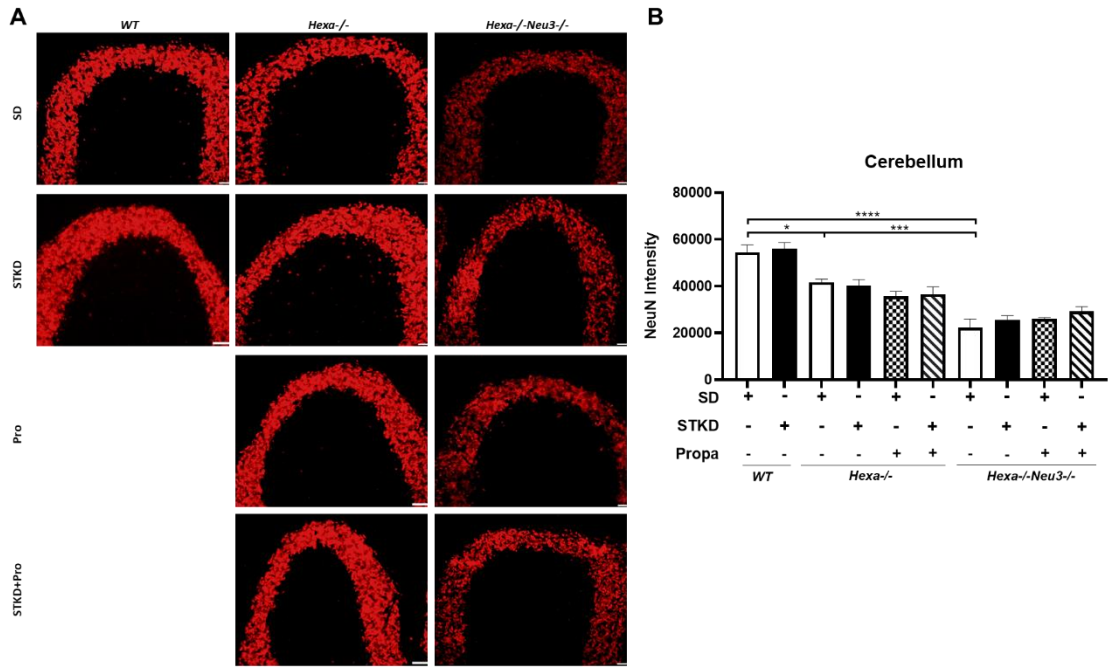


Figure 3.27 Immunostaining of the NeuN in the cerebellum of 140-day-old *WT*, *Hexa-/-* and *Hexa-/-Neu3-/-* mice brain coronal sections for short-term ketogenic diet strategy (A). Images were taken at 20X magnification and under the same light exposure. The histogram shows the intensity of the NeuN for the treated and untreated of each genotype. Intensities were measured via ImageJ program. Data show mean ± SEM of measurements. Significant levels of data were determined using the one-way ANOVA. (n=3, *p<0.05, **p<0.01, ***p<0.001 and ****p<0.0001)

The NeuN intensity significantly decreased in the cortex region of 140-day-old *Hexa-/-Neu3-/-* and *Hexa-/-* mice compared to age-matched *WT* mice. The short-term ketogenic diet and propagermanium treatments did not alter the neuronal density in the cortex of *Hexa-/-Neu3-/-* mice compared to the untreated ones (Figure 3.26 A, B). In the cerebellum, neuronal density significantly decreased in the *Hexa-/-Neu3-/-* mice, similar to the cortex compared to *WT* and *Hexa-/-* mice. The short-term ketogenic diet treatment strategy did not improve neuronal density in the cerebellum of *Hexa-/-Neu3-/- mice* (Figure 3.27 A, B).

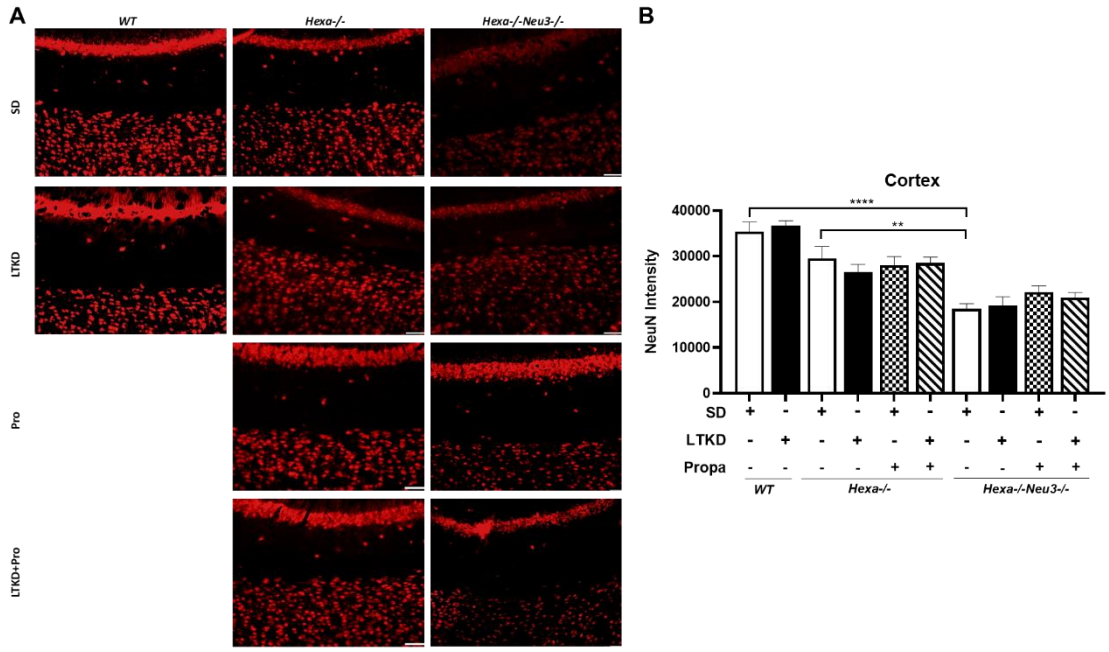


Figure 3.28 Immunostaining of the NeuN in the cortex of 140-day-old *WT*, *Hexa-/-* and *Hexa-/-Neu3-/-* mice brain coronal sections for long-term ketogenic diet strategy (A). Images were taken at 20X magnification and under the same light exposure. The histogram shows the intensity of the NeuN for the treated and untreated of each genotype. Intensities were measured via ImageJ program. Data show mean ± SEM of measurements. Significant levels of data were determined using the one-way ANOVA. (n=3, *p<0.05, **p<0.01, ***p<0.001 and ****p<0.0001)

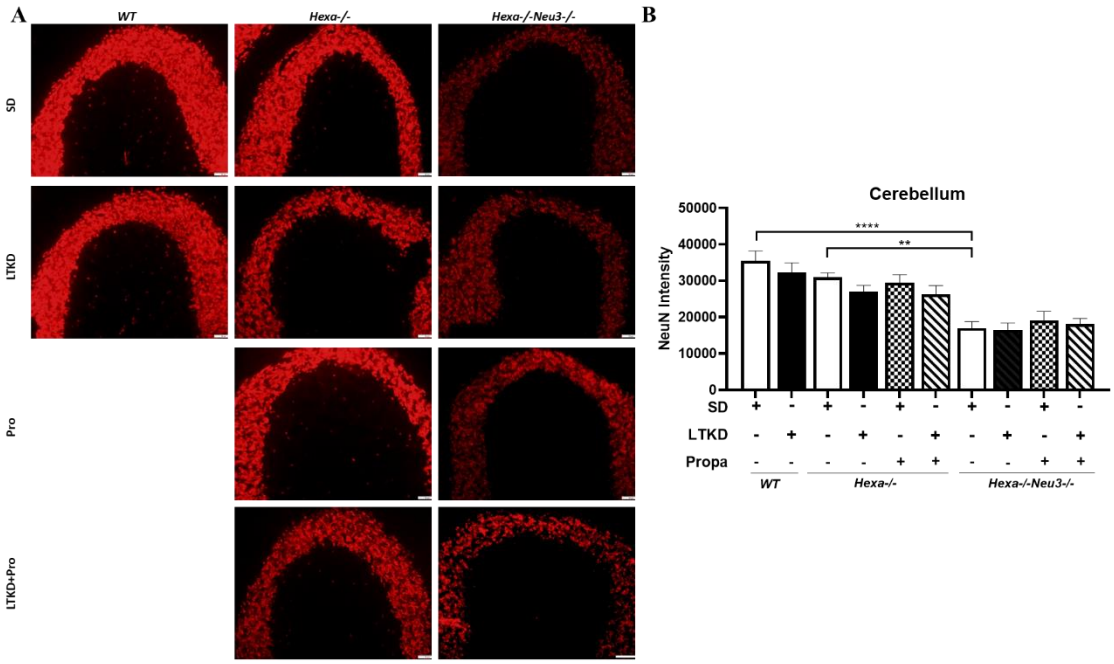


Figure 3.29 Immunostaining of the NeuN in the cerebellum of 140-day-old *WT*, *Hexa-/-* and *Hexa-/-Neu3-/-* mice brain coronal sections for long-term ketogenic diet strategy (A). Images were taken at 20X magnification and under the same light exposure. The histogram shows the intensity of the NeuN for the treated

and untreated of each genotype. Intensities were measured via ImageJ program. Data show mean ± SEM of measurements. Significant levels of data were determined using the one-way ANOVA. (n=3, *p<0.05, **p<0.01, ***p<0.001 and ****p<0.0001)

The long-term ketogenic diet treatment strategy did not ameliorate neuronal loss in the *Hexa-/-Neu3-/-* mice cortex (Figure 3.28 A, B). The results displayed neuronal loss in the *Hexa-/-Neu3-/-* cortex compared to age-matched *WT* and *Hexa-/-* mice cortex. In the cerebellum, similar to the cortex result, there is no improvement of the neuronal density in the *Hexa-/-Neu3-/-* mice compared to untreated ones (Figure 3.29 A, C).

### 3.4.3.2 GFAP Staining

The cortex and cerebellum sections from 140-day-old *WT*, *Hexa-/-* and *Hexa-/-Neu3-/-* mice were stained with the anti-GFAP to determine astrocyte activation in the two different treatment strategies (short-term and long-term).

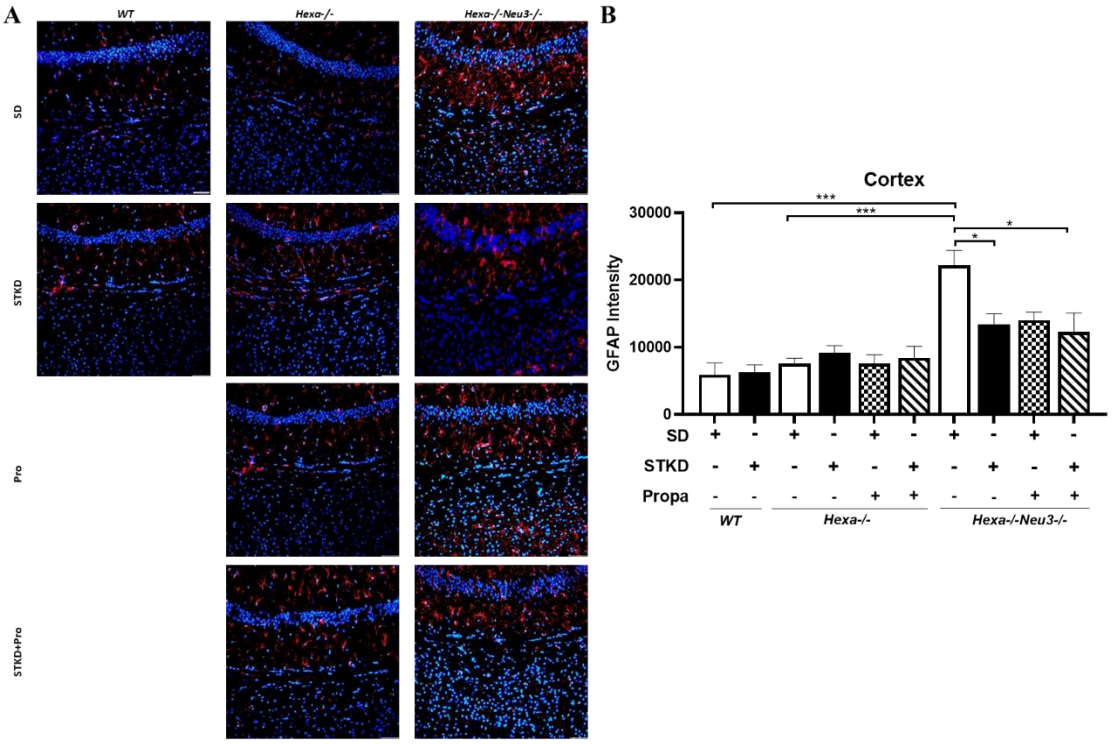


Figure 3.30 Immunostaining of the GFAP in the cortex of 140-day-old *WT*, *Hexa-/-* and *Hexa-/-Neu3-/-* mice brain coronal sections for short-term ketogenic diet strategy (A). Images were taken at 20X magnification and under the same light exposure. The histogram shows the intensity of the GFAP for the treated and untreated of each genotype. Intensities were measured via ImageJ program. Data show mean ± SEM of measurements. Significant levels of data

were determined using the one-way ANOVA. (n=3, *p<0.05, **p<0.01, ***p<0.001 and ****p<0.0001)

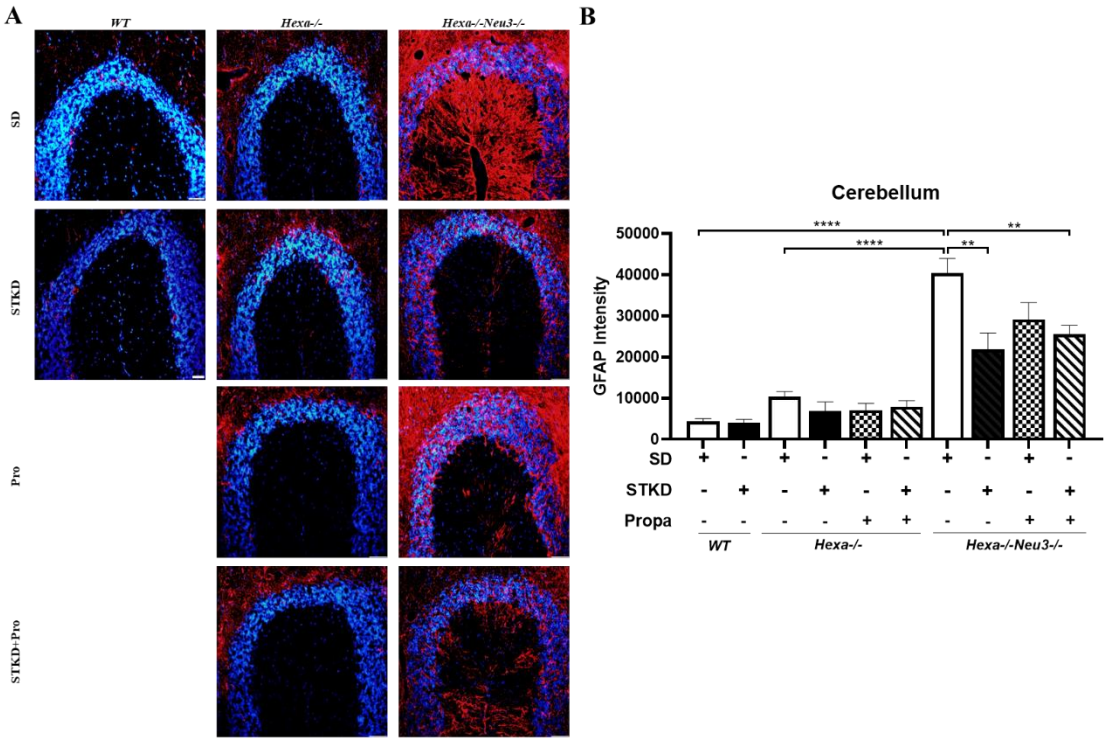


Figure 3.31 Immunostaining of the GFAP in the cerebellum of 140-day-old *WT*, *Hexa-/-* and *Hexa-/-Neu3-/-* mice brain coronal sections for short-term ketogenic diet strategy (A). Images were taken at 20X magnification and under the same light exposure. The histogram shows the intensity of the GFAP for the treated and untreated of each genotype. Intensities were measured via ImageJ program. Data show mean ± SEM of measurements. Significant levels of data were determined using the one-way ANOVA. (n=3, *p<0.05, **p<0.01, ***p<0.001 and ****p<0.0001)

The glial fibrillary associated protein (GFAP) intensity significantly increased in the 140-day-old *Hexa-/-Neu3-/-* mice cortex compared to age-matched *WT* and *Hexa-/-* mice. In addition, the short-term ketogenic diet and combined ketogenic diet and propagermanium treatments mitigated GFAP intensity which is associated with astrocyte activation (Figure 3.30 A, B). In the cerebellum, GFAP intensity is the highest in the 140-day-old *Hexa-/-Neu3-/-* mice. There was a significant reduction in GFAP density in the cerebellum of *Hexa-/-Neu3-/-* mice treated with short-term ketogenic diet and combined ketogenic diet and propagermanium, but not with propagermanium alone (Figure 3.31 A, B).

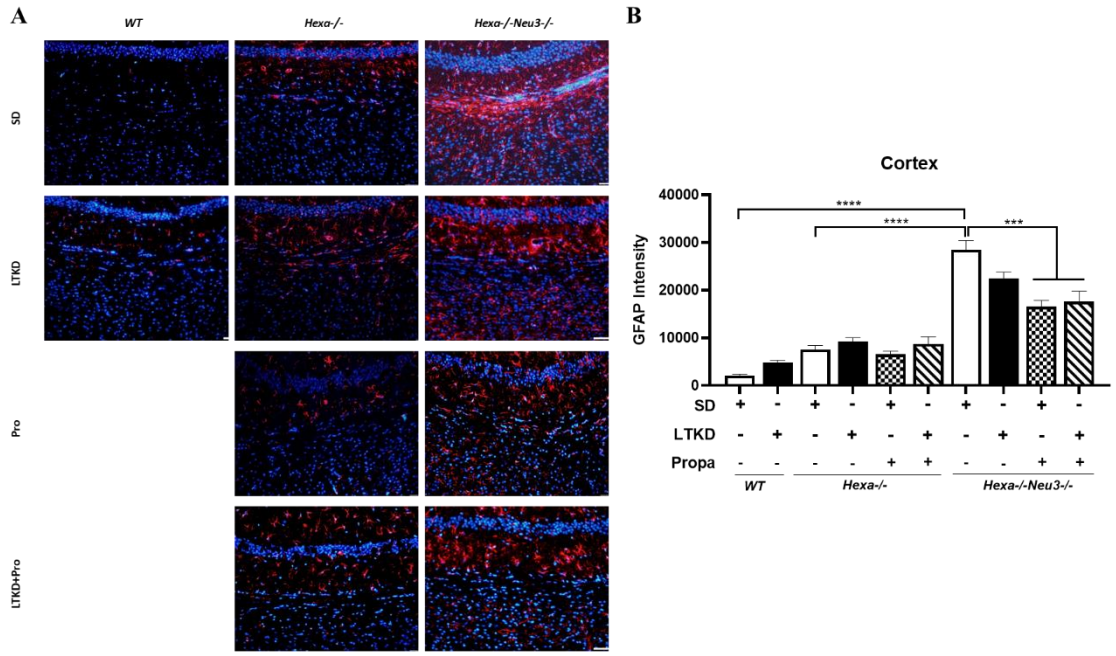


Figure 3.32 Immunostaining of the GFAP in the cortex of 140-day-old *WT*, *Hexa-/-* and *Hexa-/-Neu3-/-* mice brain coronal sections for long-term ketogenic diet strategy (A). Images were taken at 20X magnification and under the same light exposure. The histogram shows the intensity of the GFAP for the treated and untreated of each genotype. Intensities were measured via ImageJ program. Data show mean ± SEM of measurements. Significant levels of data were determined using the one-way ANOVA. (n=3, *p<0.05, **p<0.01, ***p<0.001 and ****p<0.0001)

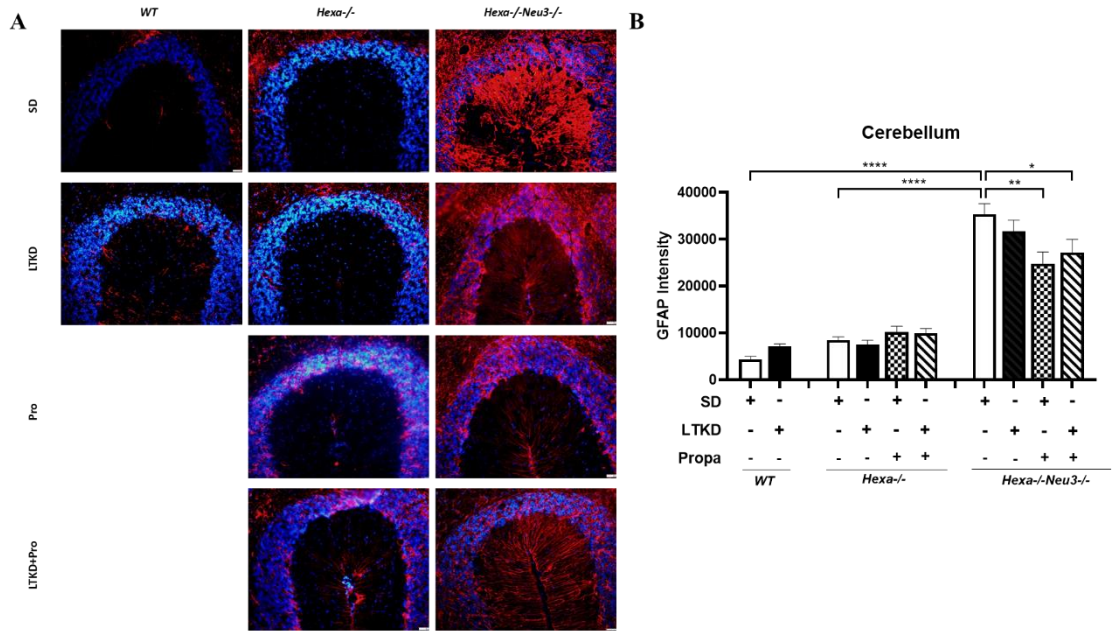


Figure 3.33 Immunostaining of the GFAP in the cerebellum of 140-day-old *WT*, *Hexa-/-* and *Hexa-/-Neu3-/-* mice brain coronal sections for long-term ketogenic diet strategy (A). Images were taken at 20X magnification and under the same light exposure. The histogram shows the intensity of the GFAP for the treated and untreated of each genotype. Intensities were measured via ImageJ

program. Data show mean ± SEM of measurements. Significant levels of data were determined using the one-way ANOVA. (n=3, *p<0.05, **p<0.01, ***p<0.001 and ****p<0.0001)

The long-term ketogenic diet strategy in the cortex significantly decreased GFAP intensity after the propagermanium alone and the combined ketogenic diet and propagermanium treatments however, long-term ketogenic diet treatment did not reduce the intensity statistically significant (Figure 3.32 A, B). Regarding cerebellum tissue, which showed similar results to the cortex, propagermanium alone and combined ketogenic diet and propagermanium treatments significantly reduced GFAP density in 140-day-old *Hexa-/-Neu3-/-* mice compared to untreated mice. (Figure 3.33 A, B).

### 3.4.3.3 MOMA-2 Staining

The MOMA-2 staining was performed to illustrate monocyte/macrophage activation in the cortex and cerebellum region of the 140-day-old *WT*, *Hexa-/-* and *Hexa-/-Neu3-/-* mice after two different treatment strategies (short-term and long-term).

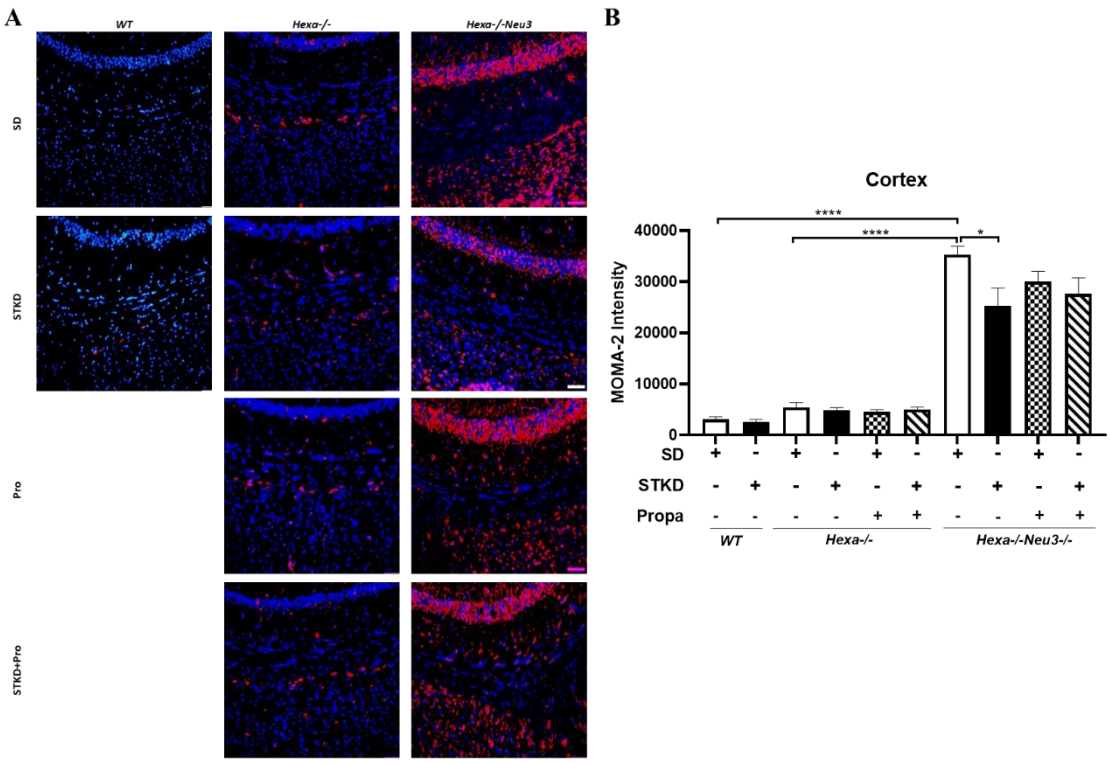


Figure 3.34 Immunostaining of the MOMA-2 in the cortex of 140-day-old *WT*, *Hexa-/-* and *Hexa-/-Neu3-/-* mice brain coronal sections for short-term ketogenic diet strategy (A). Images were taken at 20X magnification and under the same

light exposure. The histogram shows the intensity of the MOMA-2 for the treated and untreated of each genotype. Intensities were measured via ImageJ program. Data show mean ± SEM of measurements. Significant levels of data were determined using the one-way ANOVA. (n=3, *p<0.05, **p<0.01, ***p<0.001 and ****p<0.0001)

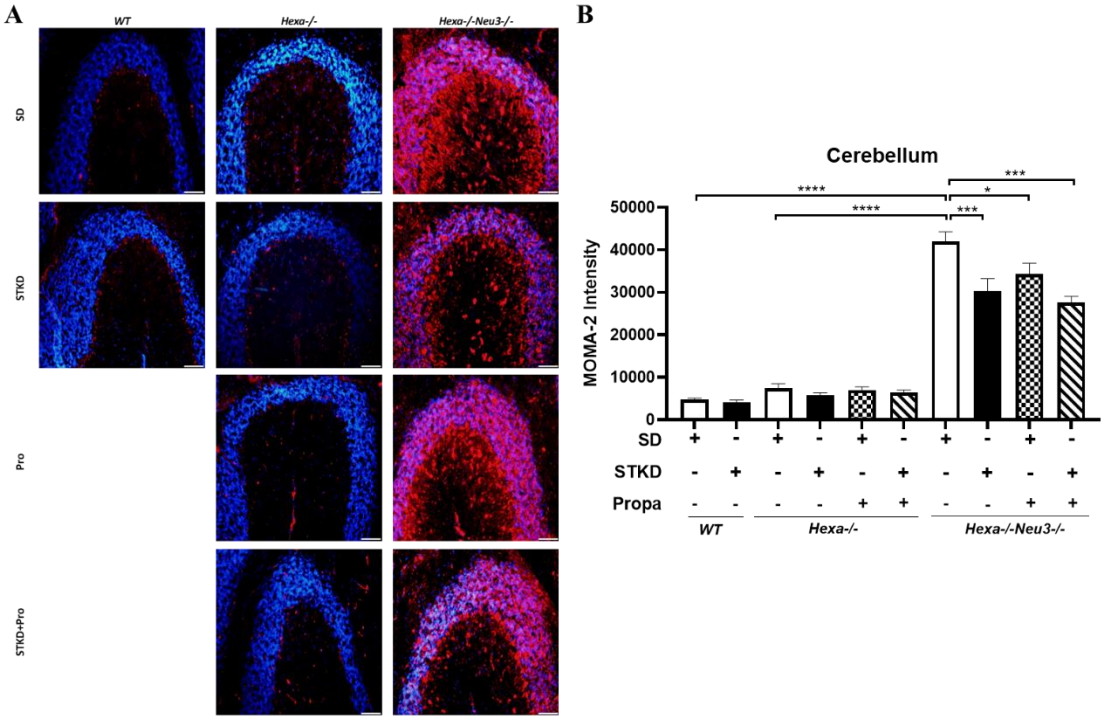


Figure 3.35 Immunostaining of the MOMA-2 in the cerebellum of 140-day-old *WT*, *Hexa-/-* and *Hexa-/-Neu3-/-* mice brain coronal sections for short-term ketogenic diet strategy (A). Images were taken at 20X magnification and under the same light exposure. The histogram shows the intensity of the MOMA-2 for the treated and untreated of each genotype. Intensities were measured via ImageJ program. Data show mean ± SEM of measurements. Significant levels of data were determined using the one-way ANOVA. (n=3, *p<0.05, **p<0.01, ***p<0.001 and ****p<0.0001)

The monocyte/macrophage marker of the MOMA-2 intensity significantly increased in the 140-day-old *Hexa-/-Neu3-/-* mice cortex compared to age-matched *WT* and *Hexa-/-* mice. After short-term ketogenic diet treatment, MOMA-2 intensity mitigated in the *Hexa-/-Neu3-/-* mice cortex but, propagermanium and combined ketogenic diet and propagermanium treatments did not reduce the MOMA-2 intensity significantly (Figure 3.34 A, B). The MOMA-2 intensity similar to cortex significantly increased in the *Hexa-/-Neu3-/-* cerebellum compared to age-matched *WT* and *Hexa-/-* mice. Unlike the cortex, there was a statistically significant decrease in MOMA-2 intensity in the cerebellum of *Hexa-/-Neu3-/-* mice compared to untreated ones after each treatment condition (Figure 3.35 A, B).

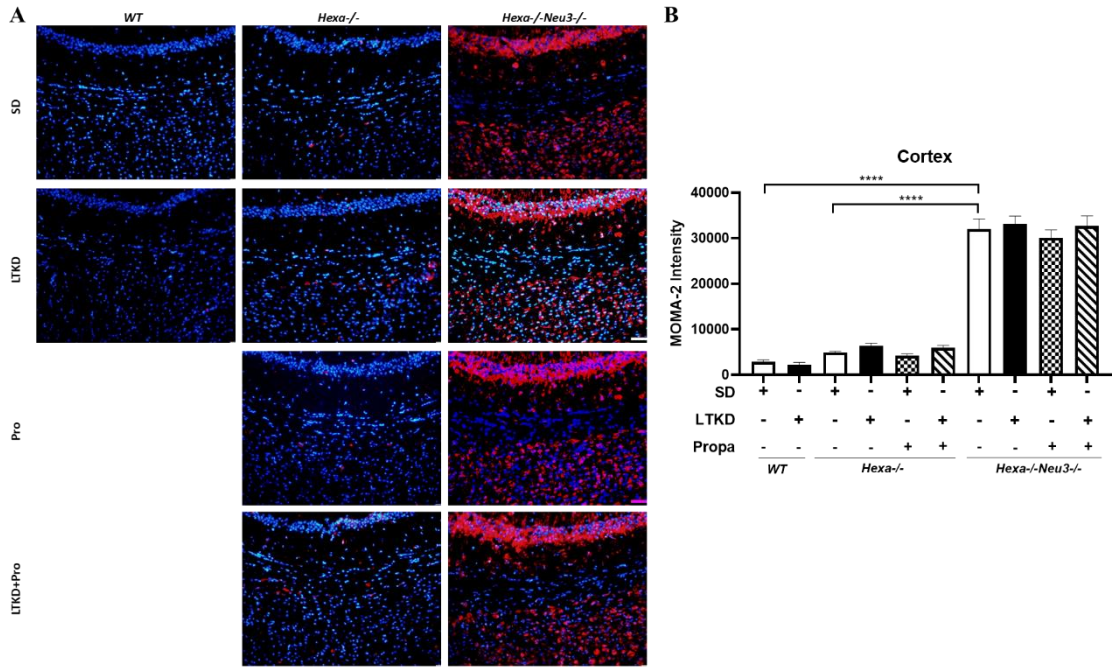


Figure 3. 36 Immunostaining of the MOMA-2 in the cortex of 140-day-old *WT*, *Hexa-/-* and *Hexa-/-Neu3-/-* mice brain coronal sections for long-term ketogenic diet strategy (A). Images were taken at 20X magnification and under the same light exposure. The histogram shows the intensity of the MOMA-2 for the treated and untreated of each genotype. Intensities were measured via ImageJ program. Data show mean ± SEM of measurements. Significant levels of data were determined using the one-way ANOVA. (n=3, *p<0.05, **p<0.01, ***p<0.001 and ****p<0.0001)

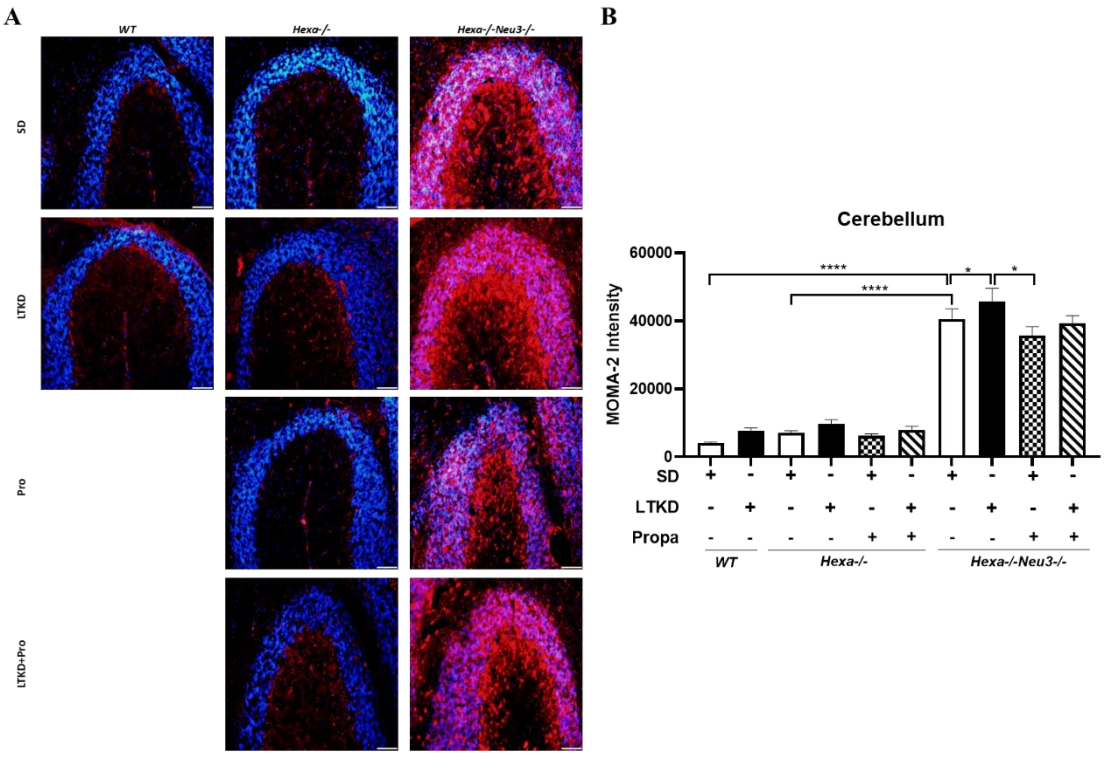

Figure 3.37 Immunostaining of the MOMA-2 in the cerebellum of 140-day-old *WT*, *Hexa-/-* and *Hexa-/-Neu3-/-* mice brain coronal sections for long-term ketogenic diet strategy (A). Images were taken at 20X magnification and under the same light exposure. The histogram shows the intensity of the MOMA-2 for the treated and untreated of each genotype. Intensities were measured via ImageJ program. Data show mean ± SEM of measurements. Significant levels of data were determined using the one-way ANOVA. (n=3, *p<0.05, **p<0.01, ***p<0.001 and ****p<0.0001)

The long-term ketogenic diet treatment strategy did not alter the MOMA-2 intensity in the *Hexa-/-Neu3-/-* mice cortex compared to untreated ones (Figure 3.36 A, B). Interestingly, the long-term ketogenic diet treatment increased the MOMA-2 intensity in the *Hexa-/-Neu3-/-* mice cerebellum compared to untreated ones (Figure 3.37 A, B) however, propagermanium alone and combined long-term ketogenic diet and propagermanium treatments did not improve the monocyte/macrophage activation in the *Hexa-/-Neu3-/-* mice cerebellum.

### 3.4.3.4 CNPase Staining

The CNPase staining was performed to measure oligodendrocyte levels after short-term and long-term ketogenic diet strategies in the 140-day-old *WT*, *Hexa-/-* and *Hexa-/-Neu3-/-* mice cortex and cerebellum.

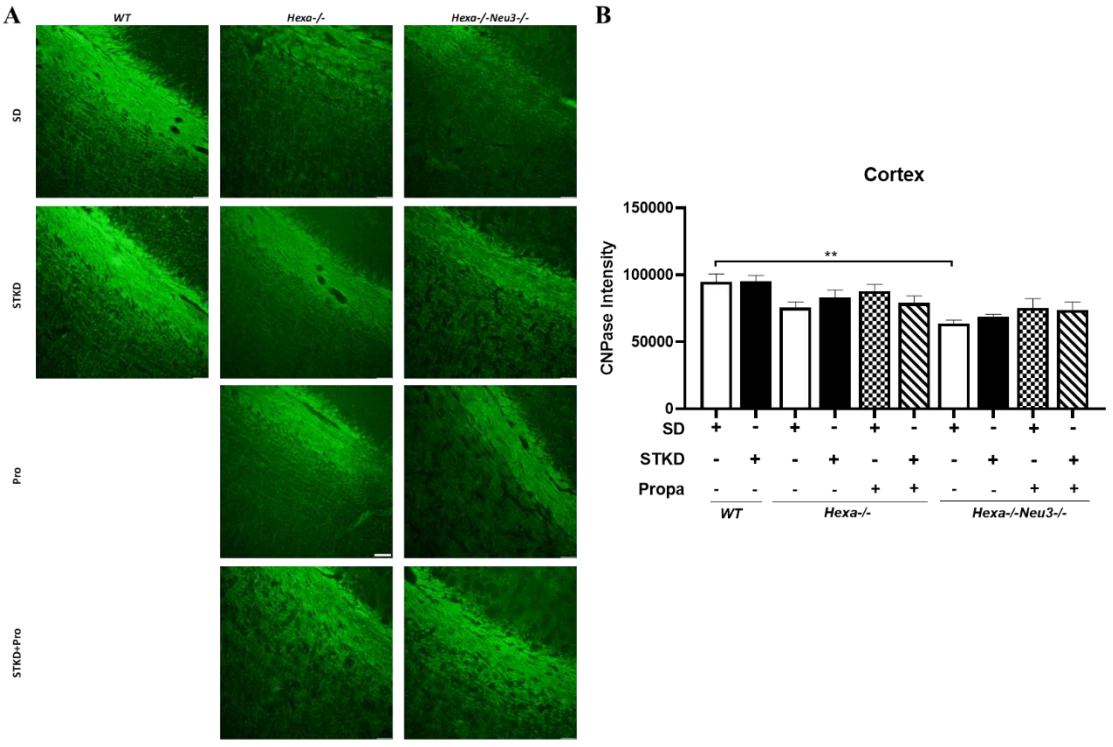

Figure 3.38 Immunostaining of the CNPase in the cortex of 140-day-old *WT*, *Hexa-/-* and *Hexa-/-Neu3-/-* mice brain coronal sections for short-term ketogenic diet strategy (A). Images were taken at 20X magnification and under the same light exposure. The histogram shows the intensity of the CNPase for the treated and untreated of each genotype. Intensities were measured via ImageJ program. Data show mean ± SEM of measurements. Significant levels of data were determined using the one-way ANOVA. (n=3, *p<0.05, **p<0.01, ***p<0.001 and ****p<0.0001)

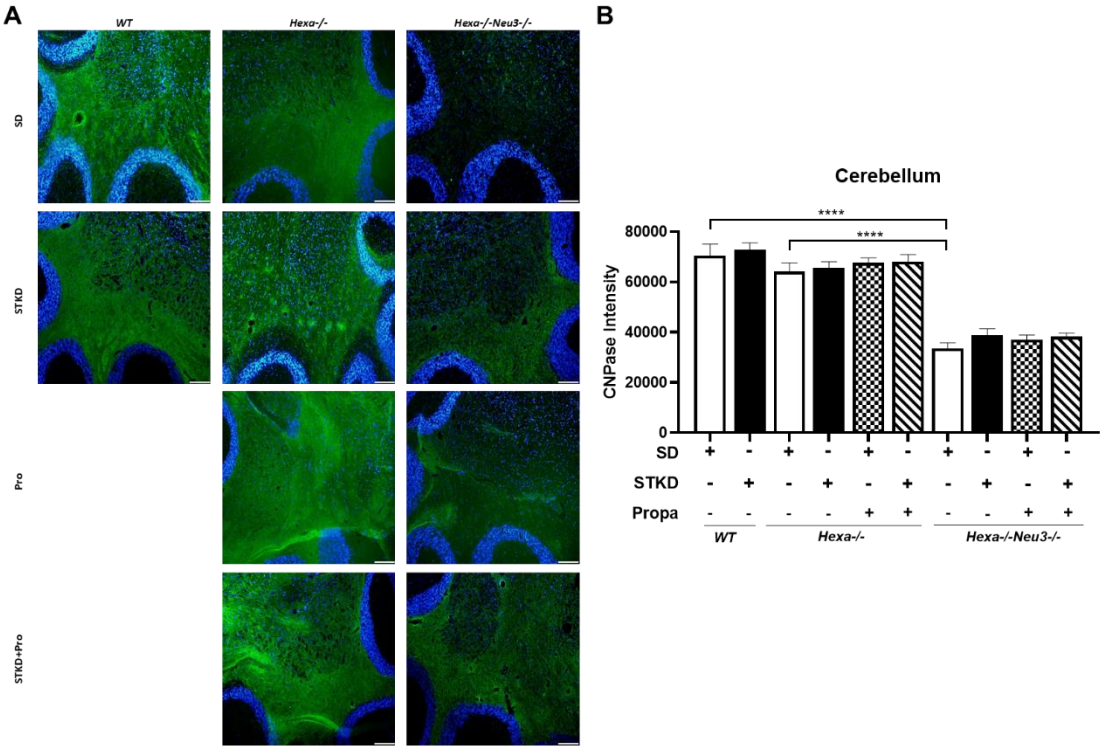


Figure 3.39 Immunostaining of the CNPase in the cerebellum of 140-day-old *WT*, *Hexa-/-* and *Hexa-/-Neu3-/-* mice brain coronal sections for short-term ketogenic diet strategy (A). Images were taken at 10X magnification and under the same light exposure. The histogram shows the intensity of the CNPase for the treated and untreated of each genotype. Intensities were measured via ImageJ program. Data show mean ± SEM of measurements. Significant levels of data were determined using the one-way ANOVA. (n=3, *p<0.05, **p<0.01, ***p<0.001 and ****p<0.0001)

The CNPase intensity significantly decreased in the 140-day-old *Hexa-/-Neu3-/-* mice cortex compared to age-matched *WT* (Figure 3.38 A, B). The short-term ketogenic diet and propagermanium treatments did not increase the CNPase intensity which is associated with the myelin sheath formation in the *Hexa-/-Neu3-/-* mice cortex. In the cerebellum, CNPase intensity significantly decreased in the *Hexa-/-Neu3-/-* mice compared to *WT* and *Hexa-/-* mice (Figure 3.39 A, B). Short-term ketogenic diet and

propagermanium treatments did not alter CNPase intensity in the cerebellum of *Hexa-/-Neu3-/-* mice compared to untreated ones.

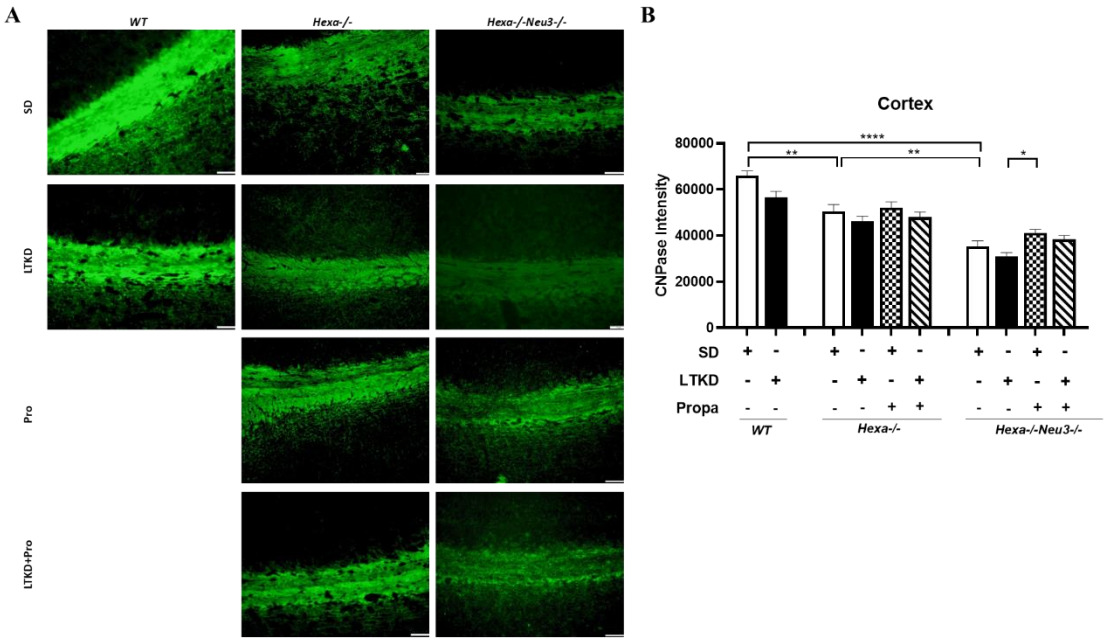


Figure 3.40 Immunostaining of the CNPase in the cortex of 140-day-old *WT*, *Hexa-/-* and *Hexa-/-Neu3-/-* mice brain coronal sections for long-term ketogenic diet strategy (A). Images were taken at 20X magnification and under the same light exposure. The histogram shows the intensity of the CNPase for the treated and untreated of each genotype. Intensities were measured via ImageJ program. Data show mean ± SEM of measurements. Significant levels of data were determined using the one-way ANOVA. (n=3, *p<0.05, **p<0.01, ***p<0.001 and ****p<0.0001)

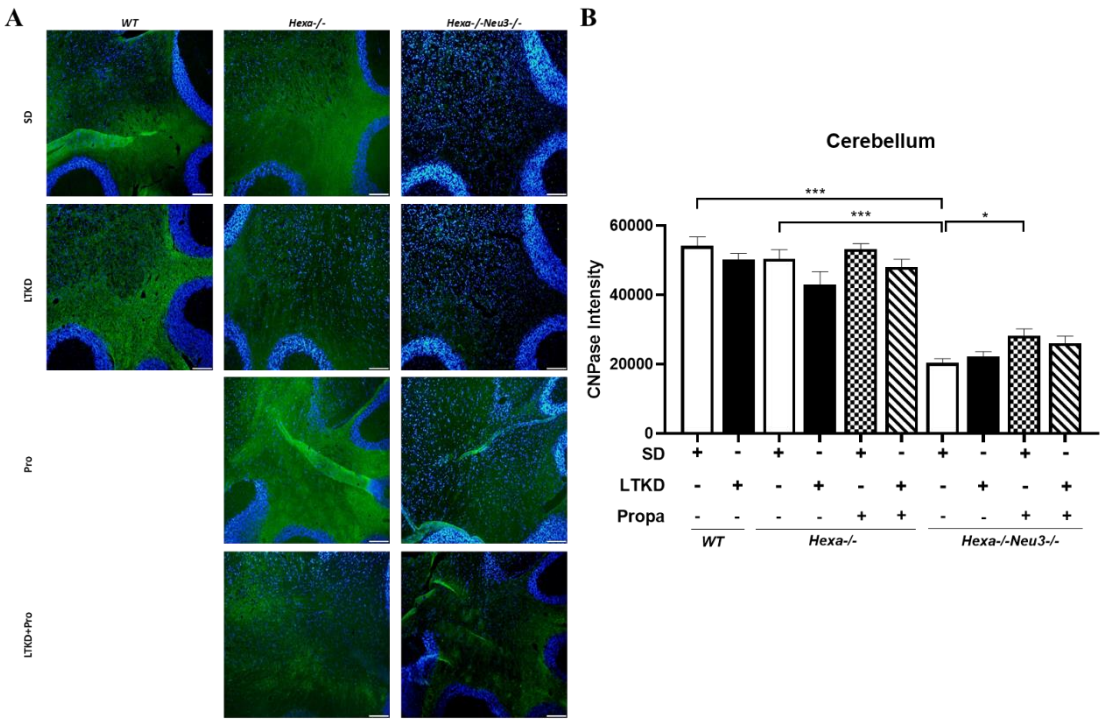


Figure 3.41 Immunostaining of the CNPase in the cerebellum of 140-day-old *WT*, *Hexa-/-* and *Hexa-/-Neu3-/-* mice brain coronal sections for long-term ketogenic diet strategy (A). Images were taken at 10X magnification and under the same light exposure. The histogram shows the intensity of the CNPase for the treated and untreated of each genotype. Intensities were measured via ImageJ program. Data show mean ± SEM of measurements. Significant levels of data were determined using the one-way ANOVA. (n=3, *p<0.05, **p<0.01, ***p<0.001 and ****p<0.0001)

Long-term ketogenic diet strategy did not improve the CNPase intensity in the *Hexa-/-Neu3-/-* mice cortex however, only statistically significant difference was observed between the long-term ketogenic diet alone and propagermanium alone treatments (Figure 3.40 A, B). In the cerebellum, CNPase intensity significantly increased after propagermanium alone treatment in the *Hexa-/-Neu3-/-* mice compared to untreated ones. The long-term ketogenic diet and combined long-term ketogenic diet and propagermanium treatments did not increase the CNPase intensity in the cerebellum of *Hexa-/-Neu3-/-* mice (Figure 3.41 A, B).

## 3.5 Autophagy Analysis

The short-term ketogenic diet and propagermanium treatment strategies effects on autophagic flux were investigated in cortex and cerebellum region for 140-day-old *WT*,

*Hexa-/-* and *Hexa-/-Neu3-/-* mice by q-PCR, western blotting and immunofluorescence staining by the support of TUBITAK-123Z087 project.

## 3.5.1 qRT-PCR Analysis

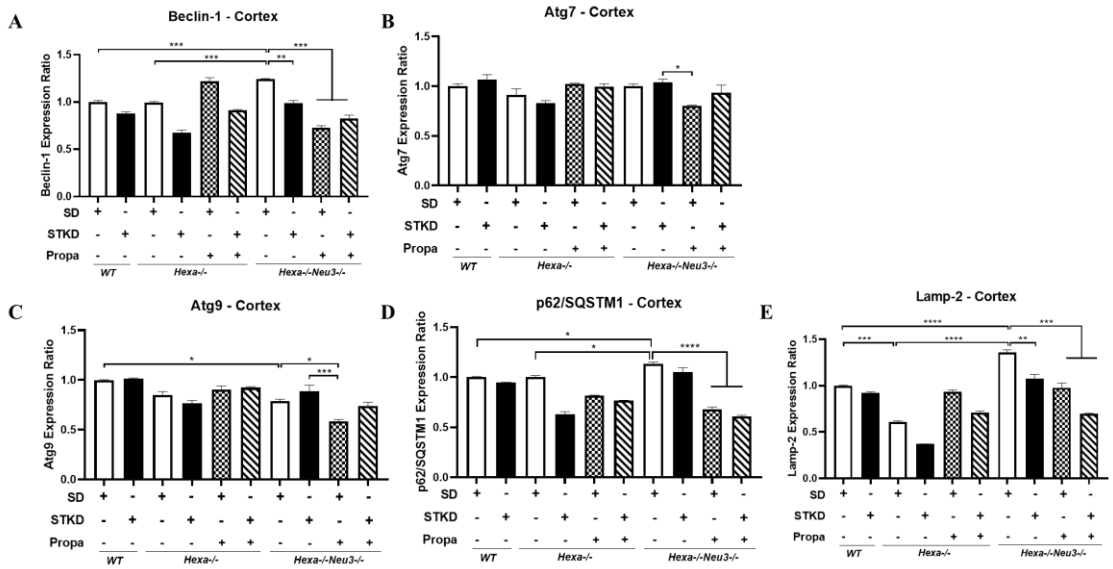


Figure 3.42 Relative expression levels of autophagy-related genes Beclin-1 (A), Atg7 (B), Atg9 (C), p62/SQSTM1 (D), and Lamp-2(E) genes in the short-term ketogenic diet strategy for 140-day-old *WT*, *Hexa-/-* and *Hexa-/-Neu3-/-* mice cortex. Data show mean ± SEM of measurements. Significant levels of data were determined using the one-way ANOVA. (n=3, *p<0.05, **p<0.01, ***p<0.001 and ****p<0.0001)

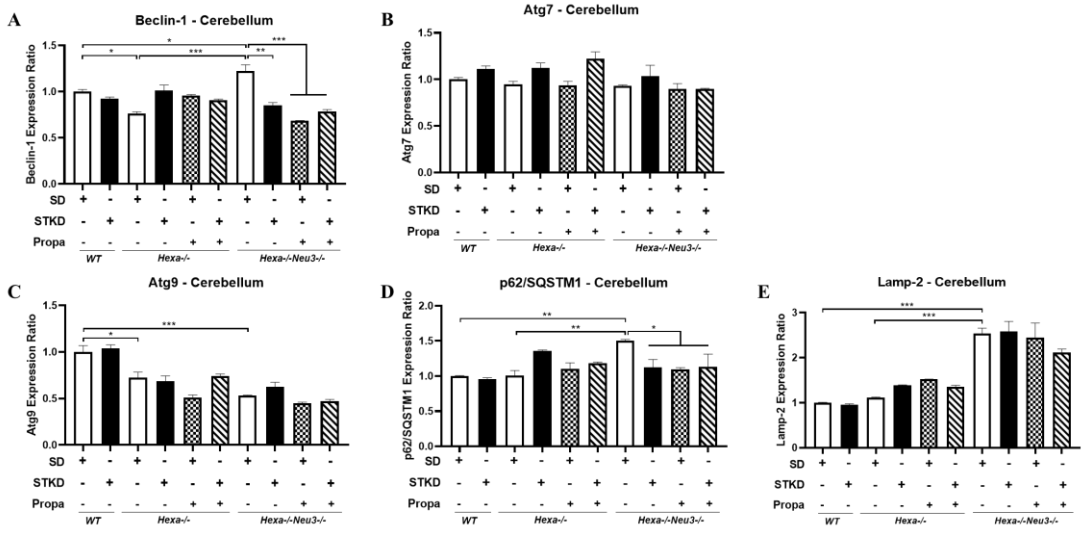


Figure 3.43 Relative expression levels of autophagy-related genes Beclin-1 (A), Atg7 (B), Atg9 (C), p62/SQSTM1 (D), and Lamp-2(E) genes in the short-term ketogenic diet strategy for 140-day-old *WT*, *Hexa-/-* and *Hexa-/-Neu3-/-* mice cerebellum. Data show mean ± SEM of measurements. Significant levels of

data were determined using the one-way ANOVA. (n=3, *p<0.05, **p<0.01, ***p<0.001 and ****p<0.0001)

The effects of short-term ketogenic diet and propagermanium treatment were analyzed in the cortex and cerebellum by q-PCR for autophagy markers including autophagic flux: *Beclin-1*, *Atg7*, *Atg9*, *p62/SQSTM1* and *Lamp2*. The *Beclin-1* gene expression level significantly increased in the 140-day-old *Hexa-/-Neu3-/-* mice cortex compared to age-matched *WT* and *Hexa-/-* mice. Each treatment condition was significantly decreased the Beclin-1 expression level in the *Hexa-/-Neu3-/-* mice cortex (Figure 3.42 A). The *Atg7* gene expression did not change in *Hexa-/-Neu3-/-* mice cortex compared to *WT* and *Hexa-/-* mice. The significant difference was observed between short-term ketogenic diet alone and propagermanium alone treatments for *Hexa-/-Neu3-/-* mice cortex (Figure 3.42 B). *Atg9* expression level significantly lower in *Hexa-/-Neu3-/-* mice cortex than *WT*. The short-term ketogenic diet treatment slightly increased the *Atg9* gene expression level in the *Hexa-/-Neu3-/-* mice cortex but this is not statistically significant. In contrast to a short-term ketogenic diet, propagermanium treatment alone significantly reduced the *Atg9* gene expression level in *Hexa-/-Neu3-/-* mouse cortex (Figure 3.42 C). p62/SQSTM1 expression level slightly increased in the *Hexa-/-Neu3-/-* mice compared to *WT* and *Hexa-/-* mice. Propagermanium alone and combined short-term ketogenic diet and propagermanium treatments significantly decreased the *p62/SQSTM1* expression level in the *Hexa-/-Neu3-/-* mice compared to untreated ones (Figure 3.42 D). In *Hexa-/-* mice cortex, *p62/SQSTM1* expression level significantly decreased after each treatment condition. *Lamp2* gene expression level is the highest in the *Hexa-/-Neu3-/-* mice cortex and each treatment condition significantly reduced this gene expression (Figure 3.42 E). In the cerebellum, *Beclin-1* gene expression level significantly increased in the *Hexa-/-Neu3-/-* mice similar to the cortex. Each treatment condition significantly mitigated the *Beclin-1* gene expression level compared to untreated ones (Figure 3.43 A). *Atg7* gene expression level did not alter after each treatment condition in *Hexa-/-Neu3-/-* mice (Figure 3.43 B). *Atg9* expression level significantly lower in *Hexa-/-Neu3-/-* mice compared to *WT*. The short-term ketogenic diet treatment slightly increased the Atg9 expression level, but it was not statistically significant (Figure 3.43 C). *p62/SQSTM1* expression level significantly increased in the *Hexa-/-Neu3-/-* mice cerebellum compared to *WT* and *Hexa-/-* mice and each treatment reduced this gene expression level in *Hexa-/-Neu3-/-* mice (Figure 3.43 D). Lamp2

expression level significantly higher in the *Hexa-/-Neu3-/-* mice cerebellum than *WT* and *Hexa-/-* mice and ketogenic diet and propagermanium treatments did not significantly alter the *Lamp2* expression level (Figure 3.43 E).

## 3.5.2 Western Blotting

The autophagic flux associated proteins (p62/SQSTM1 and LC3) were measured to examine the effects of short-term ketogenic diet and propagermanium treatments in the region of cortex and cerebellum.

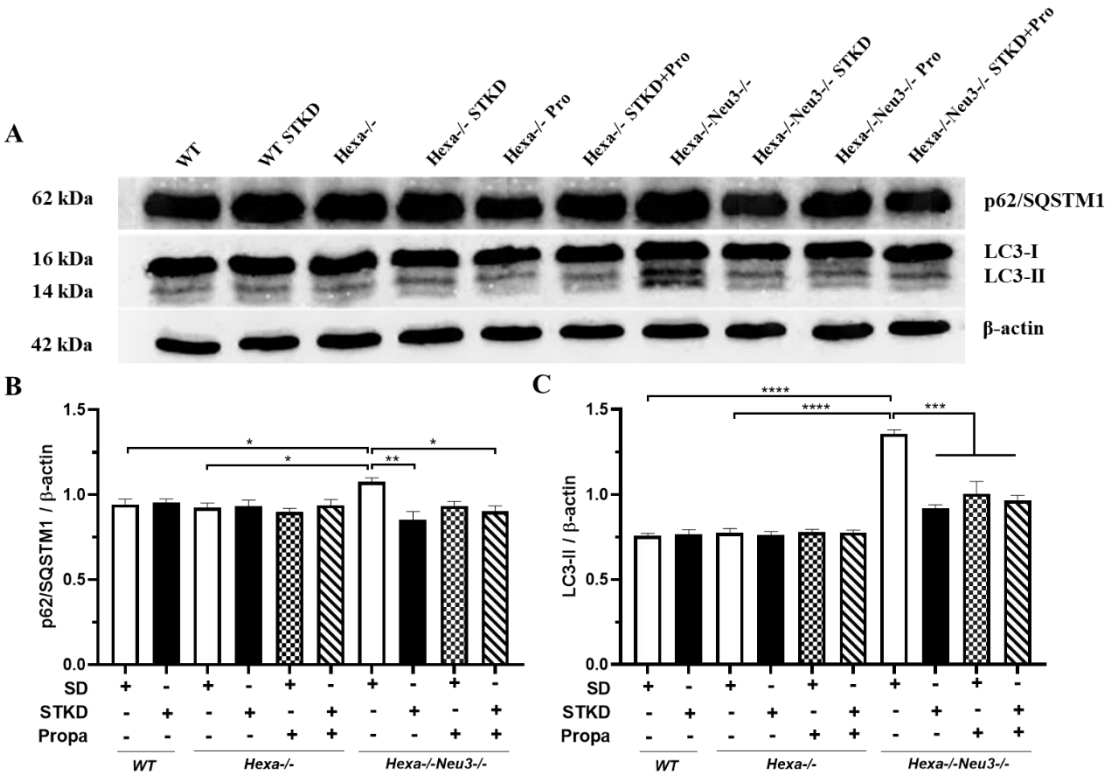


Figure 3.44 Western blotting analysis for p62/SQSTM1 and LC3-I and LC3-II in cortex region of 140-day-old *WT*, *Hexa-/-* and *Hexa-/-Neu3-/-* mice for the short-term ketogenic diet strategy (A). The histogram shows the ratio of p62/SQSTM1/β-actin (B) and LC3-II/ β-actin (C). Intensities were measured via ImageJ program. Data show mean ± SEM of measurements. Significant levels of data were determined using the one-way ANOVA. (n=3, *p<0.05, **p<0.01, ***p<0.001 and ****p<0.0001)

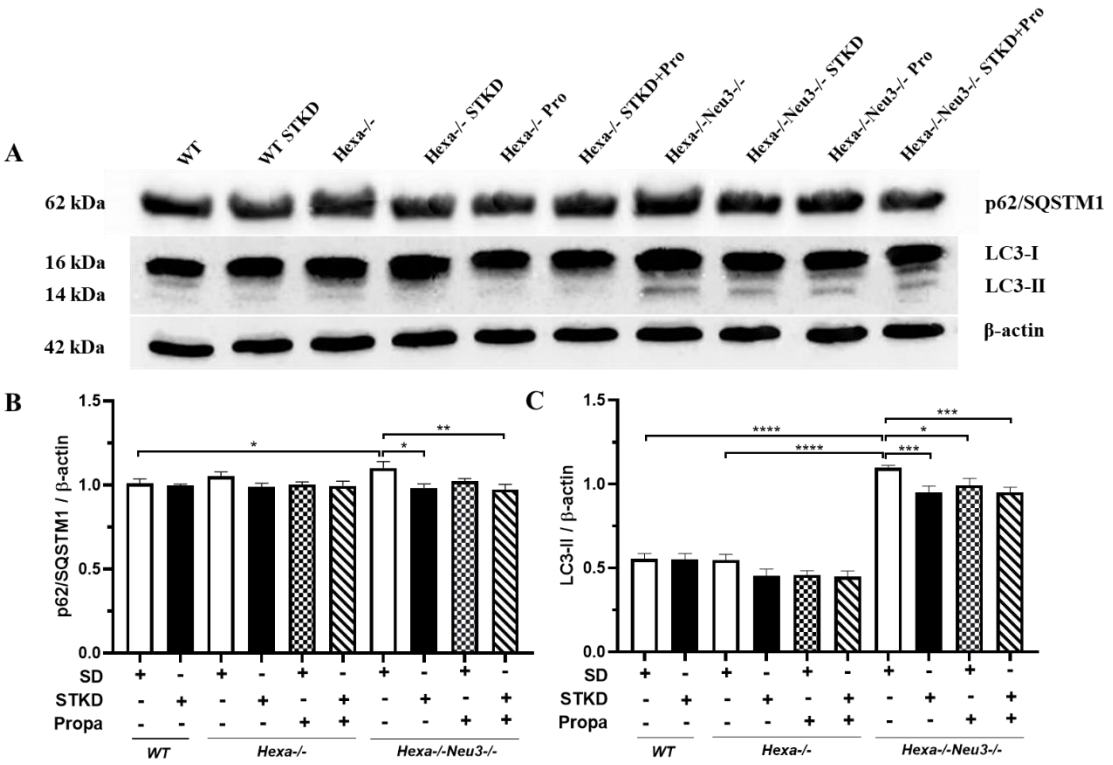


Figure 3.45 Western blotting analysis for p62/SQSTM1 and LC3-I and LC3-II in cerebellum region of 140-day-old *WT*, *Hexa-/-* and *Hexa-/-Neu3-/-* mice for the short-term ketogenic diet strategy (A). The histogram shows the ratio of p62/β-actin (B) and LC3-II/ β-actin (C). Intensities were measured via ImageJ program. Data show mean ± SEM of measurements. Significant levels of data were determined using the one-way ANOVA. (n=3, *p<0.05, **p<0.01, ***p<0.001 and ****p<0.0001)

The p62/SQSTM1 protein level is the highest in the 140-day-old *Hexa-/-Neu3-/-* mice cortex compared to age-matched *WT* and *Hexa-/-* mice. The short-term ketogenic diet and combined ketogenic diet and propagermanium treatments significantly reduced the p62/SQSTM1 in the *Hexa-/-Neu3-/-* mice cortex (Figure 3.44 A, B). When looking at the level of LC3-II protein, it was found that this protein accumulated more in the cortical region of *Hexa-/-Neu3-/-* mice compared to *WT* and *Hexa-/-* mice (Figure 3.44 A, C). In the cerebellum, p62/SQSTM1 protein level is higher in the 140-day-old *Hexa-/-Neu3-/-* mice than age-matched *WT*. Similar to what was detected in the cortex region, the p62/SQSTM1 protein level was significantly decreased in the cerebellum of *Hexa-/-Neu3-/-* mice after both the ketogenic diet and combined ketogenic diet and propagermanium administration (Figure 3.45 A, B). The LC3-II level is also higher in the *Hexa-/-Neu3-/-* mice cerebellum compared to *WT* and *Hexa-/-* mice. Each treatment condition was significantly reduced the LC3-II protein level compared to untreated ones (Figure 3.45 A, C).

### 3.5.3 Immunofluorescence Staining

The autophagic proteins of p62/SQSTM1 and LC3 were colocalized with the LAMP1 to visualize alteration of the autophagic flux after short-term ketogenic diet and propagermanium treatments in cortex and cerebellum regions of 140-day-old *WT*, *Hexa-/-* and *Hexa-/-Neu3-/-* mice.

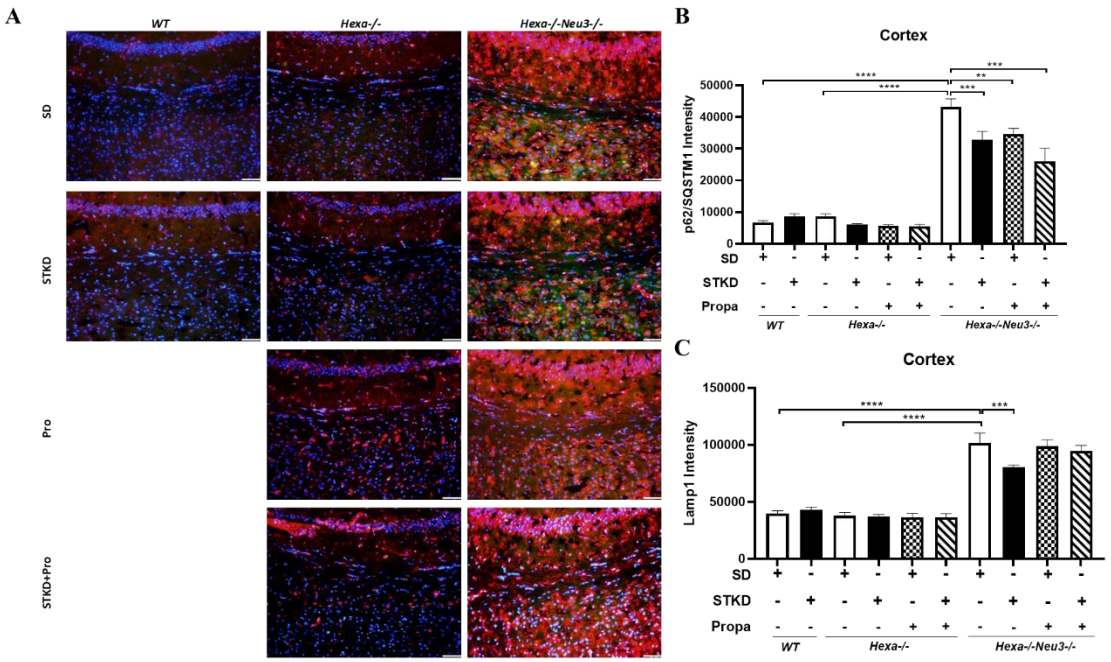


Figure 3.46 Immunostaining of the p62/SQSTM1 and Lamp1 in the cortex of 140-day-old *WT*, *Hexa-/-* and *Hexa-/-Neu3-/-* mice brain coronal sections for short-term ketogenic diet strategy (A). Images were taken at 20X magnification and under the same light exposure. The histogram shows the intensity of the p62/SQSTM1 (B) and Lamp1 (C) for the treated and untreated of each genotype. Intensities were measured via ImageJ program. Data show mean ± SEM of measurements. Significant levels of data were determined using the one-way ANOVA. (n=3, *p<0.05, **p<0.01, ***p<0.001 and ****p<0.0001)

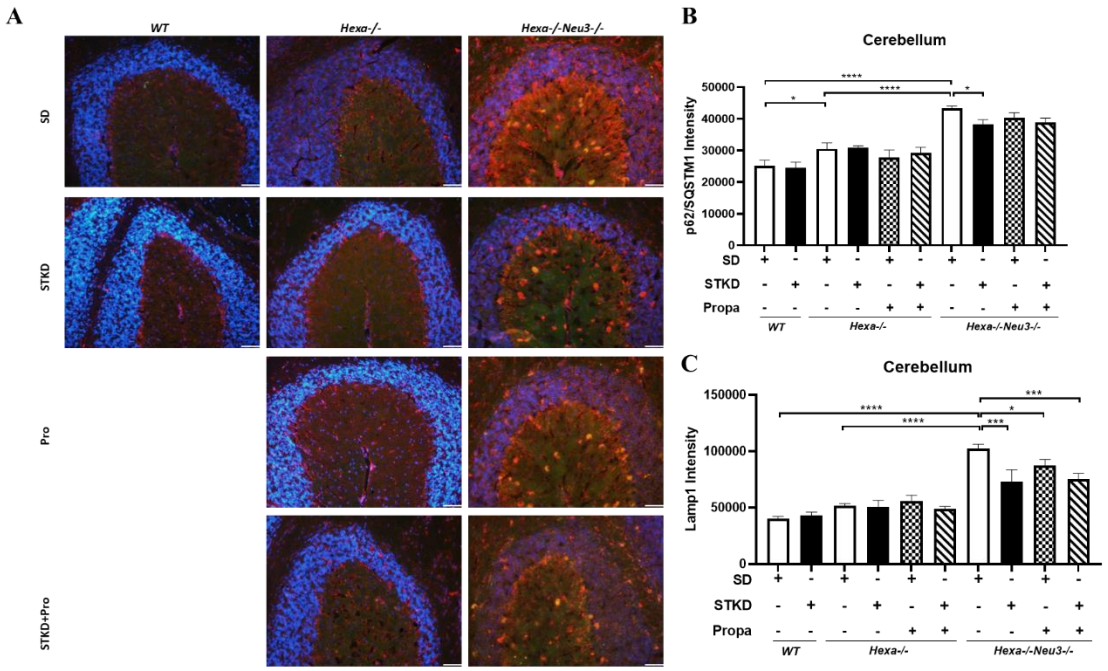


Figure 3.47 Immunostaining of the p62/SQSTM1 and Lamp1 in the cerebellum of 140-day-old *WT*, *Hexa-/-* and *Hexa-/-Neu3-/-* mice brain coronal sections for short-term ketogenic diet strategy (A). Images were taken at 20X magnification and under the same light exposure. The histogram shows the intensity of the p62/SQSTM1 (B) and Lamp1 (C) for the treated and untreated of each genotype. Intensities were measured via ImageJ program. Data show mean ± SEM of measurements. Significant levels of data were determined using the one-way ANOVA. (n=3, *p<0.05, **p<0.01, ***p<0.001 and ****p<0.0001)

The autophagic cargo protein of the p62/SQSTM1 and lysosomal membrane marker of the Lamp1 protein intensities are the highest in the 140-day-old *Hexa-/-Neu3-/-* mice cortex. The short-term ketogenic diet and propagermanium treatments and their combination significantly mitigated p62/SQSTM1 protein level in the *Hexa-/-Neu3-/-* mice compared to untreated ones (Figure 3.46 A, B). Moreover, the reduction of the Lamp1 protein level was only observed after short-term ketogenic diet alone treatment (Figure 3.46 A, C).

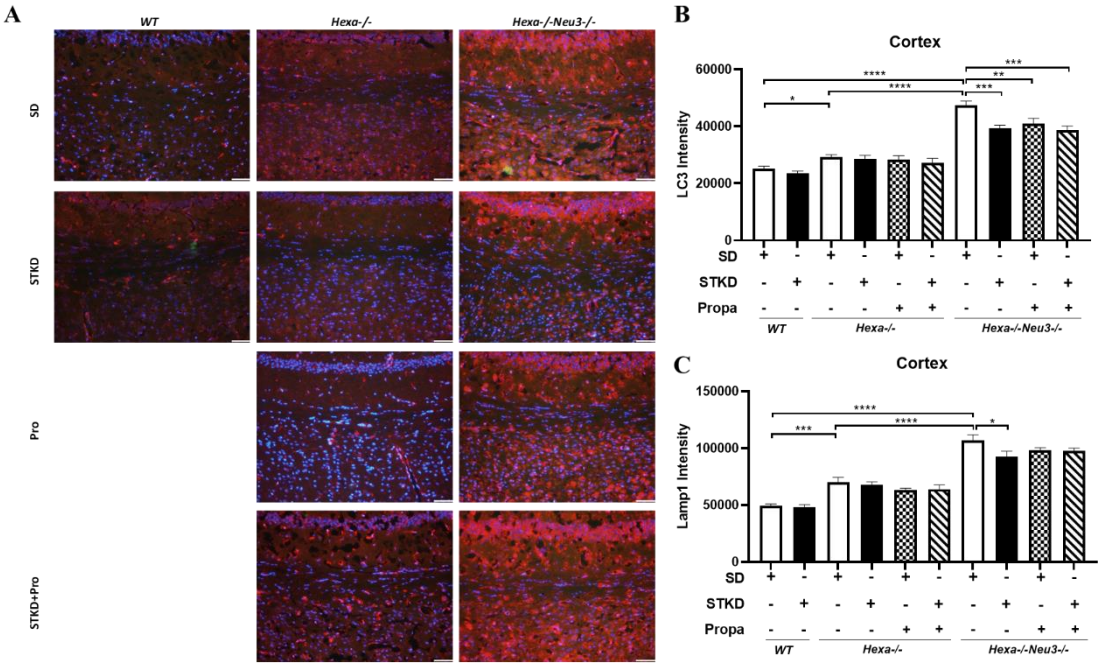


Figure 3.48 Immunostaining of the LC3 and Lamp1 in the cortex of 140-day-old *WT*, *Hexa-/-* and *Hexa-/-Neu3-/-* mice brain coronal sections for short-term ketogenic diet strategy (A). Images were taken at 20X magnification and under the same light exposure. The histogram shows the intensity of the LC3 (B) and Lamp1 (C) for the treated and untreated of each genotype. Intensities were measured via ImageJ program. Data show mean ± SEM of measurements. Significant levels of data were determined using the one-way ANOVA. (n=3, *p<0.05, **p<0.01, ***p<0.001 and ****p<0.0001)

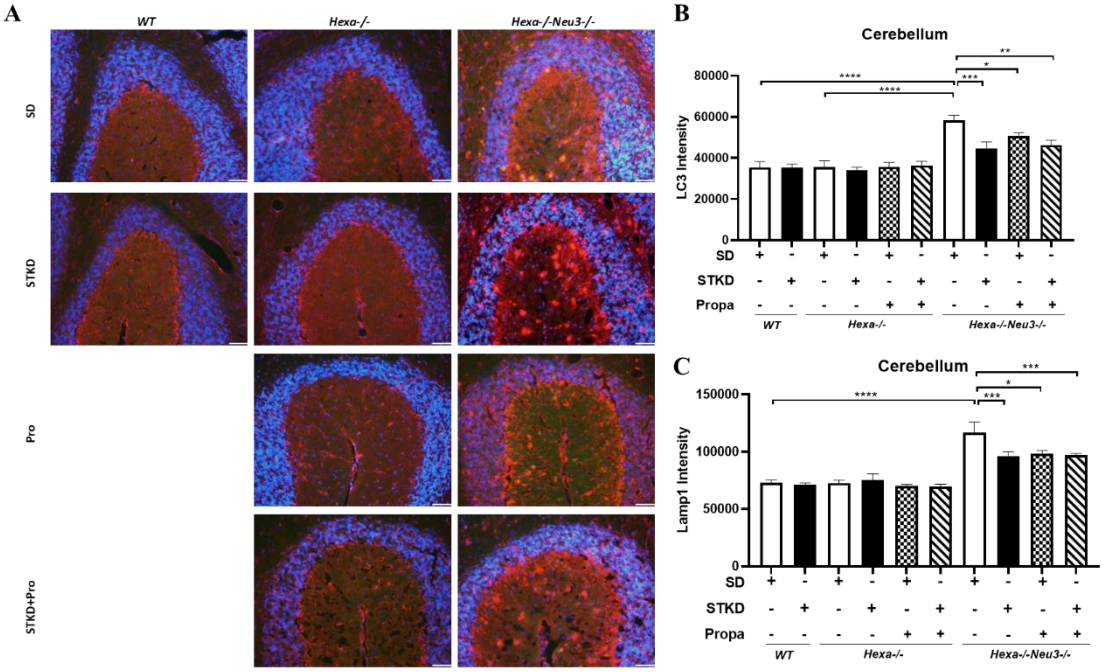


Figure 3.49 Immunostaining of the LC3 and Lamp1 in the cerebellum of 140-day-old *WT*, *Hexa-/-* and *Hexa-/-Neu3-/-* mice brain coronal sections for short-term ketogenic diet strategy (A). Images were taken at 20X magnification and under the same light exposure. The histogram shows the intensity of the LC3

(B) and Lamp1 (C) for the treated and untreated of each genotype. Intensities were measured via ImageJ program. Data show mean ± SEM of measurements. Significant levels of data were determined using the one-way ANOVA. (n=3, *p<0.05, **p<0.01, ***p<0.001 and ****p<0.0001)

LC3 protein level increased in the 140-day-old *Hexa-/-Neu3-/-* mice cortex compared to age-matched *WT* and *Hexa-/-* mice. In addition, this protein intensity is the higher in the *Hexa-/-* mice cortex than *WT*. Each treatment condition decreased the LC3 protein accumulation in the *Hexa-/-Neu3-/-* mice cortex compared to untreated ones (Figure 3.49 A, B). The Lamp1 protein level also is the highest in the *Hexa-/-Neu3-/-* mice cerebellum and the short-term ketogenic diet, propagermanium and their combined treatments significantly reduced the Lamp1 protein level in *Hexa-/-Neu3-/-* mice compared to untreated ones (Figure 3.49 A, C).

## 3.6 Histological Staining

The cortex and cerebellum tissue sections were stained by Hematoxylin&Eosin and Periodic Acid&Schiff for histopathological analysis in the 140-day-old *WT*, *Hexa-/-* and *Hexa-/- Neu3-/-* mice.

### 3.6.1 Hematoxylin&Eosin Staining

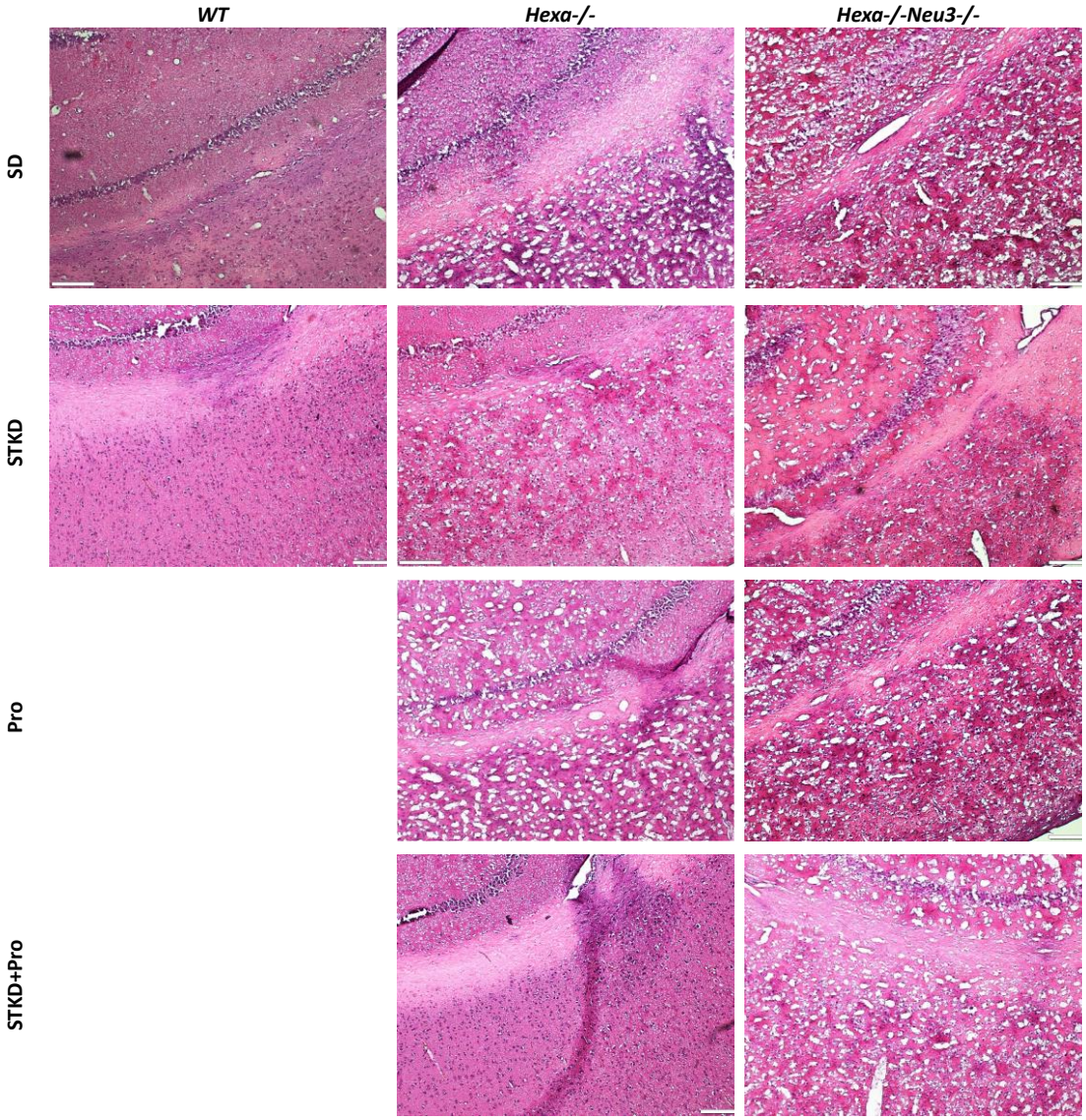


Figure 3.50 Histological staining of the Hematoxylin&Eosin in the cortex of 140-day-old *WT*, *Hexa-/-* and *Hexa-/-Neu3-/-* mice brain coronal sections for short-term ketogenic diet strategy (A). Images were taken at 10X magnification and under Olympus Light Microscope. (n=3)

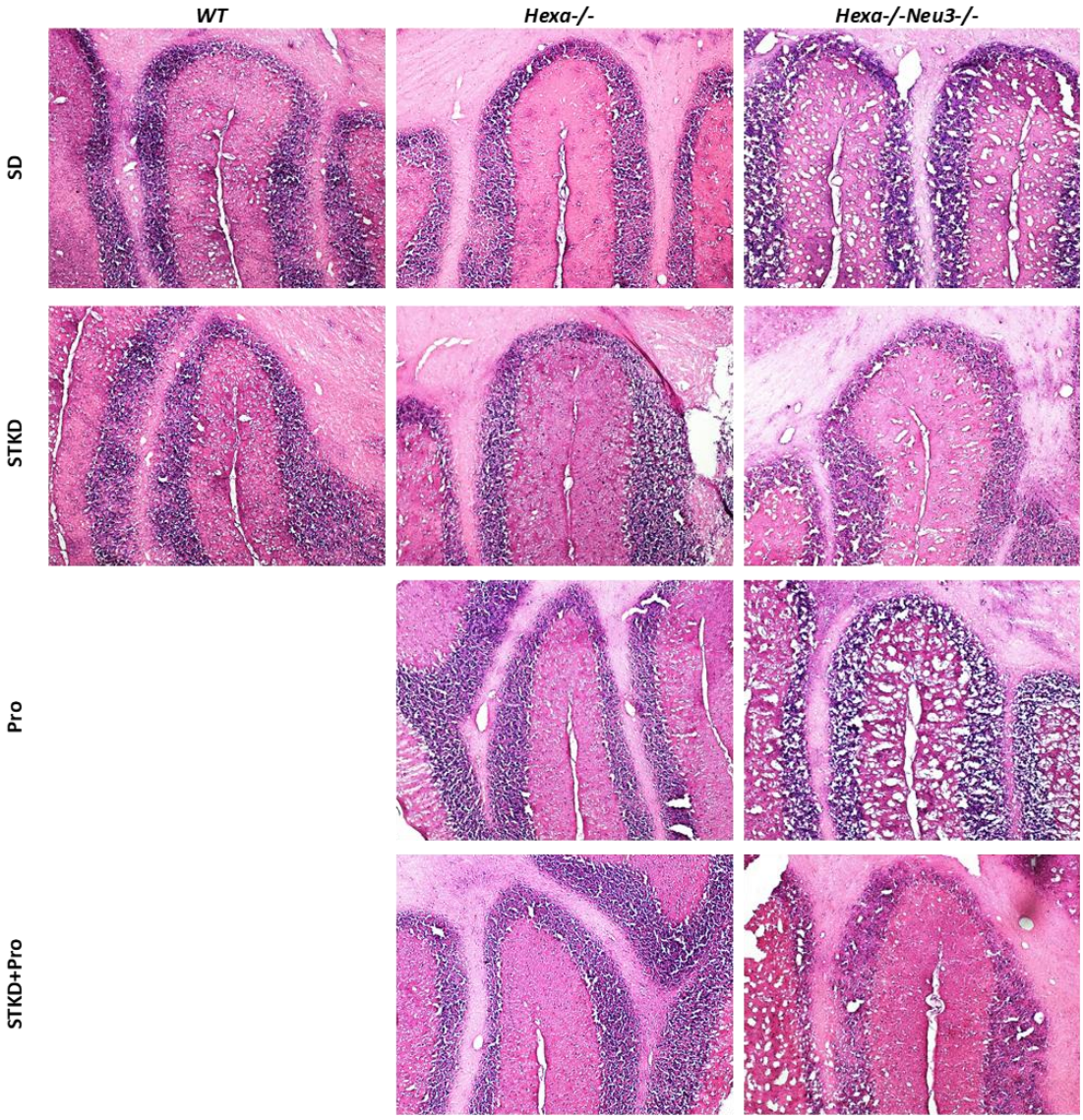


Figure 3.51 Histological staining of the Hematoxylin&Eosin in the cerebellum of 140-day-old *WT*, *Hexa-/-* and *Hexa-/-Neu3-/-* mice brain coronal sections for short-term ketogenic diet strategy (A). Images were taken at 10X magnification and under Olympus Light Microscope. (n=3)

The hematoxylin&eosin staining displayed in the cortex and cerebellum that 140-day-old mice includes vacuolization of the cell and nerve cell deteriorations. However, the short-term ketogenic diet and propagermanium treatments did not improve the pathology significantly in *Hexa-/-Neu3-/-* mice cortex (Figure 3.50). Like the cortex, cerebellum tissue included vacuolization of the neuronal cell and Purkinje cell damage in the 140-day-old *Hexa-/-Neu3-/-* mice (Figure 3.51).

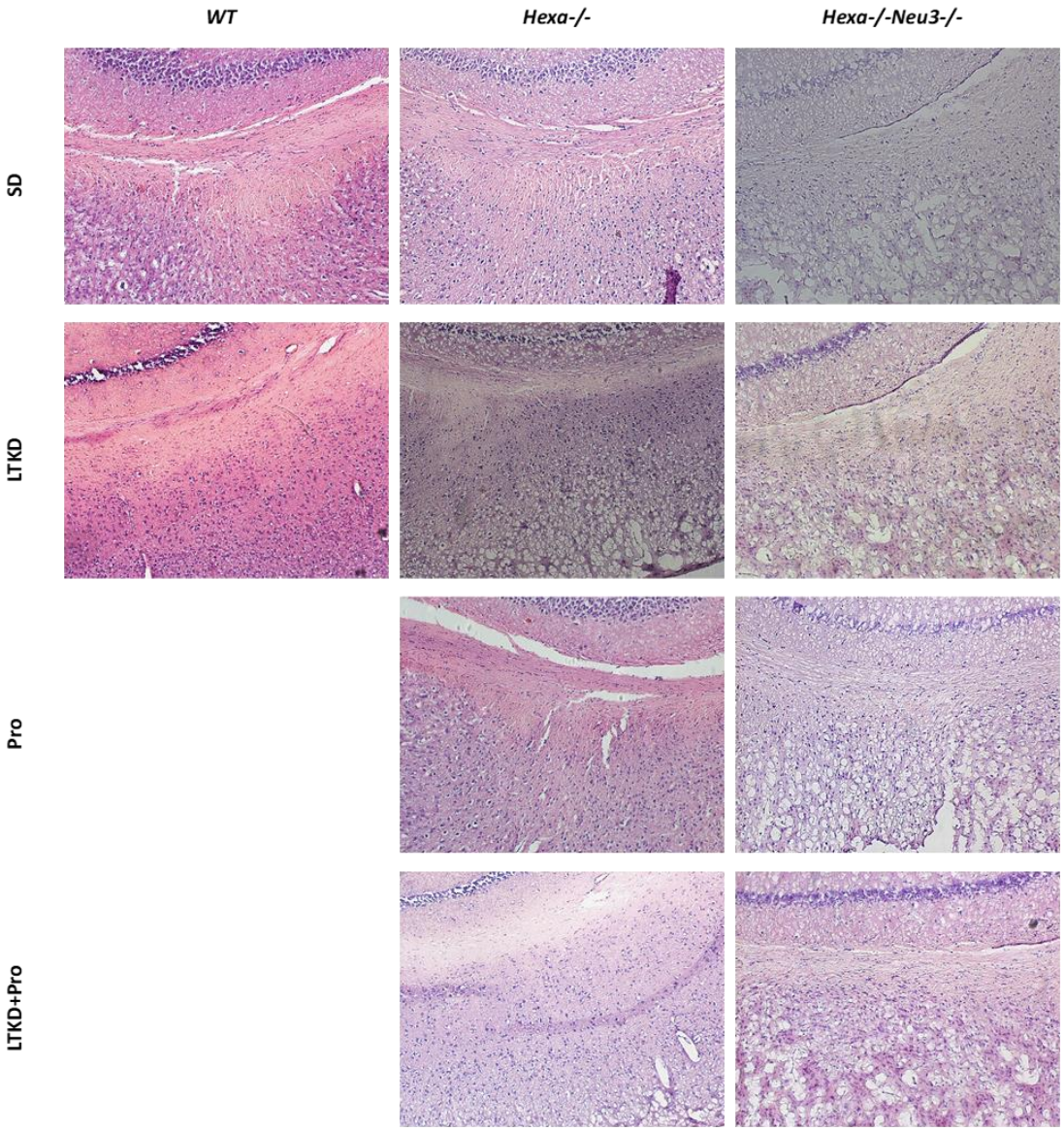


Figure 3.52 Histological staining of the Hematoxylin&Eosin in the cortex of 140-day-old *WT*, *Hexa-/-* and *Hexa-/-Neu3-/-* mice brain coronal sections for long-term ketogenic diet strategy (A). Images were taken at 10X magnification and under Olympus Light Microscope. (n=3)

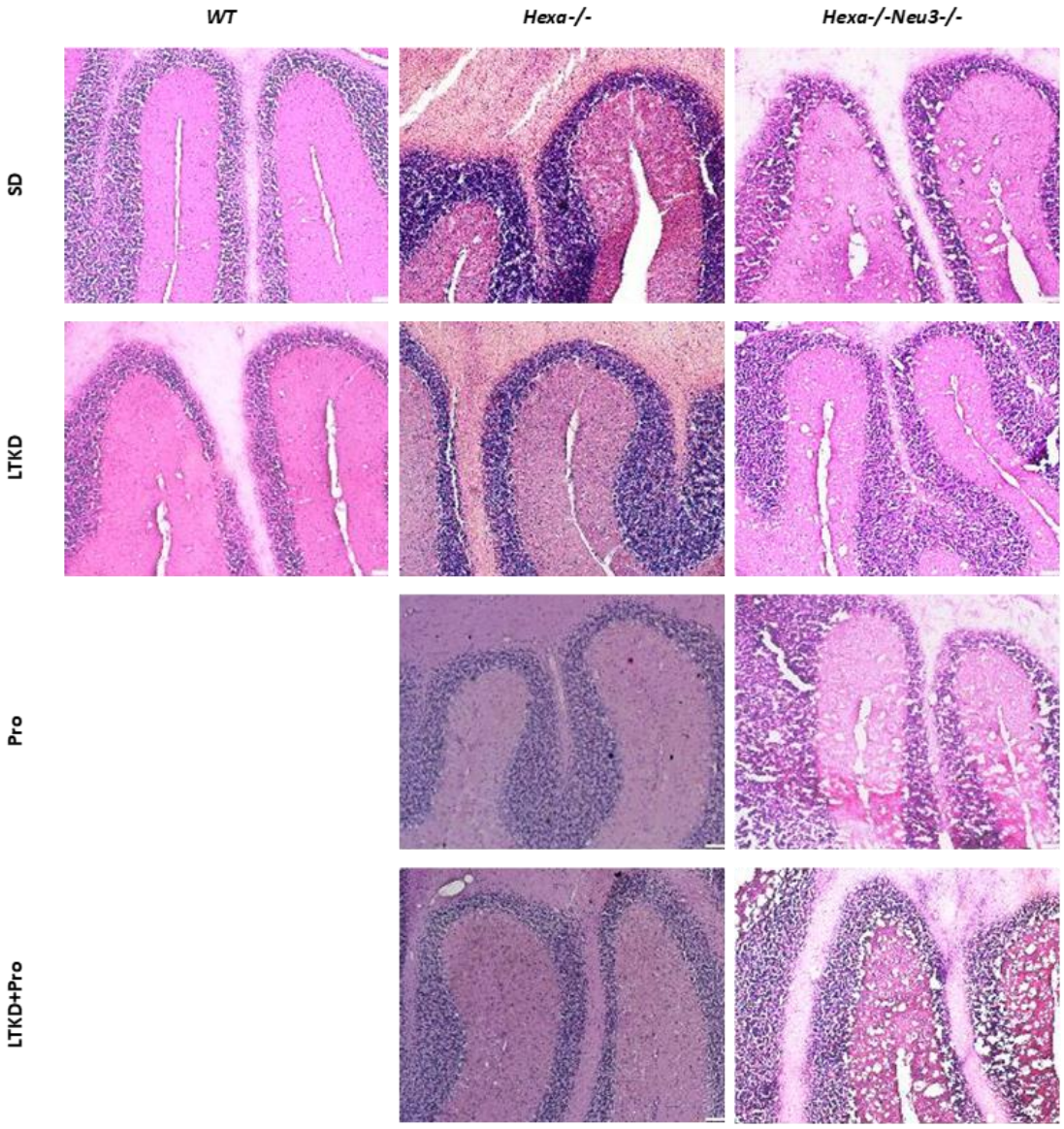


Figure 3.53 Histological staining of the Hematoxylin&Eosin in the cerebellum of 140-day-old *WT*, *Hexa-/-* and *Hexa-/-Neu3-/-* mice brain coronal sections for long-term ketogenic diet strategy (A). Images were taken at 10X magnification and under Olympus Light Microscope. (n=3)

The hematoxylin&eosin staining for the long-term ketogenic diet strategy displayed the similar patterns with the short-term ketogenic diet strategy. Each treatment did not ameliorate the cellular pathology for the *Hexa-/-Neu3-/-* mice in cortex and cerebellum (Figures 3.52, 3.53).

## 3.6.2 Periodic Acid & Schiff Staining

The Periodic acid & Schiff staining was performed to determine glycoconjugate and polysaccharide accumulation in the 140-day-old *WT*, *Hexa-/-* and *Hexa-/-Neu3-/-* mice after short-term and long-term ketogenic diet treatment strategies.

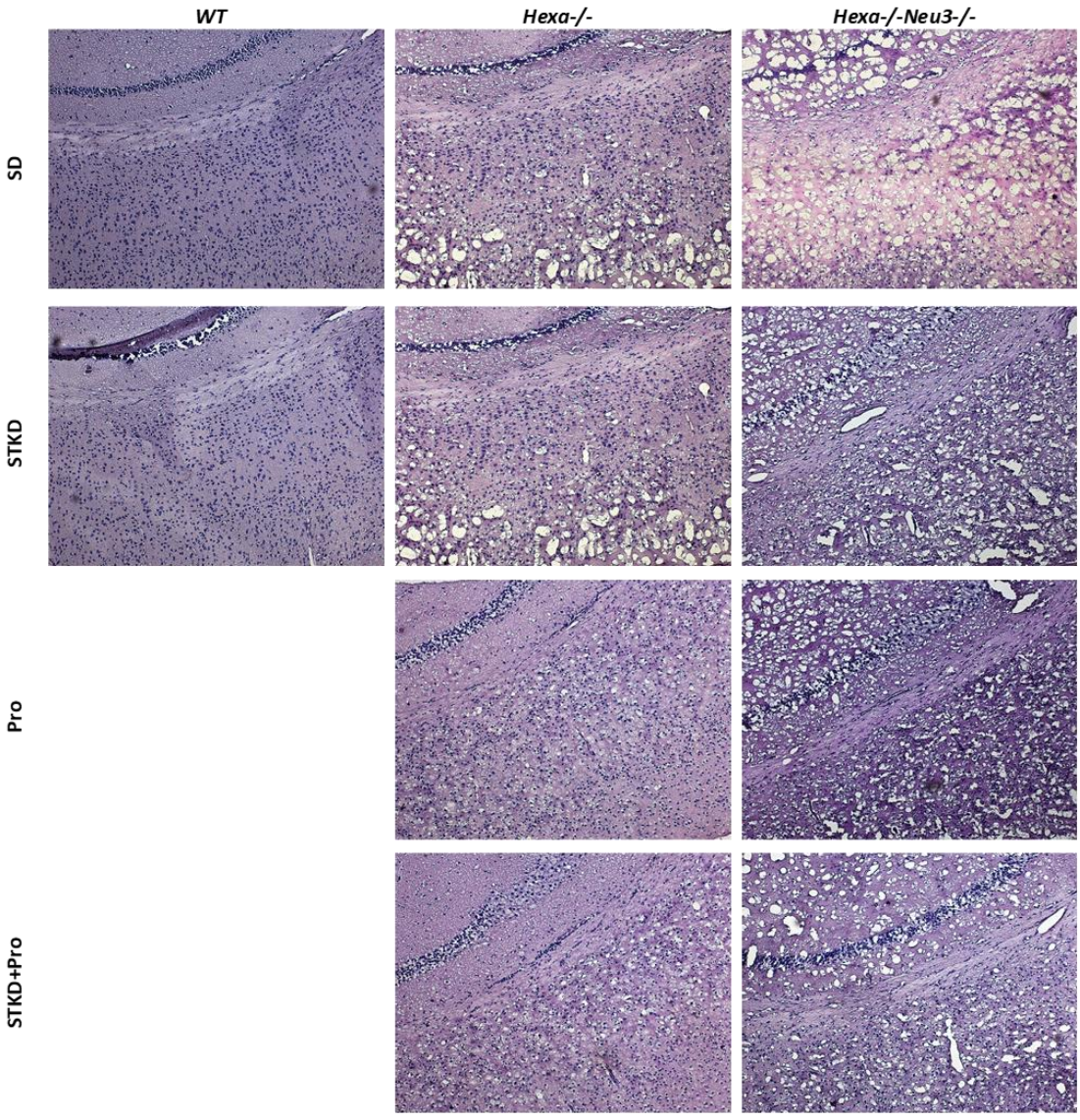


Figure 3.54 Histological staining of the Periodic acid & Schiff (PAS) in the cortex of 140-day-old *WT*, *Hexa-/-* and *Hexa-/-Neu3-/-* mice brain coronal sections for short-term ketogenic diet strategy (A). Images were taken at 10X magnification and under Olympus Light Microscope. (n=3)

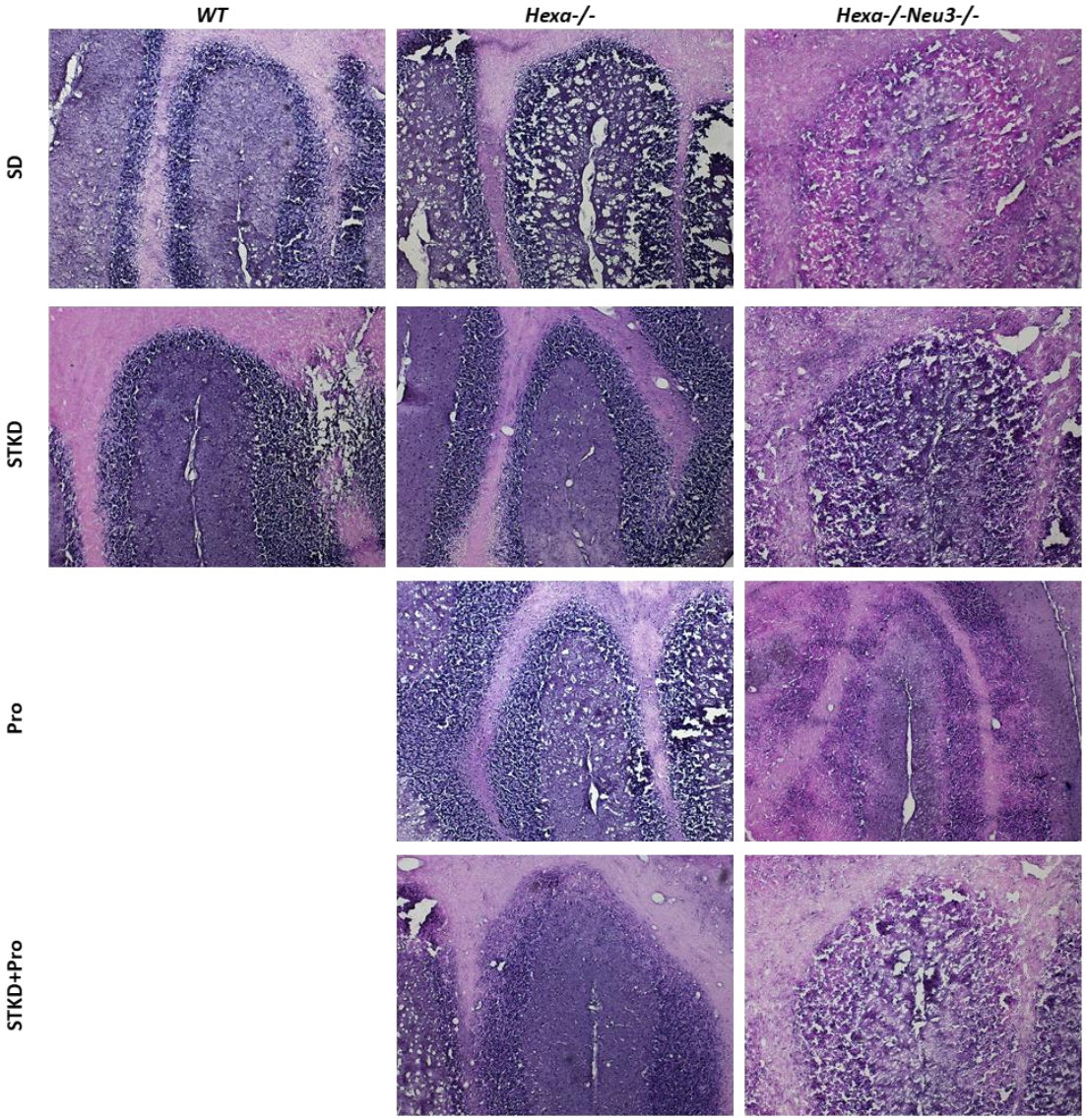


Figure 3.55 Histological staining of the Periodic acid & Schiff (PAS) in the cerebellum of 140-day-old *WT*, *Hexa-/-* and *Hexa-/-Neu3-/-* mice brain coronal sections for short-term ketogenic diet strategy (A). Images were taken at 10X magnification and under Olympus Light Microscope. (n=3)

The Periodic acid & Schiff (PAS) staining displayed that there are glycoconjugate accumulation which is pink color in the 140-day-old *Hexa-/-Neu3-/-* mice cortex compared to *WT* and *Hexa-/-* mice. The short-term ketogenic diet reduced the glycoconjugate accumulation in the *Hexa-/-Neu3-/-* mice cortex and cerebellum compared to untreated ones (Figures 3.54, 3.55).

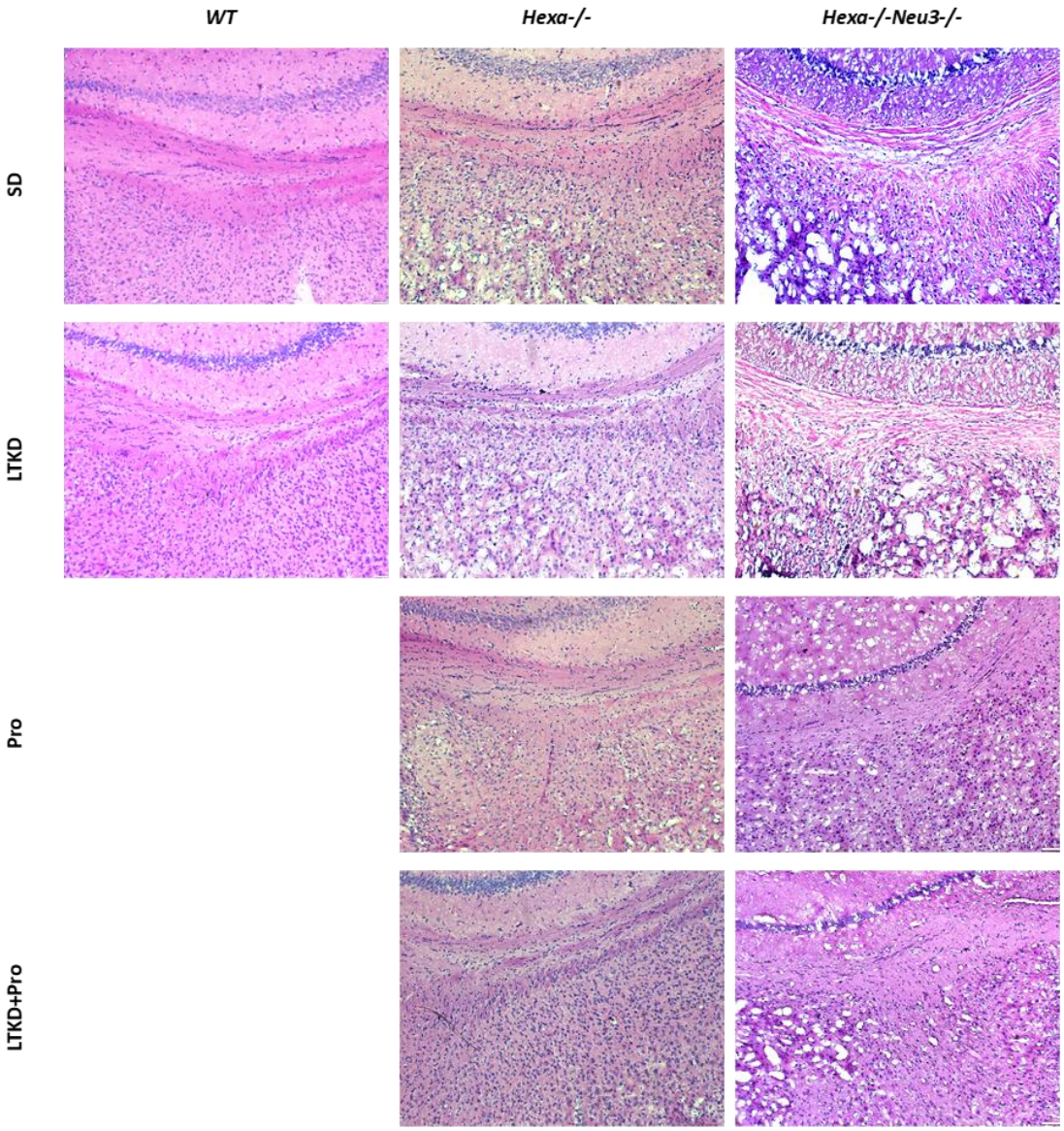


Figure 3.56 Histological staining of the Periodic acid & Schiff (PAS) in the cortex of 140-day-old *WT*, *Hexa-/-* and *Hexa-/-Neu3-/-* mice brain coronal sections for long-term ketogenic diet strategy (A). Images were taken at 10X magnification and under Olympus Light Microscope. (n=3)

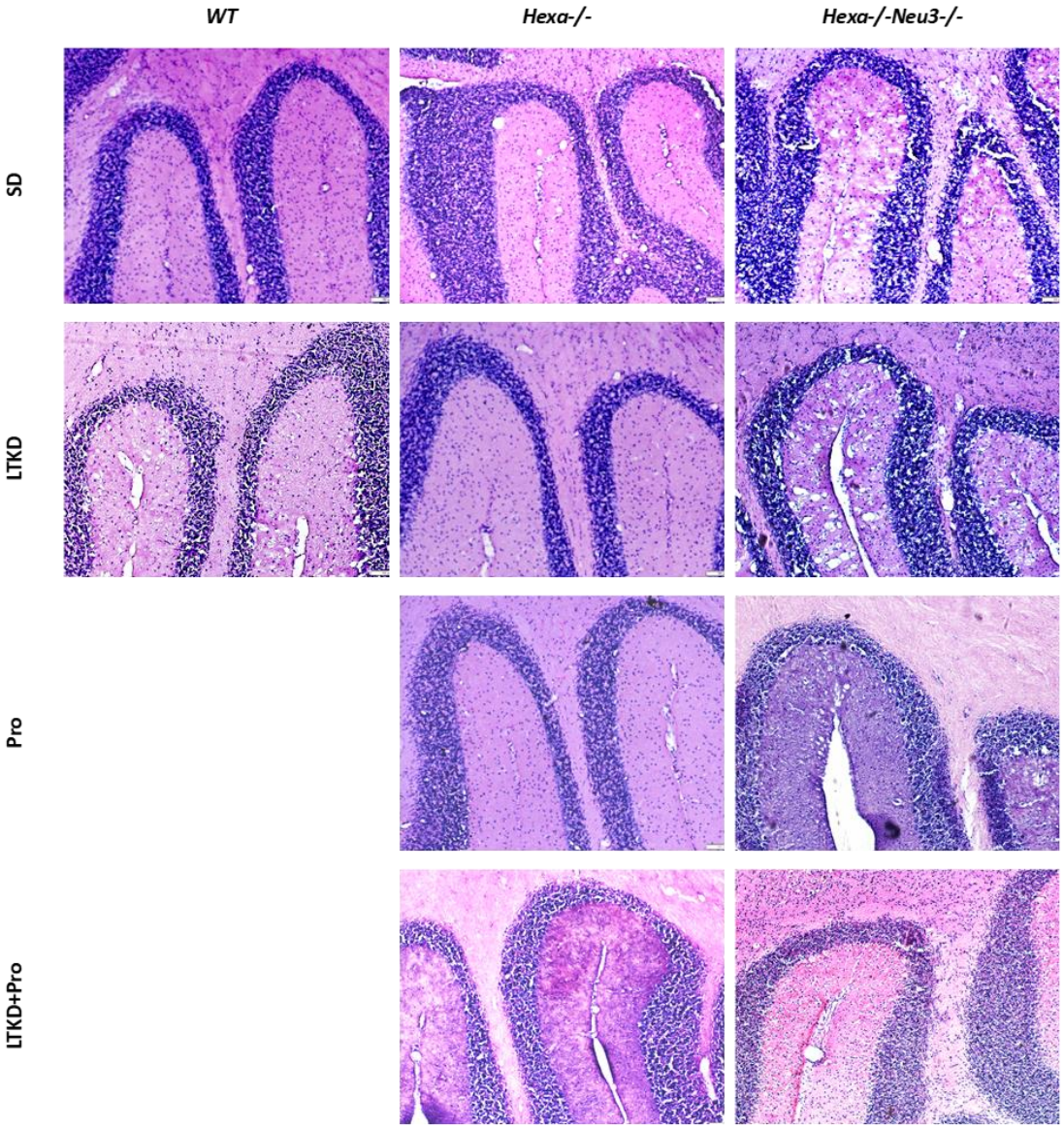


Figure 3.57 Histological staining of the Periodic acid & Schiff in the cerebellum of 140-day-old *WT*, *Hexa-/-* and *Hexa-/-Neu3-/-* mice brain coronal sections for long-term ketogenic diet strategy (A). Images were taken at 10X magnification and under Olympus Light Microscope. (n=3)

The long-term ketogenic diet strategy significantly reduced the accumulated glycoconjugate in the *Hexa-/-Neu3-/-* cortex and cerebellum compared to untreated ones due to the low carbohydrate diet content (Figures 3.56, 3.57).

## 3.7 Behavioral Analysis

Behavioral analysis for anxiety-related behavior and locomotor activity were performed after two different ketogenic diet strategies (short and long term) in the 140-day-old *WT*, *Hexa-/-* and *Hexa-/-Neu3-/-* mice by open-field and rotarod analysis, respectively.

### 3.7.1 Open Field Test

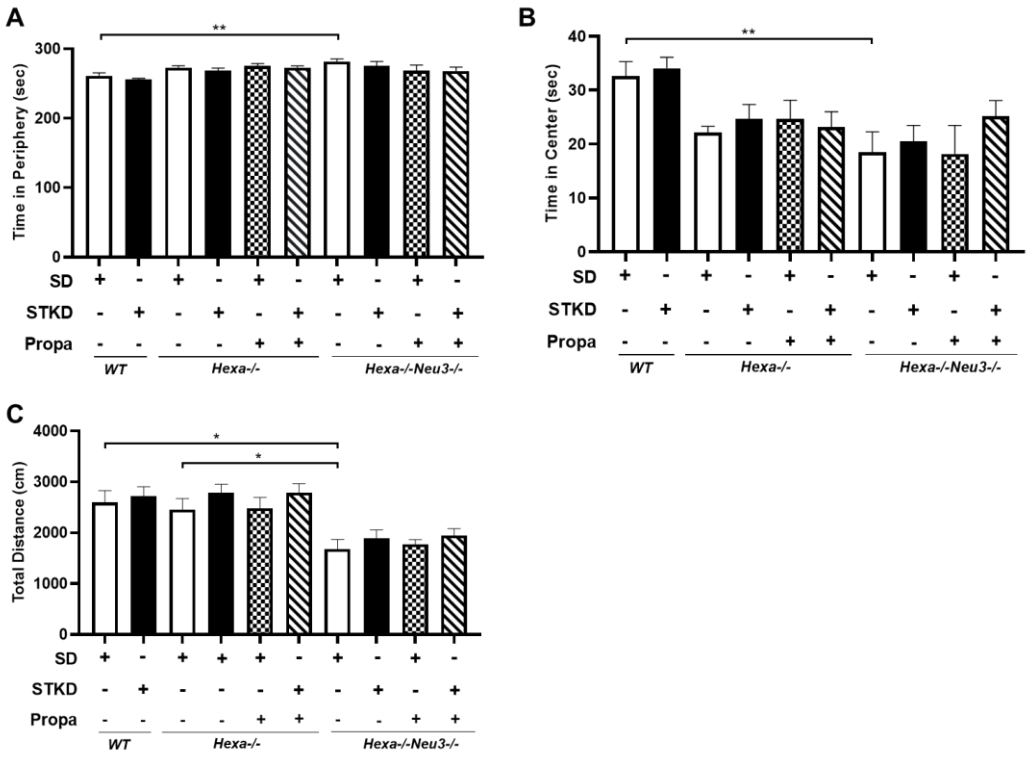


Figure 3.58 Open field analyses of the *WT*, *Hexa-/-* and *Hexa-/-Neu3-/-* mice after short-term treatments of ketogenic diet and propagermanium. Time spent in periphery (A) and center (B), total distance in the box (C) for 5 minutes were indicated. Data show mean ± SEM of measurements. Significant levels of data were determined using the one-way ANOVA. (n=3, *p<0.05, **p<0.01, ***p<0.001 and ****p<0.0001)

The open field test showed that 140-day-old *Hexa-/-Neu3-/-* mice spent much time in the periphery compared to the age-matched *WT* and *Hexa-/-* mice, as previously reported. The short-term ketogenic diet and propagermanium treatments did not reduce the time in the periphery for the *Hexa-/-Neu3-/-* mice (Figure 3.58 A). Spending time in center slightly increased in the *Hexa-/-Neu3-/-* mice compared to untreated ones but not

statistically significant (Figure 3.58 B). Looking at the total 5-min distance, *Hexa-/-Neu3-/-* mice traveled less distance than *WT* and *Hexa-/-* mice, and the short-term ketogenic diet and combined ketogenic diet and propagermanium treatments slightly increased the total distances of the *Hexa-/-Neu3-/-* mice, but it is not statistically significant (Figure 3.58 C).

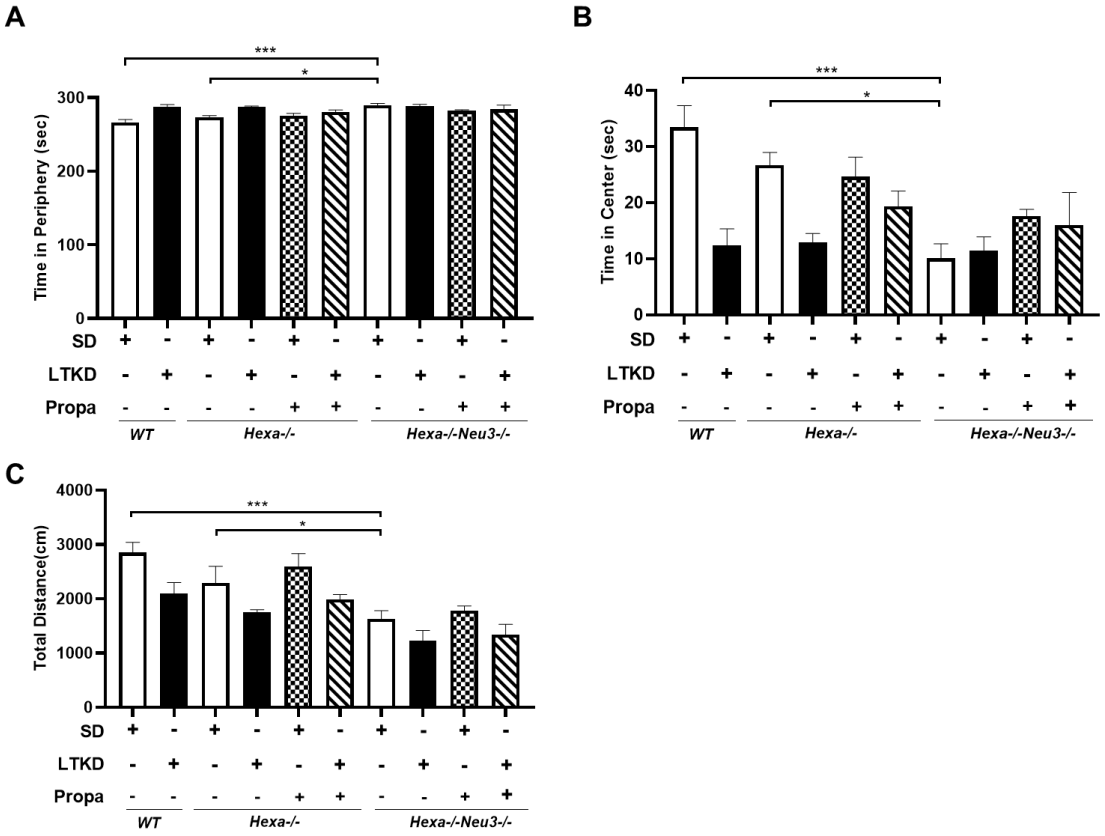


Figure 3.59 Open field analyses of the *WT*, *Hexa-/-* and *Hexa-/-Neu3-/-* mice after long-term treatments of ketogenic diet and propagermanium. Time spent in periphery (A) and center (B), total distance in the box (C) for 5 minutes were indicated. Data show mean ± SEM of measurements. Significant levels of data were determined using the one-way ANOVA. (n=3, *p<0.05, **p<0.01, ***p<0.001 and ****p<0.0001)

The long-term ketogenic diet strategy did not reduce the time in the periphery for the *Hexa-/-Neu3-/-* mice compared to untreated ones (Figure 3.59 A). Time in the center increased after propagermanium and combined ketogenic diet and propagermanium treatments in *Hexa-/-Neu3-/-* mice compared to untreated ones, but they were not statistically significant due to higher standard deviation (Figure 3.59 B). The long-term ketogenic diet also reduced the total distances in *WT*, *Hexa-/-* and *Hexa-/-Neu3-/-* mice compared to untreated ones due to the high-fat content of the diet (Figure 3.59 C).

### 3.7.2 Rotarod Test

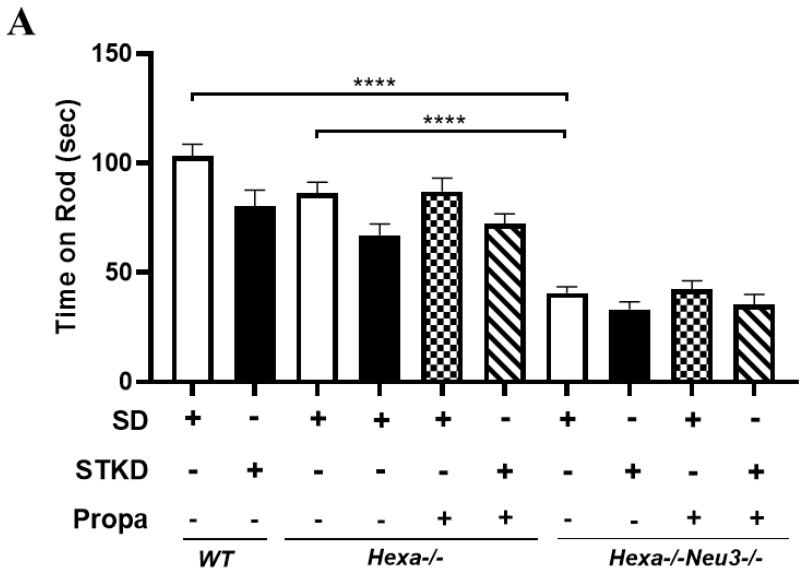


Figure 3.60 Rotarod analyses of *WT*, *Hexa-/-*, and *Hexa-/-Neu3-/-* mice on an accelerating bar (4 rpm to 40 rpm in 5 min) after short-term supplemental treatments of propagermanium and ketogenic diet. Data show mean ± SEM of measurements. Significant levels of data were determined using the one-way ANOVA. (n=3, *p<0.05, **p<0.01, ***p<0.001 and ****p<0.0001)

The rotarod analysis was performed to measure locomotor activity and the balance on the accelerated rod for the *WT*, *Hexa-/-* and *Hexa-/-Neu3-/-* mice after short-term and long-term treatment strategies. The time on rod significantly decreased in the *Hexa-/-Neu3-/-* mice compared to *WT* and *Hexa-/-* mice, as previously published. The short-term ketogenic diet slightly reduced the time on the rod in *Hexa-/-Neu3-/-* mice compared to untreated ones. Propagermanium and combined treatments also did not improve the time on the rod in *Hexa-/-Neu3-/-* mice (Figure 3.60).

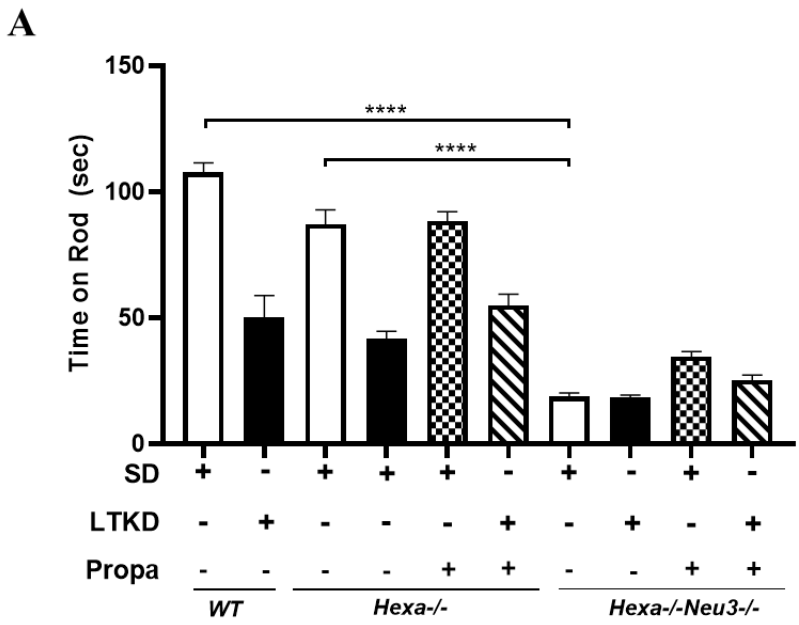


Figure 3.61 Rotarod analyses of *WT*, *Hexa-/-*, and *Hexa-/-Neu3-/-* mice on an accelerating bar (4 rpm to 40 rpm in 5 min) after long-term supplemental treatments of propagermanium and ketogenic diet. Data show mean ± SEM of measurements. Significant levels of data were determined using the one-way ANOVA. (n=3, *p<0.05, **p<0.01, ***p<0.001 and ****p<0.0001)

In the long-term ketogenic diet strategy, time on the rod slightly increased after propagermanium alone treatment for the *Hexa-/-Neu3-/-* mice compared to untreated ones, but it is not statistically significant. The long-term ketogenic diet treatment significantly reduced the time on the rod for *WT* and *Hexa-/-* mice (Figure 3.61)

# CHAPTER 4

# DISCUSSION

GM2 gangliosidosis is a group of lysosomal storage disorders that exhibit GM2 accumulation in the lysosomes due to mutations of the β-hexosaminidases or GM2 activator protein (GM2AP). One of them is the Tay-Sachs disease, or GM2 gangliosidosis B variant, which caused abnormal GM2 accumulation specifically in the central nervous system (CNS) since the dysfunction of the β-hexosaminidase A (HEXA) enzyme, which cleaved N-acetylgalactosamine residue on the GM2 ganglioside. Although the newborn is normal after birth, the disease pathology is progressive due to Hexa enzyme deficiency and abnormal GM2 ganglioside accumulation (Leal et al. 2020). To mimic the pathology of Tay-Sachs disease in an animal model, the researchers created a *Hexa-/-* mouse model, but the mouse model exhibited normal pathology due to the Neu3 sialidase-involved ganglioside bypass mechanism. The creation of *Hexa-/-Neu3-/-* mice by eliminating the Neu3 gene in addition to Hexa exhibited severe pathology mimicking the pathology of Tay-Sachs disease (Seyrantepe et al. 2018).

The high-fat/low carbohydrate diet of the ketogenic diet is a special diet to trigger ketone body production due to low glucose levels. Normally, the brain consumes glucose as its primary energy source, but when glucose levels decrease, the primary energy source is replaced by ketone bodies, which are β-hydroxybutyrate, acetoacetate, and acetone. Ketone bodies play many roles in cellular mechanisms such as regulation of energy homeostasis, inflammation, and autophagic flux (Puchalska and Crawford 2021; Koh, Dupuis, and Auvin 2020; McCarty, DiNicolantonio, and O'Keefe 2015). The main focus of this thesis is to examine the effects of the ketogenic diet and anti-inflammatory treatments on these cellular mechanisms in the GM2 gangliosidosis mouse model. The ketogenic diet saves *Hexa-/-Neu3-/-* mice from extreme weight loss at the end of their lives, both short-term and long-term, thanks to the high-fat content of the diet. However, a long-term ketogenic diet interestingly increased the body weight of *WT* and *Hexa-/-* mice. One study showed that a long-term ketogenic diet induced obesity in C57BL/6J mice by damaging the structure of γδ T cells, which is important for glucose homeostasis in adipose tissues in addition to metabolic health (Goldberg et al. 2020). Furthermore,

Ellenbroek et al. found that a long-term ketogenic diet first decreased body weight in C57BL/6J mice due to glucose intolerance and α- and β-cell depletion and then increased body weight as the duration of use increased (Ellenbroek et al. 2014).

Acidic and neutral ganglioside accumulation of GM2 and GA2 was previously shown in *Hexa-/-Neu3-/-* mice (Seyrantepe et al. 2018). In addition, Sandhoff mice (*Hexb-/-*) have an abnormal accumulation of GM2 and GA2 gangliosides, and the effects on these gangliosides after ketogenic diet intervention with N-butyldeoxynojirimycin (NB-DNJ) were measured. While the ketogenic diet did not reduce the GM2 and GA2 ganglioside levels, NB-DNJ significantly reduced the GM2 and GA2 ganglioside levels in the *Hexb-/-* mice cortex (Denny et al. 2010). Thin-layer chromatography (TLC) displayed no alteration in both acidic and neutral ganglioside levels in the cortex and cerebellum after short- or long-term ketogenic diet and propagermanium treatments except GA2 level in the *Hexa-/-Neu3-/-* cortex after short-term ketogenic diet intervention. Since there is very limited information in the literature about the effects of the ketogenic diet on ganglioside breakdown, further investigations are needed to determine the cause of the decreased amount of GA2 gangliosides after a short-term ketogenic diet. Although it has been shown that the ketogenic diet does not affect the amount of gangliosides, certain genes related to ganglioside metabolism are affected at the transcriptional level. The *B4Galnt1* gene, which encodes the GM2/GA2 synthase enzyme, is the rate-limiting enzyme for synthesizing complex gangliosides, especially in the central nervous system. The short-term but not long-term ketogenic diet treatment interestingly reduced the *B4Galnt1* gene expression in *Hexa-/-Neu3-/-* mice cortex and cerebellum. In addition, *GM3S* and *GD3S* expression levels were significantly decreased only in the cortex after short-term ketogenic diet treatment. It was shown that *B4Galnt1*, *GM3S*, and GD3S were up-regulated, and *GM2AP* was down-regulated in ganglioside expression levels after low-carbohydrate ketogenic diet treatment in the liver tissue of female B6.Cg-*Lepob*/J mice. There is no significant change in the ganglioside metabolism-associated genes except GM2AP, which significantly decreased in the cerebral cortex after the ketogenic diet (Okuda 2019; 2020). The *HexB* expression level significantly increased in the *Hexa-/-Neu3-/-* cortex and cerebellum, which was previously reported (Seyrantepe et al. 2018). The short-term ketogenic diet, propagermanium, and their combination treatments decreased the *HexB* gene expression level in the cortex and cerebellum tissues. Apart from the ganglioside degradation process, *HexB* is also used as a marker to distinguish microglia from macrophages (H.

Huang et al. 2023). On the basis of this result, the neuroprotective roles of the ketogenic diet and the anti-inflammatory propagermanium treatments may have reduced the *HexB* gene expression level in *Hexa-/-Neu3-/-* mice.

Neuroinflammation is the response of the brain immune system in the central nervous system and spinal cord by activating the glial cells, which are microglia, astrocytes, and macrophages. Activation of the glial cells secrete pro-inflammatory cytokine/chemokine, which can act either protective function or damage brain homeostasis. The neuroinflammatory response is a common pathology in various lysosomal storage disorders (Bosch and Kielian 2015). The main cause of neuroinflammation in lysosomal storage diseases is different biochemical accumulations in lysosomes, which often lead to cell death. *Hexa-/-Neu3-/-* mouse model displays abnormal GM2 accumulation in the cortex and cerebellum, which induces a neuroinflammatory response by secreting pro-inflammatory cytokine/chemokines such as CCL2, CCL3, CXCL10, etc., and reducing of the anti-inflammatory cytokine/chemokine from microglia and astrocytes (Demir et al. 2020). CCL2, or MCP-1, is a pro-inflammatory chemokine ligand that can be secreted by neurons and glial cells and recruits monocytes and other immune helpers to the site of inflammation by interacting with its receptor CCR2. CCL2 is part of neuroinflammatory processes that occur in diseases associated with the central nervous system characterized by neuronal deterioration. For example, CCL2 expression is increased in glial cells in epilepsy, Alzheimer's disease, and some lysosomal storage diseases (Foresti et al. 2009; Hickman and El Khoury 2010; F. P. S. Yu, Dworski, and Medin 2018). The downregulation of the *CCL2* expression by istradefylline administration to the Sandhoff mice reduced the microglial activation and secretion of the pro-inflammatory cytokine/chemokine secretion (Ogawa et al. 2018). Farber disease mice and patients also have elevated levels of CCL2, and elimination of the CCL2 in Farber mice attenuates leukocytosis and increases the lifespan (F. P. S. Yu, Dworski, and Medin 2018). In the light of these results, one aim of this thesis is to reduce the inflammatory response using ketogenic diet and propagermanium in the focus of CCL2/CCR2 axis. The short-term ketogenic diet, propagermanium, and combined ketogenic diet and propagermanium reduced the *CCL2* expression level in the *Hexa-/-Neu3-/-* mice cortex and cerebellum. In one study, a ketogenic diet treatment was shown to inhibit macrophage/monocyte infiltration by significantly reducing *CCL2*, *CCR2*, *CCL3*, and *CXCL10* expression levels in the spleen and spinal cord tissues of an EAE mouse model (W. Sun et al. 2023). The anti-

inflammatory propagermanium used alongside the ketogenic diet is an inhibitor of the CCL2/CCR2 axis and was used to reduce increased *CCL2* expression levels in *Hexa-/-Neu3-/-* mice. Propagermanium was administered in C57BL/6J mice on a high-fat diet and restored the ratio of pro-inflammatory and anti-inflammatory macrophages as well as reducing gene expression of inflammation markers such as *CCL2* and *CD11c* in white adipose tissue (Mulder, Van Den Hoek, and Kleemann 2017). Furthermore, propagermanium improved the microglial responses by the secretion of pro-inflammatory molecules in the cerebral ischemia/ reperfusion injured mice (He et al. 2019). The CCL3 or MIP1-α is the pro-inflammatory chemokine secreted by astrocytes, microglia, and neurons in the CNS, which interact with its receptors CCR1 and CCR5 (Zhu et al. 2012). CCL3 plays a role, especially in neutrophil and monocyte migration, and microglial activation leads to neurodegenerative conditions in Alzheimer's disease and epilepsy (Chang Liu et al. 2014; Guzik-Kornacka et al. 2011). CCL3 gene expression was significantly increased in *Hexa-/-Neu3-/-* mice and contributed to the establishment of neuroinflammatory conditions in these mice. Apart from the Tay-Sachs mouse model, it has been reported that the amount of CCL3 protein also increases in the galactosialidosis mouse model (Horii et al. 2022). When the effect of a ketogenic diet on CCL3 was examined, it was shown that the amount of CCL3 in serum samples of super-refractory status epilepticus patients increased depending on the pathology of the disease and decreased significantly after ketogenic diet treatment (Dickens et al.,. Furthermore, the CCL3 gene expression level decreased after ketogenic diet treatment in the EAE mouse model of multiple sclerosis (W. Sun et al. 2023). Since we have limited knowledge about the effects of the propagermanium, a CCL2/CCR2 inhibitor, on CCL3, additional experiments will be needed to determine how propagermanium decreases CCL3 expression. CCL5 or RANTES is found in the chemokine family and secreted by all glial cells (microglia, astrocyte, and oligodendrocyte) interacting with its receptors and regulating neuroinflammation, neuroprotection, and insulin signaling (Lanfranco et al. 2017). The *CCL5* gene expression increased in the *Hexa-/-Neu3-/-* mice and then reduced its expression after the ketogenic diet and propagermanium treatments. Moreover, the Gaucher disease mouse model (*Gba-/-*) displayed increased *CCL2*, *CCL3*, and *CCL5* gene expressions in the brain (Vitner et al. 2012). Similar to the Gaucher mouse model, the mucolipidosis type IV mouse model (*Mcoln1-/-*) showed an increased expression level of *CCL5* in serum and the microglia cells (Cougnoux et al. 2019). The effect of a ketogenic diet on CCL5 was illustrated in a mouse model of acute pancreatitis and colon tumor

allograft, where the *CCL5* gene expression level showed a significant increase in contrast to the pattern in *Hexa-/-Neu3-/-* mice (Xia et al. 2023; W. Sun et al. 2022). The effect of propagermanium on CCL5 was studied in PBMC cells, where the *CCL5* gene expression level did not change after propagermanium treatment (Yokochi et al. 2001). CXCL10 is a chemokine with important roles in controlling the entry of various leukocyte subsets into the brain and other tissues. It is expressed by neurons, glia, and stromal cells in a number of different CNS diseases, such as Alzheimer's disease and multiple sclerosis, and may play a positive or negative role in facilitating the progression or resolution of the disease process by binding to its receptor CXCR3 (Michlmayr and McKimmie 2014). Apart from neurodegenerative diseases, increased expression of the chemokine *CXCL10* is also common in lysosomal storage diseases. Firstly, *Hexa-/-Neu3-/-* mice cortex and cerebellum displayed significantly increased *CXCL10* expression level as previously published (Demir et al. 2020). In addition, the plasma and macrophage cells of the Gaucher disease type I (*Gba1-/-*), Farber disease (*Asah1-/-*) , Niemann Pick type C (*Npc1-/-*) and Krabbe disease (Twi) mouse models also showed increased CXCL10 expression levels and various cytokine/chemokine secretion in the several tissues (Manoj K Pandey et al. 2017; Dworski et al. 2017; Shin et al. 2019; Snook et al. 2014). It was reported that ketogenic diet treatment ameliorates intractable epilepsy in infantile Alexander disease patients, as well as reducing CXCL10 and CCL2 levels in serum and cerebrospinal fluid (Hamada et al. 2021). Furthermore, the ketogenic diet was shown to improve demyelination in a mouse model of cuprizone-induced demyelination while also reducing *CXCL10*, *IL1-β* and *TNF-α* gene expression (Zhang et al. 2020). A study in patients with intracerebral haemorrhage showed a common increase only in CCL2 and CXCL10 levels after 90 days in serum samples from patients. Based on this result, we suggest that propagermanium, a CCL2/CCR2 inhibitor, may decrease *CCL2* expression while decreasing *CXCL10* expression (Landreneau et al. 2018). Glial fibrillar acidic protein (GFAP) is the type III intermediate filament which is mainly secreted by astrocytes in the CNS and maintains blood-brain-barrier integrity and shape of the astrocytes. There are numerous disorders associated with defective GFAP regulation, and injuries can cause glial cells to respond in unfavourable ways. For example, astroglia cells react to brain injury and neuro-traumatic conditions with astrogliosis, a process in which astroglia cells undergo cellular hypertrophy and proliferation by elevated GFAP expression (Z. Yang and Wang 2015). GFAP also interacts with neuroinflammation and, for example, increased GFAP expression in a Tay-Sachs disease mouse cortex and cerebellum led to

activation of astrocytes and triggered astrogliosis (Demir et al. 2020). In addition, the increase in GFAP immunoreactivity in the mucolipidosis IV (ML IV) mouse model was observed at the 2nd and 3rd months and coincided with the early stages of behavioural disturbances. As the disease progressed, GFAP reactivity continued to increase until the seventh month (Grishchuk et al. 2014). A study in a mouse model of Gaucher disease showed that increased *GFAP* and *CD68* expression was reduced when neural progenitor cell lines from healthy mice were administered (Peng et al. 2019). The ketogenic diet is used to reduce astrogliosis in the various conditions. In traumatic brain-injured mice, ketogenic diet significantly reduced the GFAP level in the cortex and dentate gyrus (DG) region of hippocampus (Har-Even et al. 2021). In a study showing the effect of propagermanium on GFAP levels, it was concluded that the elevated CCL2 level in the central nervous system increased the GFAP density in the intracerebral haemorrhage mouse model and that the subsequent reduction of CCL2 levels by propagermanium indirectly decreased the GFAP level (Guo et al. 2020). The ketogenic diet, propagermanium and combined ketogenic diet and propagermanium treatments was able to attenuate gene expression levels of the pro-inflammatory cytokine/chemokines which was utilized in this thesis.

Protein levels of NfκB and IκB-α were measured after short/long term ketogenic diet and propagermanium treatments in the cortex and cerebellum tissues. NfκB is a transcription factor which is member of the Rel family and it is activated by canonical and non-canonical mechanisms. The primary mechanism for activation of NFκB is the inducible degradation of IκB-α triggered through its site-specific phosphorylation by the multi-subunit IκB-α kinase (IKK) complex (T. Liu et al. 2017). NfκB have in role to regulate in particular neuroprotection, neuroinflammation and cell survival (Li and Verma 2002; Kaltschmidt, Widera, and Kaltschmidt 2005). It was identified that activation of NFκB in patients with chronic inflammation is critically linked to several autoimmune/inflammatory diseases such as Alzheimer's disease (AD), Parkinson's disease (PD), rheumatoid arthritis and diabetes (Vallabhapurapu and Karin 2009). NfκB was decreased in *Hexa-/-Neu3-/-* mouse cortex and cerebellum after short-term ketogenic diet and propagermanium treatments, but not after long-term ketogenic diet treatment. β-hydroxybutyrate, the main ketone body formed as a result of ketogenic diet, is one of the ligands of the receptor called hydroxy-carboxylic acid receptor 2 (HCA2) and activates it. As a result of this activation, HCA2 has been shown to inhibit NfκB signaling and reduce neuroinflammation by triggering prostaglandin D2 (PGD2) production by

cyclooxygenase 1 (COX1) which activates the IKB kinase (IKK) in bone-marrow derived macrophages (Rahman et al. 2014). In another study, when NfκB levels were investigated in mice fed a high-fat/high-cholesterol diet for 8 and 16 weeks, it was observed that NfκB levels increased compared to control mice in cortex and hippocampus, but when this diet was replaced after this period and a ketogenic diet was given for 8 weeks, it was shown that NfκB levels decreased significantly (D.-T. Lin et al. 2022). Furthermore, it was shown that NfκB protein level was attenuated after ketogenic diet treatment in EAE mice model spinal cords by suppressing TLR4/MyD88/NfκB pathway and NLRP3-mediated inflammation mechanism (W. Sun et al. 2023). In one study, the elevated CCL2/CCR2 activity through AMPK downregulation in RAW264.7 macrophages is partially reversed by NfκB inhibition. This further suggested that the mechanism of action of AMPK inhibition by CCL2/CCR2 axis is modulated by the NfκB pathway (Kumase et al. 2016). IκB-α is one of the leading proteins that inhibit NfκB activity. The phosphorylation of IκB-α by IKK activates NfκB by degrading it, thereby causing the secretion of pro-inflammatory cytokines and chemokines (Gilmore 2006). However, despite the decrease in NfκB levels after ketogenic diet treatment, IκB-α levels did not change in *Hexa-/-Neu3-/-* mice cortex and cerebellum. Recent studies have revealed that bound IkB persists much longer in unstimulated cells compared to free IκB-α. However, although free IκB-α is widely used in experiments to measure IKK activity, it is not a potent substrate for IKK (O'Dea et al. 2007). Therefore, while NfκB decreased after the ketogenic diet, IκB-α levels may have remained constant. Furthermore, the IκB-α protein level was significantly increased after propagermanium treatment, and this may be due to the role of NfκB in regulating CCL2 expression and secretion, which may have contributed to the increased IκB-α protein level in the cerebellum of *Hexa-/-Neu3-/-* mice after treatment with propagermanium, a CCL2/CCR2 inhibitor (Nakatsumi, Matsumoto, and Nakayama 2017).

Neuronal cell death is one of the most prominent pathological findings in the GM2 gangliosidosis mouse model as previously published. (Seyrantepe et al. 2018). NeuN staining revealed reduced neuron density in the cortex and cerebellum of *Hexa-/-Neu3-/-* mice compared to *WT* and *Hexa-/-* mice; however, neither short- or long-term ketogenic diet nor propagermanium treatments were able to ameliorate neuron loss.

Astrogliosis is described as the most prominent findings in brain pathology in early-onset neurological LSD. The astrogliosis marker of the GFAP was shown in the cortex and cerebellum after short/long term ketogenic diet and propagermanium

treatments. GFAP protein intensity significantly increased in the *Hexa-/-Neu3-/-* mouse cortex and cerebellum as previously published (Seyrantepe et al. 2018). Furthermore, astrocytosis and microgliosis were reported to start to be observed as early as 4 months in the somatosensory cortex of MPS IIIC mouse model (Martins et al. 2015). In a neuron-specific knockout mouse model of Gaucher disease, astrogliosis in layer 5 of the cerebral cortex and thalamus nucleus regions of 10-day-old mice was described to progressively increase until neuronal cell death starting at day 14 (Vitner et al. 2010). It has also been shown that astrogliosis formation precedes neuronal cell death in different regions of the brains of mouse models of Batten disease and neuronal ceroid lipofuscinosis (Pontikis et al. 2005; Thelen et al. 2012). One of the ketone bodies of β-hydroxybutyrate may also inhibit astrocyte/microglia activation while preventing NLRP3 inflammasome activity, which induces pro-inflammatory cytokine/chemokine secretion in Alzheimer's disease pathology. (Aso et al. 2013). In addition, ketogenic diet therapy induces AQP4 activity to stabilize K+ concentration in astrocytes, and impaired AQP4 activity is implicated in neuroinflammation and astrogliosis underlying Alzheimer's disease and Parkinson's disease (Kawamura et al. 2014). In one study, the effects of the CCL2/CCR2 axis on astrogliosis were investigated in a mouse model of sciatic nerve injury, where it was shown that neuronal CCL2 first activates microglia and then activated microglia induce astrogliosis which further increases CCL2 release from astrocytes by IL18 and CXCR1 activities (Gao and Ji 2010). Thus, inhibition of the CCL2 gene expression might be related with the reduction of the astrogliosis in *Hexa-/-Neu3-/-* mice brain.

MOMA-2 is the monocyte/macrophage marker which interact with the microglia and macrophage in the CNS. MOMA-2 intensity increased in the *Hexa-/-Neu3-/-* mice cortex and cerebellum (Demir et al. 2020). Furthermore, MOMA-2+ cells, marking microglia, are also gradually increased in the cortex of MPSI and MPSIIIB mouse models (Ohmi et al. 2003). The multiple sulfatase-deficient mouse model (*Sumf1-/-*) shows high macrophage presence and severe neuroinflammation in all tissues, especially in the Purkinje cell layer in the cerebellum (Settembre et al. 2007). The short-term ketogenic diet and propagermanium reduced the MOMA-2 intensity in *Hexa-/-Neu3-/-* mice cortex and cerebellum. Ketogenic diet treatment plays a neuroprotective role by decreasing nitric oxide synthase, a marker of M1 macrophages, and increasing arginase-1, a marker of M2 macrophages in acute cervical spinal cord injured model of rat (J. Lin et al. 2020). Furthermore, EAE and cuprizone-induced MS mouse models exhibit decreased numbers of macrophages and microglia, as well as diminished pro-inflammatory responses after

ketogenic diet treatment (D. Y. Kim et al. 2012; Chunhong Liu et al. 2020). One study showed that in a mouse model of kainic acid-induced epilepsy, knockout of the CCR2 receptor and the use of anti-CCL2 antibody helped reduce the number of active microglia as well as macrophage infiltration (Tian et al. 2017). From this point of view, the positive effects of propagermanium on monocyte/macrophage activities in the brain may have been achieved in this way.

CNPase staining was performed to investigate the ketogenic diet and propagermanium treatment effects on the oligodendrocyte intensity in *Hexa-/-Neu3-/-* mice cortex and cerebellum tissues. The presence of the oligodendrocyte significantly decreased in the *Hexa-/-Neu3-/-* mice cortex and cerebellum. It has been reported that GM3 accumulation in the Niemann Pick disease type 1 (*Npc1-/-*) mouse model impairs oligodendrocyte development and persistence and that this accumulation causes demyelination due to the dysfunction of oligodendrocytes (Lee et al. 2014). In another study, psychosine accumulation was shown to have a toxic effect on oligodendrocytes in a mouse model of Krabbe disease, leading to demyelination (K Suzuki 1998). The propagermanium but not ketogenic diet treatment improved the CNPase intensity in the *Hexa-/-Neu3-/-* mice cerebellum. The miR-146a deficient cuprizone model of multiple sclerosis mice exhibited reduction level of *CCL2* gene expression as well as oligodendrocyte progenitor cell differentiation to promote remyelination (Martin et al. 2018). Therefore, inhibition of the *CCL2* expression might improve the CNPase intensity by promoting OPC differentiation in *Hexa-/-Neu3-/-* mice cerebellum.

Autophagy is a conserved degradation pathway in which unnecessary or dysfunctional intracellular material is sent to the lysosome for degradation and recycling. A problem in this pathway is classified as an autophagic failure, which is also common in various lysosomal storage disorders. It has been previously reported that abnormal level of the GM2 ganglioside impairs the autophagic flux by the accumulated autophagosomes and autophagolysosomes in the *Hexa-/-Neu3-/-* mice brain (Sengul et al. 2023). Furthermore, Pompe disease, Danon disease, Gaucher disease, Batten disease and cystinosis mouse models also have autophagic impairment in their cells due to substrate accumulation or lysosomal enzyme dysfunctions (Myerowitz, Puertollano, and Raben 2021). Autophagic flux is composed of the mainly four steps: initiation, elongation, maturation and the fusion. Beclin-1 is the regulatory protein mainly in autophagy initiation step to start autophagosome formation but also plays key role in membrane trafficking (Tran, Fairlie, and Lee 2021). *Beclin-1* gene expression level significantly

increased in *Hexa-/-Neu3-/-* mice cortex and cerebellum tissues. It has been reported in a study that increased Beclin-1 expression level in *Npc1-/-* mouse fibroblasts, as in the Tay-Sachs mouse model, is due to impaired cholesterol and sphingolipid metabolism (Christopher D Pacheco and Lieberman 2007). Furthermore, it has been shown that Beclin-1 expression is upregulated in the GM1 gangliosidosis mouse model (Takamura et al. 2008). While this has shown that autophagy is induced in these diseases, the actual autophagic defects might be due to the accumulation of these produced autophagosomes. The short-term ketogenic diet and propagermanium treatments significantly reduced the *Beclin-1* expression in *Hexa-/-Neu3-/-* mice cortex and cerebellum. Considering the impact of ketogenic diet on Beclin-1, it was shown that the protein level of Beclin-1 was higher in pentylenetetrazol-kindled rats fed a ketogenic diet compared to rats fed a control diet (Wang et al. 2018). In another study, it was reported that a ketogenic diet inhibited Beclin-1 levels, which increased in flurothyl-treated rats which induces epileptic seizure, and promoted autophagic regulation (Ni, Zhao, and Tian 2016). Pro-inflammatory cytokine secretion from microglia is closely related to autophagic flux, as autophagy-defective microglia treated with LPS under in vitro conditions secrete excess pro-inflammatory cytokines and cause neuronal apoptosis. In vivo, impaired microglial autophagy in the MPTP-induced Parkinson's and Alzheimer's mouse model causes excessive pro-inflammatory cytokine release as well as NLRP3 inflammasome activation (Qin et al. 2021; Cho et al. 2014). However, further investigations are necessary to elucidate the mechanism of the reduced *Beclin-1* expression because of propagermanium treatment, an anti-inflammatory drug. Atg7 is the another autophagic protein which plays essential role in initiation of the autophagy and the autophagosome formation as well as LC3-I to LC3-II conversion (Lieberman et al. 2012). Atg7 expression level did not vary significantly between genotypes and after each treatment condition compared to untreated ones in cortex and cerebellum. However, Atg7 is abundant excessively in the one of the lysosomal storage disorder of Pompe disease mouse muscle in addition to Beclin-1 and LC3 due to autophagic failure (Raben et al. 2008). Atg9 is a type of lipid scramblase which play role in translocation of the phospholipids between outer membrane and inner membrane of the liposomes as well as function as transmembrane protein to assist formation of the autophagosome (Matoba et al. 2020). *Atg9* expression level significantly decreased in cortex and cerebellum tissues of the *Hexa-/-Neu3-/-* mice compared to control mice. In addition, Atg9 dysregulation has been attributed to Parkinson disease mouse model due to α-syn overexpression which causes Atg9 mislocalization and

decreases omegasome formation by suppressing Rab1a (Winslow et al. 2010). The ketogenic diet slightly increased the *Atg9* expression in *Hexa-/-Neu3-/-* cortex but propagermanium decreased *Atg9* expression only in the cortex. In a study, CCL2 together with IL-6 can induce autophagy in macrophages, triggering the phenotype of M2-type microglia with anti-inflammatory function (Lv et al. 2023). Therefore, treatment of the propagermanium inhibited CCL2 expression which might indirectly reduce *Atg9* gene expression. p62/SQSTM1 is a cargo protein that functions to target other proteins by directing autophagic cargoes for selective autophagy. The p62/SQSTM1 also colocalizes with the ubiquitinated proteins which accumulate in the various neurodegenerative disorders if the autophagic flux is impaired (Bjørkøy et al. 2009). In addition to neurodegenerative disorders, p62/SQSTM1 accumulation is also a critical sign in the lysosomal storage disorders to display autophagic impairment. The p62/SQSTM1 and ubiquitinated proteins accumulates in the Niemann pick type C (*Npc1-/-*) mouse model brain lysates as well as Gaucher disease (*Gba1-/-*) mouse brain displays accumulation of p62/SQSTM1 in astrocytes and neurons (Chris D Pacheco, Elrick, and Lieberman 2009; Y. Sun et al. 2010). The short-term ketogenic diet and propagermanium treatments significantly reduced the *p62/SQSTM1* gene expression level in *Hexa-/-Neu3-/-* mice cortex and cerebellum. It has been reported that β-hydroxybutyrate, one of the ketone bodies, decreases the LC-II/LC-I ratio and decreases p62/SQSTM1 levels by triggering autophagy in the myocardium of the ischemic/reperfusion injured mouse model (Y. Yu et al. 2018). It was also shown that rats with PTZ-kindled seizures showed decreased levels of p62/SQSTM1 and increased levels of Atg5 and Beclin-1 after ketogenic diet treatment (Wang et al. 2018). A study revealed that CCL2 maintains drug resistance by activating the PI3K-Akt-mTOR signaling pathway to suppress autophagy, leading to increased *p62/SQSTM1* expression in BGC823 and SGC7901 gastric cancer cell lines (W. Xu et al. 2018). On the basis of this mechanism, it can be concluded that propagermanium, which inhibits CCL2 expression, might reduce *p62/SQSTM1* expression. Lysosome-associated membrane protein 2 (Lamp-2) is a type of the lysosomal glycoproteins which function to regulate lysosomal homeostasis such as pH and integrity (Eskelinen et al. 2002). In addition, Lamp-2 also serve as a receptor to selective lysosomal import to degrade cytosolic proteins in lysosomes (Cuervo and Dice 1996). Deficiency of the Lamp-2 protein causes Danon's disease, a type of lysosomal storage disorder in which excess glycogen and autophagic vacuoles accumulate due to impaired autophagic flux. (Nishino et al. 2000). Lamp-2 gene expression level significantly increased in *Hexa-/-Neu3-/-* mice

cortex and cerebellum compared to *WT* and *Hexa-/-* mice. Furthermore, it has been reported that Lamp2A which is the variant of the Lamp-2 protein, decreased in the mucolipidosis type IV (MLIV) fibroblasts as well as defective chaperone-mediated autophagy (CMA). Neuronopathic Gaucher disease mouse model (*Gba1-/-*) also displayed accumulation of the Lamp-2 and p62/SQSTM1 proteins due to accumulated glucosylceramide and glucosylsphingosine which impairs autophagic flux (Y. Sun et al. 2010). Lamp-2 expression was only reduced in *Hexa-/-Neu3-/-* mice cortex compared to untreated ones after short-term ketogenic diet and propagermanium treatments. The reduction in Lamp-2 gene expression observed in *Hexa-/-Neu3-/-* mouse brain may have restored the expression level to normal conditions after the ketogenic diet. It has been reported that ketogenic diet treatment increases gene and protein expressions of the Lamp-2 in cortex and cerebellum regions of the CD-1 mice (Gómora-García et al. 2023). Another study showed that D-βHB treatment prevented Lamp-2 cleavage in the striatum and cortex, leading to the restoration of lysosomal function and amelioration of the protein clearance impairment (Montiel et al. 2020). Although there is limited information about the relationship between CCL2 and Lamp-2 protein in the literature, it has been shown that the amount of CCL2 decreased while the amount of Lamp-2 protein increased in a mouse model of acute lung injury treated with rapamycin, which induces (Zhao et al. 2019).

Protein levels of p62/SQSTM1 and LC3-I/LC3-II was illustrated by western blotting and immunofluorescence staining after short-term ketogenic diet and propagermanium treatments. p62/SQSTM1 level significantly increased in the *Hexa-/-Neu3-/-* mice compared to controls. It has reported that mucolipidosis type IV (MLIV) fibroblasts included accumulation of the p62/SQSTM1 and impaired mitochondria (Vergarajauregui et al. 2008). Furthermore, mucopolysaccharidoses type II and III (MPS II/III) fibroblasts also accumulated p62/SQSTM1 as well as ubiquitin and damaged mitochondria (Otomo et al. 2009). In vivo, the MPS II mouse model (*Ids-/-*) has been shown to involve p62/SQSTM1 accumulation in neurons due to reduced degradation of autophagic cargo from lysosomes (Maeda et al. 2019). The short-term ketogenic diet and combined ketogenic diet and propagermanium treatments significantly reduced the p62/SQSTM1 protein level in *Hexa-/-Neu3-/-* mice cortex and cerebellum. It has been reported that p62/SQSTM1 protein level is inhibited by ketogenic diet to induce autophagy in the regulation of the kidney injured rat model (Kundu et al. 2022). Furthermore, plant and animal-based ketogenic diet induced the hepatic autophagy in the

C57BL/6J mouse model to reduce p62/SQSTM1 protein level (Liśkiewicz et al. 2021). In addition, PTZ-kindled mouse model displayed reduction of the p62/SQSTM1 protein level after ketogenic diet treatment (Wang et al. 2018). According to these studies, it may be speculated that ketogenic diet treatment promotes the degradation of the accumulated p62/SQSTM1 by inducing autophagy. Microtubule-associated protein 1A/1B-light chain 3 (LC3) is a autophagic protein which serve as autophagosome formation. LC3-I creates a complex with phosphotidylethanolamine (PE) to produce LC3-II through ubiquitylation like reactions. The produced LC3-II is degraded after fusion with lysosomes by the assist of lysosomal proteases (Tanida, Ueno, and Kominami 2004). It has been reported that the Tay-Sachs mouse model shows the accumulation of autophagosomes and LC3 proteins due to autophagic defect, and in addition, the CLN3, CLN6, and CLN7 mouse models also have accumulated LC3 proteins (Sengul et al. 2023; Cao et al. 2006; Thelen et al. 2012; Brandenstein et al. 2016). The ketogenic diet and propagermanium treatments significantly reduced accumulated LC3-II protein level in the *Hexa-/-Neu3-/-* mice cortex and cerebellum tissues. Intraperitoneal and epidural delivery of D-βHB significantly reduced LC3 proteins accumulated in N-methyl-D-aspartate (NMDA)-treated rat striatum (Montiel et al. 2020). Furthermore, CCL2 has been implicated in the inhibition of autophagy via PI3K/Akt mechanism in rats with spinal cord injury. Therefore, it is considered that a combined ketogenic diet and propagermanium treatment might reduce the level of accumulated LC3 protein by modulating impaired autophagy. Consequently, the ketogenic diet and propagermanium treatments had a beneficial effect on the degradation of accumulated autophagic proteins by modifying the impaired autophagic pathway in *Hexa-/-Neu3-/-* mouse brain.

Neuropathological staining of the hematoxylin&eosin (H&E) and periodic-acid&Schiff (PAS) were performed for cortex and cerebellum regions of the *Hexa-/-Neu3-/-* mice to display neuronal morphology and glycoconjugate accumulation respectively. H&E staining illustrated vacuolization of the cortical neurons and Purkinje cells due to abnormal GM2 ganglioside accumulation as previously published (Seyrantepe et al. 2018). The ketogenic diet and propagermanium treatments did not alter the neuronal morphology in the *Hexa-/-Neu3-/-* mouse brain. PAS staining displayed the accumulation of the glycoconjugates in the *Hexa-/-Neu3-/-* mouse brain compared to controls. The short/long ketogenic diet significantly reduced the accumulated glycoconjugates due to the low carbohydrate content of the ketogenic diet. It has been shown in a study conducted in the liver tissue of a respiratory chain complex III deficiency

mouse model that the number of PAS+ cells decreased when a ketogenic diet was used (Purhonen et al. 2017).

The open field analysis and rotarod tests were performed to measure the anxiety-related behaviour and motor coordination as well as balance in *Hexa-/-Neu3-/-* mice. *Hexa-/-Neu3-/-* mice showed a reduction in time spent in the center of the box, which is associated with increased anxiety-related behaviour. Furthermore, total distance travelled significantly reduced in *Hexa-/-Neu3-/-* mice compared to controls. Apart from the Tay-Sachs mouse model, it has been reported that the MPS type IIIA (MPSIIIA) mouse model has decreased total activity in the open field test (Lau et al. 2008). The ketogenic diet and propagermanium treatments did not significantly improve the total activity in the *Hexa-/-Neu3-/-* mice compared to untreated ones. The rotarod test is the motor coordination and balance test on the accelerated rod in which *Hexa-/-Neu3-/-* mice elicited reduction time on rod compared to controls. It has been reported that acid sphingomyelinase deficient mouse model (*Asm-/-*) has the lower time on the rod than controls which indicates motor impairment (Gabandé-Rodríguez et al. 2019). The ketogenic diet and propagermanium treatments did not significantly improve the motor coordination deficit in the *Hexa-/-Neu3-/-* mice. Therefore, it might be suggested that ketogenic diet and propagermanium treatments are not being suitable to improve motor coordination and balance.

# CHAPTER 5

# CONCLUSION

The ketogenic diet has anti-inflammatory and autophagy-regulating effects, especially in the clinical findings of neurodegenerative diseases, and it was considered whether its positive effects could be observed in the Tay-Sachs mouse model in which progressively increased neuroinflammation and autophagic disorder findings were published. It was considered that more efficacious results could be achieved in neuronal pathology by using propagermanium, a CCL2/CCR2 axis inhibitor, in addition to a ketogenic diet by targeting CCL2 chemokine, which increases in neuroinflammation in *Hexa-/-Neu3-/-* mouse brains. Therefore, combined ketogenic diet and anti-inflammatory drug treatment on the reduction of the neuroinflammation and induction of the autophagic flux in *Hexa-/-Neu3-/-* mouse brain was aimed in this thesis. For this purpose, two-stage ketogenic diet treatments (short and long-term) with combined propagermanium was performed. The results revealed that short-term ketogenic diet treatment decreased CCL2 expression in both cortex and cerebellum regions and even decreased the expression of other neuroinflammation-related genes, such as propagermanium, which directly targets CCL2, in contrast to the long-term. Western blot results indicated that short-term ketogenic diet and propagermanium treatments attenuated neuroinflammation by reducing the elevated amount of NfκB in the cortex and cerebellum, independent of IκB-α level, due to the role of NfκB in CCL2 regulation. Immunofluorescence staining revealed that short-term ketogenic diet and propagermanium treatments are more effective to reduce astrocyte and macrophage activations than long-term treatment. After the impact on neuroinflammation, the effects of short-term ketogenic diet and propagermanium on autophagic flux were investigated. Following short-term ketogenic diet treatment, western blot and immunofluorescence staining results revealed that the accumulation of autophagosomes and autophagolysosomes detected in the neuronal pathology of *Hexa-/-Neu3-/-* mice was effectively diminished.

In conclusion, short-term ketogenic diet and propagermanium treatment provided more effective results compared to long-term treatment, while the anti-inflammatory and autophagic regulation effects on cortex and cerebellum regions of *Hexa-/-Neu3-/-* mice

were independent of the amount of GM2 ganglioside accumulated in these regions. Therefore, besides their palliative effects, short-term ketogenic diet and propagermanium treatments, in combination with gene therapy methods, can significantly contribute to the treatment of Tay-Sachs disease.

# REFERENCES


Abed Rabbo, Muna, Yara Khodour, Laurie S. Kaguni, and Johnny Stiban. 2021. "Sphingolipid Lysosomal Storage Diseases: From Bench to Bedside." *Lipids in Health and Disease* 20 (1). https://doi.org/10.1186/S12944-021-01466-0.

Akli, S., J. E. Guidotti, E. Vigne, M. Perricaudet, K. Sandhoff, A. Kahn, and L. Poenaru. 1996. "Restoration of Hexosaminidase A Activity in Human Tay-Sachs Fibroblasts via Adenoviral Vector-Mediated Gene Transfer." *Gene Therapy* 3 (9): 769–74. https://pubmed.ncbi.nlm.nih.gov/8875224/.

Anger, F, J P Anger, L Guillou, P A Sado, and A Papillon. 1991. "[Subacute and Subchronic Oral Toxicity of Beta-Bis Carboxyethyl Sesquioxide of Germanium in the Rat]." *Journal de Toxicologie Clinique et Experimentale* 11 (7–8): 421–36. https://pubmed.ncbi.nlm.nih.gov/1841079/.

Aronson, Nathan N. 2008. "Lysosomal Storage Diseases." *Carbohydrates in Chemistry and Biology* 4–4: 944–58. https://doi.org/10.1002/9783527618255.ch96.

Aso, Ester, Jana Semakova, Laura Joda, Vladislav Semak, Lyda Halbaut, Ana Calpena, Carmen Escolano, Jose C Perales, and Isidro Ferrer. 2013. "Triheptanoin Supplementation to Ketogenic Diet Curbs Cognitive Impairment in APP/PS1 Mice Used as a Model of Familial Alzheimer's Disease." *Current Alzheimer Research* 10 (3): 290–97. https://doi.org/10.2174/1567205011209999012 8.

Ballabio, Andrea, and Volkmar Gieselmann. 2009. "Lysosomal Disorders: From Storage to Cellular Damage." *Biochimica et Biophysica Acta - Molecular Cell Research*. https://doi.org/10.1016/j.bbamcr.2008.12.001.

Banisadr, Ghazal, Romain-Daniel Gosselin, Patricia Mechighel, Patrick Kitabgi, William Rostène, and Stéphane Mélik Parsadaniantz. 2005. "Highly Regionalized Neuronal Expression of Monocyte Chemoattractant Protein-1 (MCP-1/CCL2) in Rat Brain: Evidence for Its Colocalization with Neurotransmitters and

Neuropeptides." *The Journal of Comparative Neurology* 489 (3): 275–92. https://doi.org/10.1002/cne.20598.

Barzegar, Mohammad, Mohammadreza Afghan, Vahid Tarmahi, Meysam Behtari, Soroor Rahimi Khamaneh, and Sina Raeisi. 2021. "Ketogenic Diet: Overview, Types, and Possible Anti-Seizure Mechanisms." *Nutritional Neuroscience* 24 (4): 307–16. https://doi.org/10.1080/1028415X.2019.1627769.

Bembi, B., F. Marchetti, V. I. Guerci, G. Ciana, R. Addobbati, D. Grasso, R. Barone, et al. 2006. "Substrate Reduction Therapy in the Infantile Form of Tay-Sachs Disease." *Neurology* 66 (2): 278–80. https://doi.org/10.1212/01.WNL.0000194225.78917.DE.

Bergqvist, A. G.Christina, Joan I. Schall, Paul R. Gallagher, Avital Cnaan, and Virginia A. Stallings. 2005. "Fasting versus Gradual Initiation of the Ketogenic Diet: A Prospective, Randomized Clinical Trial of Efficacy." *Epilepsia* 46 (11): 1810–19. https://doi.org/10.1111/J.1528-1167.2005.00282.X.

Bjørkøy, Geir, Trond Lamark, Serhiy Pankiv, Aud Øvervatn, Andreas Brech, and Terje Johansen. 2009. "Monitoring Autophagic Degradation of P62/SQSTM1." *Methods in Enzymology* 452: 181–97. https://doi.org/10.1016/S0076-6879(08)03612-4.

Blanchette, Marie, and Richard Daneman. 2015. "Formation and Maintenance of the BBB." *Mechanisms of Development* 138 Pt 1 (November): 8–16. https://doi.org/10.1016/j.mod.2015.07.007.

Boddeke, E W, I Meigel, S Frentzel, N G Gourmala, J K Harrison, M Buttini, O Spleiss, and P Gebicke-Härter. 1999. "Cultured Rat Microglia Express Functional Beta-Chemokine Receptors." *Journal of Neuroimmunology* 98 (2): 176–84. https://doi.org/10.1016/s0165-5728(99)00096-x.

Bosch, Megan E., and Tammy Kielian. 2015. "Neuroinflammatory Paradigms in Lysosomal Storage Diseases." *Frontiers in Neuroscience* 9 (OCT): 1–11. https://doi.org/10.3389/fnins.2015.00417.

Bose, Shambhunath, and Jungsook Cho. 2013. “Role of Chemokine CCL2 and Its Receptor CCR2 in Neurodegenerative Diseases.” *Archives of Pharmacal Research* 36 (9): 1039–50. https://doi.org/10.1007/s12272-013-0161-z.

Brandenstein, Laura, Michaela Schweizer, Jan Sedlacik, Jens Fiehler, and Stephan Storch. 2016. “Lysosomal Dysfunction and Impaired Autophagy in a Novel Mouse Model Deficient for the Lysosomal Membrane Protein Cln7.” *Human Molecular Genetics* 25 (4): 777–91. https://doi.org/10.1093/hmg/ddv615.

Brouns, Fred. 2018. “Overweight and Diabetes Prevention: Is a Low-Carbohydrate-High-Fat Diet Recommendable?” *European Journal of Nutrition* 57 (4): 1301–12. https://doi.org/10.1007/S00394-018-1636-Y.

Brunetti-Pierri, Nicola, and Fernando Scaglia. 2008. “GM1 Gangliosidosis: Review of Clinical, Molecular, and Therapeutic Aspects.” *Molecular Genetics and Metabolism* 94 (4): 391–96. https://doi.org/10.1016/j.ymgme.2008.04.012.

Cachon-Gonzalez, María Begona, Eva Zaccariotto, and Timothy Martin Cox. 2018. “Genetics and Therapies for GM2 Gangliosidosis.” *Current Gene Therapy* 18 (2). https://doi.org/10.2174/1566523218666180404162622.

Cao, Yi, Janice A Espinola, Elisa Fossale, Ashish C Massey, Ana Maria Cuervo, Marcy E MacDonald, and Susan L Cotman. 2006. “Autophagy Is Disrupted in a Knock-in Mouse Model of Juvenile Neuronal Ceroid Lipofuscinosis.” *The Journal of Biological Chemistry* 281 (29): 20483–93. https://doi.org/10.1074/jbc.M602180200.

Cheng, Clara M, Brandon Kelley, Jie Wang, David Strauss, Douglas A Eagles, and Carolyn A Bondy. 2003. “A Ketogenic Diet Increases Brain Insulin-like Growth Factor Receptor and Glucose Transporter Gene Expression.” *Endocrinology* 144 (6): 2676–82. https://doi.org/10.1210/en.2002-0057.

Cho, Mi-Hyang, Kwangmin Cho, Hoe-Jin Kang, Eun-Young Jeon, Hun-Sik Kim, Hyung-Joon Kwon, Hong-Mi Kim, Dong-Hou Kim, and Seung-Yong Yoon. 2014.

"Autophagy in Microglia Degrades Extracellular β-Amyloid Fibrils and Regulates the NLRP3 Inflammasome." *Autophagy* 10 (10): 1761–75. https://doi.org/10.4161/auto.29647.

Conductier, Grégory, Nicolas Blondeau, Alice Guyon, Jean Louis Nahon, and Carole Rovère. 2010. "The Role of Monocyte Chemoattractant Protein MCP1/CCL2 in Neuroinflammatory Diseases." *Journal of Neuroimmunology* 224 (1–2): 93–100. https://doi.org/10.1016/j.jneuroim.2010.05.010.

Cordiglieri, Chiara, and Cinthia Farina. 2010. "Astrocytes Exert and Control Immune Responses in the Brain." *Current Immunology Reviews* 6 (3): 150–59. https://doi.org/10.2174/157339510791823655.

Cougnoux, Antony, Rebecca A Drummond, Mason Fellmeth, Fatemeh Navid, Amanda L Collar, James Iben, Ashok B Kulkarni, et al. 2019. "Unique Molecular Signature in Mucolipidosis Type IV Microglia." *Journal of Neuroinflammation* 16 (1): 276. https://doi.org/10.1186/s12974-019-1672-4.

Cuervo, A M, and J F Dice. 1996. "A Receptor for the Selective Uptake and Degradation of Proteins by Lysosomes." *Science (New York, N.Y.)* 273 (5274): 501–3. https://doi.org/10.1126/science.273.5274.501.

Daikhin, Y, and M Yudkoff. 1998. "Ketone Bodies and Brain Glutamate and GABA Metabolism." *Developmental Neuroscience* 20 (4–5): 358–64. https://doi.org/10.1159/000017331.

Demir, Seçil Akylldlz, Zehra Kevser Timur, Nurselin Ateş, Luis Alarcón Martínez, and Volkan Seyrantepe. 2020. "GM2 Ganglioside Accumulation Causes Neuroinflammation and Behavioral Alterations in a Mouse Model of Early Onset Tay-Sachs Disease." *Journal of Neuroinflammation* 17 (1): 1–18. https://doi.org/10.1186/s12974-020-01947-6.

Denny, Christine A., Karie A. Heinecke, Youngho P. Kim, Rena C. Baek, Katrina S. Loh, Terry D. Butters, Roderick T. Bronson, Frances M. Platt, and Thomas N.

Seyfried. 2010. “Restricted Ketogenic Diet Enhances the Therapeutic Action of N-Butyldeoxynojirimycin towards Brain GM2 Accumulation in Adult Sandhoff Disease Mice.” *Journal of Neurochemistry* 113 (6): 1525–35. https://doi.org/10.1111/j.1471-4159.2010.06733.x.

Derecki, Noël C., Amber N. Cardani, Chun Hui Yang, Kayla M. Quinnies, Anastasia Crihfield, Kevin R. Lynch, and Jonathan Kipnis. 2010. “Regulation of Learning and Memory by Meningeal Immunity: A Key Role for IL-4.” *Journal of Experimental Medicine* 207 (5): 1067–80. https://doi.org/10.1084/jem.20091419.

Dickens, Alex M, Tory P Johnson, Santosh Lamichhane, Anupama Kumar, Carlos A Pardo, Erie G Gutierrez, Norman Haughey, and Mackenzie C Cervenka. 2023. “Changes in Lipids and Inflammation in Adults with Super-Refractory Status Epilepticus on a Ketogenic Diet.” *Frontiers in Molecular Biosciences* 10: 1173039. https://doi.org/10.3389/fmolb.2023.1173039.

Dikic, Ivan, and Zvulun Elazar. 2018. “Mechanism and Medical Implications of Mammalian Autophagy.” *Nature Reviews Molecular Cell Biology* 19 (6): 349–64. https://doi.org/10.1038/s41580-018-0003-4.

Dorf, M E, M A Berman, S Tanabe, M Heesen, and Y Luo. 2000. “Astrocytes Express Functional Chemokine Receptors.” *Journal of Neuroimmunology* 111 (1–2): 109–21. https://doi.org/10.1016/s0165-5728(00)00371-4.

Dupuis, Nina, Niccolo Curatolo, Jean François Benoist, and Stéphane Auvin. 2015. “Ketogenic Diet Exhibits Anti-Inflammatory Properties.” *Epilepsia* 56 (7): e95–98. https://doi.org/10.1111/epi.13038.

Dworski, Shaalee, Ping Lu, Aneal Khan, Bruno Maranda, John J Mitchell, Rossella Parini, Maja Di Rocco, et al. 2017. “Acid Ceramidase Deficiency Is Characterized by a Unique Plasma Cytokine and Ceramide Profile That Is Altered by Therapy.” *Biochimica et Biophysica Acta. Molecular Basis of Disease* 1863 (2): 386–94. https://doi.org/10.1016/j.bbadis.2016.11.031.

Egan, Dan, Joungmok Kim, Reuben J Shaw, and Kun-Liang Guan. 2011. “The Autophagy Initiating Kinase ULK1 Is Regulated via Opposing Phosphorylation by AMPK and MTOR.” *Autophagy* 7 (6): 643–44. https://doi.org/10.4161/auto.7.6.15123.

Ellenbroek, Johanne H., Laura van Dijck, Hendrica A. Töns, Ton J. Rabelink, Françoise Carlotti, Bart E.P.B. Ballieux, and Eelco J.P. de Koning. 2014. “Long-Term Ketogenic Diet Causes Glucose Intolerance and Reduced β- and α-Cell Mass but No Weight Loss in Mice.” *American Journal of Physiology - Endocrinology and Metabolism* 306 (5): 552–58. https://doi.org/10.1152/ajpendo.00453.2013.

Engel, Andrew G., Manuel R. Gomez, Marjorie E. Seybold, and Edward H. Lambert. 1973. “The Spectrum and Diagnosis of Acid Maltase Deficiency.” *Neurology* 23 (1): 95–106. https://doi.org/10.1212/WNL.23.1.95.

Eskelinen, Eeva-Liisa, Anna Lena Illert, Yoshitaka Tanaka, Günter Schwarzmann, Judith Blanz, Kurt Von Figura, and Paul Saftig. 2002. “Role of LAMP-2 in Lysosome Biogenesis and Autophagy.” *Molecular Biology of the Cell* 13 (9): 3355–68. https://doi.org/10.1091/mbc.e02-02-0114.

Espejo-Mojica, Angela J., Alexander Rodríguez-López, Rong Li, Wei Zheng, Carlos J. Alméciga-Díaz, Cindy Dulcey-Sepúlveda, Germán Combariza, and Luis A. Barrera. 2020. “Human Recombinant Lysosomal β-Hexosaminidases Produced in Pichia Pastoris Efficiently Reduced Lipid Accumulation in Tay-Sachs Fibroblasts.” *American Journal of Medical Genetics. Part C, Seminars in Medical Genetics* 184 (4): 885–95. https://doi.org/10.1002/AJMG.C.31849.

Fernandes Filho, Jose America, and Barbara E. Shapiro. 2004. “Tay-Sachs Disease.” *Archives of Neurology* 61 (9): 1466–68. https://doi.org/10.1001/ARCHNEUR.61.9.1466.

Foresti, Maira L., Gabriel M. Arisi, Khurshed Katki, Andres Montañez, Russell M. Sanchez, and Lee A. Shapiro. 2009. “Chemokine CCL2 and Its Receptor CCR2 Are Increased in the Hippocampus Following Pilocarpine-Induced Status

Epilepticus.” *Journal of Neuroinflammation* 6: 1–11. https://doi.org/10.1186/1742-2094-6-40.

Fukao, Toshiyuki, Xiang Qian Song, Grant A. Mitchell, Seiji Yamaguchi, Kazuko Sukegawa, Tadao Orii, and Naomi Kondo. 1997. “Enzymes of Ketone Body Utilization in Human Tissues: Protein and Messenger RNA Levels of Succinyl-Coenzyme A (CoA):3-Ketoacid CoA Transferase and Mitochondrial and Cytosolic Acetoacetyl-CoA Thiolases.” *Pediatric Research* 42 (4): 498–502. https://doi.org/10.1203/00006450-199710000-00013.

Fukushi, Yasuo, Sen Itiroh Hakomori, and Thomas Shepard. 1984. “Localization and Alteration of Mono-, Di-, and Trifucosyl Alpha 1----3 Type 2 Chain Structures during Human Embryogenesis and in Human Cancer.” *The Journal of Experimental Medicine* 160 (2): 506–20. https://doi.org/10.1084/JEM.160.2.506.

Gabandé-Rodríguez, Enrique, Azucena Pérez-Cañamás, Beatriz Soto-Huelin, Daniel N Mitroi, Sara Sánchez-Redondo, Elena Martínez-Sáez, César Venero, Héctor Peinado, and María Dolores Ledesma. 2019. “Lipid-Induced Lysosomal Damage after Demyelination Corrupts Microglia Protective Function in Lysosomal Storage Disorders.” *The EMBO Journal* 38 (2). https://doi.org/10.15252/embj.201899553.

Galimberti, Daniela, Chiara Fenoglio, Carlo Lovati, Eliana Venturelli, Ilaria Guidi, Barbara Corrà, Diego Scalabrini, et al. 2006. “Serum MCP-1 Levels Are Increased in Mild Cognitive Impairment and Mild Alzheimer’s Disease.” *Neurobiology of Aging* 27 (12): 1763–68. https://doi.org/10.1016/j.neurobiolaging.2005.10.007.

Gao, Yong-Jing, and Ru-Rong Ji. 2010. “Targeting Astrocyte Signaling for Chronic Pain.” *Neurotherapeutics : The Journal of the American Society for Experimental NeuroTherapeutics* 7 (4): 482–93. https://doi.org/10.1016/j.nurt.2010.05.016.

Gilbert-Barness, Enid. 2004. “Review: Metabolic Cardiomyopathy and Conduction System Defleas in Children.” *Annals of Clinical and Laboratory Science*. https://pubmed.ncbi.nlm.nih.gov/15038665/.

Gilmore, T D. 2006. “Introduction to NF-KappaB: Players, Pathways, Perspectives.” *Oncogene* 25 (51): 6680–84. https://doi.org/10.1038/sj.onc.1209954.

Goldberg, Emily L., Irina Shchukina, Jennifer L. Asher, Sviatoslav Sidorov, Maxim N. Artyomov, and Vishwa Deep Dixit. 2020. “Ketogenesis Activates Metabolically Protective Γδ T Cells in Visceral Adipose Tissue.” *Nature Metabolism* 2 (1): 50–61. https://doi.org/10.1038/s42255-019-0160-6.

Gómora-García, Juan Carlos, Teresa Montiel, Melanie Hüttenrauch, Ashley Salcido-Gómez, Lizbeth García-Velázquez, Yazmin Ramiro-Cortés, Juan Carlos Gomora, Susana Castro-Obregón, and Lourdes Massieu. 2023. “Effect of the Ketone Body, D-β-Hydroxybutyrate, on Sirtuin2-Mediated Regulation of Mitochondrial Quality Control and the Autophagy-Lysosomal Pathway.” *Cells* 12 (3). https://doi.org/10.3390/cells12030486.

Grishchuk, Yulia, Sarmi Sri, Nikita Rudinskiy, Weiyuan Ma, Katherine G Stember, Matthew W Cottle, Ellen Sapp, et al. 2014. “Behavioral Deficits, Early Gliosis, Dysmyelination and Synaptic Dysfunction in a Mouse Model of Mucolipidosis IV.” *Acta Neuropathologica Communications* 2 (September): 133. https://doi.org/10.1186/s40478-014-0133-7.

Guo, Fuyou, Dingkang Xu, Yazhou Lin, Guoqing Wang, Fang Wang, Qiang Gao, Qingjie Wei, and Shixiong Lei. 2020. “Chemokine CCL2 Contributes to BBB Disruption via the P38 MAPK Signaling Pathway Following Acute Intracerebral Hemorrhage.” *FASEB Journal* 34 (1): 1872–84. https://doi.org/10.1096/fj.201902203RR.

Guzik-Kornacka, Anna, Anna Sliwa, Gabriela Plucinska, and Katarzyna Lukasiuk. 2011. “Status Epilepticus Evokes Prolonged Increase in the Expression of CCL3 and CCL4 MRNA and Protein in the Rat Brain.” *Acta Neurobiologiae Experimentalis* 71 (2): 193–207. https://doi.org/10.55782/ane-2011-1840.

Hamada, Shu, Takeo Kato, Kengo Kora, Tatsuya Kawaguchi, Tenshin Okubo, Minako Ide, Takayuki Tanaka, Tomokatsu Yoshida, and Takafumi Sakakibara. 2021.

"Ketogenic Diet Therapy for Intractable Epilepsy in Infantile Alexander Disease: A Small Case Series and Analyses of Astroglial Chemokines and Proinflammatory Cytokines." *Epilepsy Research* 170 (February): 106519. https://doi.org/10.1016/j.eplepsyres.2020.106519.

Har-Even, Meirav, Vardit Rubovitch, Whitney A Ratliff, Bar Richmond-Hacham, Bruce A Citron, and Chaim G Pick. 2021. "Ketogenic Diet as a Potential Treatment for Traumatic Brain Injury in Mice." *Scientific Reports* 11 (1): 23559. https://doi.org/10.1038/s41598-021-02849-0.

Harun-Or-Rashid, Mohammad, and Denise M Inman. 2018. "Reduced AMPK Activation and Increased HCAR Activation Drive Anti-Inflammatory Response and Neuroprotection in Glaucoma." *Journal of Neuroinflammation* 15 (1): 313. https://doi.org/10.1186/s12974-018-1346-7.

He, Shucheng, Rui Liu, Binbin Li, Liangliang Huang, Wenxiang Fan, Charmaine Ruvimbo Tembachako, Xiaoya Zheng, et al. 2019. "Propagermanium, a CCR2 Inhibitor, Attenuates Cerebral Ischemia/Reperfusion Injury through Inhibiting Inflammatory Response Induced by Microglia." *Neurochemistry International* 125 (December 2018): 99–110. https://doi.org/10.1016/j.neuint.2019.02.010.

Hickman, Suzanne E, and Joseph El Khoury. 2010. "Mechanisms of Mononuclear Phagocyte Recruitment in Alzheimer's Disease." *CNS & Neurological Disorders Drug Targets* 9 (2): 168–73. https://doi.org/10.2174/187152710791011982.

Holczer, Marianna, Bence Hajdú, Tamás Lőrincz, András Szarka, Gábor Bánhegyi, and Orsolya Kapuy. 2019. "A Double Negative Feedback Loop between MTORC1 and AMPK Kinases Guarantees Precise Autophagy Induction upon Cellular Stress." *International Journal of Molecular Sciences* 20 (22). https://doi.org/10.3390/ijms20225543.

Höller, A., U. Albrecht, S. Baumgartner Sigl, T. Zöggeler, G. Ramoser, B. Bernar, D. Karall, and S. Scholl-Bürgi. 2021. "Successful Implementation of Classical Ketogenic Dietary Therapy in a Patient with Niemann-Pick Disease Type C."

*Molecular Genetics and Metabolism Reports* 27. https://doi.org/10.1016/j.ymgmr.2021.100723.

Hoops, S. L., T. Kolter, and K. Sandhoff. 2009. "Sphingolipid-Inherited Diseases of the Central Nervous System." *Handbook of Neurochemistry and Molecular Neurobiology*, 671–702. https://doi.org/10.1007/978-0-387-30378-9_27.

Horii, Yuto, Toshiki Iniwa, Masayoshi Onitsuka, Jun Tsukimoto, Yuki Tanaka, Hironobu Ike, Yuri Fukushi, et al. 2022. "Reversal of Neuroinflammation in Novel GS Model Mice by Single i.c.v. Administration of CHO-Derived RhCTSA Precursor Protein." *Molecular Therapy Methods and Clinical Development* 25 (June): 297–310. https://doi.org/10.1016/j.omtm.2022.04.001.

Huang, D R, J Wang, P Kivisakk, B J Rollins, and R M Ransohoff. 2001. "Absence of Monocyte Chemoattractant Protein 1 in Mice Leads to Decreased Local Macrophage Recruitment and Antigen-Specific T Helper Cell Type 1 Immune Response in Experimental Autoimmune Encephalomyelitis." *The Journal of Experimental Medicine* 193 (6): 713–26. https://doi.org/10.1084/jem.193.6.713.

Huang, Deren, Jerome Wujek, Graham Kidd, Toby T He, Astrid Cardona, Margaret E Sasse, Erica J Stein, et al. 2005. "Chronic Expression of Monocyte Chemoattractant Protein-1 in the Central Nervous System Causes Delayed Encephalopathy and Impaired Microglial Function in Mice." *FASEB Journal : Official Publication of the Federation of American Societies for Experimental Biology* 19 (7): 761–72. https://doi.org/10.1096/fj.04-3104com.

Huang, Hao, Wanjun He, Tao Tang, and Mengsheng Qiu. 2023. "Immunological Markers for Central Nervous System Glia." *Neuroscience Bulletin* 39 (3): 379–92. https://doi.org/10.1007/s12264-022-00938-2.

Ishii, Atsushi, Masatsugu Ohta, Yumiko Watanabe, Kazuhiro Matsuda, Keiko Ishiyama, Kumi Sakoe, Mitsuru Nakamura, Jin Ichi Inokuchi, Yutaka Sanai, and Masaki Saito. 1999. "Expression Cloning and Functional Characterization of Human CDNA for Ganglioside G(M3) Synthase." *Journal of Biological Chemistry* 273

(48): 31652–55. https://doi.org/10.1074/jbc.273.48.31652.

Jacobs, J. F.M., M. A.A.P. Willemsen, J. J. Groot-Loonen, R. A. Wevers, and P. M. Hoogerbrugge. 2005. “Allogeneic BMT Followed by Substrate Reduction Therapy in a Child with Subacute Tay-Sachs Disease.” *Bone Marrow Transplantation* 36 (10): 925–26. https://doi.org/10.1038/SJ.BMT.1705155.

Jang, Jiwon, Su Rim Kim, Jo Eun Lee, Seoyeon Lee, Hyeong Jig Son, Wonchae Choe, Kyung-Sik Yoon, Sung Soo Kim, Eui-Ju Yeo, and Insug Kang. 2023. “Molecular Mechanisms of Neuroprotection by Ketone Bodies and Ketogenic Diet in Cerebral Ischemia and Neurodegenerative Diseases.” *International Journal of Molecular Sciences* 25 (1): 124. https://doi.org/10.3390/ijms25010124.

Jarnes Utz, Jeanine R., Sarah Kim, Kelly King, Richard Ziegler, Lynn Schema, Evelyn S. Redtree, and Chester B. Whitley. 2017. “Infantile Gangliosidoses: Mapping a Timeline of Clinical Changes.” *Molecular Genetics and Metabolism* 121 (2): 170–79. https://doi.org/10.1016/j.ymgme.2017.04.011.

Jennemann, Richard, Roger Sandhoff, Shijun Wang, Eva Kiss, Norbert Gretz, Cecilia Zuliani, Ana Martin-Villalba, et al. 2005. “Cell-Specific Deletion of Glucosylceramide Synthase in Brain Leads to Severe Neural Defects after Birth.” *Proceedings of the National Academy of Sciences of the United States of America* 102 (35): 12459–64. https://doi.org/10.1073/PNAS.0500893102.

Jeyakumar, M., R. Thomas, E. Elliot-Smith, D. A. Smith, A. C. Van der Spoel, A. D’Azzo, V. Hugh Perry, T. D. Butters, R. A. Dwek, and F. M. Platt. 2003. “Central Nervous System Inflammation Is a Hallmark of Pathogenesis in Mouse Models of GM1 and GM2 Gangliosidosis.” *Brain* 126 (4): 974–87. https://doi.org/10.1093/brain/awg089.

Kaltschmidt, Barbara, Darius Widera, and Christian Kaltschmidt. 2005. “Signaling via NF-KappaB in the Nervous System.” *Biochimica et Biophysica Acta* 1745 (3): 287–99. https://doi.org/10.1016/j.bbamcr.2005.05.009.

Kang, R, H J Zeh, M T Lotze, and D Tang. 2011. “The Beclin 1 Network Regulates Autophagy and Apoptosis.” *Cell Death and Differentiation* 18 (4): 571–80. https://doi.org/10.1038/cdd.2010.191.

Kass, Hannah R., S. Parrish Winesett, Stacey K. Bessone, Zahava Turner, and Eric H. Kossoff. 2016. “Use of Dietary Therapies amongst Patients with GLUT1 Deficiency Syndrome.” *Seizure* 35 (February): 83–87. https://doi.org/10.1016/J.SEIZURE.2016.01.011.

Kawamura, Masahito Jr, David N Ruskin, Jonathan D Geiger, Detlev Boison, and Susan A Masino. 2014. “Ketogenic Diet Sensitizes Glucose Control of Hippocampal Excitability.” *Journal of Lipid Research* 55 (11): 2254–60. https://doi.org/10.1194/jlr.M046755.

Keilani, Serene, Yi Lun, Anthony C. Stevens, Hadis N. Williams, Eric R. Sjoberg, Richie Khanna, Kenneth J. Valenzano, et al. 2012. “Lysosomal Dysfunction in a Mouse Model of Sandhoff Disease Leads to Accumulation of Ganglioside-Bound Amyloid-β Peptide.” *Journal of Neuroscience* 32 (15): 5223–36. https://doi.org/10.1523/JNEUROSCI.4860-11.2012.

Kim, Do Young, Junwei Hao, Ruolan Liu, Gregory Turner, Fu-Dong Shi, and Jong M Rho. 2012. “Inflammation-Mediated Memory Dysfunction and Effects of a Ketogenic Diet in a Murine Model of Multiple Sclerosis.” *PloS One* 7 (5): e35476. https://doi.org/10.1371/journal.pone.0035476.

Kim, Kook Hwan, and Myung-Shik Lee. 2014. “Autophagy--a Key Player in Cellular and Body Metabolism.” *Nature Reviews. Endocrinology* 10 (6): 322–37. https://doi.org/10.1038/nrendo.2014.35.

Kiyota, Tomomi, Masaru Yamamoto, Huangui Xiong, Mary P Lambert, William L Klein, Howard E Gendelman, Richard M Ransohoff, and Tsuneya Ikezu. 2009. “CCL2 Accelerates Microglia-Mediated Abeta Oligomer Formation and Progression of Neurocognitive Dysfunction.” *PloS One* 4 (7): e6197. https://doi.org/10.1371/journal.pone.0006197.

Koh, Sookyong, Nina Dupuis, and Stéphane Auvin. 2020. “Ketogenic Diet and Neuroinflammation.” *Epilepsy Research* 167 (June): 1–8. https://doi.org/10.1016/j.eplepsyres.2020.106454.

Kolter, Thomas, Thomas M. Magin, and Konrad Sandhoff. 2000. “Biomolecule Function: No Reliable Prediction from Cell Culture.” *Traffic* 1 (10): 803–4. https://doi.org/10.1034/j.1600-0854.2000.011007.x.

Kolter, Thomas, and Konrad Sandhoff. 1999. “SphingolipidsĐTheir Metabolic Pathways and the Pathobiochemistry Of.” *Angewandte Chemie International Edition* 38 (11): 1532–68. https://pubmed.ncbi.nlm.nih.gov/29710982/.

Kossoff, Eric H. 2023. “The Modified Atkins Diet for Epilepsy: Two Decades of an ‘Alternative’ Ketogenic Diet Therapy.” *Pediatric Neurology* 147 (October): 82–87. https://doi.org/10.1016/J.PEDIATRNEUROL.2023.07.014.

Kumase, Fumiaki, Kimio Takeuchi, Yuki Morizane, Jun Suzuki, Hidetaka Matsumoto, Keiko Kataoka, Ahmad Al-Moujahed, Daniel E Maidana, Joan W Miller, and Demetrios G Vavvas. 2016. “AMPK-Activated Protein Kinase Suppresses Ccr2 Expression by Inhibiting the NF-KB Pathway in RAW264.7 Macrophages.” *PloS One* 11 (1): e0147279. https://doi.org/10.1371/journal.pone.0147279.

Kundu, Sushmita, Khandkar Shaharina Hossain, Akhi Moni, Md Sarwar Zahan, Md Masudur Rahman, and Md Jamal Uddin. 2022. “Potentials of Ketogenic Diet against Chronic Kidney Diseases: Pharmacological Insights and Therapeutic Prospects.” *Molecular Biology Reports* 49 (10): 9749–58. https://doi.org/10.1007/s11033-022-07460-8.

Landreneau, Margaret J, Michael T Mullen, Steven R Messé, Brett Cucchiara, Kevin N Sheth, Louise D McCullough, Scott E Kasner, and Lauren H Sansing. 2018. “CCL2 and CXCL10 Are Associated with Poor Outcome after Intracerebral Hemorrhage.” *Annals of Clinical and Translational Neurology* 5 (8): 962–70. https://doi.org/10.1002/acn3.595.

Lanfranco, Maria Fe, Italo Mocchetti, Mark P Burns, and Sonia Villapol. 2017. "Glial- and Neuronal-Specific Expression of CCL5 MRNA in the Rat Brain." *Frontiers in Neuroanatomy* 11: 137. https://doi.org/10.3389/fnana.2017.00137.

Lau, Adeline A, Allison C Crawley, John J Hopwood, and Kim M Hemsley. 2008. "Open Field Locomotor Activity and Anxiety-Related Behaviors in Mucopolysaccharidosis Type IIIA Mice." *Behavioural Brain Research* 191 (1): 130–36. https://doi.org/10.1016/j.bbr.2008.03.024.

Leal, Andrés Felipe, Eliana Benincore-Flórez, Daniela Solano-Galarza, Rafael Guillermo Garzón Jaramillo, Olga Yaneth Echeverri-Peña, Diego A. Suarez, Carlos Javier Alméciga-Díaz, and Angela Johana Espejo-Mojica. 2020. "Gm2 Gangliosidoses: Clinical Features, Pathophysiological Aspects, and Current Therapies." *International Journal of Molecular Sciences* 21 (17): 1–27. https://doi.org/10.3390/ijms21176213.

Leal, Andrés Felipe, Javier Cifuentes, Valentina Quezada, Eliana Benincore-Flórez, Juan Carlos Cruz, Luis Humberto Reyes, Angela Johana Espejo-Mojica, and Carlos Javier Alméciga-Díaz. 2022. "CRISPR/NCas9-Based Genome Editing on GM2 Gangliosidoses Fibroblasts via Non-Viral Vectors." *International Journal of Molecular Sciences* 23 (18). https://doi.org/10.3390/IJMS231810672.

Lee, Hyun, Jong Kil Lee, Yong Chul Bae, Song Hyun Yang, Nozomu Okino, Edward H Schuchman, Tadashi Yamashita, Jae-Sung Bae, and Hee Kyung Jin. 2014. "Inhibition of GM3 Synthase Attenuates Neuropathology of Niemann-Pick Disease Type C. by Affecting Sphingolipid Metabolism." *Molecules and Cells* 37 (2): 161–71. https://doi.org/10.14348/molcells.2014.2347.

Leinekugel, P., S. Michel, E. Conzelmann, and K. Sandhoff. 1992. "Quantitative Correlation between the Residual Activity of Beta-Hexosaminidase A and Arylsulfatase A and the Severity of the Resulting Lysosomal Storage Disease." *Human Genetics* 88 (5): 513–23. https://doi.org/10.1007/BF00219337.

Levine, Beth, and Guido Kroemer. 2019. “Biological Functions of Autophagy Genes: A Disease Perspective.” *Cell* 176 (1–2): 11–42. https://doi.org/10.1016/j.cell.2018.09.048.

Li, Qiutang, and Inder M Verma. 2002. “NF-KappaB Regulation in the Immune System.” *Nature Reviews. Immunology* 2 (10): 725–34. https://doi.org/10.1038/nri910.

Lieberman, Andrew P, Rosa Puertollano, Nina Raben, Susan Slaugenhaupt, Steven U Walkley, and Andrea Ballabio. 2012. “Autophagy in Lysosomal Storage Disorders.” *Autophagy* 8 (5): 719–30. https://doi.org/10.4161/auto.19469.

Lin, Dai-Ting, Ning-Juo Kao, Tzu-Wen Liu Cross, Wei-Ju Lee, and Shyh-Hsiang Lin. 2022. “Effects of Ketogenic Diet on Cognitive Functions of Mice Fed High-Fat-High-Cholesterol Diet.” *The Journal of Nutritional Biochemistry* 104 (June): 108974. https://doi.org/10.1016/j.jnutbio.2022.108974.

Lin, Junyu, Zucheng Huang, Junhao Liu, Zhiping Huang, Yapu Liu, Qi Liu, Zhou Yang, et al. 2020. “Neuroprotective Effect of Ketone Metabolism on Inhibiting Inflammatory Response by Regulating Macrophage Polarization After Acute Cervical Spinal Cord Injury in Rats.” *Frontiers in Neuroscience* 14: 583611. https://doi.org/10.3389/fnins.2020.583611.

Liśkiewicz, Daniela, Arkadiusz Liśkiewicz, Mateusz Grabowski, Marta Maria Nowacka-Chmielewska, Konstancja Jabłońska, Anna Wojakowska, Łukasz Marczak, Jarosław J Barski, and Andrzej Małecki. 2021. “Upregulation of Hepatic Autophagy under Nutritional Ketosis.” *The Journal of Nutritional Biochemistry* 93 (July): 108620. https://doi.org/10.1016/j.jnutbio.2021.108620.

Liu, Chang, Guohong Cui, Meiping Zhu, Xiangping Kang, and Haidong Guo. 2014. “Neuroinflammation in Alzheimer’s Disease: Chemokines Produced by Astrocytes and Chemokine Receptors.” *International Journal of Clinical and Experimental Pathology* 7 (12): 8342–55.

Liu, Chunhong, Ning Zhang, Ruiyan Zhang, Li Jin, Athanasios K Petridis, Gabriele Loers, Xuexing Zheng, Zhengping Wang, and Hans-Christian Siebert. 2020. "Cuprizone-Induced Demyelination in Mouse Hippocampus Is Alleviated by Ketogenic Diet." *Journal of Agricultural and Food Chemistry* 68 (40): 11215–28. https://doi.org/10.1021/acs.jafc.0c04604.

Liu, Ting, Lingyun Zhang, Donghyun Joo, and Shao Cong Sun. 2017. "NF-KB Signaling in Inflammation." *Signal Transduction and Targeted Therapy* 2 (April). https://doi.org/10.1038/sigtrans.2017.23.

Liu, Yeou Mei, and Huei Shyong Wang. 2013. "Medium-Chain Triglyceride Ketogenic Diet, an Effective Treatment for Drug-Resistant Epilepsy and a Comparison with Other Ketogenic Diets." *Biomedical Journal* 36 (1): 9–15. https://doi.org/10.4103/2319-4170.107154.

Liu, Yi, Lan Tan, and Meng-Shan Tan. 2023. "Chaperone-Mediated Autophagy in Neurodegenerative Diseases: Mechanisms and Therapy." *Molecular and Cellular Biochemistry* 478 (10): 2173–90. https://doi.org/10.1007/s11010-022-04640-9.

Longo, Raffaella, Carolina Peri, Dalma Cricrì, Lara Coppi, Donatella Caruso, Nico Mitro, Emma De Fabiani, and Maurizio Crestani. 2019. "Ketogenic Diet: A New Light Shining on Old but Gold Biochemistry." *Nutrients* 11 (10). https://doi.org/10.3390/nu11102497.

Lu, B, B J Rutledge, L Gu, J Fiorillo, N W Lukacs, S L Kunkel, R North, C Gerard, and B J Rollins. 1998. "Abnormalities in Monocyte Recruitment and Cytokine Expression in Monocyte Chemoattractant Protein 1-Deficient Mice." *The Journal of Experimental Medicine* 187 (4): 601–8. https://doi.org/10.1084/jem.187.4.601.

Lv, Xiaodi, Weifeng Tang, Jingjing Qin, Wenqian Wang, Jingcheng Dong, and Ying Wei. 2023. "The Crosslinks between Ferroptosis and Autophagy in Asthma." *Frontiers in Immunology* 14: 1140791. https://doi.org/10.3389/fimmu.2023.1140791.

Maeda, Mitsuyo, Toshiyuki Seto, Chiho Kadono, Hideto Morimoto, Sachiho Kida, Mitsuo Suga, Motohiro Nakamura, Yosky Kataoka, Takashi Hamazaki, and Haruo Shintaku. 2019. "Autophagy in the Central Nervous System and Effects of Chloroquine in Mucopolysaccharidosis Type II Mice." *International Journal of Molecular Sciences* 20 (23). https://doi.org/10.3390/ijms20235829.

Maegawa, Gustavo H.B., Tracy Stockley, Michael Tropak, Brenda Banwell, Susan Blaser, Fernando Kok, Roberto Giugliani, Don Mahuran, and Joe T.R. Clarke. 2006. "The Natural History of Juvenile or Subacute GM2 Gangliosidosis: 21 New Cases and Literature Review of 134 Previously Reported." *Pediatrics* 118 (5). https://doi.org/10.1542/PEDS.2006-0588.

Mandon, E. C., I. Ehses, J. Rother, G. Van Echten, and K. Sandhoff. 1992. "Subcellular Localization and Membrane Topology of Serine Palmitoyltransferase, 3-Dehydrosphinganine Reductase, and Sphinganine N- Acyltransferase in Mouse Liver." *Journal of Biological Chemistry* 267 (16): 11144–48. https://doi.org/10.1016/s0021-9258(19)49887-6.

Marosi, Krisztina, Sang Woo Kim, Keelin Moehl, Morten Scheibye-Knudsen, Aiwu Cheng, Roy Cutler, Simonetta Camandola, and Mark P Mattson. 2016. "3-Hydroxybutyrate Regulates Energy Metabolism and Induces BDNF Expression in Cerebral Cortical Neurons." *Journal of Neurochemistry* 139 (5): 769–81. https://doi.org/10.1111/jnc.13868.

Martin, Nellie A, Viktor Molnar, Gabor T Szilagyi, Maria L Elkjaer, Arkadiusz Nawrocki, Justyna Okarmus, Agnieszka Wlodarczyk, et al. 2018. "Experimental Demyelination and Axonal Loss Are Reduced in MicroRNA-146a Deficient Mice." *Frontiers in Immunology* 9: 490. https://doi.org/10.3389/fimmu.2018.00490.

Martino, S., P. Marconi, B. Tancini, D. Dolcetta, M. G.Cusella De Angelis, P. Montanucci, G. Bregola, et al. 2005. "A Direct Gene Transfer Strategy via Brain Internal Capsule Reverses the Biochemical Defect in Tay-Sachs Disease." *Human Molecular Genetics* 14 (15): 2113–23. https://doi.org/10.1093/HMG/DDI216.

Martins, Carla, Helena Hůlková, Larbi Dridi, Virginie Dormoy-Raclet, Lubov Grigoryeva, Yoo Choi, Alexander Langford-Smith, et al. 2015. "Neuroinflammation, Mitochondrial Defects and Neurodegeneration in Mucopolysaccharidosis III Type C Mouse Model." *Brain : A Journal of Neurology* 138 (Pt 2): 336–55. https://doi.org/10.1093/brain/awu355.

Masingue, Marion, Louis Dufour, Timothée Lenglet, Lisa Saleille, Cyril Goizet, Xavier Ayrignac, Fabienne Ory-Magne, et al. 2020. "Natural History of Adult Patients with GM2 Gangliosidosis." *Annals of Neurology* 87 (4): 609–17. https://doi.org/10.1002/ANA.25689.

Masino, Susan A, and Jong M Rho. 2012. "Mechanisms of Ketogenic Diet Action." In , edited by Jeffrey L Noebels, Massimo Avoli, Michael A Rogawski, Richard W Olsen, and Antonio V Delgado-Escueta. Bethesda (MD).

Matoba, Kazuaki, Tetsuya Kotani, Akihisa Tsutsumi, Takuma Tsuji, Takaharu Mori, Daisuke Noshiro, Yuji Sugita, et al. 2020. "Atg9 Is a Lipid Scramblase That Mediates Autophagosomal Membrane Expansion." *Nature Structural & Molecular Biology* 27 (12): 1185–93. https://doi.org/10.1038/s41594-020-00518-w.

McCarty, Mark F, James J DiNicolantonio, and James H O'Keefe. 2015. "Ketosis May Promote Brain Macroautophagy by Activating Sirt1 and Hypoxia-Inducible Factor-1." *Medical Hypotheses* 85 (5): 631–39. https://doi.org/10.1016/j.mehy.2015.08.002.

McPherson, Peter Andrew C., and Jane McEneny. 2012. "The Biochemistry of Ketogenesis and Its Role in Weight Management, Neurological Disease and Oxidative Stress." *Journal of Physiology and Biochemistry* 68 (1): 141–51. https://doi.org/10.1007/s13105-011-0112-4.

Mehrpour, Maryam, Audrey Esclatine, Isabelle Beau, and Patrice Codogno. 2010. "Overview of Macroautophagy Regulation in Mammalian Cells." *Cell Research* 20 (7): 748–62. https://doi.org/10.1038/cr.2010.82.

Michlmayr, Daniela, and Clive S. McKimmie. 2014. “Role of CXCL10 in Central Nervous System Inflammation.” *International Journal of Interferon, Cytokine and Mediator Research* 6 (1): 1–18. https://doi.org/10.2147/IJICMR.S35953.

Mitchell, G. A., S. Kassovska-Bratinova, Y. Boukaftane, M. F. Robert, S. P. Wang, L. Ashmarina, M. Lambert, P. Lapierre, and E. Potier. 1995. “Medical Aspects of Ketone Body Metabolism.” *Clinical and Investigative Medicine*. https://pubmed.ncbi.nlm.nih.gov/7554586/.

Miyagi, Taeko, and Kazunori Yamaguchi. 2012. “Mammalian Sialidases: Physiological and Pathological Roles in Cellular Functions.” *Glycobiology* 22 (7): 880–96. https://doi.org/10.1093/GLYCOB/CWS057.

Mizushima, Noboru, and Tamotsu Yoshimori. 2007. “How to Interpret LC3 Immunoblotting.” *Autophagy* 3 (6): 542–45. https://doi.org/10.4161/auto.4600.

Monti, Eugenio, Erik Bonten, Alessandra D’Azzo, Roberto Bresciani, Bruno Venerando, Giuseppe Borsani, Roland Schauer, and Guido Tettamanti. 2010. “Sialidases in Vertebrates: A Family of Enzymes Tailored for Several Cell Functions.” *Advances in Carbohydrate Chemistry and Biochemistry* 64 (C): 403–79. https://doi.org/10.1016/S0065-2318(10)64007-3.

Montiel, Teresa, Juan Carlos Gómora-García, Cristian Gerónimo-Olvera, Yessica Heras-Romero, Berenice N Bernal-Vicente, Xochitl Pérez-Martínez, Luis B Tovar-Y-Romo, and Lourdes Massieu. 2023. “Modulation of the Autophagy-Lysosomal Pathway and Endoplasmic Reticulum Stress by Ketone Bodies in Experimental Models of Stroke.” *Journal of Neurochemistry* 166 (1): 87–106. https://doi.org/10.1111/jnc.15852.

Montiel, Teresa, Luis A Montes-Ortega, Susana Flores-Yáñez, and Lourdes Massieu. 2020. “Treatment with the Ketone Body D-β-Hydroxybutyrate Attenuates Autophagy Activated by NMDA and Reduces Excitotoxic Neuronal Damage in the Rat Striatum In Vivo.” *Current Pharmaceutical Design* 26 (12): 1377–87. https://doi.org/10.2174/1381612826666200115103646.

Mulder, Petra, Anita M. Van Den Hoek, and Robert Kleemann. 2017. "The CCR2 Inhibitor Propagermanium Attenuates Diet-Induced Insulin Resistance, Adipose Tissue Inflammation and Non-Alcoholic Steatohepatitis." *PLoS ONE* 12 (1): 1–14. https://doi.org/10.1371/journal.pone.0169740.

Murakami, Mari, and Paola Tognini. 2022. "Molecular Mechanisms Underlying the Bioactive Properties of a Ketogenic Diet." *Nutrients* 14 (4): 1–17. https://doi.org/10.3390/nu14040782.

Myerowitz, Rachel, Douglas Lawson, Hiroki Mizukami, Yide Mi, Cynthia J Tifft, and Richard L Proia. 2002. "Molecular Pathophysiology in Tay-Sachs and Sandhoff Diseases as Revealed by Gene Expression Profiling." *Human Molecular Genetics* 11 (11): 1343–50. https://doi.org/10.1093/hmg/11.11.1343.

Myerowitz, Rachel, Rosa Puertollano, and Nina Raben. 2021. "Impaired Autophagy: The Collateral Damage of Lysosomal Storage Disorders." *EBioMedicine* 63 (January): 103166. https://doi.org/10.1016/j.ebiom.2020.103166.

Myers, Kenneth A., Mark F. Bennett, Chung W. Chow, Susan M. Carden, Simone A. Mandelstam, Melanie Bahlo, and Ingrid E. Scheffer. 2018. "Mosaic Uniparental Disomy Results in GM1 Gangliosidosis with Normal Enzyme Assay." *American Journal of Medical Genetics, Part A* 176 (1): 230–34. https://doi.org/10.1002/ajmg.a.38549.

Nakamura, Shuhei, and Tamotsu Yoshimori. 2017. "New Insights into Autophagosome-Lysosome Fusion." *Journal of Cell Science* 130 (7): 1209–16. https://doi.org/10.1242/jcs.196352.

Nakatsumi, Hirokazu, Masaki Matsumoto, and Keiichi I Nakayama. 2017. "Noncanonical Pathway for Regulation of CCL2 Expression by an MTORC1-FOXK1 Axis Promotes Recruitment of Tumor-Associated Macrophages." *Cell Reports* 21 (9): 2471–86. https://doi.org/10.1016/j.celrep.2017.11.014.

Ni, Hong, Dong-Jing Zhao, and Tian Tian. 2016. “Ketogenic Diet Change CPLA2/Clusterin and Autophagy Related Gene Expression and Correlate with Cognitive Deficits and Hippocampal MFs Sprouting Following Neonatal Seizures.” *Epilepsy Research* 120 (February): 13–18. https://doi.org/10.1016/j.eplepsyres.2015.11.021.

Nishie, Toshikazu, Yoko Hikimochi, Kota Zama, Yoshiyasu Fukusumi, Mitutoshi Ito, Haruka Yokoyama, Chie Naruse, Makoto Ito, and Masahide Asano. 2010. “Beta4-Galactosyltransferase-5 Is a Lactosylceramide Synthase Essential for Mouse Extra-Embryonic Development.” *Glycobiology* 20 (10): 1311–22. https://doi.org/10.1093/GLYCOB/CWQ098.

Nishino, I, J Fu, K Tanji, T Yamada, S Shimojo, T Koori, M Mora, et al. 2000. “Primary LAMP-2 Deficiency Causes X-Linked Vacuolar Cardiomyopathy and Myopathy (Danon Disease).” *Nature* 406 (6798): 906–10. https://doi.org/10.1038/35022604.

O’Dea, Ellen L, Derren Barken, Raechel Q Peralta, Kim T Tran, Shannon L Werner, Jeffrey D Kearns, Andre Levchenko, and Alexander Hoffmann. 2007. “A Homeostatic Model of IkappaB Metabolism to Control Constitutive NF-KappaB Activity.” *Molecular Systems Biology* 3: 111. https://doi.org/10.1038/msb4100148.

Ogawa, Yasuhiro, Eiri Furusawa, Takahiro Saitoh, Hiroki Sugimoto, Takumi Omori, Shinya Shimizu, Hisatsugu Kondo, Mika Yamazaki, Hitoshi Sakuraba, and Kazuhiko Oishi. 2018. “Inhibition of Astrocytic Adenosine Receptor A2A Attenuates Microglial Activation in a Mouse Model of Sandhoff Disease.” *Neurobiology of Disease* 118 (July): 142–54. https://doi.org/10.1016/j.nbd.2018.07.014.

Ohmi, Kazuhiro, David S Greenberg, Kavitha S Rajavel, Sergey Ryazantsev, Hong Hua Li, and Elizabeth F Neufeld. 2003. “Activated Microglia in Cortex of Mouse Models of Mucopolysaccharidoses I and IIIB.” *Proceedings of the National Academy of Sciences of the United States of America* 100 (4): 1902–7. https://doi.org/10.1073/pnas.252784899.

Okuda, Tetsuya. 2019. “A Low-Carbohydrate Ketogenic Diet Promotes Ganglioside Synthesis via the Transcriptional Regulation of Ganglioside Metabolism-Related Genes.” *Scientific Reports* 9 (1): 1–11. https://doi.org/10.1038/s41598-019-43952-7.

Otomo, Takanobu, Katsumi Higaki, Eiji Nanba, Keiichi Ozono, and Norio Sakai. 2009. “Inhibition of Autophagosome Formation Restores Mitochondrial Function in Mucolipidosis II and III Skin Fibroblasts.” *Molecular Genetics and Metabolism* 98 (4): 393–99. https://doi.org/10.1016/j.ymgme.2009.07.002.

Pacheco, Chris D, Matthew J Elrick, and Andrew P Lieberman. 2009. “Tau Deletion Exacerbates the Phenotype of Niemann-Pick Type C Mice and Implicates Autophagy in Pathogenesis.” *Human Molecular Genetics* 18 (5): 956–65. https://doi.org/10.1093/hmg/ddn423.

Pacheco, Christopher D, and Andrew P Lieberman. 2007. “Lipid Trafficking Defects Increase Beclin-1 and Activate Autophagy in Niemann-Pick Type C Disease.” *Autophagy* 3 (5): 487–89. https://doi.org/10.4161/auto.4586.

Pandey, Manoj K, Thomas A Burrow, Reena Rani, Lisa J Martin, David Witte, Kenneth D Setchell, Mary A Mckay, et al. 2017. “Complement Drives Glucosylceramide Accumulation and Tissue Inflammation in Gaucher Disease.” *Nature* 543 (7643): 108–12. https://doi.org/10.1038/nature21368.

Pandey, Manoj Kumar. 2023. “Exploring Pro-Inflammatory Immunological Mediators: Unraveling the Mechanisms of Neuroinflammation in Lysosomal Storage Diseases.” *Biomedicines* 11 (4). https://doi.org/10.3390/biomedicines11041067.

Pandey, Manoj Kumar, and Gregory A Grabowski. 2013. “Immunological Cells and Functions in Gaucher Disease.” *Critical Reviews in Oncogenesis* 18 (3): 197–220. https://doi.org/10.1615/critrevoncog.2013004503.

Pandey, Manoj Kumar, Reena Rani, Wujuan Zhang, Kenneth Setchell, and Gregory A Grabowski. 2012. “Immunological Cell Type Characterization and Th1-Th17

Cytokine Production in a Mouse Model of Gaucher Disease." *Molecular Genetics and Metabolism* 106 (3): 310–22. https://doi.org/10.1016/j.ymgme.2012.04.020.

Peng, Yanyan, Benjamin Liou, Venette Inskeep, Rachel Blackwood, Christopher N Mayhew, Gregory A Grabowski, and Ying Sun. 2019. "Intravenous Infusion of IPSC-Derived Neural Precursor Cells Increases Acid β-Glucosidase Function in the Brain and Lessens the Neuronopathic Phenotype in a Mouse Model of Gaucher Disease." *Human Molecular Genetics* 28 (20): 3406–21. https://doi.org/10.1093/hmg/ddz184.

Pfeifer, Heidi H., David A. Lyczkowski, and Elizabeth A. Thiele. 2008. "Low Glycemic Index Treatment: Implementation and New Insights into Efficacy." *Epilepsia* 49 Suppl 8 (SUPPL. 8): 42–45. https://doi.org/10.1111/J.1528-1167.2008.01832.X.

Pfeifer, Heidi H., and Elizabeth A. Thiele. 2005. "Low-Glycemic-Index Treatment: A Liberalized Ketogenic Diet for Treatment of Intractable Epilepsy." *Neurology* 65 (11): 1810–12. https://doi.org/10.1212/01.WNL.0000187071.24292.9E.

Pietrzak, Diana, Kamila Kasperek, Paweł Rękawek, and Iwona Piątkowska-Chmiel. 2022. "The Therapeutic Role of Ketogenic Diet in Neurological Disorders." *Nutrients* 14 (9). https://doi.org/10.3390/nu14091952.

Pinto, Alessandro, Alessio Bonucci, Elisa Maggi, Mariangela Corsi, and Rita Businaro. 2018. "Anti-Oxidant and Anti-Inflammatory Activity of Ketogenic Diet: New Perspectives for Neuroprotection in Alzheimer's Disease." *Antioxidants (Basel, Switzerland)* 7 (5). https://doi.org/10.3390/antiox7050063.

Platt, Frances M., Alessandra d'Azzo, Beverly L. Davidson, Elizabeth F. Neufeld, and Cynthia J. Tifft. 2018. "Lysosomal Storage Diseases." *Nature Reviews. Disease Primers* 4 (1). https://doi.org/10.1038/S41572-018-0025-4.

Pontikis, Charlie C, Susan L Cotman, Marcy E MacDonald, and Jonathan D Cooper. 2005. "Thalamocortical Neuron Loss and Localized Astrocytosis in the Cln3Deltaex7/8 Knock-in Mouse Model of Batten Disease." *Neurobiology of*

*Disease* 20 (3): 823–36. https://doi.org/10.1016/j.nbd.2005.05.018.

Puchalska, Patrycja, and Peter A. Crawford. 2017. "Multi-Dimensional Roles of Ketone Bodies in Fuel Metabolism, Signaling, and Therapeutics." *Cell Metabolism* 25 (2): 262–84. https://doi.org/10.1016/J.CMET.2016.12.022.

Purhonen, Janne, Jayasimman Rajendran, Matthias Mörgelin, Kristiina Uusi-Rauva, Shintaro Katayama, Kaarel Krjutskov, Elisabet Einarsdottir, et al. 2017. "Ketogenic Diet Attenuates Hepatopathy in Mouse Model of Respiratory Chain Complex III Deficiency Caused by a Bcs1l Mutation." *Scientific Reports* 7 (1): 957. https://doi.org/10.1038/s41598-017-01109-4.

Puri, Vishwajeet, Rikio Watanabe, Michel Dominguez, Xiaofeng Sun, Christine L. Wheatley, David L. Marks, and Richard E. Pagano. 1999. "Cholesterol Modulates Membrane Traffic along the Endocytic Pathway in Sphingolipid-Storage Diseases." *Nature Cell Biology* 1 (6): 386–88. https://doi.org/10.1038/14084.

Qin, Yue, Jingru Qiu, Ping Wang, Jia Liu, Yong Zhao, Fan Jiang, and Haiyan Lou. 2021. "Impaired Autophagy in Microglia Aggravates Dopaminergic Neurodegeneration by Regulating NLRP3 Inflammasome Activation in Experimental Models of Parkinson's Disease." *Brain, Behavior, and Immunity* 91 (January): 324–38. https://doi.org/10.1016/j.bbi.2020.10.010.

Raben, Nina, Victoria Hill, Lauren Shea, Shoichi Takikita, Rebecca Baum, Noboru Mizushima, Evelyn Ralston, and Paul Plotz. 2008. "Suppression of Autophagy in Skeletal Muscle Uncovers the Accumulation of Ubiquitinated Proteins and Their Potential Role in Muscle Damage in Pompe Disease." *Human Molecular Genetics* 17 (24): 3897–3908. https://doi.org/10.1093/hmg/ddn292.

Rahman, Mahbubur, Sajjad Muhammad, Mahtab A Khan, Hui Chen, Dirk A Ridder, Helge Müller-Fielitz, Barbora Pokorná, et al. 2014. "The β-Hydroxybutyrate Receptor HCA2 Activates a Neuroprotective Subset of Macrophages." *Nature Communications* 5 (May): 3944. https://doi.org/10.1038/ncomms4944.

Ransohoff, Richard M., Dorothy Schafer, Angela Vincent, Nathalie E. Blachère, and Amit Bar-Or. 2015. "Neuroinflammation: Ways in Which the Immune System Affects the Brain." *Neurotherapeutics : The Journal of the American Society for Experimental NeuroTherapeutics* 12 (4): 896–909. https://doi.org/10.1007/S13311-015-0385-3.

Rollins, B J. 1996. "Monocyte Chemoattractant Protein 1: A Potential Regulator of Monocyte Recruitment in Inflammatory Disease." *Molecular Medicine Today* 2 (5): 198–204. https://doi.org/10.1016/1357-4310(96)88772-7.

Rui, Liangyou. 2014. "Energy Metabolism in the Liver." *Comprehensive Physiology* 4 (1): 177–97. https://doi.org/10.1002/CPHY.C130024.

Rumi, M., R. Romeo, F. De Filippi, R. Marcelli, E. Del Ninno, P. Van Eyken, V. Desmet, and M. Colombo. 1993. "A Multicentre Randomized Clinical Trial of Recombinant Alpha-2a Interferon Therapy in Patients with Chronic Hepatitis B." *The Italian Journal of Gastroenterology* 25 (3): 117–20. https://pubmed.ncbi.nlm.nih.gov/8507888/.

Sandhoff, Roger, and Konrad Sandhoff. 2018. "Emerging Concepts of Ganglioside Metabolism." *FEBS Letters* 592 (23): 3835–64. https://doi.org/10.1002/1873-3468.13114.

Sardiello, Marco, and Andrea Ballabio. 2009. "Lysosomal Enhancement: A CLEAR Answer to Cellular Degradative Needs." *Cell Cycle (Georgetown, Tex.)*. United States. https://doi.org/10.4161/cc.8.24.10263.

Schultz, Mark L., Luis Tecedor, Michael Chang, and Beverly L. Davidson. 2011. "Clarifying Lysosomal Storage Diseases." *Trends in Neurosciences* 34 (8): 401–10. https://doi.org/10.1016/J.TINS.2011.05.006.

Semple, Bridgette D, Thomas Kossmann, and Maria Cristina Morganti-Kossmann. 2010. "Role of Chemokines in CNS Health and Pathology: A Focus on the CCL2/CCR2 and CXCL8/CXCR2 Networks." *Journal of Cerebral Blood Flow*

*and Metabolism : Official Journal of the International Society of Cerebral Blood Flow and Metabolism* 30 (3): 459–73. https://doi.org/10.1038/jcbfm.2009.240.

Sengul, Tugce, Melike Can, Nurselin Ateş, and Volkan Seyrantepe. 2023. "Autophagic Flux Is Impaired in the Brain Tissue of Tay-Sachs Disease Mouse Model." *PLoS ONE* 18 (3 March): 1–15. https://doi.org/10.1371/journal.pone.0280650.

Settembre, Carmine, Ida Annunziata, Carmine Spampanato, Daniela Zarcone, Gilda Cobellis, Edoardo Nusco, Ester Zito, Carlo Tacchetti, Maria Pia Cosma, and Andrea Ballabio. 2007. "Systemic Inflammation and Neurodegeneration in a Mouse Model of Multiple Sulfatase Deficiency." *Proceedings of the National Academy of Sciences of the United States of America* 104 (11): 4506–11. https://doi.org/10.1073/pnas.0700382104.

Settembre, Carmine, Alessandro Fraldi, Luca Jahreiss, Carmine Spampanato, Consuelo Venturi, Diego Medina, Raquel de Pablo, Carlo Tacchetti, David C. Rubinsztein, and Andrea Ballabio. 2008. "A Block of Autophagy in Lysosomal Storage Disorders." *Human Molecular Genetics* 17 (1): 119–29. https://doi.org/10.1093/hmg/ddm289.

Settembre, Carmine, Chiara Di Malta, Vinicia Assunta Polito, Moises Garcia Arencibia, Francesco Vetrini, Serkan Erdin, Serpil Uckac Erdin, et al. 2011. "TFEB Links Autophagy to Lysosomal Biogenesis." *Science (New York, N.Y.)* 332 (6036): 1429–33. https://doi.org/10.1126/science.1204592.

Seyrantepe, Volkan, Secil Akyildiz Demir, Zehra Kevser Timur, Johanna Von Gerichten, Christian Marsching, Esra Erdemli, Emin Oztas, et al. 2018. "Murine Sialidase Neu3 Facilitates GM2 Degradation and Bypass in Mouse Model of Tay-Sachs Disease." *Experimental Neurology* 299 (July 2017): 26–41. https://doi.org/10.1016/j.expneurol.2017.09.012.

Seyrantepe, Volkan, Pablo Lema, Aurore Caqueret, Larbi Dridi, Samar Bel Hadj, Stephane Carpentier, Francine Boucher, et al. 2010. "Mice Doubly-Deficient in Lysosomal Hexosaminidase a and Neuraminidase 4 Show Epileptic Crises and

Rapid Neuronal Loss." *PLoS Genetics* 6 (9). https://doi.org/10.1371/journal.pgen.1001118.

Shi, Xiaoxia, Xinwei Li, Dangdang Li, Yu Li, Yuxiang Song, Qinghua Deng, Jianguo Wang, et al. 2014. "β-Hydroxybutyrate Activates the NF-KB Signaling Pathway to Promote the Expression of pro-Inflammatory Factors in Calf Hepatocytes." *Cellular Physiology and Biochemistry : International Journal of Experimental Cellular Physiology, Biochemistry, and Pharmacology* 33 (4): 920–32. https://doi.org/10.1159/000358664.

Shimazu, Tadahiro, Matthew D Hirschey, John Newman, Wenjuan He, Kotaro Shirakawa, Natacha Le Moan, Carrie A Grueter, et al. 2013. "Suppression of Oxidative Stress by β-Hydroxybutyrate, an Endogenous Histone Deacetylase Inhibitor." *Science (New York, N.Y.)* 339 (6116): 211–14. https://doi.org/10.1126/science.1227166.

Shin, Samuel D, Alexandra Shin, Karina Mayagoitia, Lorraine Siebold, Marsilio Rubini, Christopher G Wilson, Denise L Bellinger, and Salvador Soriano. 2019. "Loss of Amyloid Precursor Protein Exacerbates Early Inflammation in Niemann-Pick Disease Type C." *Journal of Neuroinflammation* 16 (1): 269. https://doi.org/10.1186/s12974-019-1663-5.

Snook, Eric R, Jeanne M Fisher-Perkins, Hope A Sansing, Kim M Lee, Xavier Alvarez, Andrew G MacLean, Karin E Peterson, Andrew A Lackner, and Bruce A Bunnell. 2014. "Innate Immune Activation in the Pathogenesis of a Murine Model of Globoid Cell Leukodystrophy." *The American Journal of Pathology* 184 (2): 382–96. https://doi.org/10.1016/j.ajpath.2013.10.011.

Stamatovic, Svetlana M, Parvin Shakui, Richard F Keep, Bethany B Moore, Steven L Kunkel, Nico Van Rooijen, and Anuska V Andjelkovic. 2005. "Monocyte Chemoattractant Protein-1 Regulation of Blood-Brain Barrier Permeability." *Journal of Cerebral Blood Flow and Metabolism : Official Journal of the International Society of Cerebral Blood Flow and Metabolism* 25 (5): 593–606. https://doi.org/10.1038/sj.jcbfm.9600055.

Stenson, Peter D., Matthew Mort, Edward V. Ball, Katy Evans, Matthew Hayden, Sally Heywood, Michelle Hussain, Andrew D. Phillips, and David N. Cooper. 2017. "The Human Gene Mutation Database: Towards a Comprehensive Repository of Inherited Mutation Data for Medical Research, Genetic Diagnosis and next-Generation Sequencing Studies." *Human Genetics* 136 (6): 665–77. https://doi.org/10.1007/S00439-017-1779-6.

Stepien, Karolina M., Su Han Lum, J. Edmond Wraith, Christian J. Hendriksz, Heather J. Church, David Priestman, Frances M. Platt, Simon Jones, Ana Jovanovic, and Robert Wynn. 2018. "Haematopoietic Stem Cell Transplantation Arrests the Progression of Neurodegenerative Disease in Late-Onset Tay-Sachs Disease." *JIMD Reports* 41: 17–23. https://doi.org/10.1007/8904_2017_76.

Stumpf, Sina K., Stefan A. Berghoff, Andrea Trevisiol, Lena Spieth, Tim Düking, Lennart V. Schneider, Lennart Schlaphoff, et al. 2019. "Ketogenic Diet Ameliorates Axonal Defects and Promotes Myelination in Pelizaeus–Merzbacher Disease." *Acta Neuropathologica* 138 (1): 147–61. https://doi.org/10.1007/s00401-019-01985-2.

Sun, Wei, Qingpeng Wang, Ruiyan Zhang, and Ning Zhang. 2023. "Ketogenic Diet Attenuates Neuroinflammation and Induces Conversion of M1 Microglia to M2 in an EAE Model of Multiple Sclerosis by Regulating the NF-KB/NLRP3 Pathway and Inhibiting HDAC3 and P2X7R Activation." *Food & Function* 14 (15): 7247–69. https://doi.org/10.1039/d3fo00122a.

Sun, Wei, Junrong Yang, Bingyi Liu, Quiqin Liu, Ting Wang, Qingpeng Wang, Min Liu, et al. 2022. "Ketogenic Diet Inhibits Tumor Growth by Enhancing Immune Response, Attenuating Immunosuppression, Inhibiting Angiogenesis and EMT in CT26 Colon Tumor Allografts Mouse Model." *Journal of Functional Foods* 92: 105067. https://doi.org/https://doi.org/10.1016/j.jff.2022.105067.

Sun, Ying, Benjamin Liou, Huimin Ran, Matthew R Skelton, Michael T Williams, Charles V Vorhees, Kazuyuki Kitatani, et al. 2010. "Neuronopathic Gaucher Disease in the Mouse: Viable Combined Selective Saposin C Deficiency and

Mutant Glucocerebrosidase (V394L) Mice with Glucosylsphingosine and Glucosylceramide Accumulation and Progressive Neurological Deficits." *Human Molecular Genetics* 19 (6): 1088–97. https://doi.org/10.1093/hmg/ddp580.

Suzuki, K. 1998. "Twenty Five Years of the 'Psychosine Hypothesis': A Personal Perspective of Its History and Present Status." *Neurochemical Research* 23 (3): 251–59. https://doi.org/10.1023/a:1022436928925.

Suzuki, Kunihiko, Marie T. Vanier, and Kinuko Suzuki. 1998. "Induced Mouse Models of Abnormal Sphingolipid Metabolism." *Journal of Biochemistry* 124 (1): 8–19. https://doi.org/10.1093/OXFORDJOURNALS.JBCHEM.A022101.

Svennerholm, Lars. 1994. "Designation and Schematic Structure of Gangliosides and Allied Glycosphingolipids." *Progress in Brain Research* 101 (C): xi–xiv. https://doi.org/10.1016/S0079-6123(08)61935-4.

Takamura, Ayumi, Katsumi Higaki, Kenya Kajimaki, Susumu Otsuka, Haruaki Ninomiya, Junichiro Matsuda, Kousaku Ohno, Yoshiyuki Suzuki, and Eiji Nanba. 2008. "Enhanced Autophagy and Mitochondrial Aberrations in Murine G(M1)-Gangliosidosis." *Biochemical and Biophysical Research Communications* 367 (3): 616–22. https://doi.org/10.1016/j.bbrc.2007.12.187.

Tamura, Yukinori, Masayuki Sugimoto, Toshinori Murayama, Yukihiko Ueda, Hiroshi Kanamori, Koh Ono, Hiroyuki Ariyasu, et al. 2008. "Inhibition of CCR2 Ameliorates Insulin Resistance and Hepatic Steatosis in Db/Db Mice." *Arteriosclerosis, Thrombosis, and Vascular Biology* 28 (12): 2195–2201. https://doi.org/10.1161/ATVBAHA.108.168633.

Tanida, Isei, Takashi Ueno, and Eiki Kominami. 2004. "LC3 Conjugation System in Mammalian Autophagy." *The International Journal of Biochemistry & Cell Biology* 36 (12): 2503–18. https://doi.org/10.1016/j.biocel.2004.05.009.

Tettamanti, G., F. Bonali, S. Marchesini, and V. Zambotti. 1973. “A New Procedure for the Extraction, Purification and Fractionation of Brain Gangliosides.” *Biochimica et Biophysica Acta* 296 (1): 160–70. https://doi.org/10.1016/0005-2760(73)90055-6.

Thameem Dheen, S., Charanjit Kaur, and Eng-Ang Ling. 2007. “Microglial Activation and Its Implications in the Brain Diseases.” *Current Medicinal Chemistry* 14 (11): 1189–97. https://doi.org/10.2174/092986707780597961.

Thelen, Melanie, Markus Damme, Michaela Schweizer, Christian Hagel, Andrew M S Wong, Jonathan D Cooper, Thomas Braulke, and Giovanna Galliciotti. 2012. “Disruption of the Autophagy-Lysosome Pathway Is Involved in Neuropathology of the Nclf Mouse Model of Neuronal Ceroid Lipofuscinosis.” *PloS One* 7 (4): e35493. https://doi.org/10.1371/journal.pone.0035493.

Tian, Dai Shi, Jiyun Peng, Madhuvika Murugan, Li Jie Feng, Jun Li Liu, Ukpong B. Eyo, Li Jun Zhou, Rochelle Mogilevsky, Wei Wang, and Long Jun Wu. 2017. “Chemokine CCL2-CCR2 Signaling Induces Neuronal Cell Death via STAT3 Activation and IL-1β Production after Status Epilepticus.” *Journal of Neuroscience* 37 (33): 7878–92. https://doi.org/10.1523/JNEUROSCI.0315-17.2017.

Tokuda, Noriyo, Shinichiro Numata, Xiaojin Li, Tomoko Nomura, Minoru Takizawa, Yuji Kondo, Yoriko Yamashita, et al. 2013. “B4GalT6 Is Involved in the Synthesis of Lactosylceramide with Less Intensity than B4GalT5.” *Glycobiology* 23 (10): 1175–83. https://doi.org/10.1093/GLYCOB/C*WT*054.

Toro, Camilo, Mosufa Zainab, and Cynthia J Tifft. 2021. “The GM2 Gangliosidoses: Unlocking the Mysteries of Pathogenesis and Treatment.” *Neuroscience Letters* 764 (November): 136195. https://doi.org/10.1016/j.neulet.2021.136195.

Tran, Sharon, W Douglas Fairlie, and Erinna F Lee. 2021. “BECLIN1: Protein Structure, Function and Regulation.” *Cells* 10 (6). https://doi.org/10.3390/cells10061522.

Ubogu, Eroboghene E. 2020. “Biology of the Human Blood-Nerve Barrier in Health and Disease.” *Experimental Neurology* 328 (February): 113272. https://doi.org/10.1016/j.expneurol.2020.113272.

Vallabhapurapu, Sivakumar, and Michael Karin. 2009. “Regulation and Function of NF-KappaB Transcription Factors in the Immune System.” *Annual Review of Immunology* 27: 693–733. https://doi.org/10.1146/annurev.immunol.021908.132641.

Vergarajauregui, Silvia, Patricia S Connelly, Mathew P Daniels, and Rosa Puertollano. 2008. “Autophagic Dysfunction in Mucolipidosis Type IV Patients.” *Human Molecular Genetics* 17 (17): 2723–37. https://doi.org/10.1093/hmg/ddn174.

Verkhratsky, Alexei, Maiken Nedergaard, and Leif Hertz. 2015. “Why Are Astrocytes Important?” *Neurochemical Research* 40 (2): 389–401. https://doi.org/10.1007/S11064-014-1403-2.

Villamizar-Schiller, Ives T., Laudy A. Pabón, Sophia B. Hufnagel, Norma C. Serrano, Gabriela Karl, John L. Jefferies, Robert J. Hopkin, and Carlos E. Prada. 2015. “Neurological and Cardiac Responses after Treatment with Miglustat and a Ketogenic Diet in a Patient with Sandhoff Disease.” *European Journal of Medical Genetics* 58 (3): 180–83. https://doi.org/10.1016/j.ejmg.2014.12.009.

Vitner, Einat B. 2020. “The Role of Brain Innate Immune Response in Lysosomal Storage Disorders: Fundamental Process or Evolutionary Side Effect?” *FEBS Letters* 594 (22): 3619–31. https://doi.org/10.1002/1873-3468.13980.

Vitner, Einat B., Tamar Farfel-Becker, Raya Eilam, Inbal Biton, and Anthony H. Futerman. 2012. “Contribution of Brain Inflammation to Neuronal Cell Death in Neuronopathic Forms of Gaucher’s Disease.” *Brain* 135 (6): 1724–35. https://doi.org/10.1093/brain/aws095.

Vitner, Einat B, Hani Dekel, Hila Zigdon, Tamar Shachar, Tamar Farfel-Becker, Raya Eilam, Stefan Karlsson, and Anthony H Futerman. 2010. “Altered Expression and

Distribution of Cathepsins in Neuronopathic Forms of Gaucher Disease and in Other Sphingolipidoses." *Human Molecular Genetics* 19 (18): 3583–90. https://doi.org/10.1093/hmg/ddq273.

Wada, R, C J Tifft, and R L Proia. 2000. "Microglial Activation Precedes Acute Neurodegeneration in Sandhoff Disease and Is Suppressed by Bone Marrow Transplantation." *Proceedings of the National Academy of Sciences of the United States of America* 97 (20): 10954–59. https://doi.org/10.1073/pnas.97.20.10954.

Wain, J H, J A Kirby, and S Ali. 2002. "Leucocyte Chemotaxis: Examination of Mitogen-Activated Protein Kinase and Phosphoinositide 3-Kinase Activation by Monocyte Chemoattractant Proteins-1, -2, -3 and -4." *Clinical and Experimental Immunology* 127 (3): 436–44. https://doi.org/10.1046/j.1365-2249.2002.01764.x.

Wang, Bao Hui, Qun Hou, Yu Qiang Lu, Meng Meng Jia, Tao Qiu, Xiao Hang Wang, Zheng Xiang Zhang, and Yan Jiang. 2018. "Ketogenic Diet Attenuates Neuronal Injury via Autophagy and Mitochondrial Pathways in Pentylenetetrazol-Kindled Seizures." *Brain Research* 1678 (January): 106–15. https://doi.org/10.1016/J.BRAINRES.2017.10.009.

Wheless, James W. 2008. "History of the Ketogenic Diet." *Epilepsia* 49 (SUPPL. 8): 3–5. https://doi.org/10.1111/j.1528-1167.2008.01821.x.

Winslow, Ashley R, Chien-Wen Chen, Silvia Corrochano, Abraham Acevedo-Arozena, David E Gordon, Andrew A Peden, Maike Lichtenberg, et al. 2010. "α-Synuclein Impairs Macroautophagy: Implications for Parkinson's Disease." *The Journal of Cell Biology* 190 (6): 1023–37. https://doi.org/10.1083/jcb.201003122.

Xia, He, Jing Guo, Jian Shen, Shiman Jiang, Shengyi Han, and Lanjuan Li. 2023. "Ketogenic Diet Exacerbates L-Arginine-Induced Acute Pancreatitis and Reveals the Therapeutic Potential of Butyrate." *Nutrients* 15 (20). https://doi.org/10.3390/nu15204427.

Xu, Sengen, Mikhail Galperin, Gary Melvin, Robert Horowits, Nina Raben, Paul Plotz, and Leepo Yu. 2010. “Impaired Organization and Function of Myofilaments in Single Muscle Fibers from a Mouse Model of Pompe Disease.” *Journal of Applied Physiology (Bethesda, Md. : 1985)* 108 (5): 1383–88. https://doi.org/10.1152/japplphysiol.01253.2009.

Xu, Wenxia, Qi Wei, Mengjiao Han, Bingluo Zhou, Hanying Wang, Jianbing Zhang, Qiang Wang, et al. 2018. “CCL2-SQSTM1 Positive Feedback Loop Suppresses Autophagy to Promote Chemoresistance in Gastric Cancer.” *International Journal of Biological Sciences* 14 (9): 1054–66. https://doi.org/10.7150/ijbs.25349.

Yamada, Takashi, Shi-Jin Zhang, Hakan Westerblad, and Abram Katz. 2010. “{beta}-Hydroxybutyrate Inhibits Insulin-Mediated Glucose Transport in Mouse Oxidative Muscle.” *American Journal of Physiology. Endocrinology and Metabolism* 299 (3): E364-73. https://doi.org/10.1152/ajpendo.00142.2010.

Yamanaka, Shoji, Mark D. Johnson, Alex Grinberg, Heiner Westphal, Jacqueline N. Crawley, Masako Taniike, Kinuko Suzuki, and Richard L. Proia. 1994. “Targeted Disruption of the Hexa Gene Results in Mice with Biochemical and Pathologic Features of Tay-Sachs Disease.” *Proceedings of the National Academy of Sciences of the United States of America* 91 (21): 9975–79. https://doi.org/10.1073/PNAS.91.21.9975.

Yang, Jie, Mingzi Ran, Hongyu Li, Ye Lin, Kui Ma, Yuguang Yang, Xiaobing Fu, and Siming Yang. 2022. “New Insight into Neurological Degeneration: Inflammatory Cytokines and Blood-Brain Barrier.” *Frontiers in Molecular Neuroscience* 15: 1013933. https://doi.org/10.3389/fnmol.2022.1013933.

Yang, Zhihui, and Kevin K W Wang. 2015. “Glial Fibrillary Acidic Protein: From Intermediate Filament Assembly and Gliosis to Neurobiomarker.” *Trends in Neurosciences* 38 (6): 364–74. https://doi.org/10.1016/j.tins.2015.04.003.

Yokochi, S., H. Hashimoto, Y. Ishiwata, H. Shimokawa, M. Haino, Y. Terashima, and K. Matsushima. 2001. “An Anti-Inflammatory Drug, Propagermanium, May

Target GPI-Anchored Proteins Associated with an MCP-1 Receptor, CCR2." *Journal of Interferon & Cytokine Research : The Official Journal of the International Society for Interferon and Cytokine Research* 21 (6): 389–98. https://doi.org/10.1089/107999001750277862.

Yong, Heather Y.F., Khalil S. Rawji, Samira Ghorbani, Mengzhou Xue, and V. Wee Yong. 2019. "The Benefits of Neuroinflammation for the Repair of the Injured Central Nervous System." *Cellular & Molecular Immunology* 16 (6): 540–46. https://doi.org/10.1038/S41423-019-0223-3.

Young, Andrew R J, Edmond Y W Chan, Xiao Wen Hu, Robert Köchl, Samuel G Crawshaw, Stephen High, Dale W Hailey, Jennifer Lippincott-Schwartz, and Sharon A Tooze. 2006. "Starvation and ULK1-Dependent Cycling of Mammalian Atg9 between the TGN and Endosomes." *Journal of Cell Science* 119 (Pt 18): 3888–3900. https://doi.org/10.1242/jcs.03172.

Yu, Fabian P.S., Shaalee Dworski, and Jeffrey A. Medin. 2018. "Deletion of MCP-1 Impedes Pathogenesis of Acid Ceramidase Deficiency." *Scientific Reports* 8 (1): 1–16. https://doi.org/10.1038/s41598-018-20052-6.

Yu, Yongsheng, Yunhua Yu, Yuefan Zhang, Zhigang Zhang, Weishuai An, and Xianxian Zhao. 2018. "Treatment with D-β-Hydroxybutyrate Protects Heart from Ischemia/Reperfusion Injury in Mice." *European Journal of Pharmacology* 829 (June): 121–28. https://doi.org/10.1016/j.ejphar.2018.04.019.

Yudkoff, M, Y Daikhin, I Nissim, A Lazarow, and I Nissim. 2001. "Ketogenic Diet, Amino Acid Metabolism, and Seizure Control." *Journal of Neuroscience Research* 66 (5): 931–40. https://doi.org/10.1002/jnr.10083.

Yuziuk, Jeffrey A., Carmen Bertoni, Tommaso Beccari, Aldo Orlacchio, Yan Yun Wu, Su Chen Li, and Yu Teh Li. 1998. "Specificity of Mouse GM2 Activator Protein and Beta-N-Acetylhexosaminidases A and B. Similarities and Differences with Their Human Counterparts in the Catabolism of GM2." *The Journal of Biological Chemistry* 273 (1): 66–72. https://doi.org/10.1074/JBC.273.1.66.

Zhang, Ning, Chunhong Liu, Ruiyan Zhang, Li Jin, Xiaohan Yin, Xuexing Zheng, Hans Christian Siebert, et al. 2020. “Amelioration of Clinical Course and Demyelination in the Cuprizone Mouse Model in Relation to Ketogenic Diet.” *Food and Function* 11 (6): 5647–63. https://doi.org/10.1039/c9fo02944c.

Zhao, Hongying, Hongguang Chen, Meng Xiaoyin, Guotao Yang, Ying Hu, Keliang Xie, and Yonghao Yu. 2019. “Autophagy Activation Improves Lung Injury and Inflammation in Sepsis.” *Inflammation* 42 (2): 426–39. https://doi.org/10.1007/s10753-018-00952-5.

Zhu, X B, Y B Wang, O Chen, D Q Zhang, Z H Zhang, A H Cao, S Y Huang, and R P Sun. 2012. “Characterization of the Expression of Macrophage Inflammatory Protein-1α (MIP-1α) and C-C Chemokine Receptor 5 (CCR5) after Kainic Acid-Induced Status Epilepticus (SE) in Juvenile Rats.” *Neuropathology and Applied Neurobiology* 38 (6): 602–16. https://doi.org/10.1111/j.1365-2990.2012.01251.x.

# VITA

## EDUCATIONAL INFORMATION

- September 2018 – March 2024 Izmir Institute of Technology, Turkey

**Ph.D.** Department of Molecular Biology and Genetics, Faculty of Science

- September 2013 – July 2018 Izmir Institute of Technology, Turkey

**B.Sc.** Department of Molecular Biology and Genetics, Faculty of Science

## PUBLICATIONS

Leal, A. F., Inci, O. K., Seyrantepe, V., Rintz, E., Celik, B., Ago, Y., León, D., Suarez, D. A., Alméciga-Díaz, C. J., & Tomatsu, S. (2023). Molecular Trojan Horses for treating lysosomal storage diseases. *Molecular genetics and metabolism*, *140*(3), 107648. https://doi.org/10.1016/j.ymgme.2023.107648

Can, M., Sengül, T., Demir, S. A., İnci, O. K., Basırlı, H., & Seyrantepe, V. (2022). Analysis of Brain Lipids in the Early-Onset Tay-Sachs Disease Mouse Model with the Combined Deficiency of β-Hexosaminidase A and Neuraminidase 3. *Frontiers in molecular biosciences*, *9*, 892248. https://doi.org/10.3389/fmolb.2022.892248

Timur, Z. K., Inci, O. K., Demir, S. A., & Seyrantepe, V. (2021). Sialidase neu4 deficiency is associated with neuroinflammation in mice. *Glycoconjugate journal*, *38*(6), 649–667. https://doi.org/10.1007/s10719-021-10017-9

## SCHOLARSHIPS

- TUBITAK BIDEB 2211- A National Scholarship Program for Ph.D. Students
- Turkish Higher Education Council's 100/2000 Ph.D. Fellowship Program